RECENT ADVANCES IN THE CONTROVERSIAL HUMAN PATHOGENS PNEUMOCYSTIS, MICROSPORIDIA AND BLASTOCYSTIS

EDITED BY: Olga Matos and Lihua Xiao

PUBLISHED IN: Frontiers in Microbiology and Frontiers in Public Health

frontiers Research Topics

frontiers

ISSN 1664-8714
ISBN 978-2-88971-156-7
DOI 10.3389/978-2-88971-156-7

About Frontiers

Frontiers is more than just an open-access publisher of scholarly articles: it is a pioneering approach to the world of academia, radically improving the way scholarly research is managed. The grand vision of Frontiers is a world where all people have an equal opportunity to seek, share and generate knowledge. Frontiers provides immediate and permanent online open access to all its publications, but this alone is not enough to realize our grand goals.

Frontiers Journal Series

The Frontiers Journal Series is a multi-tier and interdisciplinary set of open-access, online journals, promising a paradigm shift from the current review, selection and dissemination processes in academic publishing. All Frontiers journals are driven by researchers for researchers; therefore, they constitute a service to the scholarly community. At the same time, the Frontiers Journal Series operates on a revolutionary invention, the tiered publishing system, initially addressing specific communities of scholars, and gradually climbing up to broader public understanding, thus serving the interests of the lay society, too.

Dedication to Quality

Each Frontiers article is a landmark of the highest quality, thanks to genuinely collaborative interactions between authors and review editors, who include some of the world's best academicians. Research must be certified by peers before entering a stream of knowledge that may eventually reach the public - and shape society; therefore, Frontiers only applies the most rigorous and unbiased reviews.
Frontiers revolutionizes research publishing by freely delivering the most outstanding research, evaluated with no bias from both the academic and social point of view. By applying the most advanced information technologies, Frontiers is catapulting scholarly publishing into a new generation.

What are Frontiers Research Topics?

Frontiers Research Topics are very popular trademarks of the Frontiers Journals Series: they are collections of at least ten articles, all centered on a particular subject. With their unique mix of varied contributions from Original Research to Review Articles, Frontiers Research Topics unify the most influential researchers, the latest key findings and historical advances in a hot research area! Find out more on how to host your own Frontiers Research Topic or contribute to one as an author by contacting the Frontiers Editorial Office: frontiersin.org/about/contact

RECENT ADVANCES IN THE CONTROVERSIAL HUMAN PATHOGENS PNEUMOCYSTIS, MICROSPORIDIA AND BLASTOCYSTIS

Topic Editors:
Olga Matos, New University of Lisbon, Portugal
Lihua Xiao, South China Agricultural University, China

Citation: Matos, O., Xiao, L., eds. (2021). Recent Advances in the Controversial Human Pathogens Pneumocystis, Microsporidia and Blastocystis. Lausanne: Frontiers Media SA. doi: 10.3389/978-2-88971-156-7

Table of Contents

frontiers in Microbiology

EDITORIAL
published: 02 August 2021
doi: 10.3389/fmicb.2021.701879

Editorial: Recent Advances in the Controversial Human Pathogens *Pneumocystis*, Microsporidia and *Blastocystis*

Olga Matos[1,2]* *and Lihua Xiao*[3,4]*

[1] Medical Parasitology Unit, Group of Opportunistic Protozoa/HIV and Other Protozoa, Global Health and Tropical Medicine, Instituto de Higiene e Medicina Tropical, Universidade NOVA de Lisboa, Lisboa, Portugal, [2] Faculdade de Medicina, Instituto de Saúde Ambiental, Universidade de Lisboa, Lisboa, Portugal, [3] Center for Emerging and Zoonotic Diseases, College of Veterinary Medicine, South China Agricultural University, Guangzhou, China, [4] Guangdong Laboratory for Lingnan Modern Agriculture, Guangzhou, China

Keywords: opportunistic protists, *Pneumocystis*, microsporidia, *Blastocystis*, epidemiology, diagnosis, therapy

Editorial on the Research Topic

Recent Advances in the Controversial Human Pathogens *Pneumocystis*, Microsporidia and *Blastocystis*

OPEN ACCESS

Edited by:
Axel Cloeckaert, Institut National de recherche pour l'agriculture, l'alimentation et l'environnement (INRAE), France

Reviewed by:
Louis Weiss, Albert Einstein College of Medicine, United States

***Correspondence:**
Olga Matos
omatos@ihmt.unl.pt
Lihua Xiao
lxiao1961@gmail.com

Specialty section:
This article was submitted to Infectious Diseases, a section of the journal Frontiers in Microbiology

Received: *28 April 2021*
Accepted: *07 July 2021*
Published: *02 August 2021*

Citation:
Matos O and Xiao L (2021) Editorial: Recent Advances in the Controversial Human Pathogens Pneumocystis, Microsporidia and Blastocystis. Front. Microbiol. 12:701879. doi: 10.3389/fmicb.2021.701879

Pneumocystis spp. are ubiquitous atypical fungi that develop extracellularly in the alveolar cavities of mammalian lungs with a not-completely defined lifecycle (Cushion, 2010). Similarly, microsporidia are a diverse group (>1,400 species) of obligate intracellular fungi, with a broad range of vertebrate and invertebrate hosts and poorly understood mechanisms of invasion, growth and reproduction (Han and Weiss, 2017). *Blastocystis* spp. are ubiquitous anaerobic eukaryotes that have a unique phylogenetic origin but are widely present in various mammals, including humans (Scanlan and Stensvold, 2013). All these organisms have environmental stages required for the initiation of infection in new hosts, and were previously considered protozoa. Further controversies remain on the species structure, zoonotic potential, transmission routes, and pathogenicity/clinical significance of each group of organisms (Didier, 2005; Morris and Norris, 2012; Scanlan and Stensvold, 2013). Recently, with the development of various molecular tools for the identification and characterization and the availability of whole genome sequences, metagenomics tools, animal models and/or cultivation, there have been significant advances in our understanding of the biology and epidemiology of these controversial pathogens. The 2019–2020 Research Topic on Recent Advances in the Controversial Human Pathogens *Pneumocystis*, Microsporidia and *Blastocystis* has published 11 manuscripts, nine in Frontiers in Microbiology and two in Frontiers in Public Health. This topic aimed to gather articles from research groups who are active on these neglected and opportunistic pathogens. They highlight the potential of new tools and approaches in resolving some longstanding issues. These research articles are contributions from several major research groups in these three areas, significantly improving our knowledge of *P. jirovecii*, microsporidia and *Blastocystis* infections in different contexts.

PNEUMOCYSTIS

The articles gathered in this Research Topic addressed issues in epidemiology and risk factors of PCP in industrialized nations and low-income countries, especially on the genetic diversity of the pathogen. Attention was given to the use of modern diagnostic approaches. The pathogenesis of

PCP and host defenses against *P. jirovecii* and its relationship with new therapies were discussed.

Knowing the prevalence and risk factors of PCP is a basic requirement for the prevention and control of the disease. Pereira-Díaz et al. conducted a nationwide study in Spain with this objective. It was a descriptive study of PCP patients registered in the Hospital Discharge Records Database of the country between 2008 and 2012. There was an increase in the annual incidence of PCP cases in non-HIV-infected patients and a decrease in HIV-infected patients. Risk factors identified in the HIV-negative group included hematological neoplasm, chronic lung diseases and non-hematological cancers. The mean mortality and the hospitalization costs observed were higher in non-HIV-infected patients with PCP than in HIV-infected patients with PCP. These observations indicate that PCP is an emerging problem in non-HIV-infected patients.

In another retrospective study of specimens from PCP patients from Réunion (a French island in the Indian Ocean), French Guiana (a French South American territory) and Brest (Brittany, metropolitan France), Le Gal et al. compared multilocus genotypes of *P. jirovecii* among these very different populations. A multilocus sequence typing (MLST) based on three distinct loci of *P. jirovecii* was used for the analysis of specimens. The data generated revealed significant genetic diversity of *P. jirovecii* in the islands and the existence of geographically segregated pathogen populations.

Morilla et al. addressed the issue of colonization by *P. jirovecii*. They analyzed epidemiological data from PCP patients and *P. jirovecii*-colonized individuals in Spain and data on the distribution of superoxide dismutase (SOD) genotypes of *P. jirovecii* isolates. Only two *SOD* genotypes were found in the country, with one being the dominant genotype in the colonized individuals. *SOD* is a single copy nuclear gene commonly used in genotyping studies. Based on the data obtained, the authors concluded that although SOD-PCR is not an attractive tool for genotyping *P. jirovecii*, it could be useful in distinguishing colonization from PCP.

The diagnosis of PCP relies heavily on microscopic visualization of organisms or DNA detection in respiratory specimens obtained by invasive/costly techniques, which are difficult to implement in low-income countries. As an alternative, blood biomarkers, reflecting the host-pathogen interaction, were tested (Matos and Esteves, 2016). Elevated serum levels of (1-3)-β-D-Glucan (cell wall component of *P. jirovecii* cystic forms or ascus) were related to PCP and proposed as marker of the disease, especially in non-HIV-infected immunocompromised patients (Esteves et al., 2014; Matos and Esteves, 2016). Recent studies propose the immunodiagnosis of PCP, based on the detection of IgM anti-*P. jirovecii* antibodies, using recombinant synthetic antigens, as a new diagnostic alternative (Tomás et al., 2016, 2020). However, the relationship between serology and the detection of *P. jirovecii* DNA in respiratory specimens is not yet clear. In this topic, Tomás et al. presented an innovative approach based on the development of a prototype for point-of-care serological diagnosis of PCP. Synthetic multiepitope antigens were designed, produced, and conjugated to gold nanoparticles. They were used in the development of two strip-based bionanodiagnostic assays for the specific detection of IgM against *P. jirovecii* in patient sera. This technology may offer an alternative to the conventional diagnosis of PCP, reducing the use of invasive procedures in collecting respiratory specimens. This new PCP diagnostic tool could be particularly useful in low-income countries, where this disease is emerging.

PCP therapy remains a challenge. The contribution of innate immunity to *Pneumocystis*-induced pathology is largely unexplored. Excess mucus and goblet-cell-derived CLCA1 protein activation appear to be associated with *Pneumocystis* infection in immunocompetent infants and animal models, and innate immunity related airway mucus responses may play a relevant role in the immunopathology of PCP. Existing treatment of PCP depend on anti-*Pneumocystis* drugs plus steroids that reduce cellular responses. Using a steroid-induced-immunosuppression rat model of PCP, Pérez et al. documented *Pneumocystis*-related pulmonary edema and progressive goblet-cell-derived CLCA1-related immunopathology. After the administration of the potent CLCA1-blocker Niflumic acid there were progressive reversal of mucous changes and improved animal survival. CLCA1 blockers could be used as an adjunctive therapy to improve clinical outcome, especially in steroid-induced PCP.

MICROSPORIDIA

Microsporidia have an environmental stage, the spore, which contains a coiled polar tube anchored to the spore wall. It is the developmental stage used in transmission of microsporidia and invasion of host cells. Once the spores are ingested, the polar tube inside ejects, delivering the sporoplasm into host cells (Tamim El Jarkass and Reinke, 2020). The invasion mechanism of microsporidia remains poorly explored. In the Research Topic, Han B. et al. reviewed recent developments in the structure and composition of the spore wall and polar tube and the invasion process of microsporidia. The involvement of various polar tube proteins in the invasion of host cells was discussed in detail.

Immune responses to microsporidia have attracted recent attention. Studies in this area were done mostly with the three human-pathogenic *Encephalitozoon* species, which have various rodent models and can be cultured easily. Another review by Han Y. et al. has summarized recent understandings of the innate and acquired immune responses to microsporidia, especially the role of various immune cells (macrophages, dendritic cells, natural killer cells, etc.), the toll-like receptor-MyD88 pathway in innate immunity, and antibody, CD4+ lymphocyte and CD8+ lymphocyte responses in acquired immunity against microsporidia.

Enterocytozoon bieneusi is another major human-pathogenic microsporidian species, responsible for over 90% human microsporidiosis cases (Li and Xiao, 2021). Sequence analysis of the ribosomal internal transcribed spacer (ITS) has identified over 500 genotypes of various host ranges and zoonotic potential. They belong to at least 11 genogroups, with Group 1 containing most genotypes from humans and many genotypes from animals. Other groups have more restricted host ranges, therefore,

representing host-adapted *E. bieneusi* populations. Therefore, genetic characterizations of isolates have been used in studies of the transmission dynamics, infection sources, and public health significance of *E. bieneusi* in humans and animals (Li et al., 2019). As a result, molecular epidemiology is a very active area in microsporidiosis research (Matos et al., 2012).

In the collection of articles for the Research Topic, three of the five ones on microsporidia were on molecular characterizations of *E. bieneusi*, all from the same research group. Data from the three studies suggest that domestic animals are infected with diverse *E. bieneusi* genotypes. In a study conducted on seven large-scale pig farms in Xinjiang, China by Li et al., a very high prevalence (48.6% or 389/801) of *E. bieneusi* was found. Altogether, 15 Group 1 genotypes were found, with the pig-adapted genotypes EbpA ($n = 129$) and EbpC ($n = 168$) as the dominant ones. These two genotypes and six other Group 1 genotypes were also found in a study by Zhao et al. of *E. bieneusi* in racehorses. A low frequency (prevalence = 4.8% or 30/621) of *E. bieneusi* was found in animals in 17 equestrian clubs in 15 Chinese cities. Among the *E. bieneusi* genotypes found, horse 1 ($n = 16$) was the dominant genotype. In addition to the Group 1 genotypes, one genotype each from Group 2 and Group 6 were found in 1–2 animals. In contrast, in another report by Wang et al., 11 *E. bieneusi* genotypes were found in dairy cattle (prevalence = 14.2% or 501/3527) in three provinces in China, with two bovine-adapted Group 2 genotypes I ($n = 226$) and J ($n = 225$) as the dominant genotypes. Therefore, cattle, pigs and horses in China are mostly infected with different groups of ITS genotypes of *E. bieneusi*. This has important implications in understanding cross-species transmission of *E. bieneusi*.

BLASTOCYSTIS

The pathogenicity of *Blastocystis* spp. remains controversial. Some major contributors to this debate include the influences of co-infections, microbiome, and subtype identity of *Blastocystis* spp. (Deng et al., 2021). In one study presented in the Research Topic by Betts et al., the subtype identity of *Blastocystis* spp., concurrence of *Cryptosporidium* spp., *Eimeria* spp., *Isospora* spp., *Entamoeba* spp., and *Giardia* spp. were examined in 231 fecal samples collected from asymptomatic animals in two conservation parks in the United Kingdom. Among the 38 vertebrate species examined, 47.4% (18/38) were positive for *Blastocystis* spp. Altogether, 10 known subtypes were identified, with ST2 as the most common one (31.4% or 80/255). Among the animal species with significant *Blastocystis*-positive samples, voles were mainly infected with ST4 (89.7% or 78/87), while non-human primates were mostly infected with ST1 (24.8% or 27/109), ST2 (56.9% or 62/109), and ST3 (11.0% or 12/109). Of the 81 *Blastocystis*-positive samples analyzed for other protists, 43 (53.1%) were positive for co-pathogens. These data suggest that co-infection and subtype identity should be considered in studies of pathogenicity of *Blastocystis* spp. in humans and animals.

AUTHOR CONTRIBUTIONS

Both authors listed have made a substantial, direct and intellectual contribution to the work, and approved it for publication.

FUNDING

Research was supported in part by the Guangdong Major Project of Basic and Applied Basic Research (Grant No. 2020B0301030007), the 111 Project (D20008), Innovation Team Project of Guangdong University (2019KCXTD001), and by grants from Foundation for Science and Technology, Portugal: UID/04413/2020 (GHTM) and UIDB/04295/2020 (ISAMB).

ACKNOWLEDGMENTS

We thank the authors of publications in this Research Topic for their contributions.

REFERENCES

Cushion, M. T. (2010). Are members of the fungal genus pneumocystis (a) commensals; (b) opportunists; (c) pathogens; or (d) all of the above? *PLoS Pathog.* 6:e1001009. doi: 10.1371/journal.ppat.1001009

Deng, L., Wojciech, L., Gascoigne, N. R. J., Peng, G., and Tan, K. S. W. (2021). New insights into the interactions between *Blastocystis*, the gut microbiota, and host immunity. *PLoS Pathog.* 17:e1009253. doi: 10.1371/journal.ppat.1009253

Didier, E. S. (2005). Microsporidiosis: an emerging and opportunistic infection in humans and animals. *Acta Tropica* 94, 61–76. doi: 10.1016/j.actatropica.2005.01.010

Esteves, F., Le, C.-H., De Sousa, B., Badura, R., Seringa, M., Fernandes, C., et al. (2014). (1-3)-Beta-D-glucan in association with lactate dehydrogenase as biomarkers of *Pneumocystis pneumonia* (PcP) in HIV-infected patients. *Eur. J. Clin. Microbiol. Infect. Dis.* 33, 1173–1180. doi: 10.1007/s10096-014-2054-6

Han, B., and Weiss, L. M. (2017). Microsporidia: obligate intracellular pathogens within the fungal kingdom. *Microbiol. Spectr.* 5:FUNK-0018-2016. doi: 10.1128/9781555819583.ch5

Li, W., Feng, Y., and Santin, M. (2019). Host specificity of *Enterocytozoon bieneusi* and public health implications. *Trends Parasitol.* 35, 436–451. doi: 10.1016/j.pt.2019.04.004

Li, W., and Xiao, L. (2021). Ecological and public health significance of *Enterocytozoon bieneusi*. *One Health* 12:100209. doi: 10.1016/j.onehlt.2020.100209

Matos, O., and Esteves, F. (2016). "Laboratory diagnosis of Pneumocystis jirovecii pneumonia," in *Microbiology of Respiratory System Infection*, eds K. Kon and M. Rai (London: Elsevier), 185–210. doi: 10.1016/B978-0-12-804543-5.00013-0

Matos, O., Lobo, M. L., and Xiao, L. (2012). Epidemioloy of *Enterocytozoon bieneusi* Infection in humans. *J. Parasitol. Res.* 2012:981424. doi: 10.1155/2012/981424

Morris, A., and Norris, K. A. (2012). Colonization by *Pneumocystis jirovecii* and its role in disease. *Clin. Microbiol. Rev.* 25, 297–317 doi: 10.1128/CMR.00013-12

Scanlan, P. D., and Stensvold, C. R. (2013). Blastocystis: getting to grips with our guileful guest. *Trends Parasitol.* 29, 523–529. doi: 10.1016/j.pt.2013.08.006

Tamim El Jarkass, H., and Reinke, A. W. (2020). The ins and outs of host-microsporidia interactions during invasion, proliferation and exit. *Cell. Microbiol.* 22:e13247. doi: 10.1111/cmi.13247

Tomás, A. L., Cardoso, F., De Sousa, B., and Matos, O. (2020). Detection of anti-*Pneumocystis jirovecii* antibodies in human serum using a recombinant synthetic multi-epitope kexin-based antigen. *Eur. J. Clin. Microbiol. Infect. Dis* 39: 2205–2209. doi: 10.1007/s10096-020-03936-2

Tomás, A. L., Cardoso, F., Esteves, F., and Matos, O. (2016). Serological diagnosis of pneumocystosis: production of a synthetic recombinant antigen for immunodetection of *Pneumocystis jirovecii*. *Sci. Rep*. 6:36287. doi: 10.1038/srep36287

Conflict of Interest: The authors declare that the research was conducted in the absence of any commercial or financial relationships that could be construed as a potential conflict of interest.

Publisher's Note: All claims expressed in this article are solely those of the authors and do not necessarily represent those of their affiliated organizations, or those of the publisher, the editors and the reviewers. Any product that may be evaluated in this article, or claim that may be made by its manufacturer, is not guaranteed or endorsed by the publisher.

frontiers in Microbiology

ORIGINAL RESEARCH
published: 25 June 2019
doi: 10.3389/fmicb.2019.01399

Prevalence and Population Genetics Analysis of *Enterocytozoon bieneusi* in Dairy Cattle in China

Hai-Yan Wang[1,2], Meng Qi[3], Ming-Fei Sun[4], Dong-Fang Li[2], Rong-Jun Wang[2], Su-Mei Zhang[2], Jin-Feng Zhao[2], Jun-Qiang Li[2], Zhao-Hui Cui[2], Yuan-Cai Chen[2], Fu-Chun Jian[2], Rui-Ping Xiang[1], Chang-Shen Ning[2] and Long-Xian Zhang[2]**

[1] Experimental and Research Center, Henan University of Animal Husbandry and Economy, Zhengzhou, China, [2] College of Animal Science and Veterinary Medicine, Henan Agricultural University, Zhengzhou, China, [3] College of Animal Science, Tarim University, Alar, China, [4] Institute of Animal Health, Guangdong Academy of Agricultural Sciences, Guangzhou, China

OPEN ACCESS

Edited by:
Olga Matos,
NOVA University Lisbon, Portugal

Reviewed by:
Majid Fasihi Harandi,
Kerman University of Medical Sciences, Iran
Na Li,
South China Agricultural University, China

***Correspondence:**
Hai-Yan Wang
wangheng800220@126.com
Long-Xian Zhang
zhanglx8999@henau.edu.cn;
zhanglx8999@gmail.com

Specialty section:
This article was submitted to Infectious Diseases, a section of the journal Frontiers in Microbiology

Received: 07 April 2019
Accepted: 04 June 2019
Published: 25 June 2019

Citation:
Wang H-Y, Qi M, Sun M-F, Li D-F, Wang R-J, Zhang S-M, Zhao J-F, Li J-Q, Cui Z-H, Chen Y-C, Jian F-C, Xiang R-P, Ning C-S and Zhang L-X (2019) Prevalence and Population Genetics Analysis of Enterocytozoon bieneusi in Dairy Cattle in China. Front. Microbiol. 10:1399. doi: 10.3389/fmicb.2019.01399

Enterocytozoon bieneusi, an obligate intracellular pathogen, can infect various hosts. In this study, 3527 dairy cattle fecal specimens were collected from different geographic locations in China (including 673 from Shandong province, 1,440 from Guangdong province and 1,414 from Gansu province) and examined for the presence of *E. bieneusi* using polymerase chain reactions targeting the ribosomal internal transcribed spacer (ITS). The dominant genotypes identified were further subtyped by multilocus sequence typing. The overall prevalence of *E. bieneusi* was 14.2% (501/3527), with a significant difference in prevalence among the different geographical locations ($P < 0.001$). Our logistic regression analysis showed that all four variables (farming model, location, age, and clinical manifestations) had strong effects on the risk of contracting *E. bieneusi*. Sequence analysis revealed 11 genotypes: eight known genotypes (J, I, BEB4, BEB10, D, EbpC, CM19, and CM21) and three novel genotypes (named here as CGC1, CGC2, and CGC3). Genotypes J and I, the commonest, were found on all farms across the three provinces. Our linkage disequilibrium analysis showed a clonal population structure in the *E. bieneusi* dairy cattle population but the ITS genotypes had different population structures. Phylogenetic and haplotype network analysis showed the absence of geographical segregation in the *E. bieneusi* dairy cattle populations. Instead, they revealed the presence of host adaptation to the *E. bieneusi* populations in various animals. Our findings augment the current understanding of *E. bieneusi* transmission dynamics.

Keywords: *Enterocytozoon bieneusi*, prevalence, dairy cattle, China, multilocus genotyping, zoonotic infection

INTRODUCTION

Microsporidia, a diverse group of emerging opportunistic pathogens with more than 1,300 named species, are classified as fungi (Mathis et al., 2005). Among approximately 17 human infective microsporidia species, *Enterocytozoon bieneusi* is the most commonly detected (Matos et al., 2012). *E. bieneusi* can cause gastrointestinal illnesses such as wasting syndrome and chronic diarrhea in immunocompromised people (organ transplant recipients, patients with cancer or AIDS), but

remains asymptomatic in the immunocompetent (Didier and Weiss, 2011). *E. bieneusi* has also been detected in livestock, companion animals and wildlife, and even in environmental water samples (Santín and Fayer, 2011; Guo et al., 2014).

The DNA sequence of the ribosomal internal transcribed spacer (ITS) has been frequently used as the standard method for determining the genotypes of *E. bieneusi* (Santín and Fayer, 2009b), and phylogenetic analysis has revealed that over 300 *E. bieneusi* ITS genotypes cluster into at least 11 large groups (Li et al., 2018). Group 1 contains most genotypes found in humans (e.g., EbpC, D, EbpD, Peru8, Peru11, and type IV), and with its likely transmission between humans and other animals this group is considered to be zoonotic. Groups 2–11 have a narrow host range and only infect particular animals (e.g., ruminants, non-human primates, horses, and dogs) (Guo et al., 2014). To date, over 40 *E. bieneusi* genotypes have been identified in cattle worldwide, most of which belong to Group 2 (Fayer et al., 2003, 2007; Sulaiman et al., 2004; Santin et al., 2012; Del Coco et al., 2014; Ma et al., 2015; Zhao et al., 2015; da Silva Fiuza et al., 2016; Li J. et al., 2016; Wang et al., 2016; Zhang et al., 2018). However, some genotypes (I, J, BEB4, and BEB6) from Group 2, which were originally regarded as ruminant-specific, are considered to have reduced host specificity because of the sporadic infections they cause in other hosts including humans (Sak et al., 2011; Zhang et al., 2011; Wang et al., 2013; Jiang et al., 2015), implying the possibility of them having zoonotic transmission.

Nevertheless, the use of a single-marker typing method has limitations in representing the whole genome of *E. bieneusi* (∼ 6 Mb total length), and with the possibility of a sexual phase in the *E. bieneusi* lifecycle (Widmer and Akiyoshi, 2010) such an approach will be inadequate for inferring subgroup-level phylogenies. The multilocus sequence typing (MLST) tool approach, which has higher resolution, has been effectively used to characterize the population genetic structures of *Cryptosporidium*, *E. bieneusi,* and *Cyclospora cayetanensis* (Feng et al., 2011; Li et al., 2012, 2013; 2017; Karim et al., 2014; Guo et al., 2016; Wan et al., 2016). Geographical regions, transmission intensities, genetic variation and adaptive selection within species contribute to shape diverse population structures: clonal, epidemic, and panmictic (Tanriverdi et al., 2006). These evoluting processes have caused the association of the population structures with specific transmission patterns, parasite virulence, the emergence of host-adapted and geographical segregation and hypertransmissible populations with different genetic structures and public health potential (Feng et al., 2018).

As one of the largest animal husbandry countries, China raises very large numbers of dairy cattle annually. Although many studies have reported the prevalence and genotypes of *E. bieneusi* in dairy cattle from different Chinese provinces or cities, including Henan, Hebei, Tianjin, Ningxia, and Xinjiang (Li J. et al., 2016; Wang et al., 2016; Hu et al., 2017; Qi et al., 2017), these observations on *E. bieneusi* in China would benefit from substantiation by studies conducted in other geographic locations to fully determine the overall picture. Therefore, in this study, we investigated the prevalence of *E. bieneusi* in dairy cattle from other geographic locations in China and assessed the population structure of the common *E. bieneusi* ITS genotypes by MLST analyses.

MATERIALS AND METHODS

Ethics Statement

This study was performed strictly according to the recommendations of the Guide for the Care and Use of Laboratory Animals of the Ministry of Health, China. Our protocol was reviewed and approved by the Research Ethics Committee (Approval No. LVRIAEC 2016-011) of Henan Agricultural University (Zhengzhou city, China). The locations where we sampled did not involve endangered or protected species and no specific permits were required. All fecal specimens were collected based on the accessibility of the animals for sampling and each owner's willingness to participate in the study.

Collection of Fecal Samples and DNA Extraction

In total, 3527 feces samples from dairy cattle under 1 year of age from 24 farms in Shandong (673 samples from 5 farms), Guangdong (1,440 samples from 10 farms), and Gansu province (1,414 samples from 9 farms) were collected and examined. Each dairy farm was sampled on one occasion between November 2017 and September 2018, and 15–20% of the each herd was sampled. The fecal samples were collected from the rectum or immediately picked up using sterile gloves after defecation, and then stored on ice. Genomic DNA was extracted from each sample using the E.Z.N.A.® Stool DNA Kit (D4015-02, Omega Bio-Tek, Inc., Norcross, GA, United States) according to the manufacturer's instructions and then stored at −20°C until used for polymerase chain reaction (PCR) analyses. All samples were processed within 24 h of collection.

PCR Amplification

Enterocytozoon bieneusi genotypes from the dairy cattle residing in different geographical regions were determined by nested PCR amplification of an ∼390 bp fragment of the ribosomal ITS spacer, and using primers whose sequences have been described previously (Buckholt et al., 2002) (**Table 1**). Each PCR was conducted in a 25 μL volume, containing 0.3 μM of each primer, 12.5 μL 2 × EasyTaq PCR SuperMix (TransGen Biotech Co., Ltd., Beijing, China), 1 μL of genomic DNA for the primary PCR and 1 μL of the primary amplification product for the secondary PCR, and 10.9 μL of deionized water. Positive (dairy cattle-derived genotype J DNA) and negative controls (sterile water) were included in each test.

MLST PCR and Sequencing

Together with the ITS, one minisatellite (MS4) and three microsatellite markers (MS1, MS3, and MS7) were used in the MLST analysis. The PCR primers and amplification conditions

TABLE 1 | PCR primers used in this study.

Gene locus	Primer	Sequence (5′–3′)	Amplicon length (bp) (GenBank accession number)	Annealing temperature (°C)
ITS	EBITS3	GGTCATAGGGATGAAGAG	435	57
	BITS4	TTCGAGTTCTTTCGCGCTC		
	BITS1	GCTCTGAATATCTATGGCT	390 (MK559494–MK559496)	55
	EBITS2.4	ATCGCCGACGGATCCAAGTG		
MS1	F1	CAAGTTGCAAGTTCAGTGTTTGAA	843	58
	R1	GATGAATATGCATCCATTGATGTT		
	F2	TTGTAAATCGACCAAATGTGCTAT	676 (MH560534–MH560563)	58
	R2	GGACATAAACCACTAATTAATGTAAC		
MS3	F1	CAAGCACTGTGGTTACTGTT	702	55
	R1	AAGTTAGGGCATTTAATAAAATTA		
	F2	GTTCAAGTA ATTGATACCAGTCT	537 (MH560519–MH560526)	55
	R2	CTCATTGAATCTAAATGTGTATAA		
MS4	F1	GCATATCGTCTCATAGGAACA	965	55
	R1	GTTCATGGTTATTAATTCCAGAA		
	F2	CGAAGTGTACTACATGTCTCT	885 (MH560527–MH560533)	55
	R2	GGACTTTAATAAGTTACCTATAGT		
MS7	F1	GTTGATCGTCCAGATGGAATT	684	55
	R1	GACTATCAGTATTACTGATTATAT		
	F2	CAATAGTAAAGGAAGATGGTCA	471 (MH560564–MH560566)	55
	R2	CGTCGCTTTGTTTCATAATCTT		

used for the four markers were the same as those previously described (Feng et al., 2011) (**Table 1**). Considering *E. bieneusi* ITS genotypes J, I, and BEB4 as being the dominant genotypes found in different geographic locations in China and their recently certified potential zoonotic properties, specimens that belonged to these genotypes were selected for further MLST analysis. Specifically, 2–3 isolates were chosen from each *E. bieneusi*-positive farm in the different geographical locations (**Figure 1**). With these selected samples, we tried to incorporate representatives of the different dominant pathogen genotypes, and representatives of the different clinical signs and age groups for the dairy cattle. A total of 155 *E. bieneusi* specimens were used in this study. The number of isolates and their ITS genotype designations by geographic location are shown in **Table 2**. Most of the specimens were genotyped in this study, whereas the remaining specimens from Shaanxi and Shanghai were included and genotyped by the same technique in previous studies (Wang et al., 2016; Tang et al., 2018).

Secondary PCR products were agarose gel electrophoresed, and then visualized and examined after GelRed™ (Biotium Inc., Hayward, CA, United States) staining. The secondary PCR products were bidirectionally sequenced on an ABI PRISM™ 3730 XL DNA Analyzer using the BigDye Terminator v3.1 Cycle Sequencing Kit (Applied Biosystems, Foster City, CA, United States). Raw sequences were assembled and edited with Chromas Pro version 2.1.3 (Technelysium Pty., Ltd., Helensvale, QLD, Australia). The sequences obtained were compared with the reference sequences downloaded from the National Center for Biotechnology Information[1] using Clustal X 2.0[2].

Linkage Disequilibrium (LD) Analysis

The values for the standardized index of association (I^S_A) were calculated using the LIAN 3.5 program[3] on the five-locus haplotypes. Moreover, the variance of pair-wise differences (V_D) and 95% confidence limits (L) were also calculated as another test of LD.

Phylogenetic and Sub-Population Analysis

An analysis of the phylogenetic relationships among the *E. bieneusi* isolates was performed by ITS sequencing and the resultant sequences were concatenated for all 5 polymorphic markers by a neighbor-joining (NJ) analysis in MEGA 7.01, as based on the Kimura 2-parameter model using 1000 bootstrap replicates. Additionally, median-joining phylogenies were generated using Network software version 5.0[4] under the default parameters. Networks were then arranged by hand and nodes colored using Network Publisher version 5.0.0.0[5]. *E. bieneusi* isolates from different hosts and geographic origins, including the *E. bieneusi* isolates belonging to ITS zoonotic Group 1 (genotypes D, EbpC, type IV, horse1, Nig2, EBITS3, Henan-1, WL11, CM1, and CM2), Group 6 (genotypes horse2 and Nig3), Group 10 (genotypes CHB1, CSK1, and ABB1) and an outlier genotype (Nig5) were also included in the multilocus phylogeny and haplotype network analysis (Karim et al., 2014; Wan et al., 2016; Li et al., 2019).

[1]https://www.ncbi.nlm.nih.gov/

[2]http://www.clustal.org

[3]http://guanine.evolbio.mpg.de/cgi-bin/lian/lian.cgi.pl

[4]www.fluxus-engineering.com/sharenet.htm

[5]http://fluxus-engineering.com/nwpub.htm

FIGURE 1 | Specific locations where the samples were collected in this study. Locations ▲.

Statistical Analysis

Comparisons of *E. bieneusi* prevalence (*ó*) in dairy cattle between the different geographical locations ($x1$), ages ($x2$), clinical signs in the animals ($x3$), and farming model ($x4$) were performed using the chi-squared test. All results were considered statistically significant at $P < 0.01$. Odds ratios (ORs) and 95% confidence intervals (95% CIs) were calculated to explore the strength of the association between *E. bieneusi* positivity and the variables tested. The impacts of the multiple variables were also evaluated by multivariable regression analysis using SPSS 22.0 version (SPSS Inc., Chicago, IL, United States).

TABLE 2 | The *E. bieneusi* isolates used for further intra-genotypic variation analysis in this study and their associated ITS genotypes.

Location	Number	ITS genotype (number)	References
Beijing	14	J (5); I (4); BEB4 (5)	Hu et al., 2017
Tianjin	15	J (11); BEB4 (4)	Hu et al., 2017
Henan	20	J (11); I (5), BEB4 (4)	Li J. et al., 2016
Guangdong	23	J (12); I (8); BEB4 (3)	This study
Shandong	21	J (18); I (1); BEB4 (2)	This study
Gansu	21	J (8); I (8); BEB4 (5)	This study
Xinjiang	21	J (4); I (9); BEB4 (8)	Qi et al., 2017
Shaanxi	10	J (5); I (5)	Wang et al., 2016
Shanghai	10	J (8); BEB4 (2)	Tang et al., 2018
Total	155	J (82); I (40); BEB4 (33)	

RESULTS

Prevalence of *E. bieneusi*

Of the 3,527 dairy cattle fecal specimens we tested, 501 (14.2%) were found to be *E. bieneusi*-positive by nested PCR amplification of the ITS region. *E. bieneusi* was detected in 21 of the 24 farms surveyed, with infection rates ranging between 0 and 42.4% (**Table 3**). The results of the univariate and multiple analyses are summarized in **Table 4**. In the final model, all four variables had strong effects on *E. bieneusi* prevalence, as described by the equation $y = -0.455 \times x4 + 2.069 \times x1 + 0.929 \times x2 + 0.970 \times x3 - 4.124$. Farming model had a negative effect on the risk of *E. bieneusi*, for which the OR was 0.65 (95% CI 0.52–0.82). Dairy cattle managed by outdoor-free practices (18.6% positive) showed a significantly higher *E. bieneusi* prevalence compared with those managed by intensive-closed practices (13.1% positive). Notably, clinical manifestations in the cattle, age and the geographical region also had strong effects on the risk of contracting *E. bieneusi*. Dairy cattle in Gansu Province (22.6% positive) were considered to have higher positivity rates compared with those from the two other

TABLE 3 | *Enterocytozoon bieneusi* genotypes identified in dairy cattle from different farms in three Chinese geographic regions.

Location	Farm ID	Farming model	No. tested	No. positive (%)	Genotype (n)
Shandong Province	1	Intensive-closed	141	5 (3.54%)	J (5)
	2	Intensive-closed	136	0	–
	3	Intensive-closed	121	6 (4.41%)	BEB4 (1), J (5)
	4	Intensive-closed	135	3 (2.22)	J (3)
	5	Outdoor-free	140	7 (5.0%)	J (5), I (1), BEB4 (1)
Subtotal			673	21 (3.12)	J (18), BEB4 (2), I (1)
Guangdong Province	1	Intensive-closed	82	6 (7.3%)	J (6)
	2	Outdoor-free	67	9 (13.4%)	I (9)
	3	Outdoor-free	40	0	–
	4	Intensive-closed	111	25 (22.5%)	I (7), J (14), D (4)
	5	Outdoor-free	138	23 (16.7%)	I (9), J (13), BEB4 (1)
	6	Intensive-closed	118	17 (14.4%)	J (13), BEB4 (2), EbpC (2)
	7	Intensive-closed	374	28 (7.4%)	I (18), J (10)
	8	Outdoor-free	12	0	–
	9	Intensive-closed	319	27 (8.4%)	I (23), J (4)
	10	Intensive-closed	179	25 (13.9%)	I (25)
Subtotal			1440	160 (11.1%)	J (60), I (91), BEB4 (3), EbpC (2), D (4)
Gansu Province	1	Intensive-closed	125	30 (24)	J (20), I (10)
	2	Intensive-closed	55	8 (14.5%)	I (8)
	3	Intensive-closed	94	22 (23.4%)	J (18), I (4)
	4	Outdoor-free	125	53 (42.4%)	J (30), I (6), CGC 3[a] (11), BEB4 (5), CM21 (1)
	5	Outdoor-free	137	31 (22.6%)	J (15), I (7), CGC 1[a] (6), BEB10 (3)
	6	Outdoor-free	57	10 (17.5%)	J (9), I (1)
	7	Intensive-closed	226	8 (3.5%)	J (8)
	8	Intensive-closed	200	4 (2%)	J (4)
	9	Intensive-closed	395	154 (40%)	J (43), I (98), CGC 2[a] (8), CM19 (5)
Subtotal			1414	320 (22.6%)	J (155), I (126), BEB4 (5), BEB10 (3), CM19 (5), CM21 (1), CGC1 (6)[a], CGC2 (8)[a], CGC3 (11)[a]
Total	24		3527	01 (14.2)	J (225), I (226), BEB4 (10), BEB10 (3), D (4), EbpC (2), CM19 (5), CM21 (1), CGC1 (6)[a], CGC2 (8)[a], CGC3 (11)[a]

[a]*Novel types from this study.*

TABLE 4 | Factors associated with the prevalence of *E. bieneusi* in dairy cattle in three Chinese geographic regions.

Factor	Category	No. tested	No. positive	% (95% CI)	OR (95% CI)[a]	*P*-value[a]	OR (95% CI)[b]	*P*-value[b]
Location	Shandong Province	673	21	3.1 (1.8–4.4)	Reference	$P < 0.01$	Reference	$P < 0.01$
	Guangdong Province	1440	160	11.1 (9.5–12.7)	3.88 (2.44–6.18)		4.77 (2.97–7.65)	
	Gansu Province	1441	320	22.6 (20.4–24.8)	9.08 (5.78–14.27)		13.20 (8.28–21.04)	
Age	Pre-weaned	897	82	9.1 (7.3–11.0)	Reference	$P < 0.01$	Reference	$P < 0.01$
	Post-weaned	2630	419	15.9 (14.5–17.3)	1.88 (1.47–2.42)		2.98 (2.28–3.89)	
Clinical symptom	Non-diarrhea	3196	431	13.5 (12.3–14.7)	Reference	$P < 0.01$	Reference	$P < 0.01$
	Diarrhea	331	70	21.1 (16.7–25.6)	1.72 (1.30–2.28)		3.19 (2.32–4.38)	
Farming model	Outdoor-free	716	133	18.6 (18.0–19.2)	Reference	$P < 0.01$	Reference	$P < 0.01$
	Intensive-closed	2811	368	13.1 (12.9–13.3)	0.66 (0.53–0.82)		0.65 (0.52–0.82)	
Total		3527	501	14.2 (13.1–15.4)				

[a]*Univariate analysis;* [b]*Multivariate analysis.*

provinces (Guangdong, 11.1%; Shandong, 3.1%). Furthermore, post-weaned (15.9% positive) dairy cattles and diarrheal animals (21.1% positive) were more susceptible to *E. bieneusi* than pre-weaned cattles (9.1% positive) and animals with clinical signs (13.5% positive), respectively, for which the ORs were 2.98 (95% CI 2.28–3.89) and 3.19 (95% CI 2.32–4.38), respectively.

Genotype Distribution

A total of 11 *E. bieneusi* ITS genotypes were identified from the 501 successfully sequenced specimens, including eight known genotypes (J, I, BEB4, BEB10, D, EbpC, CM19, and CM21) and three novel genotypes (CGC1, CGC2, and CGC3). Among them, *E. bieneusi* ITS genotypes J ($n = 225$, 44.9%) and I ($n = 226$, 45.1%) were the dominant ones in our study (**Table 3**). The remaining genotypes were seen in only 0–10 *E. bieneusi*-positive calves. Two genotypes (D and EbpC) clustered into zoonotic Group 1, while the remaining genotypes clustered into Group 2 (**Figure 2**). Among the three geographic locations, Gansu province showed the highest genetic diversity in its sampled cattle (nine *E. bieneusi* ITS genotypes) compared with Guangdong province (with five genotypes) and Shandong province (with three genotypes).

Multilocus Sequence Typing (MLST) and Analysis

Altogether, 106 specimens were successfully amplified at all five loci, generating 30, 8, 7, and 3 genotypes at MS1, MS3, MS4, and MS7 loci, respectively. A total of 71 multilocus genotypes (MLGs) were formed (**Supplementary Table S1**). The I^S_A values for the overall dairy cattle population and ITS genotype subpopulations are shown in **Table 5**. When all the isolates were used in the analysis, I^S_A was >0 and V_D was greater than L, indicating the presence of LD and a clonal population structure for *E. bieneusi* in the overall dairy cattle population of China. Considering each group of isolates with the same MLST subtype as one individual, the I^S_A value obtained was still above zero for the overall dairy cattle population ($I^S_A = 0.0513$, $V_D > L$) and ITS genotype J ($I^S_A = 0.0917$, $V_D > L$), suggesting a clonal population structure. In contrast, evidence for linkage equilibrium (LE) was obtained for ITS genotype I and BEB4 (genotypes I: $I^S_A = 0.0394$, $P_{MC} = 0.0134$, and $V_D < L$; genotypes BEB4: $I^S_A = 0.0484$, $P_{MC} = 0.0079$, and $V_D < L$), finally indicating that the two subpopulations under comparison had epidemic population structures.

Phylogenetic and Structure Analysis

We performed multilocus phylogenetic and genetic network analyses for the *E. bieneusi* isolates from dairy cattle ($n = 71$) and other hosts (pigs, horse, humans, non-human primates, bears, and kangaroo, $n = 44$). All specimens used in the phylogenetic analysis formed three main clusters; one contained zoonotic MLGs from NHPs, humans and pigs, the remaining two contained MLGs with Group 2 and Group 10 that are specific to cattles and bears, respectively. No clear geographically segregated groups were seen among all the dairy cattle specimens (**Figure 3**). Median-joining network analysis showed the zoonotic MLGs were in the central position, while isolates from dairy cattles and bears occupied the peripheral position.

DISCUSSION

In the present study, the overall infection rate for *E. bieneusi* was 14.2% (501/3527). Different infection rates in dairy cattle have been reported for studies from China, including Henan and Ningxia (29.3%), Hebei and Tianjin (19.4%), Shaanxi (19.5%), Xinjiang (17.7%), and Shanghai (26.5%) (Li J. et al., 2016; Wang et al., 2016; Hu et al., 2017; Qi et al., 2017; Tang et al., 2018), and for North America (17.0 and 24.0%) (Fayer et al., 2003; Santín and Fayer, 2009b), Brazil (17.5%) (da Silva Fiuza et al., 2016), Argentina (14.3%) (Del Coco et al., 2014), and the Czechia (2.5%) (Juránková et al., 2013). The discrepant values among these studies might result from various factors, such as differences in the animal management systems, sample sizes, climatic and environmental conditions, as well as the health status of the animals. In our analysis of the effects of multiple variables on *E. bieneusi*, post-weaned dairy cattles were more susceptible to *E. bieneusi* than pre-weaned animals, which agreed with a previous study in Maryland where pre-weaned calves (11.7%) showed a significantly lower prevalence than post-weaned calves (44.4%) (Santín and Fayer, 2009a). Moreover, the farming management system showed a strong effect on the risk of contracting an *E. bieneusi* infection, probably because free-range dairy cattle have more opportunities to come into contact with contaminated food and water than those kept indoors.

Sequence analysis of the ITS sequences from the *E. bieneusi*-positive isolates highlighted the presence of high genetic diversity in the *E. bieneusi* genotypes. We identified genotypes I and J as the dominant ones in the present study. Similar results to ours have been reported in the Czechia, United States, Brazil, Argentina, and China (Sulaiman et al., 2004; Fayer et al., 2007; Santin et al., 2012; Juránková et al., 2013; Del Coco et al., 2014; Jiang et al., 2015; Ma et al., 2015; Zhao et al., 2015; da Silva Fiuza et al., 2016; Li J. et al., 2016; Wang et al., 2016). These dominant genotypes (notably I, J, BEB4, and BEB6), which were previously considered to be adapted to ruminants, can have a broad-host range and are therefore becoming of increasing zoonotic concern. For example, genotype I was detected in monkeys (Karim et al., 2014), and genotype J in deer (Santín and Fayer, 2015), chickens (Reetz et al., 2002), and pigeons (Pirestani et al., 2013), while BEB4 was detected in pigs, and BEB6 in deer (Zhao et al., 2014), horses (Qi et al., 2016), and pet chinchillas (Qi et al., 2015). The common *E. bieneusi* genotypes have also been reported in children in China and in immunocompetent people in the Czechia (Sak et al., 2011; Zhang et al., 2011; Wang et al., 2013; Jiang et al., 2015). The occurrence of zoonotic genotypes suggests that dairy cattle may be potential reservoirs of infection and play a role in the epidemiology of *E. bieneusi*.

In the present study, strong LD has revealed a clonal population structure in the overall population of dairy cattle, further supporting the finding that *E. bieneusi* undergoes predominantly clonal propagation in dairy cattle, which probably reflects the narrow-host range and lower transmission intensity of *E. bieneusi* genotypes. This observation is similar to what has been reported elsewhere; specifically that *E. bieneus*i isolates from AIDS patients in Peru, Nigeria, and India have a clonal population structure (Li et al., 2013). A clonal population structure for *E. bieneusi* was also found in non-human primates, pigs, pandas, and fur animals (Karim et al., 2014; Li W. et al., 2016, 2017; Wan et al., 2016). Nevertheless, the possibility of genetic recombination among some of the genotypes cannot be

FIGURE 2 | Phylogenetic relationships among the *E. bieneusi* genotypes identified in this study and other reported genotypes. The phylogeny was inferred from the Neighbor-joining (NJ) analysis of the ITS sequences based on the distances calculated using the Kimura 2-parameter model. Bootstrap values of $N > 50\%$ from 1,000 replicates are shown at the nodes. Known and new genotypes are indicated by hollow and filled triangles, respectively.

TABLE 5 | Results of the linkage disequilibrium analysis based on the allelic profile data from five genetic loci.

Population	No.	Hd	I^S_A	P_{MC}	V_D	*L*	$V_D > L$
All (10 locations)	106	0.6386 ± 0.1449	0.1126	<0.001	1.0649	0.7673	Y
All (10 locations)[a]	71	0.9392 ± 0.1505	0.0513	<0.001	0.8442	0.7472	Y
I	32	0.4303 ± 0.1550	0.1154	<0.001	1.0890	0.8916	Y
J	43	0.4901 ± 0.1967	0.1064	<0.001	0.6780	0.5228	Y
BEB4	31	0.4413 ± 0.1562	0.2100	<0.001	1.3711	0.8797	Y
I[a]	22	0.4877 ± 0.1687	0.0394	0.0134	0.7869	0.8583	N
J[a]	32	0.5015 ± 0.1989	0.0917	<0.001	0.6275	0.5130	Y
BEB4[a]	17	0.4926 ± 0.1861	0.0484	0.0079	0.6653	0.6801	N

Hd, mean genetic diversity; I^S_A, standardized index of association calculated using the LIAN 3.5 program; P_{MC}, significance of obtaining this value in 1,000 simulations using the Monte Carlo method; V_D, variance of pairwise differences; L, 95% critical value for V_D; $V_D > L$ indicates linkage disequilibrium. [a]Considering isolates with the same MLG as one individual.

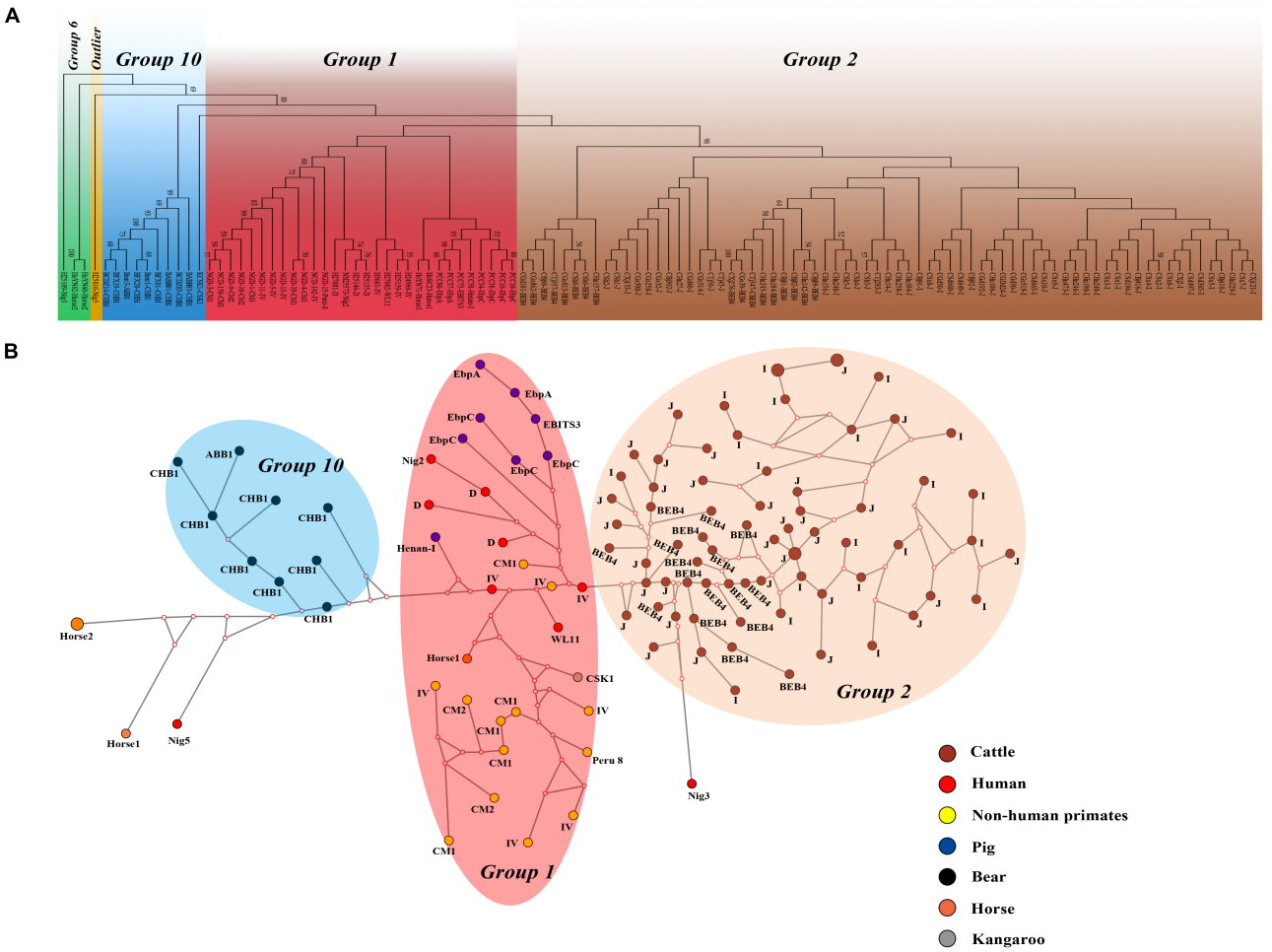

FIGURE 3 | Phylogenetic and haplotype network of *E. bieneusi* isolates from different hosts and geographic origins. All dairy cattle *E. bieneusi* isolates (*n* = 71) identified in this study were included in the analyses and some of the Group 1 isolates (*n* = 30) with genotypes being D, EbpC, type IV, horse1, Nig2, EBITS3, Henan-1, WL11, CM1, and CM2, Group 6 isolates (*n* = 3) with genotypes being horse2 and Nig3, Group 10 isolates (*n* = 10) with genotypes being CHB1, CSK1, and ABB1, and an outlier isolate genotype Nig5 were selected for comparative analysis. **(A)** NJ phylogenetic analysis of all *E. bieneusi* isolates by the Kimura 2-parameter model, implemented in MEGA version 7.01. The letters B, H, Ho, P, C, N, and K, indicate the isolates were sampled from bear, human, horse, pig, cattle, non-human primates, and kangaroo, respectively. Bootstrap values of *N* > 50% from 1,000 replicates are displayed. **(B)** Median-joining analysis of the MLST data from all *E. bieneusi* specimens using the Network program. Circles are proportional to the frequency of each genotype and node sizes are proportional to the total haplotype frequencies. The colors within the circles represent the different ITS genotypes.

excluded. Our analysis of the allelic profile data showed that ITS genotypes I and BEB4 are in LE and have epidemic population structures (I^S_A was >0 and $V_D < L$), which indicates that genetic recombination has occurred among them. This situation is similar to that reported previously where a clonal population was reported for the zoonotic ITS genotypes D and Type IV and an epidemic population in genotype A, which only infects human AIDS patients (Li et al., 2012, 2013). Further information was reported by Karim et al. (2014) who observed that the ITS genotypes CM1, Type IV and D had epidemic population structures, while Li W. et al. (2016) revealed population differentiation in fur animals with ITS genotype D from two known human *E. bieneusi* populations with ITS genotypes D and IV (a clonal structure) and with ITS genotype A (an epidemic structure) in their study. Collectively, the observations on the overall clonality and epidemic population structures of sub-population structures in dairy cattle, AIDS patients in Peru, Nigeria, and India, non-human primates, and fur animals further support the probability of sexual recombination occurring in *E. bieneusi* (Lee et al., 2008). The determination of the population genetic structure of *E. bieneusi* is undoubtedly vital to the understanding of its transmission patterns.

The high MLG diversity revealed in the present study on *E. bieneusi* is based on only three ITS genotypes (I, J, and BEB4). The *E. bieneusi* MLGs from dairy cattle showed no signs of geographical segregation by phylogenetic and haplotype networks analysis, indicating that they most likely originate from a single clonal type. Although this phenomenon might be related to frequent animal transport, the food and feed trade, and frequent floods, the *E. bieneusi* MLST data from different hosts shows a clear host separation, revealing the potential occurrence of directed genetic differentiation from zoonotic to host-adapted in *E. bieneusi* (Li and Xiao, 2019; Li et al., 2019). More MLST data are patently needed to further assess the level of host specificity for this species.

CONCLUSION

Enterocytozoon bieneusi in dairy cattle in China exhibits a high level of genetic diversity in our study. The detection of *E. bieneusi* zoonotic genotypes suggests that dairy cattle may be reservoir hosts for zoonotic *E. bieneusi* infections and play a role in the epidemiology of this fungal pathogen. MLST analysis revealed a high level of MLG diversity in the same ITS gene sequences. LD analysis revealed a clonal structure within the overall population of dairy cattle. No significant geographic segregation in *E. bieneusi* MLGs from dairy cattle was observed. Instead, the data have revealed the presence of host adaptation of *E. bieneusi* to different hosts. The findings presented here enhance our current understanding of the transmission dynamics of this pathogen.

DATA AVAILABILITY

The data sets supporting the conclusions of this article are included in the article. All ITS, MS1, MS3, MS4, and MS7 nucleotide sequences from dairy cattle-isolated *E. bieneusi* in this study are deposited in the GenBank database under accession numbers MK559494–MK559496, MH560534–MH560563, MH560519–MH560526, MH560527–MH560533, and MH560564–MH560566, respectively.

AUTHOR CONTRIBUTIONS

L-XZ conceived and designed the research. M-FS, Z-HC, and MQ collected the samples. H-YW, J-FZ, S-MZ, J-QL, Y-CC, and MQ performed the experiments. D-FL, R-JW, F-CJ, R-PX, and C-SN analyzed the data. H-YW wrote the manuscript. All authors read and approved the final manuscript.

FUNDING

This study was supported, in part, by the National Natural Science Foundation of China (31802181), the Natural Science Foundation of Henan Province (162300410129), and the open fund of the Key Laboratory of Livestock Disease Prevention of Guangdong Province (YDWS1704).

ACKNOWLEDGMENTS

We thank Sandra Cheesman, Ph.D. from Liwen Bianji, Edanz Group China (www.liwenbianji.cn/ac), for editing the English text of a draft of this manuscript.

SUPPLEMENTARY MATERIAL

The Supplementary Material for this article can be found online at: https://www.frontiersin.org/articles/10.3389/fmicb.2019.01399/full#supplementary-material

REFERENCES

Buckholt, M. A., Lee, J. H., and Tzipori, S. (2002). Prevalence of *Enterocytozoon bieneusi* in swine: an 18-month survey at a slaughterhouse in Massachusetts. *Appl. Environ. Microbiol.* 68, 2595–2599. doi: 10.1128/AEM.68.5.2595-2599.2002

da Silva Fiuza, V. R., Lopes, C. W., de Oliveira, F. C., Fayer, R., and Santin, M. (2016). New findings of *Enterocytozoon bieneusi* in beef and dairy cattle in Brazil. *Vet. Parasitol.* 216, 46–51. doi: 10.1016/j.vetpar.2015.12.008

Del Coco, V. F., Cordoba, M. A., Bilbao, G., de Almeida Castro, P., Basualdo, J. A., and Santin, M. (2014). First report of *Enterocytozoon bieneusi* from dairy cattle in Argentina. *Vet. Parasitol.* 199, 112–115. doi: 10.1016/j.vetpar.2013.09.024

Didier, E. S., and Weiss, L. M. (2011). Microsporidiosis: not just in AIDS patients. *Curr. Opin. Infect. Dis.* 24, 490–495. doi: 10.1097/QCO.0b013e32834aa152

Fayer, R., Santín, M., and Trout, J. M. (2003). First detection of *microsporidia* in dairy calves in North America. *Parasitol. Res.* 90, 383–386. doi: 10.1007/s00436-003-0870-1

Fayer, R., Santin, M., and Trout, J. M. (2007). *Enterocytozoon bieneusi* in mature dairy cattle on farms in the eastern United States. *Parasitol. Res.* 102, 15–20. doi: 10.1007/s00436-007-0746-x

Feng, Y., Li, N., Dearen, T., Lobo, M. L., Matos, O., Cama, V., et al. (2011). Development of a multilocus sequence typing tool for high-resolution genotyping of *Enterocytozoon bieneusi*. *Appl. Environ. Microbiol.* 77, 4822–4828. doi: 10.1128/AEM.02803-10

Feng, Y., Ryan, U. M., and Xiao, L. (2018). Genetic diversity and population structure of *Cryptosporidium*. *Trends Parasitol.* 34, 997–1011. doi: 10.1016/j.pt.2018.07.009

Guo, Y., Roellig, D. M., Li, N., Tang, K., Frace, M., Ortega, Y., et al. (2016). Multilocus sequence typing tool for *Cyclospora cayetanensis*. *Emerg. Infect. Dis.* 22, 1464–1467. doi: 10.3201/eid2208.150696

Guo, Y. Q., Alderisio, K. A., Yang, W. L., Cama, V., Feng, Y. Y., and Xiao, L. H. (2014). Host specificity and source of *Enterocytozoon bieneusi* genotypes in a drinking source watershed. *Appl. Environ. Microbiol.* 80, 218–225. doi: 10.1128/AEM.02997-13

Hu, S., Liu, Z., Yan, F., Zhang, Z., Zhang, G., Zhang, L., et al. (2017). Zoonotic and host-adapted genotypes of *Cryptosporidium* spp., *Giardia duodenalis* and *Enterocytozoon bieneusi* in dairy cattle in Hebei and Tianjin, China. *Vet. Parasitol.* 248, 68–73. doi: 10.1016/j.vetpar.2017.10.024

Jiang, Y., Tao, W., Wan, Q., Li, Q., Yang, Y., Lin, Y., et al. (2015). Zoonotic and potentially host-adapted *Enterocytozoon bieneusi* genotypes in sheep and cattle in northeast China and an increasing concern about the zoonotic importance of previously considered ruminant-adapted genotypes. *Appl. Environ. Microbiol.* 81, 3326–3335. doi: 10.1128/AEM.00328-15

Juránková, J., Kamler, M., Kovařčí, K., and Koudela, B. (2013). *Enterocytozoon bieneusi* in bovine viral diarrhea virus (BVDV) infected and noninfected cattle herds. *Res. Vet. Sci.* 94, 100–104. doi: 10.1016/j.rvsc.2012.07.016

Karim, M. R., Wang, R., He, X., Zhang, L., Li, J., Rume, F. I., et al. (2014). Multilocus sequence typing of *Enterocytozoon bieneusi* in nonhuman primates in China. *Vet. Parasitol.* 200, 13–23. doi: 10.1016/j.vetpar.2013.12.004

Lee, S. C., Corradi, N., Byrnes, E. J. III, Torres-Martinez, S., Dietrich, F. S., Keeling, P. J., et al. (2008). *Microsporidia* evolved from ancestral sexual fungi. *Curr. Biol.* 18, 1675–1679. doi: 10.1016/j.cub.2008.09.030

Li, D., Zheng, S., Zhou, C., Karim, M. R., Wang, L., Wang, H., et al. (2019). Multilocus typing of *Enterocytozoon bieneusi* in pig reveals the high prevalence, zoonotic potential, host adaptation and geographical segregation in China. *J. Eukaryot. Microbiol.* doi: 10.1111/jeu.12715 [Epub ahead of print].

Li, J., Luo, N., Wang, C., Meng, Q., Cao, J., Cui, Z., et al. (2016). Occurrence, molecular characterization and predominant genotypes of *Enterocytozoon bieneusi* in dairy cattle in Henan and Ningxia, China. *Parasit. Vectors* 9:142. doi: 10.1186/s13071-016-1425-5

Li, N., Ayinmode, A. B., Zhang, H., Feng, Y., and Xiao, L. (2018). Host-adapted cryptosporidium and *Enterocytozoon bieneusi* genotypes in straw-colored fruit bats in Nigeria. *Int. J. Parasitol. Parasites Wildl.* 8, 19–24. doi: 10.1016/j.ijppaw.2018.12.001

Li, W., Cama, V., Akinbo, F. O., Ganguly, S., Kiulia, N. M., Zhang, X., et al. (2013). Multilocus sequence typing of *Enterocytozoon bieneusi*: lack of geographic segregation and existence of genetically isolated sub-populations. *Infect. Genet. Evol.* 14, 111–119. doi: 10.1016/j.meegid.2012.11.021

Li, W., Cama, V., Feng, Y., Gilman, R. H., Bern, C., Zhang, X., et al. (2012). Population genetic analysis of *Enterocytozoon bieneusi* in humans. *Int. J. Parasitol.* 42, 287–293. doi: 10.1016/j.ijpara.2012.01.003

Li, W., Song, Y., Zhong, Z., Huang, X., Wang, C., Li, C., et al. (2017). Population genetics of *Enterocytozoon bieneusi* in captive giant pandas of China. *Parasit. Vectors* 10:499. doi: 10.1186/s13071-017-2459-z

Li, W., Wan, Q., Yu, Q., Yang, Y., Tao, W., Jiang, Y., et al. (2016). Genetic variation of mini- and microsatellites and a clonal structure in *Enterocytozoon bieneusi* population in foxes and raccoon dogs and population differentiation of the parasite between fur animals and humans. *Parasitol. Res.* 115, 2899–2904. doi: 10.1007/s00436-016-5069-3

Li, W., and Xiao, L. (2019). Multilocus sequence typing and population genetic analysis of *Enterocytozoon bieneusi*: host specificity and its impacts on public health. *Front. Genet.* 10:307. doi: 10.3389/fgene.2019.00307

Ma, J., Li, P., Zhao, X., Xu, H., Wu, W., Wang, Y., et al. (2015). Occurrence and molecular characterization of *Cryptosporidium* spp. and *Enterocytozoon bieneusi* in dairy cattle, beef cattle and water buffaloes in China. *Vet. Parasitol.* 207, 220–227. doi: 10.1016/j.vetpar.2014.10.011

Mathis, A., Weber, R., and Deplazes, P. (2005). Zoonotic potential of the *microsporidia*. *Clin. Microbiol. Rev.* 18, 423–445. doi: 10.1128/cmr.18.3.423-445.2005

Matos, O., Lobo, M. L., and Xiao, L. (2012). Epidemiology of *Enterocytozoon bieneusi* infection in humans. *J. Parasitol. Res.* 2012:981424. doi: 10.1155/2012/981424

Pirestani, M., Sadraei, J., and Forouzandeh, M. (2013). Molecular characterization and genotyping of human related *microsporidia* in free-ranging and captive pigeons of Tehran, Iran. *Infect. Genet. Evol.* 20, 495–499. doi: 10.1016/j.meegid.2013.10.007

Qi, M., Jing, B., Jian, F., Wang, R., Zhang, S., Wang, H., et al. (2017). Dominance of *Enterocytozoon bieneusi* genotype J in dairy calves in Xinjiang, Northwest China. *Parasitol. Int.* 66, 960–963. doi: 10.1016/j.parint.2016.10.019

Qi, M., Luo, N., Wang, H., Yu, F., Wang, R., Huang, J., et al. (2015). Zoonotic *Cryptosporidium* spp. and Enterocytozoon bieneusi in pet chinchillas (Chinchilla lanigera) in China. *Parasitol. Int.* 64, 339–341. doi: 10.1016/j.parint.2015.05.007

Qi, M., Wang, R., Wang, H., Jian, F., Li, J., Zhao, J., et al. (2016). *Enterocytozoon bieneusi* genotypes in grazing horses in China and their zoonotic transmission potential. *J. Eukaryot. Microbiol.* 63, 591–597. doi: 10.1111/jeu.12308

Reetz, J., Rinder, H., Thomschke, A., Manke, H., Schwebs, M., and Bruderek, A. (2002). First detection of the *microsporidium Enterocytozoon bieneusi* in non-mammalian hosts (chickens). *Int. J. Parasitol.* 32, 785–787. doi: 10.1016/s0020-7519(02)00045-0

Sak, B., Brady, D., Pelikanova, M., Kvetonova, D., Rost, M., Kostka, M., et al. (2011). Unapparent microsporidial infection among immunocompetent humans in the Czech Republic. *J. Clin. Microbiol.* 49, 1064–1070. doi: 10.1128/JCM.01147-10

Santin, M., Dargatz, D., and Fayer, R. (2012). Prevalence and genotypes of *Enterocytozoon bieneusi* in weaned beef calves on cow-calf operations in the USA. *Parasitol. Res.* 110, 2033–2041. doi: 10.1007/s00436-011-2732-6

Santín, M., and Fayer, R. (2009a). A longitudinal study of *Enterocytozoon bieneusi* in dairy cattle. *Parasitol. Res.* 105, 141–144. doi: 10.1007/s00436-009-1374-4

Santín, M., and Fayer, R. (2009b). *Enterocytozoon bieneusi* genotype nomenclature based on the internal transcribed spacer sequence: a consensus. *J. Eukaryot. Microbiol.* 56, 34–38. doi: 10.1111/j.1550-7408.2008.00380.x

Santín, M., and Fayer, R. (2011). Microsporidiosis: *Enterocytozoon bieneusi* in domesticated and wild animals. *Res. Vet. Sci.* 90, 363–371. doi: 10.1016/j.rvsc.2010.07.014

Santín, M., and Fayer, R. (2015). *Enterocytozoon bieneus i, giardia*, and *Cryptosporidium* infecting white-tailed deer. *J. Eukaryot. Microbiol.* 62, 34–43. doi: 10.1111/jeu.12155

Sulaiman, I. M., Fayer, R., Yang, C., Santin, M., Matos, O., and Xiao, L. (2004). Molecular characterization of *Enterocytozoon bieneusi* in cattle indicates that only some isolates have zoonotic potential. *Parasitol. Res.* 92, 328–334. doi: 10.1007/s00436-003-1049-5

Tang, C., Cai, M., Wang, L., Guo, Y., Li, N., Feng, Y., et al. (2018). Genetic diversity within dominant *Enterocytozoon bieneusi* genotypes in pre-weaned calves. *Parasit. Vectors* 11:170. doi: 10.1186/s13071-018-2768-x

Tanriverdi, S., Markovics, A., Arslan, M. O., Itik, A., Shkap, V., and Widmer, G. (2006). Emergence of distinct genotypes of *Cryptosporidium parvum* in structured host populations. *Appl. Environ. Microbiol.* 72, 2507–2513. doi: 10.1128/AEM.72.4.2507-2513.2006

Wan, Q., Xiao, L., Zhang, X., Li, Y., Lu, Y., Song, M., et al. (2016). Clonal evolution of *Enterocytozoon bieneusi* populations in swine and genetic differentiation in subpopulations between isolates from swine and humans. *PLoS Negl. Trop. Dis.* 10:e0004966. doi: 10.1371/journal.pntd.0004966

Wang, L., Xiao, L., Duan, L., Ye, J., Guo, Y., Guo, M., et al. (2013). Concurrent infections of *Giardia duodenalis*, *Enterocytozoon bieneusi*, and *Clostridium* difficile in children during a cryptosporidiosis outbreak in a pediatric hospital in China. *PLoS Negl. Trop. Dis.* 7:e2437. doi: 10.1371/journal.pntd.0002437

Wang, X. T., Wang, R. J., Ren, G. J., Yu, Z. Q., Zhang, L. X., Zhang, S. Y., et al. (2016). Multilocus genotyping of *Giardia duodenalis* and *Enterocytozoon bieneusi* in dairy and native beef (Qinchuan) calves in Shaanxi province,

northwestern China. *Parasitol. Res.* 115, 1355–1361. doi: 10.1007/s00436-016-4908-6

Widmer, G., and Akiyoshi, D. E. (2010). Host-specific segregation of ribosomal nucleotide sequence diversity in the microsporidian *Enterocytozoon bieneusi*. *Infect. Genet. Evol.* 10, 122–128. doi: 10.1016/j.meegid.2009.11.009

Zhang, Q., Cai, J., Li, P., Wang, L., Guo, Y., Li, C., et al. (2018). *Enterocytozoon bieneusi* genotypes in Tibetan sheep and yaks. *Parasitol. Res.* 117, 721–727. doi: 10.1007/s00436-017-5742-1

Zhang, X., Wang, Z., Su, Y., Liang, X., Sun, X., Peng, S., et al. (2011). Identification and genotyping of *Enterocytozoon bieneusi* in China. *J. Clin. Microbiol.* 49, 2006–2008. doi: 10.1128/JCM.00372-11

Zhao, W., Zhang, W., Wang, R., Liu, W., Liu, A., Yang, D., et al. (2014). Enterocytozoon bieneusi in sika deer (Cervus nippon) and red deer (*Cervus elaphus*): deer specificity and zoonotic potential of ITS genotypes. *Parasitol. Res.* 113, 4243–4250. doi: 10.1007/s00436-014-4100-9

Zhao, W., Zhang, W., Yang, F., Zhang, L., Wang, R., Cao, J., et al. (2015). *Enterocytozoon bieneusi* in dairy cattle in the northeast of China: genetic diversity of ITS gene and evaluation of zoonotic transmission potential. *J. Eukaryot. Microbiol.* 62, 553–560. doi: 10.1111/jeu.12210

Conflict of Interest Statement: The authors declare that the research was conducted in the absence of any commercial or financial relationships that could be construed as a potential conflict of interest.

frontiers in Microbiology

ORIGINAL RESEARCH
published: 05 July 2019
doi: 10.3389/fmicb.2019.01522

Niflumic Acid Reverses Airway Mucus Excess and Improves Survival in the Rat Model of Steroid-Induced *Pneumocystis* Pneumonia

*Francisco J. Pérez, Pablo A. Iturra, Carolina A. Ponce, Fabien Magne, Víctor Garcia-Angulo and Sergio L. Vargas**

Programa de Microbiología y Micología, Instituto de Ciencias Biomédicas (ICBM), Facultad de Medicina, Universidad de Chile, Santiago, Chile

Although the role of adaptive immunity in fighting *Pneumocystis* infection is well known, the role of the innate, airway epithelium, responses remains largely unexplored. The concerted interaction of innate and adaptive responses is essential to successfully eradicate infection. Increased expression of goblet-cell-derived CLCA1 protein plus excess mucus in infant autopsy lungs and in murine models of primary *Pneumocystis* infection alert of innate immune system immunopathology associated to *Pneumocystis* infection. Nonetheless, whether blocking mucus-associated innate immune pathways decreases *Pneumocystis*-related immunopathology is unknown. Furthermore, current treatment of *Pneumocystis* pneumonia (PcP) relying on anti-*Pneumocystis* drugs plus steroids is not ideal because removes cellular immune responses against the fungal pathogen. In this study, we used the steroid-induced rat model of PcP to evaluate inflammation and mucus progression, and tested the effect of niflumic acid (NFA), a fenamate-type drug with potent CLCA1 blocker activity, in decreasing *Pneumocystis*-associated immunopathology. In this model, animals acquire *Pneumocystis* spontaneously and pneumonia develops owing to the steroids-induced immunodeficiency. Steroids led to decreased animal weight evidencing severe immunosuppression and to significant *Pneumocystis*-associated pulmonary edema as evidenced by wet-to-dry lung ratios that doubled those of uninfected animals. Inflammatory cuffing infiltrates were noticed first around lung blood vessels followed by bronchi, and both increased progressively. Similarly, airway epithelial and lumen mucus progressively increased. This occurred in parallel to increasing levels of MUC5AC and mCLCA3, the murine homolog of hCLCA1. Administration of NFA caused a significant decrease in total mucus, MUC5AC and mCLCA3 and also, in *Pneumocystis*-associated inflammation. Most relevant, NFA treatment improved survival at 8 weeks of steroids. Results suggest an important role of innate immune responses in immunopathology of steroid-induced PcP. They warrant evaluation of CLCA1 blockers as adjunctive therapy in this condition and describe a simple model to evaluate therapeutic interventions for steroid resistant mucus, a common condition in patients with chronic lung disease like asthma, chronic obstructive pulmonary disease (COPD) and cystic fibrosis.

Keywords: *Pneumocystis* pneumonia, steroid-resistant-mucus, animal model, mucus, Innate Immunity, CLCA1, MUC5AC, niflumic acid

OPEN ACCESS

Edited by:
Olga Matos,
New University of Lisbon, Portugal

Reviewed by:
Gee W. Lau,
University of Illinois at Urbana-Champaign, United States
Rodrigo Tinoco Figueiredo,
Federal University of Rio de Janeiro, Brazil

****Correspondence:***
Sergio L. Vargas
svargas@med.uchile.cl;
svargas.uchile@gmail.com

Specialty section:
This article was submitted to Infectious Diseases, a section of the journal Frontiers in Microbiology

Received: *16 May 2019*
Accepted: *18 June 2019*
Published: *05 July 2019*

Citation:
Pérez FJ, Iturra PA, Ponce CA, Magne F, Garcia-Angulo V and Vargas SL (2019) Niflumic Acid Reverses Airway Mucus Excess and Improves Survival in the Rat Model of Steroid-Induced Pneumocystis Pneumonia. Front. Microbiol. 10:1522. doi: 10.3389/fmicb.2019.01522

INTRODUCTION

Progression of a mild fungal infection by *Pneumocystis* to the life-threatening *Pneumocystis* pneumonia (PcP) occurs in immunocompromised hosts largely because T-cell defects halt the coordinated action of the innate and adaptive immune systems required to clear infections (Iwasaki and Medzhitov, 2015). Research attention has mainly focused on the adaptive response. However, airway mucus is an essential component of the innate immune defense mechanisms of the lung and finely regulated mucus levels are critical for effective airway mucociliary clearance and lung health (Fahy and Dickey, 2010; Perez B.F. et al., 2014; Ha and Rogers, 2016).

Recent reports describe increased production of mucus and of specific MUC5AC and MUC5B mucus proteins during *Pneumocystis* primary infection in infants (Vargas et al., 2013; Perez F. J. et al., 2014; Rojas et al., 2019) and in immunocompetent rodent models (Meissner et al., 2005; Hernandez-Novoa et al., 2008; Vargas et al., 2013; Eddens et al., 2016; Rojas et al., 2019). Importantly, mucus excess as a pathologic feature in PcP remains unexplored. "Hydropically swollen muco-proteins" were histochemically identified by H. S. Baar in 1955 within the amorphous foamy material or acellular eosinophilic exudate characteristic of PcP thus emphasizing the increased fluid accumulation aspect of PcP related pathology (Baar, 1955). Characterization of the role of mucus in PcP is therefore a priority as excess airway mucus indicates inflammation, may limit airflow, impair mucociliary clearance and favor mucostasis, airway collapse and the development of mucus plugging which may therefore, contribute to the respiratory failure in PcP (Fahy and Dickey, 2010; Ha and Rogers, 2016; Perez B.F. et al., 2014; Ma et al., 2018).

Unfortunately, there is not an effective treatment for mucus hypersecretion. The options are few (Ha and Rogers, 2016), and they have limited efficacy in part explained by the multiple inflammatory pathways, inflammatory mediators and cytokines that drive mucus production (Hauber and Zabel, 2008; Ha and Rogers, 2016). Even corticosteroids, the best anti-inflammatory drug available, have low efficacy in PcP (Wieruszewski et al., 2018) and are unable to suppress goblet cell hyperplasia (Kibe et al., 2003; Nakano et al., 2006), emphasizing the need to investigate the mechanistic insights of excess mucus production associated to this fungal infection. Relevant to this research, steroids are strong inducers of PcP in cancer and other diseases in a dose dependent manner (Park et al., 2018). The capacity of steroids to induce PcP has been utilized for decades to model PcP in animals for *Pneumocystis* research. PcP develops in nearly 100% of the animals after administration of glucocorticoids during a period of 8 to 10 weeks (Hughes et al., 1994). The more accepted explanation for this effect is that systemic use of corticosteroids leads to profound cell-mediated immunosuppression encompassing apoptosis of immune cells including CD4+, CD8+, and other T cell lymphocyte subsets (Walzer et al., 1984; Barnes, 2016). This blunting of the adaptive immune responses halts the clearance of the infection (Iwasaki and Medzhitov, 2015) and therefore, allows a growing fungal burden of *Pneumocystis* in the lungs (Screpanti et al., 1989; Adcock and Mumby, 2017; Hu et al., 2017; Rong et al., 2018) that keeps stimulating the airway epithelium (Screpanti et al., 1989; Swain et al., 2012; Eddens et al., 2016; Adcock and Mumby, 2017; Iturra et al., 2018). Collectively, available data suggest that *Pneumocystis* infection overcomes the anti-inflammatory effects of corticosteroids and induces a steroid-resistant mucus phenotype in this model.

Host recognition of *Pneumocystis* and triggering of immune responses is an area of intense research (Hoving and Kolls, 2017; Hoving, 2018; Hauser, 2019). The cyst (ascus) and trofozoite (nuclei) forms exhibit different antigens and both display differing strategies to evade host recognition (Hoving and Kolls, 2017; Hoving, 2018; Hauser, 2019). It is well described that β-glucans present in the thick *Pneumocystis* cyst wall are recognized by host pattern-recognition receptors such as Dectin-1 and Mincle located in macrophages and by HSPA5 in the airway epithelium thereby activating airway innate immune responses (Krajicek et al., 2009; Ricks et al., 2013; Hoving and Kolls, 2017; Hoving, 2018; Kottom et al., 2018; Hauser, 2019). *Pneumocystis*-mediated overexpression of the goblet-cell-derived calcium-activated chloride channel (CLCA) regulator CLCA1, also known as Gob5 or mCLCA3 (the murine homolog), was first suggested by Kovacs et al. using microarray technology (Hernandez-Novoa et al., 2008), and more recently confirmed by us and others (Swain et al., 2012; Perez F. J. et al., 2014; Iturra et al., 2018). CLCA1 is a secreted signaling protein that regulates airway target cells in healthy and disease conditions with a role in the development of mucous metaplasia and increased airway mucus production (Patel et al., 2009; Sala-Rabanal et al., 2015). Consensus STAT6-binding sites have been identified in the mClca3 and human Clca1 gene regulatory regions suggesting that it directly mediates responsiveness to IL-13 stimulation (Patel et al., 2009). *Pneumocystis* elicits a STAT6 innate immune response that can result in airway hyperresponsiveness (Swain et al., 2012). The emerging evidence of excess mucus and goblet cell metaplasia associated to CLCA1 pathway activation by *Pneumocystis* with upregulation of MUC5AC and MUC5B mucin expression suggests that this fungus induces strong stimuli of mucus related host airway responses whose role in immunopathology warrants characterization (Patel et al., 2009; Swain et al., 2012; Perez F. J. et al., 2014; Iturra et al., 2018).

We hypothesized that the persistent stimulation of CLCA1 mediated immune responses in the airway epithelium by *Pneumocystis* leads to mucus related immunopathology, and selected the classic steroid-induced rat model of PcP to characterize the histological progression of mucus and to further do a case control experiment blocking CLCA1 to evaluate the role of this protein in this immunopathology. We selected this rat model because resembles the circulation of *Pneumocystis* in the human community where the infection is unnoticeably acquired in a non-closed environment, and furthermore, because the progression of *Pneumocystis* infection to PcP is highly host-dependent, determined by host factors, like apoptosis of T-cell CD4 counts, that in this model are induced by administration of high-dose steroids (Walzer et al., 1984; Sukura et al., 1995).

More importantly, steroids represent the most relevant risk factor for development of PcP in non-HIV-infected population (Park et al., 2018; Wieruszewski et al., 2018). In addition, we selected niflumic acid (NFA), a non-steroidal anti-inflammatory drug, because NFA has a potent, although not completely specific, blocker activity over the CLCA family of proteins (Famaey, 1997; Parai and Tabrizchi, 2002; Zhou et al., 2002; Ledoux et al., 2005; Nakano et al., 2006; Fukuyama et al., 2009). Of relevance, it is well documented that NFA inhibits goblet cell hyperplasia, mucus overproduction and airway hyperresponsiveness in mice as well as in human bronchial epithelial cells, through the reduction of hCLCA1 and MUC5AC expression (Hauber et al., 2005; Nakano et al., 2006; Yasuo et al., 2006; Hegab et al., 2007; Kim et al., 2007; Fukuyama et al., 2009). Documenting an effect of NFA in decreasing steroid resistant *Pneumocystis*-related immunopathology would lead to evaluate anti-CLCA1 related drugs as novel adjuvant treatments for PcP.

MATERIALS AND METHODS

Ethics Statement

Ethical approval was obtained from the Institutional Animal Welfare Ethics Committee of the University of Chile School of Medicine (Santiago, Chile) under protocol number CBA0634. Animal experiments were conducted in accordance to the Animal Protection Law of Chile (Law 20.380) and following international directions of the Guide for the Care and Use of Laboratory Animals (Eighth Edition, National Academies Press, Washington, DC).

Animal Model of Steroid-Induced *Pneumocystis* Pneumonia

Sprague Dawley juvenile female rats (180–200 g body weight) from a single colony were used in each experiment. They were housed in a standard animal room to let them acquire *Pneumocystis* from the air and given oxytetracycline (0.4 mg/mL) in the drinking water starting 3 weeks prior to the start of immunosuppression and maintained throughout the experiment to eliminate eventual respiratory bacterial pathogens, specially *Mycoplasma pulmonis* (Banerjee et al., 1987). PcP was induced using high dose betamethasone (3 mg/L). This experimental scheme is highly effective in inducing PcP and cysts can be detected after 2 weeks of immunosuppression (Hughes et al., 1974). Two animals per experimental group were sacrificed at the end of week two to confirm *Pneumocystis* in lungs by microscopy using Grocott-Gomori methenamine silver stain before the animals were moved a high-efficiency particulate-filtered air environment (One Cage 2100, Lab Products Inc.) to prevent acquisition of new infections. Corticosteroids were given for a total of 8 weeks. A control group of rats given anti-*Pneumocystis* prophylaxis with trimethoprim (50 mg/Kg) sulfamethoxazole (250 mg/Kg) (TMP-SMZ) (Hughes et al., 1974) *ad libitum* in the drinking water was used for comparison to characterize the progression of mucus, inflammation and lung edema (**Figure 1A**). The individual weight of the animals was recorded weekly.

Niflumic Acid Administration

The effect of NFA was evaluated in animals with steroid-induced PcP. Animals were randomized to receive NFA or vehicle (placebo). The NFA dose used was 6 mg/Kg/day, 7 days/week, starting at week 4 of steroid administration. NFA (Sigma-Aldrich) was dissolved daily in 0.4 M $NaHCO_3$ in 5% glucose, adjusted to pH 7.5, passed through 0.22 μm filters and administered via the intraperitoneal (IP) route. Control animals received equivalent volumes of filtered 0.4 M NaHCO3 in 5% glucose pH 7.5 alone as vehicle/placebo (**Figure 1B**). The dose of NFA was chosen based on previous reports of *in vivo* experiments (Parai and Tabrizchi, 2002; Nakano et al., 2006; Hegab et al., 2007) and confirmed after in-house safety evaluations. Liver toxicity of 3 and 12 mg/kg/day dose was evaluated by measuring liver function tests in serum samples of 5 healthy rats per dose IP and of control rats receiving vehicle alone, daily, for 28 days prior to the start of experiments (**Supplementary Figure S1**).

Lung Samples

Eight rats and their respective controls given TMP-SMZ were subject to the experimental scheme depicted in **Figure 1A** and let to develop PcP to evaluate body weight progression during steroid-induced immunosuppression, pulmonary edema, and survival at 8 weeks. Rats were sacrificed by exsanguination under deep anesthesia with ketamine (100 mg/kg) and xylazine (10 mg/kg), their lungs were extracted immediately, weighed, and put in an oven at 85°C during 24 h to determine the wet-to dry lung weight ratio as a measure of PcP-associated pulmonary edema. In subsequent experiments eight animals per group were sacrificed at 4, 6, and 8 weeks of immunosuppression under deep anesthesia as described above. Half of them were exsanguinated, their lungs removed, and their upper right lung lobes immediately separated, cut and stored at −20°C until protein extraction. Lungs in the other half were fixed using *in situ* vascular-perfusion as previously reported (Iturra et al., 2018). Briefly, 3.7% PBS-buffered formalin (pH 7.2) was perfused via the inferior cava vein at a pressure of 25 cm H_2O. Perfused lungs were maintained inside the thorax for 12 h at room temperature and then were extracted and immersed in buffered formalin for additional 12 h. The upper right lung lobe was dissected, and paraffin-embedded for histology sections.

Pneumocystis Diagnosis, Histologic, and Morphometric Assessments

Longitudinal 5 μm-thick lung tissue sections were observed using an OLYMPUS BX60 microscope connected to a QImaging MicroPublisher 3.3 RTV camera (QImaging). Morphometry assessments were performed by observers that were unaware of the experimental group using the Image-Pro Plus software version 5.1 (Media Cybernetics, Inc.). *Pneumocystis* was examined in lung imprints using Grocott-Gomori methenamine silver stain and pneumonia confirmed by Hematoxylin and Eosin (H&E) stain (Hughes et al., 1974). Peribronchial and perivascular inflammation was evaluated in lung sections stained with H&E stain measuring cellular cuffs around <300 μm bronchioles and its associated blood vessels using a modified

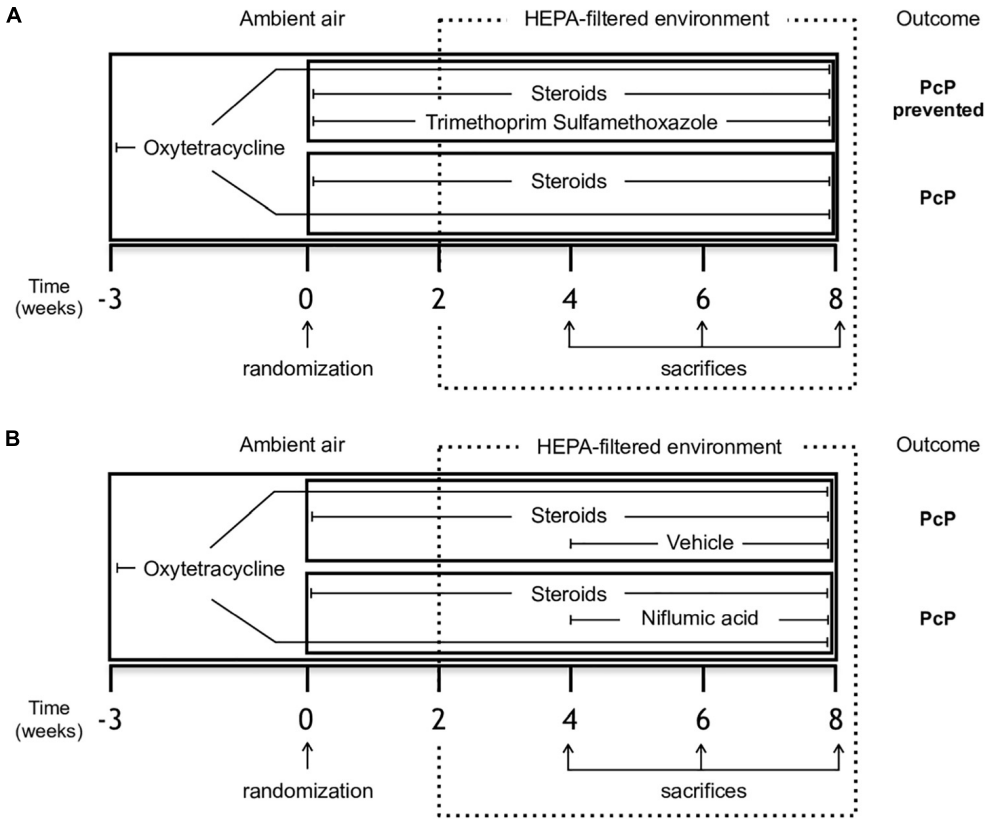

FIGURE 1 | Study design. Female Sprague-Dawley rats from a single colony were treated with oxytetracycline starting 3 weeks before immunosuppressive regimen and kept throughout the experiment in both groups to prevent bacterial infections. **(A)** Experiment 1 - Rats were randomized to receive either steroids (*Pneumocystis*-infected group) or steroids plus anti-*Pneumocystis* prophylaxis consisting of trimethoprim/sulfamethoxazole (controls) for 8 weeks. **(B)** Experiment 2 - Rats receiving steroids and oxytetracycline were randomized at week 4 to continue with steroids plus NFA treatment (6 mg/Kg/day) or to steroids plus the vehicle solution without NFA (control group) for additional 4 weeks. Eight rats per group were sacrificed on weeks 4, 6, and 8 of immunosuppression. At each time point, four rats per group underwent vascular perfusion of lungs *in situ* using buffered formalin to preserve lung architecture for histological analysis. Lungs from the other four rats per group were fresh-extracted for use in molecular determinations. HEPA: High-Efficiency Particulate Air; NFA: Niflumic acid (6 mg/Kg/day); Pc (–): uninfected control group; Pc (+): *Pneumocystis*- infected group.

semiquantitative scoring system as described (Iturra et al., 2018). Briefly, 0 indicates no surrounding cuffs seen; 1: cuffs in <25% of bronchioles or vessels; 2: cuffs in 25% to 50% of bronchioles or vessels; and 3: cuffs in >50% of bronchioles or vessels. Mucus was assessed in lung sections stained with Alcian blue/periodic acid-Schiff (AB/PAS) stain and evaluated for the presence of mucin glycoconjugates in the epithelium and in the lumen. The AB/PAS-positive epithelium area and the percentage of lumen area occupied by mucus were quantified separately. Morphometry measurements were done in five randomly selected <300 μm bronchioles per animal in all four rats per group/time point (using a random table). *Pneumocystis* DNA was studied at the end of the experiment 2 (week 8) in all animals that received steroids or steroids plus NFA, using DNA amplification as described (Vargas et al., 1995).

Western Blotting

A 300 mg aliquot of lung tissue were disrupted with Tissue Tearor (BioSpec Products Inc.) in chilled modified RIPA buffer (50 mM Tris–HCl pH 7.4; 150 mM NaCl; 1 mM EDTA; 1% NP-40; 0.5% sodium deoxicolate; 1 mM PMSF; 1 μg/ml of each Aprotinin, Leupeptin, and Pepstatin). Total protein was quantified in supernatants using the Bradford assay (BIO-RAD). 30 μg protein samples were subjected to SDS-PAGE with 4% stacking and 8% resolving Tris-Glycine gels. Proteins were transferred to polyvinylidene difluoride membranes and blocked with 5% low-fat milk. Mouse anti-MUC5AC IgG antibody (1:500, 45M1, Santa Cruz Biotechnology) and Goat anti-mouse IgG-HRP antibody (1:2000, Santa Cruz Biotechnology) were used to detect MUC5AC. Rabbit anti-CLCA3 IgG antibody (1:200, Santa Cruz Biotechnology) and Chicken anti-rabbit IgG-HRP antibody (1:2000, Santa Cruz Biotechnology) were used to detect mCLCA3. Membranes were stripped, blocked and reprobed for Actin detection using a Goat anti-Actin IgG (1:500, Santa Cruz Biotechnology) and a Donkey anti-goat IgG-HRP (1:2000, Santa Cruz Biotechnology) antibodies. Enhanced chemiluminescence reagent was used for membrane development (Pierce ECL) with X-ray films (CL-XPosure, Thermo Fisher Scientific). Films were analyzed using ImageJ software (NIH, United States).

Data Analyses and Statistics

Data was expressed as mean ± SD. Groups were compared using one-way ANOVA with Tukey *post hoc* test. When two factors were evaluated a two-way ANOVA with Bonferroni *post hoc* test was performed. Survival analysis was performed using the Kaplan-Meier estimator and survival distributions were compared using the Mantel-Cox test. In all data analysis values of $p < 0.05$ were considered significant. Statistical analysis was performed using Prism 5.0 software (GraphPad Software, Inc.).

RESULTS

Steroid Induced PcP Model

Effect of Steroids in Weight, *Pneumocystis*, Lung Edema, and Survival

We evaluated body weight changes, lung fluid accumulation and survival in the steroid-induced PcP model rats as per "A" experimental scheme (**Figure 1**). Animals receiving steroids steadily lost body weight regardless of anti-*Pneumocystis* prophylaxis while control rats without steroids progressively gained body weight (**Figure 2A**). This group of rats was sacrificed at the eighth week of immunosuppression and *Pneumocystis* cysts were detected in lung imprints of all animals receiving steroids and not detected in those receiving TMP-SMZ or in the healthy controls (**Figure 2B**). Increased weight of the wet portion of the lung was detected in the *Pneumocystis*-infected animals. The wet-to-dry lung ratio, a measure of lung edema, increased in the *Pneumocystis* infected animals with respect to healthy controls and to rats receiving anti-*Pneumocystis* prophylaxis (**Figure 2C**). No differences in the dry lung weight were detected across all groups (data not shown). Survival of rats with PcP rounded 60% at week eighth of steroid administration and TMP-SMZ was 100% efficient in preventing *Pneumocystis* and associated mortality (**Figure 2D**).

Steroid-Induced PcP Promotes Perivascular and Peribronchial "Cuffing" Inflammation and Excess in Total Mucus With Increased MUC5AC and mCLCA3 Mucus Markers

Pneumocystis Induces Progressive Increase in Peribronchial and Perivascular Inflammatory Cuffs

Inflammatory response as assessed in H&E-stained lung sections at 4, 6, and 8 weeks of steroid administration documented a progressive increase in *Pneumocystis*-associated inflammatory cuffs surrounding blood vessels and bronchioles

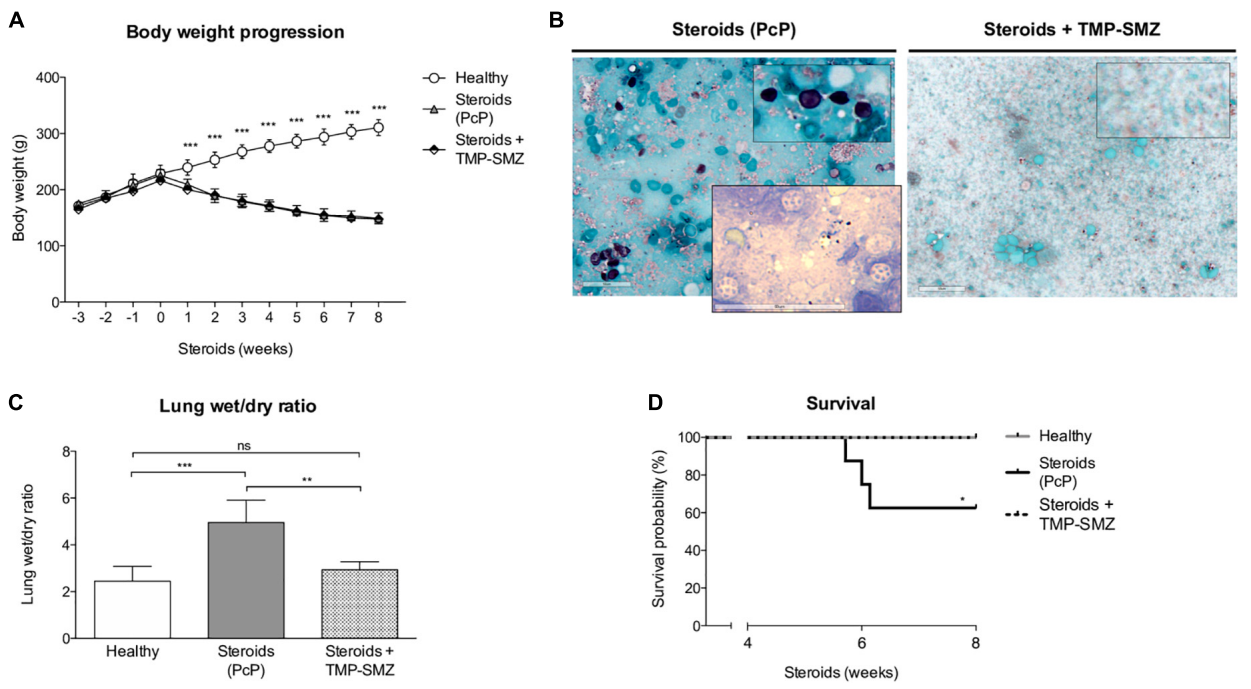

FIGURE 2 | Effect of steroids on body weight, *Pneumocystis* infection, pulmonary edema, and PcP-associated survival. **(A)** Progression of body weight in animals receiving steroids with and without anti-*Pneumocystis* prophylaxis and in healthy controls. **(B)** Grocott-Gomori silver methenamine stain of *Pneumocystis* cysts in lung imprints of rats after 8 weeks of receiving steroids alone versus steroids plus anti-*Pneumocystis* prophylaxis with trimethoprim sulfamethoxazole. Insert documenting nuclei forms of *Pneumocystis* using Giemsa stain in rats without prophylaxis. Scale bar = 50 μm. **(C)** Pulmonary fluid accumulation determined by the wet / dry lung weight ratios at 8 weeks of steroids administration. **(D)** Kaplan–Meier survival plots at the eighth week of immunosuppression of rats healthy rats, with PcP, and rats receiving PcP prophylaxis. PcP: *Pneumocystis* pneumonia; TMP-SMZ: Trimethoprim Sulfamethoxazole. **(A,C)** Data are expressed as mean ± SD; **(A)** $n = 8$; ANOVA test: $^{***}P < 0.001$; **(C)** $n = 5$; ANOVA test: ^{ns}no significant; $^{**}P < 0.01$; $^{***}P < 0.001$. **(D)** $n = 8$; Mantel-Cox test: $^{*}P < 0.05$. Dataset for this figure available in **Supplementary Data Sheet S1**.

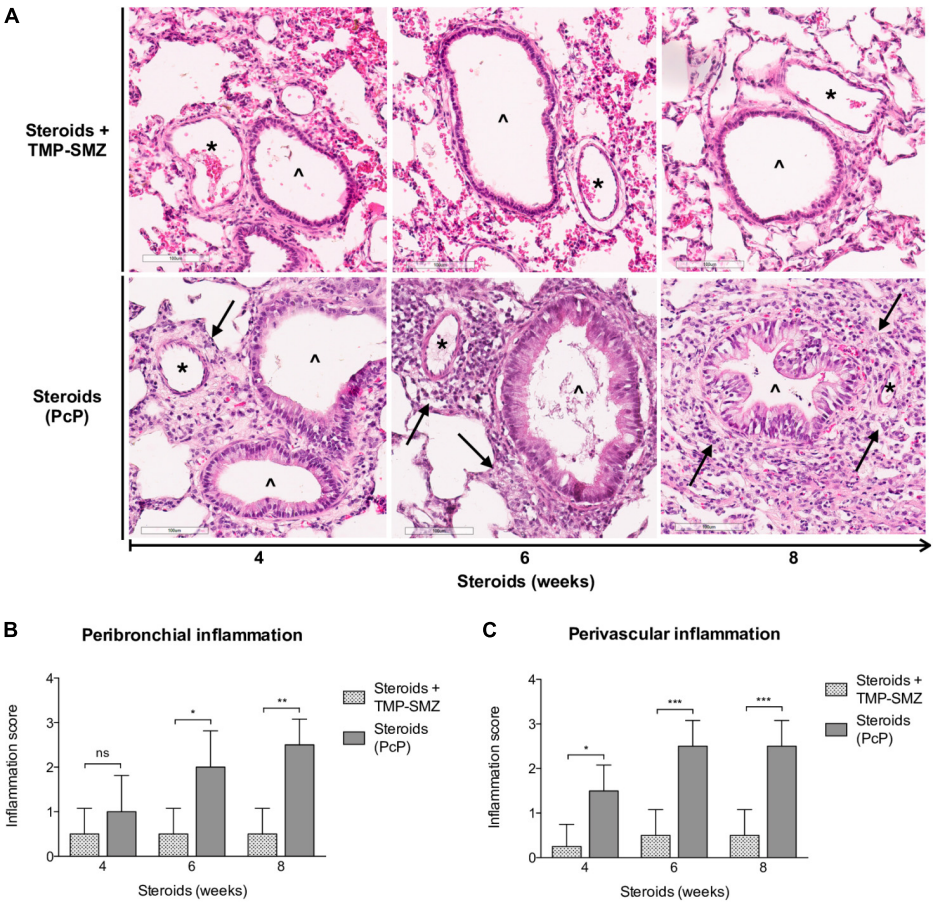

FIGURE 3 | Sequential inflammatory changes in rats on steroids receiving and not-receiving anti-*Pneumocystis* prophylaxis. **(A)** Representative microscopic images of H&E-stained lung sections at 4, 6, and 8 weeks of immunosuppression. Blood vessels (*); bronchioles (^); PcP: *Pneumocystis* pneumonia; TMP-SMZ: Trimethoprim Sulfamethoxazole. H&E stain, Scale bar = 100 μm. **(B,C)** Proportion of bronchioles and blood vessels surrounded by inflammatory cuffs infiltrates classified using a semiquantitative score (see Section "Materials and Methods"). Data are expressed as mean ± SD; $n = 4$; ANOVA test: ^{ns}no significant; $^{*}P < 0.05$; $^{**}P < 0.01$; $^{***}P < 0.001$. Dataset for this figure available in **Supplementary Data Sheet S1**.

(**Figure 3A** arrows). Semiquantitative score measurements showed that cellular cuff infiltrates appeared significantly earlier around blood vessels than around bronchioles (4 versus 6 weeks of immunosuppression). Control animals receiving TMP-SMZ prophylaxis did not develop significant inflammation (**Figures 3B,C**).

Pneumocystis Induces Progressive Increase of Total Mucus Production

Progressive overproduction of mucus associated to *Pneumocystis* was documented by histology morphometry quantification of AB/PAS-stained area at 4, 6, and 8 weeks in rat lung sections of steroid-receiving rats (**Figures 4A,B**). Increase in intracellular mucin granules was also detected in the respiratory epithelium (**Figure 4A**, arrowheads). AB/PAS stained cells were absent to rare in control animals receiving TMP-SMZ at every measured time point (**Figures 4A,B**). Mucus plugs occupying the airway lumen increased in association to *Pneumocystis* with significant differences at 8 weeks of immunosuppression (**Figures 4A** arrows, **4C**).

Pneumocystis Induces Progressive Increase in MUC5AC and mCLCA3 Protein Expression

A significant increase in MUC5AC (**Figures 5A,C**) and mCLCA3 (**Figures 5B,D**) expression was noticed at 6 and 4 weeks of steroid administration, respectively. Control animals showed no MUC5AC or mCLCA3 expression changes.

Taken together, the findings in rats with steroid-induced PcP indicate that *Pneumocystis* induces progressive inflammation, and mucus overproduction with increased expression of MUC5AC and mCLCA3.

Niflumic Acid Is Well-Tolerated and Reverses Inflammation, Mucus Excess and Improves Survival in the Steroid-Induced PcP Model

Safety and Tolerance of Niflumic Acid

The safety of 3 and 12 mg/Kg/day NFA administered daily for 28 days intraperitoneally was evaluated in healthy rats prior to efficacy evaluations in PcP. Animals receiving NFA

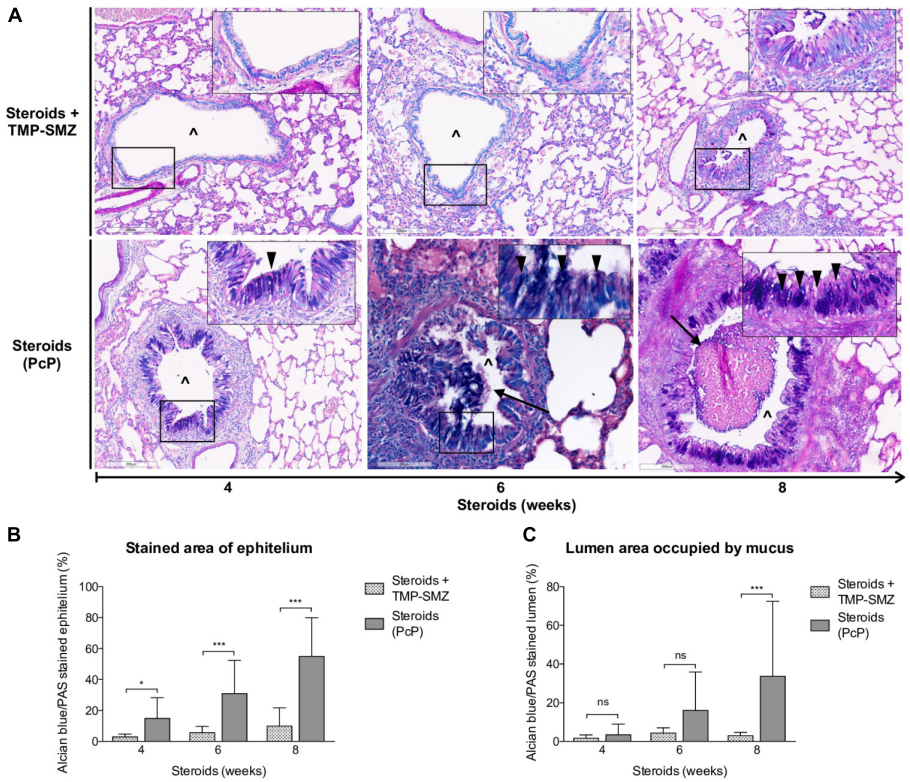

FIGURE 4 | Sequential changes in mucus in rats on steroids receiving and not-receiving anti-*Pneumocystis* prophylaxis. **(A)** Representative microscopic images of AB/PAS-stained lung sections at 4, 6, and 8 weeks of immunosuppression. Intracellular mucin granules (arrowheads); Mucus plugs (arrows); PcP: *Pneumocystis* pneumonia; TMP-SMZ: Trimethoprim Sulfamethoxazole; (^): Bronchiolar lumen. AB/PAS stain, Scale bar = 200 μm. **(B,C)** Percent of AB/PAS stained epithelium **(B)** and lumen **(C)**. Data are expressed as mean ± SD; $n = 4$; ANOVA test: ^{ns}no significant; $^{*}P < 0.05$; $^{***}P < 0.001$. Dataset for this figure available in **Supplementary Data Sheet S1**.

as well as the control rats receiving vehicle alone increased in body weight (**Supplementary Figure S1A**). Urea blood levels showed a dose-dependent increase in NFA-treated animals (**Supplementary Figure S1B**) and alkaline phosphatases increased in NFA 3 mg/Kg/day-treated animals compared to control rats (**Supplementary Figure S1C**). Liver (Total and conjugated bilirubin, AST, ALT, and GGT) and renal (creatinine) function tests were within reference ranges for Sprague-Dawley rats in all the animals. These findings indicate that intraperitoneal administration of NFA at these doses is safe and well tolerated by the animals.

NFA Administration Decreases Inflammation and Mucus Overproduction in Rats With Steroid Induced PcP

Next, steroids were administered to two groups of rats, with one group receiving NFA and the other receiving vehicle alone. *Pneumocystis* cysts were detected in lung imprints of all rats, regardless of whether they received NFA or vehicle (controls). In addition, *Pneumocystis* spp.-DNA was detected in all rats receiving steroids alone or steroids plus NFA (**Supplementary Figure S2**). Of relevance, treatment with NFA slowed the progression of cellular cuffing infiltrates around blood vessels (*) and bronchioles (^) regardless of the presence of Pneumocystis (**Figure 6A** arrows) and this decrease in progression reached significance respect to vehicle at the eighth week of steroid administration, corresponding to 4 weeks of continuous NFA treatment (**Figures 6B,C**). Animals that receive vehicle alone showed progressive inflammation. Furthermore, NFA stopped and reverted mucus overproduction as evidenced by a significant decrease of AB/PAS-stained area (**Figures 7A,B**), a reduction of intracellular mucin granules in the epithelia (**Figure 7A** arrowheads) and a depletion of mucous plugs in airway lumen (**Figures 7A** arrows, **7C**). The reduction in mucus production became significant after 2 weeks of NFA continuous administration (6 weeks of steroids) (**Figures 7B,C**). Rats that received placebo (steroids + vehicle) showed progressive mucus overproduction. Moreover, the continuous administration of NFA suppressed the increased expression of both MUC5AC (**Figures 8A,C**) and mCLCA3 (**Figures 8B,D**) starting from 2 weeks of NFA treatment.

Niflumic Acid Increases Survival in Animals With Steroid-Induced PcP

Survival plots were determined for animals that received steroids versus animals that received steroids + TMP-SMZ (Experiment 1 - **Figure 1A**), and for animals receiving steroids versus steroids + NFA (Experiment 2 - **Figure 1B**). Prevention

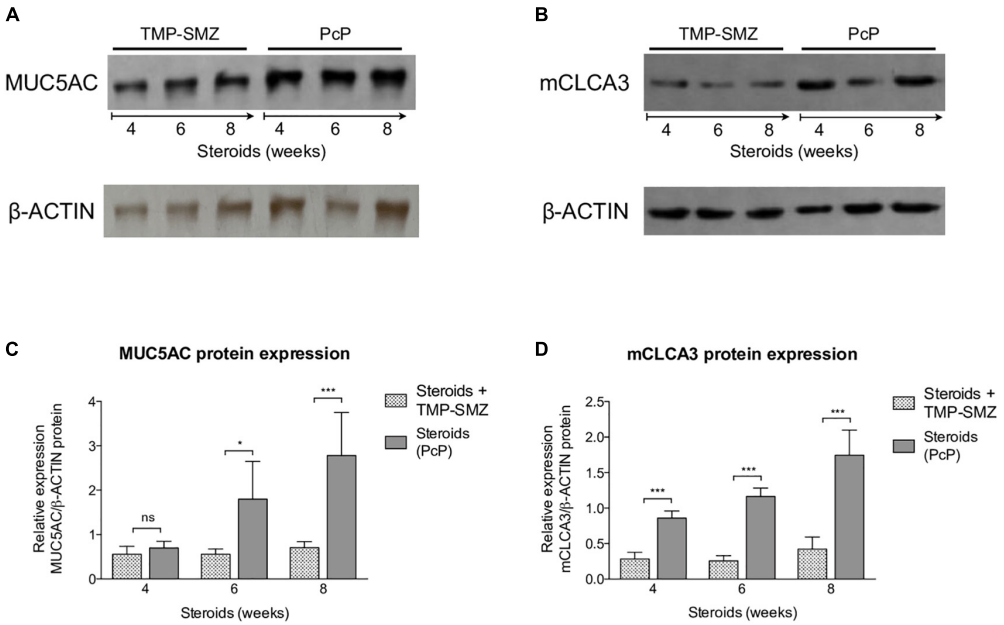

FIGURE 5 | Sequential changes in MUC5AC and mCLCA3 protein levels in rats on steroids receiving and not-receiving anti-*Pneumocystis* prophylaxis (PcP). **(A,B)** Representative images of Western Blot analysis of MUC5AC **(A)** and mCLCA3 **(B)** protein expression levels in fresh lung tissue at 4, 6, and 8 weeks of immunosuppression. **(C,D)** Relative densitometric quantitation of MUC5AC **(C)** and mCLCA3 **(D)** expression. PcP: *Pneumocystis* pneumonia; TMP-SMZ: Trimethoprim Sulfamethoxazole. Data are expressed as mean ± SD; $n = 4$; ANOVA test: ^{ns}no significant; $^{*}P < 0.05$; $^{***}P < 0.001$. Dataset for this figure available in **Supplementary Data Sheet S1**.

of *Pneumocystis* conferred a significant survival improvement compared to animals that developed PcP (100% versus 60%) (**Figure 9A**). Animals developing steroid-induced PcP in the second experiment had a survival of 60%; similar to the animals developing steroid-induced PcP in the first experiment. However, animals receiving continuous treatment with NFA for 4 weeks (28 days) reached an 80% survival that was significantly improved respect to animals receiving steroids and placebo (vehicle) (**Figure 9B**). This survival improvement was lost if administration of NFA was intermittent (i.e., 5 days / week) and animals interrupting NFA approached their survival values to those of non-treated animals in 2 days, at first interruption of NFA treatment (**Supplementary Figure S3**). Increased lung volumes leading to greater slice sections areas were noticed in lungs of rats with PcP (Steroids or Steroids + vehicle) compared to rats that received prophylaxis with TMP-SMZ. This is consistent with increased lung edema in rats with PcP (**Figure 2C**). Also, rats with PcP receiving NFA treatment had smaller lungs than those with PcP receiving steroids + placebo (vehicle). Rats with PcP in experiment 1 **(A)** or with steroids plus placebo (**B**) developed mucus plugs (see also **Figures 4**, **7**), and collapse of important areas of the lung was frequently observed among them.

DISCUSSION

In this work we show that the *Pneumocystis*-induced mucus response of the airway epithelium is highly activated during PcP and can be attenuated by treatment with Niflumic acid. This suggests a relevant role for the innate immune system in immunopathology of this fungal infection. The pathology features documented in this model consisted of steroid-resistant mucus excess with significantly increased protein expression of MUC5AC and mCLCA3. All these endpoints were reverted by the administration of niflumic acid, a specific and strong CLCA1 blocker, albeit not full blocker of mucus responses and with pleiotropic anti-inflammatory effects. Moreover, rats receiving this drug had increased survival suggesting the important participation of CLCA1-associated mechanisms in mediating *Pneumocystis*-associated immunopathology.

The first experiments aimed to document the progression of the disease in the rat model of steroid-induced PcP (**Figures 2–5**). Importantly, in addition to pulmonary edema they showed that mucus excess is a relevant disease feature during PcP by histologically documenting airway plugs and extensive shunting (**Figure 9A**). Differences in lung size are attributed to slight differences in rat size, magnitude of lung edema, or genetic differences in response to PcP Further results suggest that the mechanism for this pathogenic feature is mediated by CLCA1 which hints into a strong involvement of innate immune pathways that have been previously associated with *Pneumocystis* infection in immune competent human and animal hosts (Wang et al., 2005; Hernandez-Novoa et al., 2008; Swain et al., 2012; Vargas et al., 2013; Bello-Irizarry et al., 2014; Perez F. J. et al., 2014; Eddens et al., 2016; Iturra et al., 2018) and could help explain the low sensitivity to high dose steroids observed in PcP (Maeda et al., 2015; Wieruszewski et al., 2018).

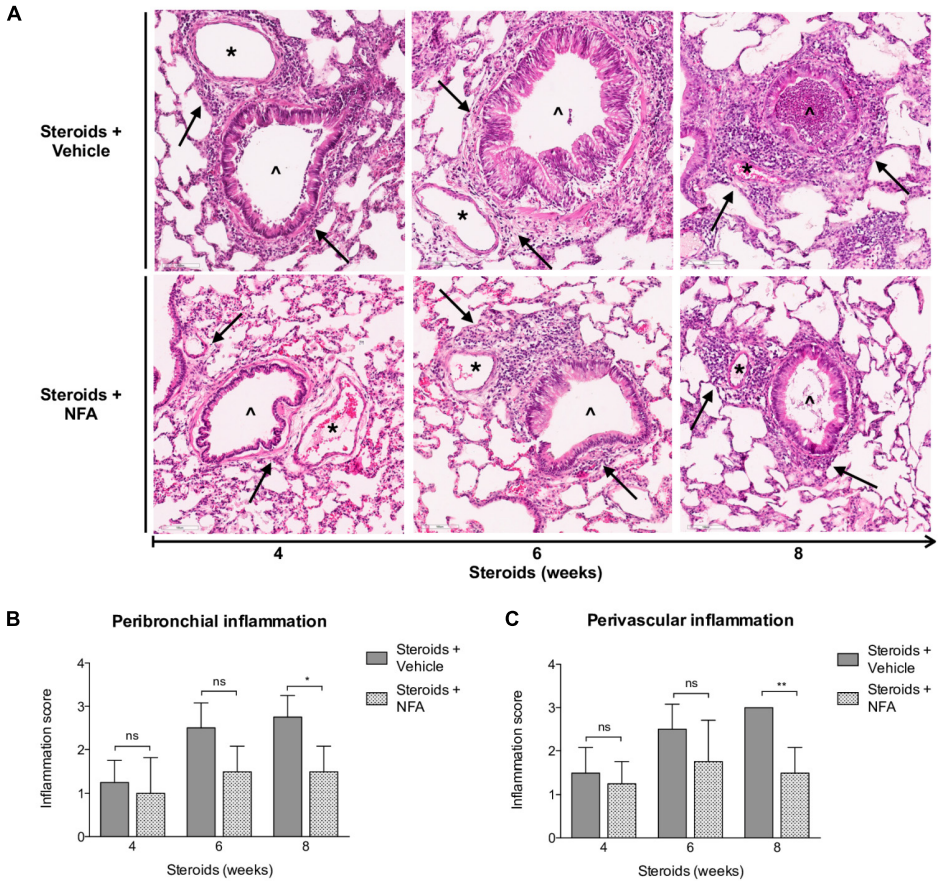

FIGURE 6 | Effect of NFA in the inflammatory response during PcP. **(A)** Representative microscopic images of H&E-stained lung sections at 4, 6, and 8 weeks of immunosuppression. Cuff infiltrates (arrows); blood vessels (*); bronchioles (^). NFA: Niflumic acid; Scale bar = 100 μm. **(B,C)** Proportion of bronchioles and blood vessels surrounded by inflammatory cuff infiltrates (see Section "Materials and Methods"). Data are expressed as mean ± SD; $n = 4$; ANOVA test: ^{ns}no significant; $^{*}P < 0.05$; $^{**}P < 0.01$. Dataset for this figure available in **Supplementary Data Sheet S1**.

Pneumocystis pneumonia induced perivascular inflammatory infiltrates, mucus overproduction and increased mCLCA3 protein levels were noticed after 4 weeks of steroid-induced immunosuppression; at the first sacrifice date. Increase in peribronchial infiltrates and in MUC5AC protein levels followed. This sequence of progression of inflammatory changes was similar to the sequence documented previously in immunocompetent rats with primary infection (Iturra et al., 2018) ($P < 0.001$), (**Figures 3**, **4**).

Extrapolation of this model to pathogenesis of specific types of PcP needs to be cautious. The immunopathogenesis of PcP is incompletely understood and may vary in patients depending on their underlying immunosuppressive etiology (Eddens and Kolls, 2015; Kutty et al., 2016; Bhagwat et al., 2018). This work did not measure T-cell levels. However, T-cell blunting is a well-documented feature of steroid-induced PcP and is expected as a result of steroid administration in this model (Walzer et al., 1984; Sukura et al., 1995). Therefore, the pathology features and response to NFA therapy determined here may not necessarily extrapolate to other types of PcP. For example, PcP in patients with immune reconstitution inflammatory syndrome (IRIS) display high lymphocyte counts after antiretroviral-therapy-related T-cell recovery (Eddens and Kolls, 2015; Gopal et al., 2017; Aggarwal et al., 2018). A progressive increase in CLCA1 as in this model may more likely occur in the setting of the slowly developing PcP of untreated AIDS or in cancer patients receiving steroids, than in the context of recovering CD4+ T-cell counts able to trigger a strong cellular immune response, or of other underlying etiologies.

The mucus excess in this model developed despite the potent anti-inflammatory activity of high-dose steroids. The effect of steroids was overcome by the effect of *Pneumocystis* in stimulating mucus-related pathways indicating that mucus in this model is steroid resistant. This may be partially explained because CLCA1 activates MAP kinases (Alevy et al., 2012), and MAP kinases phosphorylate the glucocorticoid receptor thereby inhibiting steroid signaling (Rhen and Cidlowski, 2005). However, there is currently no complete explanation for steroid resistant mucus (Barnes, 2013). Several mechanisms have been identified which include familial glucocorticoid resistance, glucocorticoid receptor modifications, increased glucocorticoid receptor-β expression, increased proinflammatory transcription

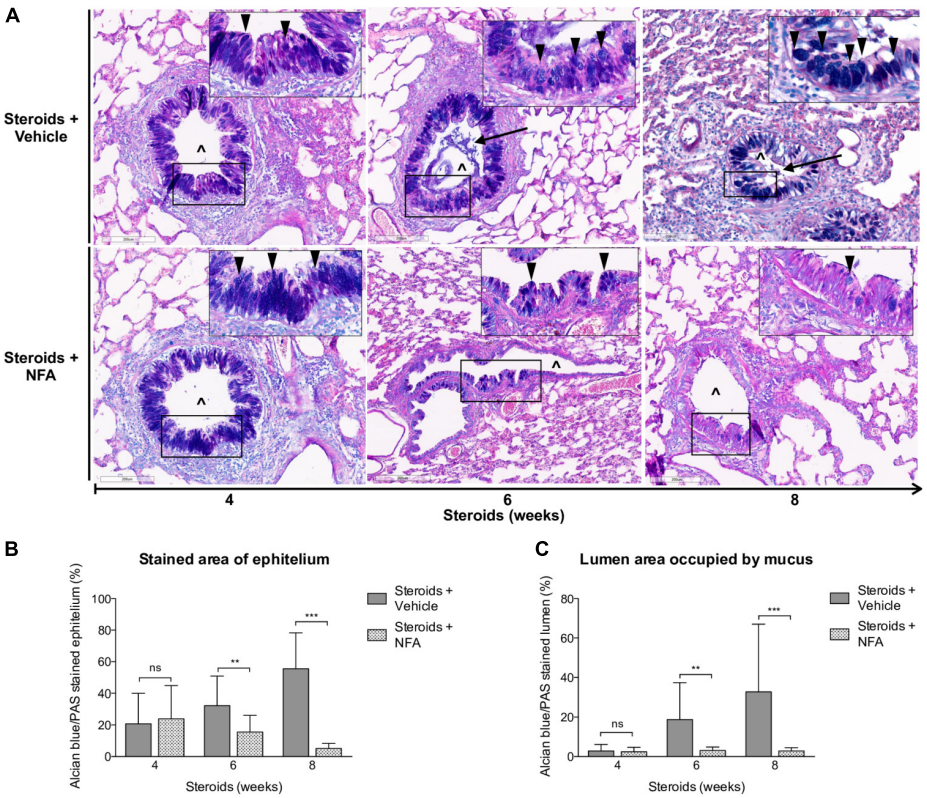

FIGURE 7 | Effect of NFA in mucus production during PcP. **(A)** Representative microscopy images of AB/PAS-stained lung sections at 4, 6, and 8 weeks of immunosuppression. Intracellular mucin granules (arrowheads); mucus plugs (arrows); NFA: Niflumic acid; (^): bronchiolar lumen; Scale bar = 200 μm. **(B,C)** Percent of AB/PAS stained epithelium **(B)** and lumen **(C)**. Data are expressed as mean ± SD; $n = 4$; ANOVA test: ^{ns}no significant; $^{**}P < 0.01$; $^{***}P < 0.001$. Dataset for this figure available in **Supplementary Data Sheet S1**.

factors, and defective histone acetylation (Barnes, 2016). Importantly, corticosteroids have been shown to be unable to control IL-13-induced mucus (Liu et al., 2004; Kanoh et al., 2011) and are also incapable of suppressing IL-13-induced goblet cell hyperplasia in mice (Kibe et al., 2003), suggesting that CLCA1-associated mucus response was beyond the anti-inflammatory reach potential of steroids (Kibe et al., 2003; Nakano et al., 2006; Alevy et al., 2012) as occurred in this model. Corticosteroids are used as adjuvant therapy in severe HIV-related PcP because inflammation is a well-known pathology feature of PcP and they are the best anti-inflammatory drugs available (Krajicek et al., 2009; Wieruszewski et al., 2018). Paradoxically, corticosteroids offer no therapeutic benefit to patients with Non-HIV-related PCP in whom inflammation is characteristically worse (Wieruszewski et al., 2018). Results of this model raise the hypothesis that the lack of response to steroid treatment observed in these patients reflects that a relevant proportion of their immunopathology is steroid-resistant. There is no clear understanding of why therapeutic response to corticosteroids in patients with PcP may vary in hosts with different causes of underlying immunosuppression. Provided that the efficacy of anti-*Pneumocystis* drugs in killing the fungus is independent of the patient condition, this host-to-host variation in response to treatment suggests the need to tailor anti-PcP therapy to the underlying cause of immunosuppression. A highly intriguing example is provided by patients with rheumatic diseases that may have different *Pneumocystis* burden thresholds for developing PcP (Shimada et al., 2018) suggesting that drugs used for underlying medical conditions could affect immune pathways differently and thus trigger different levels of immune responses (Shimada et al., 2018). In addition to PcP, corticosteroids are widely used clinically via the inhalation route to treat patients with asthma or chronic obstructive pulmonary disease (COPD) (Barnes, 2006; Adcock and Mumby, 2017) where steroid-resistance is observed (Christenson et al., 2019). Relatedly, pathways and signals activating mucus cell metaplasia in non-asthma-related chronic airway diseases like COPD and cystic fibrosis are induced by mediators that are distinct from those involved in allergic airway disease (McGuckin et al., 2015). All patients with COPD and some patients with asthma display steroid resistance that is to certain extent clinically unresponsive to corticosteroids (Barnes, 2013). Glucocorticoids exert their anti-inflammatory action by binding to the glucocorticoid receptor that inhibits transcription factors as c-Jun, NF-kB, and other signal transcription pathways that control the expression of pro-inflammatory mediators (Rhen and Cidlowski, 2005; Barnes, 2006). Some of these pathways are activated by *Pneumocystis* (Wang et al., 2005; Swain et al., 2012; Bello-Irizarry et al., 2014).

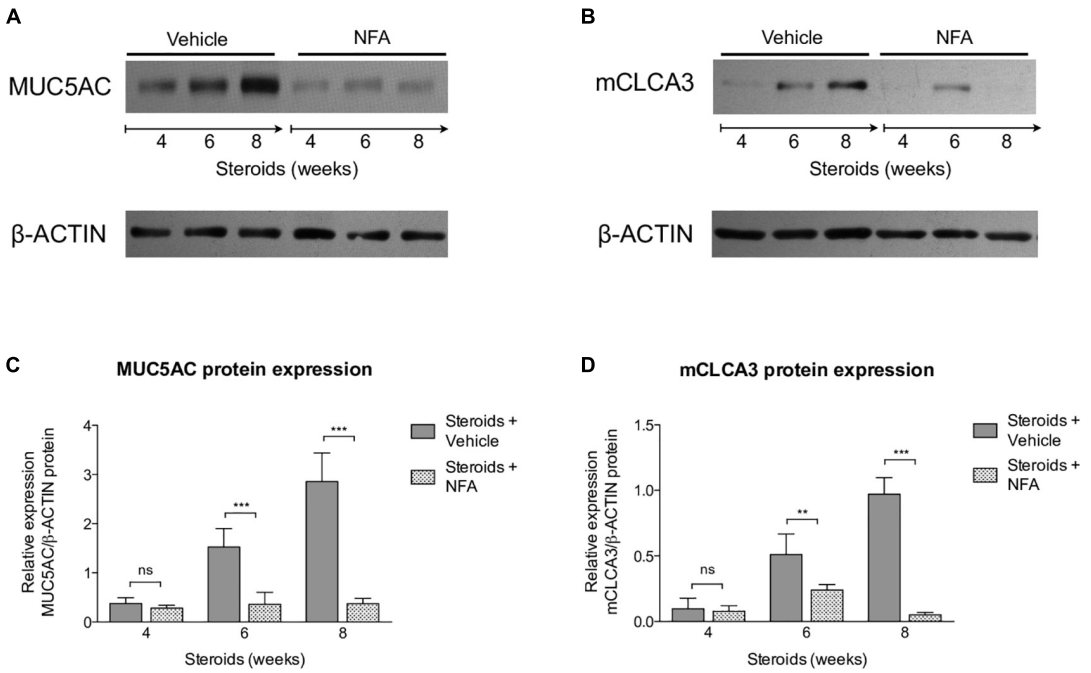

FIGURE 8 | Effect of NFA in MUC5AC and mCLCA3 protein levels during PcP. **(A,B)** Representative images of Western Blot analysis of MUC5AC **(A)** and mCLCA3 **(B)** protein expression levels in fresh lung tissue of rats with or without NFA administration at 4, 6, and 8 weeks of immunosuppression. **(C,D)** Relative densitometric quantitation of MUC5AC **(C)** and mCLCA3 **(D)** expression. NFA: Niflumic acid. Data are expressed as mean ± SD; $n = 4$; ANOVA test: ^{ns}no significant; $^{**}P < 0.01$; $^{***}P < 0.001$. Dataset for this figure available in **Supplementary Data Sheet S1**.

They may also decrease mucin protein production by reducing transcription of mucin genes (Barnes, 2016). The wide anatomic availability of the glucocorticoid receptor explains that corticosteroids have multiple beneficial and detrimental effects (Rhen and Cidlowski, 2005; Barnes, 2006).

Results also suggest that the progressive increase in mucus, mCLCA3 and MUC5AC was also CLCA1-associated as demonstrated by mucus inhibition, lesser inflammation and improved survival after administration of the CLCA1 blocker NFA (**Figures 8**, **9**). Induction of the CLCA1 pathway with increased mucins has been shown to correlate with *Pneumocystis* infection in humans (Vargas et al., 2013; Perez F. J. et al., 2014; Rojas et al., 2019) and in animal models (Swain et al., 2012; Eddens et al., 2016; Iturra et al., 2018; Rojas et al., 2019) and is strongly related to IL-13 driven mucus cell metaplasia, STAT6 activation and MUC5AC and MUC5B expression in the airways (Swain et al., 2012; Eddens et al., 2016; Iturra et al., 2018; Rojas et al., 2019). These models document increased IL-13 and mucus associated to *Pneumocystis* infection in the immunocompetent host providing an indication of activation of innate immune pathways. Germane to this work, it has been shown that NFA decreases mucus excess without affecting the expression of IL-13 receptors (Nakano et al., 2006) and, therefore, IL-13 was not measured in this model. Clinically, CLCA1 has been associated with innate airway immune response, airway inflammation (Long et al., 2006; Zhang and He, 2010), asthma (Hoshino et al., 2002; Mei et al., 2013), and COPD (Hauber et al., 2005; Hegab et al., 2007). CLCA1 may also act as a molecular signal to induce cytokine release by airway macrophages (Ching et al., 2013). All the above, suggests that CLCA1 protein is a relevant mediator of innate immune responses providing an explanation to the increase in survival of PcP-infected rats after administration of NFA via modulation of mucus responses. Furthermore, antibody blockage of the mouse homolog mCLCA3 suppresses symptoms and mucus overproduction in a murine model of asthma emphasizing the relevance of this pathway (Song et al., 2013).

Importantly, the exact contribution of mCLCA3 to mucus production is not completely elucidated. For example a knockout model to a putative transmembrane domain of mCLCA3 shows that MUC5AC production in response to an allergic challenge remained unchanged respect to wild type control mice (Robichaud et al., 2005) suggesting that mCLCA3 is not required for mucus production at least in its native conformation. Whether fragments of mCLCA3 could induce physiologic effects is unknown. This possibility is suggested by the demonstration that hCLCA1 and mCLCA3 are secreted non-integral membrane proteins (Gibson et al., 2005; Mundhenk et al., 2006). Beyond mCLCA3, many other pathways participate in mucus production. This is a complex process that involves transcription factors like STAT6, CREB, SP-1 and AP-1, the NAPDH oxidase component NOX-4, mitogen-activated protein (MAP) kinases and the transmembrane protein TM16A (Whitsett and Alenghat, 2015).

Niflumic acid is a non-steroidal anti-inflammatory drug and similar to glucocorticoids inhibits cyclooxygenase-2 (COX2) which is a potent mediator of inflammatory pathways. However,

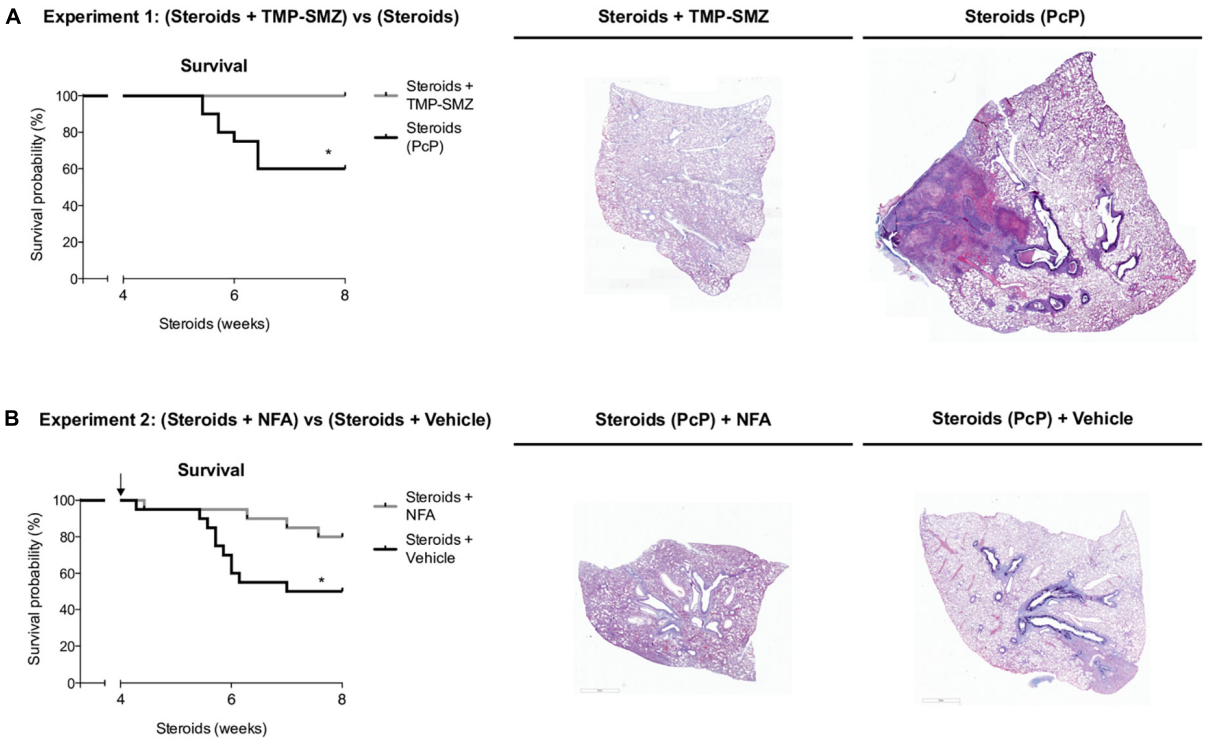

FIGURE 9 | Niflumic acid treatment improves animal survival in PcP. Kaplan–Meier survival plots and representative lung sections stained with Alcian Blue/PAS at 8 weeks of steroid treatment for animals with steroid-induced PcP versus animals receiving steroids plus anti-*Pneumocystis* prophylaxis with TMP-SMZ in experiment 1 **(A)**, or for animals receiving NFA plus steroids alone versus steroids plus placebo (NFA vehicle) in experiment 2 **(B)**. PcP: *Pneumocystis* pneumonia; TMP-SMZ: Trimethoprim Sulfamethoxazole; NFA: Niflumic acid. $n = 20$; Mantel–Cox test: $^*P < 0.05$. Dataset for this figure available in **Supplementary Data Sheet S1**.

in this work NFA treatment led first to decrease mucus excess followed by decreasing inflammatory cuffing infiltrates evidencing a faster anti-mucus than anti-inflammatory effect. This suggests that the anti-mucus effect of NFA observed in our model would be unrelated to COX2 inhibition. Of note, administration of indomethacin, a non-selective inhibitor of cyclooxygenase 1 and 2, is not accompanied by mucus decrease (Nakano et al., 2006). Whether anti-inflammatory synergy between glucocorticoids and NFA occurs would be interesting to determine. This was not possible to evaluate in this model as steroids were given to all rats. Moreover, NFA is also a potent inhibitor of phospholipase A2 that favors hydrolysis of pulmonary surfactant (Cremonesi and Cavalieri, 2015). Hughes et al. (1998) documented that aerosolized administration of synthetic surfactant, which overcomes the activity of phospholipase A2, increases survival of rats with steroid-induced PcP to levels comparable to those obtained in this model (**Figure 9**). A potential effect of NFA in surfactant levels remains to be determined.

Data about NFA dosage, route of administration, tolerance and toxicity in rats is scarce despite previous use to inhibit goblet cell hyperplasia, airway hyperresponsiveness and mucus overproduction in murine models and in human bronchial epithelial cells. Therefore, we did preliminary experiments to document tolerance and safety of NFA in healthy rats. Results of these experiments indicate that for protective effects, NFA administration needs to be uninterrupted, using 7 days a week daily administration scheme (**Figures 1B**, **9**). The survival advantage conferred by NFA was lost if continuous administration was not maintained (**Supplementary Figure S3**).

To show a mechanism of action for NFA effects in mucus production is beyond the reach of this work. However, regardless of the limitations of our model, this work demonstrates for the first time that NFA treatment effectively decreased inflammation, mucus production and significantly improved animal survival in steroid-induced PcP.

CONCLUSION

Results advocate CLCA1-mediated innate immune responses having a probable causal relationship for *Pneumocystis* mediated mucus immunopathology in steroid-induced PcP and propose steroid resistant mucus as an explanation to the lack of response to steroids in patients with PcP. A fully specific target inhibition of CLCA1 will prove the concept. Drugs aiming to revert mucus excess during PcP may have a role as adjuvants to drugs with anti-*Pneumocystis* activity and the potential efficacy of therapies to block innate-immune pathways including CLCA1 protein needs to be explored in this condition.

In addition, taking together the potential of *Pneumocystis* to induce mucus-associated immunopathology and the striking

anti-mucus effects documented for NFA, we recommend this steroid-induced PcP model as an appropriate tool to evaluate therapeutic approaches to control mucus excess in chronic respiratory diseases including steroid-resistant mucus excess.

DATA AVAILABILITY

All datasets generated for this study are included in the manuscript and/or **Supplementary Files**.

AUTHOR CONTRIBUTIONS

FP and SV designed the study and wrote the manuscript. FP and CP performed animal experiments. PI and FP performed the morphometric determinations. FP performed the molecular determinations. FP, PI, FM, VG-A, and SV analyzed and interpreted data. All authors reviewed and contributed to the final version of the manuscript.

FUNDING

This work was supported by the Fondo Nacional de Desarrollo Científico y Tecnológico (FONDECYT-Chile) grant number 1140412 (SV); by CONICYT under ERANet LAC Grant ELAC2014/HID-0254 (SV); Vicerrectoría de Investigación y Deaserrollo Universidad de Chile grant ENL 30/19 (SV); and by the Chilean Doctoral Scholarship Fund (FP).

ACKNOWLEDGMENTS

This work was presented at the 18th Annual St. Jude/PIDS Pediatric Infectious Diseases Research Conference, March 8–9, 2019 held at St. Jude Children's Research Hospital, Memphis, TN, United States. We thank Rebeca Bustamante BA and Nelson Ponce Faculty of Medicine, University of Chile, Santiago, Chile, for excellent assistance with microscopy determinations, and for excellent animal care support, respectively.

SUPPLEMENTARY MATERIAL

The Supplementary Material for this article can be found online at: https://www.frontiersin.org/articles/10.3389/fmicb.2019.01522/full#supplementary-material

FIGURE S1 | Safety of intraperitoneal administration of NFA in rats. NFA safety was tested at 3 or 12 mg/Kg/day doses administered via intraperitoneal injections during 28 consecutive days to healthy rats. Control animals received intraperitoneal injections with vehicle alone. **(A)** Animals treated with each NFA dose or with vehicle alone showed no significant differences in weight gain. **(B,C)** Safety blood tests showed all values within normal reference ranges for Sprague-Dawley rats. However, a dose-dependent increase in UREA levels was seen in NFA-treated animals, and a non- dose-dependent increase in ALKP in the NFA 3 mg/Kg/day-treated animals was also detected. NFA: Niflumic acid; CREA: Creatinine; UREA: Urea nitrogen; TBIL: Total bilirubin; DBIL: Direct bilirubin; AST: Aspartate transaminase; ALKP: Alkaline phosphatase; ALT: Alanine transaminase; GGT: Gamma glutamyl transferase. $n = 5$; ANOVA test: ^{ns}no significant; $^{***}P < 0.001$.

FIGURE S2 | *Pneumocystis* spp.-DNA amplification in rats receiving steroids alone or steroids plus Niflumic acid. All rats received oxytetracycline starting 3 weeks before and throughout the duration of the experiment as depicted in **Figure 1B**.

FIGURE S3 | Survival of rats after interruption of NFA administration. A 5-day a week administration scheme was attempted to reduce animal stress. NFA was delivered daily via intraperitoneal injection starting after 4 weeks of steroid administration (arrow) and interrupted after 5 days of NFA treatment (arrowhead and dotted line). $n = 8$; Mantel–Cox test: ^{ns} no significant.

DATA SHEET S1 | Dataset for figures: MS Excel dataset tables for each figure.

REFERENCES

Adcock, I. M., and Mumby, S. (2017). Glucocorticoids. *Handb. Exp. Pharmacol.* 237, 171–196. doi: 10.1007/164_2016_98

Aggarwal, N., Barclay, W., and Shinohara, M. L. (2018). Understanding mechanisms underlying the pathology of immune reconstitution inflammatory syndrome (IRIS) by using animal models. *Curr. Clin. Microbiol. Rep.* 5, 201–209. doi: 10.1007/s40588-018-0099-5

Alevy, Y. G., Patel, A. C., Romero, A. G., Patel, D. A., Tucker, J., Roswit, W. T., et al. (2012). IL-13-induced airway mucus production is attenuated by MAPK13 inhibition. *J. Clin. Invest.* 122, 4555–4568. doi: 10.1172/JCI64896

Baar, H. H. (1955). Interstitial plasmacellular pneumonia due to *Pneumocystis carinii*. *J. Clin. Pathol.* 8, 19–24.

Banerjee, A. K., Angulo, A. F., Polak-Vogelzang, A. A., and Kershof, A. M. (1987). An alternative method for the decontamination of rats carrying Mycoplasma pulmonis without the use of germfree isolators. *Lab. Anim.* 21, 138–142.

Barnes, P. J. (2006). How corticosteroids control inflammation: Quintiles Prize Lecture 2005. *Br. J. Pharmacol.* 148, 245–254. doi: 10.1038/sj.bjp.0706736

Barnes, P. J. (2013). Corticosteroid resistance in patients with asthma and chronic obstructive pulmonary disease. *J. Allergy Clin. Immunol.* 131, 636–645. doi: 10.1016/j.jaci.2012.12.1564

Barnes, P. J. (2016). "Glucocorticosteroids," in *Pharmacology and Therapeutics of Asthma and COPD*, eds C. P. Page and P. J. Barnes (Cham: Springer), 93–115.

Bello-Irizarry, S. N., Wang, J., Johnston, C. J., Gigliotti, F., and Wright, T. W. (2014). MyD88 signaling regulates both host defense and immunopathogenesis during pneumocystis infection. *J. Immunol.* 192, 282–292. doi: 10.4049/jimmunol.1301431

Bhagwat, S. P., Gigliotti, F., Wang, J., Wang, Z., Notter, R. H., Murphy, P. S., et al. (2018). Intrinsic programming of alveolar macrophages for protective antifungal innate immunity against pneumocystis infection. *Front. Immunol.* 9:2131. doi: 10.3389/fimmu.2018.02131

Ching, J. C., Lobanova, L., and Loewen, M. E. (2013). Secreted hCLCA1 is a signaling molecule that activates airway macrophages. *PLoS One* 8:e83130. doi: 10.1371/journal.pone.0083130

Christenson, S. A., van den Berge, M., Faiz, A., Inkamp, K., Bhakta, N., Bonser, L. R., et al. (2019). An airway epithelial IL-17A response signature identifies a steroid-unresponsive COPD patient subgroup. *J. Clin. Invest.* 129, 169–181. doi: 10.1172/JCI121087

Cremonesi, G., and Cavalieri, L. (2015). Efficacy and safety of morniflumate for the treatment of symptoms associated with soft tissue inflammation. *J. Int. Med. Res.* 43, 290–302. doi: 10.1177/0300060514567212

Eddens, T., Campfield, B. T., Serody, K., Manni, M. L., Horne, W., Elsegeiny, W., et al. (2016). A novel CD4(+) T cell-dependent murine model of pneumocystis-driven asthma-like pathology. *Am. J. Respir. Crit. Care Med.* 194, 807–820. doi: 10.1164/rccm.201511-2205OC

Eddens, T., and Kolls, J. K. (2015). Pathological and protective immunity to Pneumocystis infection. *Semin. Immunopathol.* 37, 153–162. doi: 10.1007/s00281-014-0459-z

Fahy, J. V., and Dickey, B. F. (2010). Airway mucus function and dysfunction. *N. Engl. J. Med.* 363, 2233–2247. doi: 10.1056/NEJMra0910061

Famaey, J. P. (1997). In vitro and in vivo pharmacological evidence of selective cyclooxygenase-2 inhibition by nimesulide: an overview. *Inflamm. Res.* 46, 437–446. doi: 10.1007/s000110050221

Fukuyama, S., Nakano, T., Matsumoto, T., Oliver, B. G., Burgess, J. K., Moriwaki, A., et al. (2009). Pulmonary suppressor of cytokine signaling-1 induced by IL-13 regulates allergic asthma phenotype. *Am. J. Respir. Crit. Care Med.* 179, 992–998. doi: 10.1164/rccm.200806-992OC

Gibson, A., Lewis, A. P., Affleck, K., Aitken, A. J., Meldrum, E., and Thompson, N. (2005). hCLCA1 and mCLCA3 are secreted non-integral membrane proteins and therefore are not ion channels. *J. Biol. Chem.* 280, 27205–27212. doi: 10.1074/jbc.M504654200

Gopal, R., Rapaka, R. R., and Kolls, J. K. (2017). Immune reconstitution inflammatory syndrome associated with pulmonary pathogens. *Eur. Respir. Rev.* 26:160042. doi: 10.1183/16000617.0042-2016

Ha, E. V., and Rogers, D. F. (2016). Novel therapies to inhibit mucus synthesis and secretion in airway hypersecretory diseases. *Pharmacology* 97, 84–100. doi: 10.1159/000442794

Hauber, H. P., Daigneault, P., Frenkiel, S., Lavigne, F., Hung, H. L., Levitt, R. C., et al. (2005). Niflumic acid and MSI-2216 reduce TNF-alpha-induced mucin expression in human airway mucosa. *J. Allergy Clin. Immunol.* 115, 266–271. doi: 10.1016/j.jaci.2004.09.039

Hauber, H. P., and Zabel, P. (2008). Emerging mucus regulating drugs in inflammatory and allergic lung disease. *Inflamm. Allergy Drug Targets* 7, 30–34.

Hauser, P. M. (2019). Is the unique camouflage strategy of Pneumocystis associated with its particular niche within host lungs? *PLoS Pathog.* 15:e1007480. doi: 10.1371/journal.ppat.1007480

Hegab, A. E., Sakamoto, T., Nomura, A., Ishii, Y., Morishima, Y., Iizuka, T., et al. (2007). Niflumic acid and AG-1478 reduce cigarette smoke-induced mucin synthesis: the role of hCLCA1. *Chest* 131, 1149–1156. doi: 10.1378/chest.06-2031

Hernandez-Novoa, B., Bishop, L., Logun, C., Munson, P. J., Elnekave, E., Rangel, Z. G., et al. (2008). Immune responses to Pneumocystis murina are robust in healthy mice but largely absent in CD40 ligand-deficient mice. *J. Leukoc. Biol.* 84, 420–430. doi: 10.1189/jlb.1207816

Hoshino, M., Morita, S., Iwashita, H., Sagiya, Y., Nagi, T., Nakanishi, A., et al. (2002). Increased expression of the human Ca2+-activated Cl- channel 1 (CaCC1) gene in the asthmatic airway. *Am. J. Respir. Crit. Care Med.* 165, 1132–1136. doi: 10.1164/ajrccm.165.8.2107068

Hoving, J. C. (2018). Pneumocystis and interactions with host immune receptors. *PLoS Pathog.* 14:e1006807. doi: 10.1371/journal.ppat.1006807

Hoving, J. C., and Kolls, J. K. (2017). New advances in understanding the host immune response to Pneumocystis. *Curr. Opin. Microbiol.* 40, 65–71. doi: 10.1016/j.mib.2017.10.019

Hu, Y., Wang, D., Zhai, K., and Tong, Z. (2017). Transcriptomic analysis reveals significant B lymphocyte suppression in corticosteroid-treated hosts with pneumocystis pneumonia. *Am. J. Respir. Cell Mol. Biol.* 56, 322–331. doi: 10.1165/rcmb.2015-0356OC

Hughes, W. T., Killmar, J. T., and Oz, H. S. (1994). Relative potency of 10 drugs with anti-*Pneumocystis carinii* activity in an animal model. *J. Infect. Dis.* 170, 906–911.

Hughes, W. T., McNabb, P. C., Makres, T. D., and Feldman, S. (1974). Efficacy of trimethoprim and sulfamethoxazole in the prevention and treatment of *Pneumocystis carinii* pneumonitis. *Antimicrob. Agents Chemother.* 5, 289–293.

Hughes, W. T., Sillos, E. M., LaFon, S., Rogers, M., Woolley, J. L., Davis, C., et al. (1998). Effects of aerosolized synthetic surfactant, atovaquone, and the combination of these on murine *Pneumocystis carinii* pneumonia. *J. Infect. Dis.* 177, 1046–1056.

Iturra, P. A., Rojas, D. A., Perez, F. J., Mendez, A., Ponce, C. A., Bonilla, P., et al. (2018). Progression of Type 2 Helper T cell-type inflammation and airway remodeling in a rodent model of naturally acquired subclinical primary pneumocystis infection. *Am. J. Pathol.* 188, 417–431. doi: 10.1016/j.ajpath.2017.10.019

Iwasaki, A., and Medzhitov, R. (2015). Control of adaptive immunity by the innate immune system. *Nat. Immunol.* 16, 343–353. doi: 10.1038/ni.3123

Kanoh, S., Tanabe, T., and Rubin, B. K. (2011). IL-13-induced MUC5AC production and goblet cell differentiation is steroid resistant in human airway cells. *Clin. Exp. Allergy* 41, 1747–1756. doi: 10.1111/j.1365-2222.2011.03852.x

Kibe, A., Inoue, H., Fukuyama, S., Machida, K., Matsumoto, K., Koto, H., et al. (2003). Differential regulation by glucocorticoid of interleukin-13-induced eosinophilia, hyperresponsiveness, and goblet cell hyperplasia in mouse airways. *Am. J. Respir. Crit. Care Med.* 167, 50–56. doi: 10.1164/rccm.2110084

Kim, Y. M., Won, T. B., Kim, S. W., Min, Y. G., Lee, C. H., and Rhee, C. S. (2007). Histamine induces MUC5AC expression via a hCLCA1 pathway. *Pharmacology* 80, 219–226. doi: 10.1159/000104419

Kottom, T. J., Hebrink, D. M., and Limper, A. H. (2018). Binding of *Pneumocystis carinii* to the lung epithelial cell receptor HSPA5 (GRP78). *J. Med. Microbiol.* 67, 1772–1777. doi: 10.1099/jmm.0.000864

Krajicek, B. J., Thomas, C. F. Jr., and Limper, A. H. (2009). Pneumocystis pneumonia: current concepts in pathogenesis, diagnosis, and treatment. *Clin. Chest Med.* 30, 265–278. doi: 10.1016/j.ccm.2009.02.005

Kutty, G., Davis, A. S., Ferreyra, G. A., Qiu, J., Huang, da, W., et al. (2016). beta-glucans are masked but contribute to pulmonary inflammation during pneumocystis pneumonia. *J. Infect. Dis.* 214, 782–791. doi: 10.1093/infdis/jiw249

Ledoux, J., Greenwood, I. A., and Leblanc, N. (2005). Dynamics of Ca2+-dependent Cl- channel modulation by niflumic acid in rabbit coronary arterial myocytes. *Mol. Pharmacol.* 67, 163–173. doi: 10.1124/mol.104.004168

Liu, J., Zhang, Z., Xu, Y., Xing, L., and Zhang, H. (2004). Effects of glucocorticoid on IL-13-induced Muc5ac expression in airways of mice. *J. Huazhong Univ. Sci. Technol. Med. Sci.* 24, 575–577.

Long, A. J., Sypek, J. P., Askew, R., Fish, S. C., Mason, L. E., Williams, C. M., et al. (2006). Gob-5 contributes to goblet cell hyperplasia and modulates pulmonary tissue inflammation. *Am. J. Respir. Cell Mol. Biol.* 35, 357–365. doi: 10.1165/rcmb.2005-0451OC

Ma, J., Rubin, B. K., and Voynow, J. A. (2018). Mucins, mucus, and goblet cells. *Chest* 154, 169–176. doi: 10.1016/j.chest.2017.11.008

Maeda, T., Babazono, A., Nishi, T., Matsuda, S., Fushimi, K., and Fujimori, K. (2015). Quantification of the effect of chemotherapy and steroids on risk of Pneumocystis jiroveci among hospitalized patients with adult T-cell leukaemia. *Br. J. Haematol.* 168, 501–506. doi: 10.1111/bjh.13154

McGuckin, M. A., Thornton, David, J., Whitsett, and Jeffrey, A. (2015). "Mucins and mucus," in *Mucosal Immunology*, eds W. Strober, J. Mestecky, M. W. Russell, B. L. Kelsall, H. Cheroutre, and B. N. Lambrecht (Amsterdam: Elsevier), 231–250.

Mei, L., He, L., Wu, S. S., Zhang, B., Xu, Y. J., Zhang, Z. X., et al. (2013). Murine calcium-activated chloride channel family member 3 induces asthmatic airway inflammation independently of allergen exposure. *Chin. Med. J.* 126, 3283–3288.

Meissner, N. N., Swain, S., Tighe, M., Harmsen, A., and Harmsen, A. (2005). Role of type I IFNs in pulmonary complications of Pneumocystis murina infection. *J. Immunol.* 174, 5462–5471.

Mundhenk, L., Alfalah, M., Elble, R. C., Pauli, B. U., Naim, H. Y., and Gruber, A. D. (2006). Both cleavage products of the mCLCA3 protein are secreted soluble proteins. *J. Biol. Chem.* 281, 30072–30080. doi: 10.1074/jbc.M606489200

Nakano, T., Inoue, H., Fukuyama, S., Matsumoto, K., Matsumura, M., Tsuda, M., et al. (2006). Niflumic acid suppresses interleukin-13-induced asthma phenotypes. *Am. J. Respir. Crit. Care Med.* 173, 1216–1221. doi: 10.1164/rccm.200410-1420OC

Parai, K., and Tabrizchi, R. (2002). A comparative study of the effects of Cl(-) channel blockers on mesenteric vascular conductance in anaesthetized rat. *Eur. J. Pharmacol.* 448, 59–66.

Park, J. W., Curtis, J. R., Moon, J., Song, Y. W., Kim, S., and Lee, E. B. (2018). Prophylactic effect of trimethoprim-sulfamethoxazole for pneumocystis pneumonia in patients with rheumatic diseases exposed to prolonged high-dose glucocorticoids. *Ann. Rheum. Dis.* 77, 644–649. doi: 10.1136/annrheumdis-2017-211796

Patel, A. C., Brett, T. J., and Holtzman, M. J. (2009). The role of CLCA proteins in inflammatory airway disease. *Annu. Rev. Physiol.* 71, 425–449. doi: 10.1146/annurev.physiol.010908.163253

Perez, B. F., Mendez, G. A., Lagos, R. A., and Vargas, M. S. (2014). [Mucociliary clearance system in lung defense]. *Rev. Med. Chil.* 142, 606–615. doi: 10.4067/S0034-98872014000500009

Perez, F. J., Ponce, C. A., Rojas, D. A., Iturra, P. A., Bustamante, R. I., Gallo, M., et al. (2014). Fungal colonization with Pneumocystis correlates to increasing

chloride channel accessory 1 (hCLCA1) suggesting a pathway for up-regulation of airway mucus responses, in infant lungs. *Results Immunol.* 4, 58–61. doi: 10.1016/j.rinim.2014.07.001

Rhen, T., and Cidlowski, J. A. (2005). Antiinflammatory action of glucocorticoids–new mechanisms for old drugs. *N. Engl. J. Med.* 353, 1711–1723. doi: 10.1056/NEJMra050541

Ricks, D. M., Chen, K., Zheng, M., Steele, C., and Kolls, J. K. (2013). Dectin immunoadhesins and pneumocystis pneumonia. *Infect. Immun.* 81, 3451–3462. doi: 10.1128/IAI.00136-13

Robichaud, A., Tuck, S. A., Kargman, S., Tam, J., Wong, E., Abramovitz, M., et al. (2005). Gob-5 is not essential for mucus overproduction in preclinical murine models of allergic asthma. *Am. J. Respir. Cell Mol. Biol.* 33, 303–314. doi: 10.1165/rcmb.2004-0372OC

Rojas, D. A., Iturra, P. A., Mendez, A., Ponce, C. A., Bustamante, R., Gallo, M., et al. (2019). Increase in secreted airway mucins and partial Muc5b STAT6/FoxA2 regulation during Pneumocystis primary infection. *Sci. Rep.* 9:2078. doi: 10.1038/s41598-019-39079-4

Rong, H. M., Li, T., Zhang, C., Wang, D., Hu, Y., Zhai, K., et al. (2018). IL-10 producing B Cells Regulate Th1/Th17 cell immune responses in pneumocystis pneumonia. *Am. J. Physiol. Lung Cell. Mol. Physiol.* 316, L291–L301. doi: 10.1152/ajplung.00210.2018

Sala-Rabanal, M., Yurtsever, Z., Berry, K. N., and Brett, T. J. (2015). Novel roles for chloride channels, exchangers, and regulators in chronic inflammatory airway diseases. *Mediat. Inflamm.* 2015: 497387. doi: 10.1155/2015/497387

Screpanti, I., Morrone, S., Meco, D., Santoni, A., Gulino, A., Paolini, R., et al. (1989). Steroid sensitivity of thymocyte subpopulations during intrathymic differentiation. Effects of 17 beta-estradiol and dexamethasone on subsets expressing T cell antigen receptor or IL-2 receptor. *J. Immunol.* 142, 3378–3383.

Shimada, K., Yokosuka, K., Nunokawa, T., and Sugii, S. (2018). Differences in clinical Pneumocystis pneumonia in rheumatoid arthritis and other connective tissue diseases suggesting a rheumatoid-specific interstitial lung injury spectrum. *Clin. Rheumatol.* 37, 2269–2274. doi: 10.1007/s10067-018-4157-4

Song, L., Liu, D., Wu, C., Wu, S., Yang, J., Ren, F., et al. (2013). Antibody to mCLCA3 suppresses symptoms in a mouse model of asthma. *PLoS One* 8:e82367. doi: 10.1371/journal.pone.0082367

Sukura, A., Konttinen, Y. T., Sepper, R., and Lindberg, L. A. (1995). Recovery from *Pneumocystis carinii* pneumonia in dexamethasone-treated Wistar rats. *Eur. Respir. J.* 8, 701–708.

Swain, S. D., Meissner, N. N., Siemsen, D. W., McInnerney, K., and Harmsen, A. G. (2012). Pneumocystis elicits a STAT6-dependent, strain-specific innate immune response and airway hyperresponsiveness. *Am. J. Respir. Cell Mol. Biol.* 46, 290–298. doi: 10.1165/rcmb.2011-0154OC

Vargas, S. L., Hughes, W. T., Wakefield, A. E., and Oz, H. S. (1995). Limited persistence in and subsequent elimination of *Pneumocystis carinii* from the lungs after *P. carinii* pneumonia. *J. Infect. Dis.* 172, 506–510.

Vargas, S. L., Ponce, C. A., Gallo, M., Perez, F., Astorga, J. F., Bustamante, R., et al. (2013). Near-universal prevalence of Pneumocystis and associated increase in mucus in the lungs of infants with sudden unexpected death. *Clin. Infect. Dis.* 56, 171–179. doi: 10.1093/cid/cis870

Walzer, P. D., LaBine, M., Redington, T. J., and Cushion, M. T. (1984). Lymphocyte changes during chronic administration of and withdrawal from corticosteroids: relation to *Pneumocystis carinii* pneumonia. *J. Immunol.* 133, 2502–2508.

Wang, J., Gigliotti, F., Maggirwar, S., Johnston, C., Finkelstein, J. N., and Wright, T. W. (2005). *Pneumocystis carinii* activates the NF-kappaB signaling pathway in alveolar epithelial cells. *Infect. Immun.* 73, 2766–2777. doi: 10.1128/IAI.73.5.2766-2777.2005

Whitsett, J. A., and Alenghat, T. (2015). Respiratory epithelial cells orchestrate pulmonary innate immunity. *Nat. Immunol.* 16, 27–35. doi: 10.1038/ni.3045

Wieruszewski, P. M., Barreto, J. N., Frazee, E., Daniels, C. E., Tosh, P. K., Dierkhising, R. A., et al. (2018). Early corticosteroids for pneumocystis pneumonia in adults without HIV are not associated with better outcome. *Chest* 154, 636–644. doi: 10.1016/j.chest.2018.04.026

Yasuo, M., Fujimoto, K., Tanabe, T., Yaegashi, H., Tsushima, K., Takasuna, K., et al. (2006). Relationship between calcium-activated chloride channel 1 and MUC5AC in goblet cell hyperplasia induced by interleukin-13 in human bronchial epithelial cells. *Respiration* 73, 347–359. doi: 10.1159/000091391

Zhang, H. L., and He, L. (2010). Overexpression of mclca3 in airway epithelium of asthmatic murine models with airway inflammation. *Chin. Med. J.* 123, 1603–1606.

Zhou, Y., Shapiro, M., Dong, Q., Louahed, J., Weiss, C., Wan, S., et al. (2002). A calcium-activated chloride channel blocker inhibits goblet cell metaplasia and mucus overproduction. *Novartis Found. Symp* .248, 150–165; discussion165–170, 277–182.

Conflict of Interest Statement: The authors declare that the research was conducted in the absence of any commercial or financial relationships that could be construed as a potential conflict of interest.

frontiers in Microbiology

ORIGINAL RESEARCH
published: 16 August 2019
doi: 10.3389/fmicb.2019.01920

Molecular Detection and Genotyping of *Enterocytozoon bieneusi* in Racehorses in China

Aiyun Zhao[1], Dongfang Li[2], Zilin Wei[1], Ying Zhang[1], Yushi Peng[3], Yixuan Zhu[1], Meng Qi[1] and Longxian Zhang[2]**

[1] College of Animal Science, Tarim University, Alar, China, [2] College of Animal Science and Veterinary Medicine, Henan Agricultural University, Zhengzhou, China, [3] Equivets, Beijing, China

Enterocytozoon bieneusi is a widely distributed human and animal pathogen. However, few data are available on the distribution of *E. bieneusi* genotypes in racehorses. In this study, 621 fecal specimens were collected from racehorses at 17 equestrian clubs in 15 Chinese cities. *E. bieneusi* was detected via nested polymerase chain reaction (PCR) amplification of the internal transcribed spacer (ITS) gene. The overall infection rate of *E. bieneusi* was 4.8% (30/621). Statistically significant differences were found in the prevalence of this parasite among the equestrian clubs (χ^2 = 78.464, *df* = 16, $p < 0.01$) and age groups (χ^2 = 23.686, *df* = 1, $p < 0.01$), but no sex bias was found among the racehorses for the *E. bieneusi* infections (χ^2 = 1.407, *df* = 2, $p > 0.05$). Ten *E. bieneusi* genotypes were identified, including seven known genotypes (EbpC, EbpA, Peru6, horse1, horse2, CAF1, and TypeIV) and three novel genotypes (HBH-1, SXH-1, and BJH-1). Phylogenetic analysis showed that EbpC, EbpA, Peru6, horse2, CAF1, TypeIV, BJH-1, and SXH-1 belonged to Group 1 of *E. bieneusi*, HBH-1 belonged to Group 2, and horse2 belonged to Group 6. Our findings advance the current knowledge of *E. bieneusi* prevalence and genotypes in racehorses in China.

Keywords: *Enterocytozoon bieneusi*, racehorse, prevalence, genotype, zoonotic

OPEN ACCESS

Edited by:
Lihua Xiao,
South China Agricultural University, China

Reviewed by:
Aiqin Liu,
Harbin Medical University, China
Guangneng Peng,
Sichuan Agricultural University, China
Yu Juan Shen,
National Institute of Parasitic Diseases, China

****Correspondence:***
Meng Qi
qimengdz@163.com
Longxian Zhang
zhanglx8999@henau.edu.cn

Specialty section:
This article was submitted to Infectious Diseases, a section of the journal Frontiers in Microbiology

Received: *22 May 2019*
Accepted: *05 August 2019*
Published: *16 August 2019*

Citation:
Zhao A, Li D, Wei Z, Zhang Y, Peng Y, Zhu Y, Qi M and Zhang L (2019) Molecular Detection and Genotyping of Enterocytozoon bieneusi in Racehorses in China. Front. Microbiol. 10:1920. doi: 10.3389/fmicb.2019.01920

INTRODUCTION

Enterocytozoon bieneusi, an obligate intracellular eukaryotic pathogen, infects a wide variety of vertebrates and invertebrates, including humans (Santín and Fayer, 2011). Clinical symptoms caused by *E. bieneusi* vary depending on the health status of the infected hosts. Asymptomatic infections or self-limiting diarrhea often occur in immunocompetent or healthy individuals, while chronic or life-threatening diarrhea occur in immunocompromised individuals (Didier and Weiss, 2006; Maikai et al., 2012). Most *E. bieneusi* infections in humans result from fecal-oral transmission of spores from infected hosts through contaminated food or water. A foodborne outbreak was reported in Sweden in 2009 (Decraene et al., 2012). Environmentally resistant, infective spores have been detected in various water bodies, including irrigation water, a drinking-source watershed, recreational water, and wastewater from treatment plants, suggesting the possibility of waterborne transmission (Ben et al., 2012; Li et al., 2012; Galván et al., 2013). Because of the clinical and public health importance of *E. bieneusi*, the National Institutes of Health has ranked it on the category

B list[1], and the Environmental Protection Agency has placed it on the microbial contaminant candidate list of concern for waterborne transmission (Didier et al., 2009). To date, based on sequence analysis of the ribosomal internal transcribed spacer (ITS) gene, 474 *E. bieneusi* ITS genotypes have been identified, and 11 phylogenetic groups have been recognized (Li et al., 2019). Group 2 does not include ruminant-specific genotypes, nor does it specify the zoonotic potential of some genotypes (notably BEB4, BEB6, I, and J); thus, Group 2 genotypes are not host-specific (Wang et al., 2018; Li and Xiao, 2019).

Most reports on *E. bieneusi* infections in animals involve cattle, sheep and other livestock, pets, non-human primates and wildlife; however, few reports are available on horses (Thellier and Breton, 2008; Santín et al., 2018; Zhang et al., 2018). In 2010, Santín et al. first reported on *E. bieneusi* infections in horses in Colombia, after which, *E. bieneusi* infections in horses were reported in Algeria, the Czechia, the United States and China (**Table 1**). To date, 37 *E. bieneusi* genotypes have been identified in horses. To our knowledge, the following eight genotypes have been reported as having infected humans: BEB6, CZ3, CS-4, D, EbpA, EbpC, O, and Peru8 (Leelayoova et al., 2006; Thellier and Breton, 2008; Sak et al., 2011; Wang et al., 2013, 2018; Liu et al., 2017; **Table 1**).

Horses are common animals worldwide and have been used for leisure activities, sports, and working purposes, including agricultural production, transportation, and military combat. In recent years, horse racing, as one of the oldest known sports, has become more popular in China, and the value of racehorses has increased. However, only one study has been published on *E. bieneusi* infections in racehorses in China, reporting the prevalence of this pathogen in two equestrian clubs in Sichuan at 10.4% (5/48) and 9.6% (5/52; Deng et al., 2016b). To better understand *E. bieneusi* transmission in racehorses in China, we investigated the occurrence of *E. bieneusi* genotypes in racehorses from 17 equestrian clubs.

[1]https://www.niaid.nih.gov/research/emerging-infectious-diseases-pathogens

MATERIALS AND METHODS

Fecal Specimen Collection and DNA Extraction

From December 2016 to May 2018, 621 fresh fecal specimens were collected from 30 to 50% of the racehorses at 17 equestrian clubs in 15 Chinese cities (**Figure 1** and **Table 2**). Among the 621 specimens, 74 were from young horses, 547 were from adult horses, 186 were from stallions, 350 were from mares, and 85 were from castrated horses. All horses appeared healthy. Each specimen (30–50 g) was collected directly from the rectum or from the ground immediately after defecation using a sterile disposable latex glove and placed into an individual plastic zip-lock bag. Each individual was identified by the name or number provided by the veterinarians at the equestrian clubs. Specimens were stored in a cooler with ice packs and immediately transferred to the laboratory for testing. The specimens were stored at 4°C, and DNA was extracted within 1 week after collection.

Ten grams of each fecal specimen was thoroughly mixed with 30 mL of distilled water. The suspension was passed through a 250-μm pore wire mesh sieve and centrifuged at 3000 × g for 5 min. The precipitates were used for DNA extraction. Genomic DNA was directly extracted from each (200 mg) precipitate using the E.Z.N.A.® Stool DNA Kit (D4015-02, Omega Bio-tek, Inc., Norcross, GA, United States) per the manufacturer's instructions with minor modifications. The extracted DNA specimens were stored at −20°C prior to polymerase chain reaction (PCR) analysis.

TABLE 1 | *Enterocytozoon bieneusi* occurrence and genotype distribution among horses worldwide.

Country (region)	No. Positive/No. examined (%)	Genotype (n)	References
Algeria	15/219 (6.8)[a]	**CZ3** (2), **D** (1), horse1 (6), horse2 (1)	Laatamna et al., 2015
China (Xinjiang)	81/262 (30.9)	**BEB6** (9), CS-4 (5), CM7 (2), CM8 (1), CS-1 (1), **D** (1), **EbpA** (20), **EbpC** (21), G (3), horse1 (4), horse2 (2), **O** (4), **Peru8** (1), PigEBITS4 (2), XJH1 (2), ESH-01 (1), XJH3 (1), XJH4 (1)	Qi et al., 2016
China (Sichuan and Yunnan)	75/333 (22.5)	**D** (1), horse1 (13), horse2 (39), SC02 (16), SCH1 (1), SCH2 (1), SCH3 (1), SCH4 (1), YNH1 (1), YNH2 (1)	Deng et al., 2016b
Colombia	21/195 (10.8)	**D** (4), horse1 (13), horse2 (4)	Santín et al., 2010
Czechia	66/377 (17.5)	**D** (34), **EbpA** (2), G (3), horse1 (7), horse2 (8), horse3 (2), horse4 (1), horse5 (1), horse6 (1), horse7 (1), horse8 (1), horse9 (1), horse10 (1), horse11 (2), **WL15**(1)	Wagnerová et al., 2012
Switzerland	0/24 (0)		Breitenmoser et al., 1999
Spain	0/10 (0)		Lores et al., 2002
United States	7/84 (8.3)	horse1 (7)	Wagnerová et al., 2016
Total	265/1504 (17.6)	**BEB6** (9), CS-4 (5), CM7 (2), CM8 (1), CS-1 (1), **CZ3** (2), **D** (41), **EbpA** (22), **EbpC** (21), ESH-01 (1), G (6), horse1 (50), horse2 (54), horse3 (2), horse4 (1), horse5 (1), horse6 (1), horse7 (1), horse8 (1), horse9 (1), horse10 (1), horse11 (2), **O** (4), **Peru8** (1), PigEBITS4 (2), SC02 (16), SCH1 (1), SCH2 (1), SCH3 (1), SCH4 (1), **WL15** (1), XJH1 (2), XJH3 (1), XJH4 (1), YNH1 (1), YNH2 (1)	

[a]*Unsuccessful resequencing of five positive specimens. Genotypes detected in humans are shown in bold.*

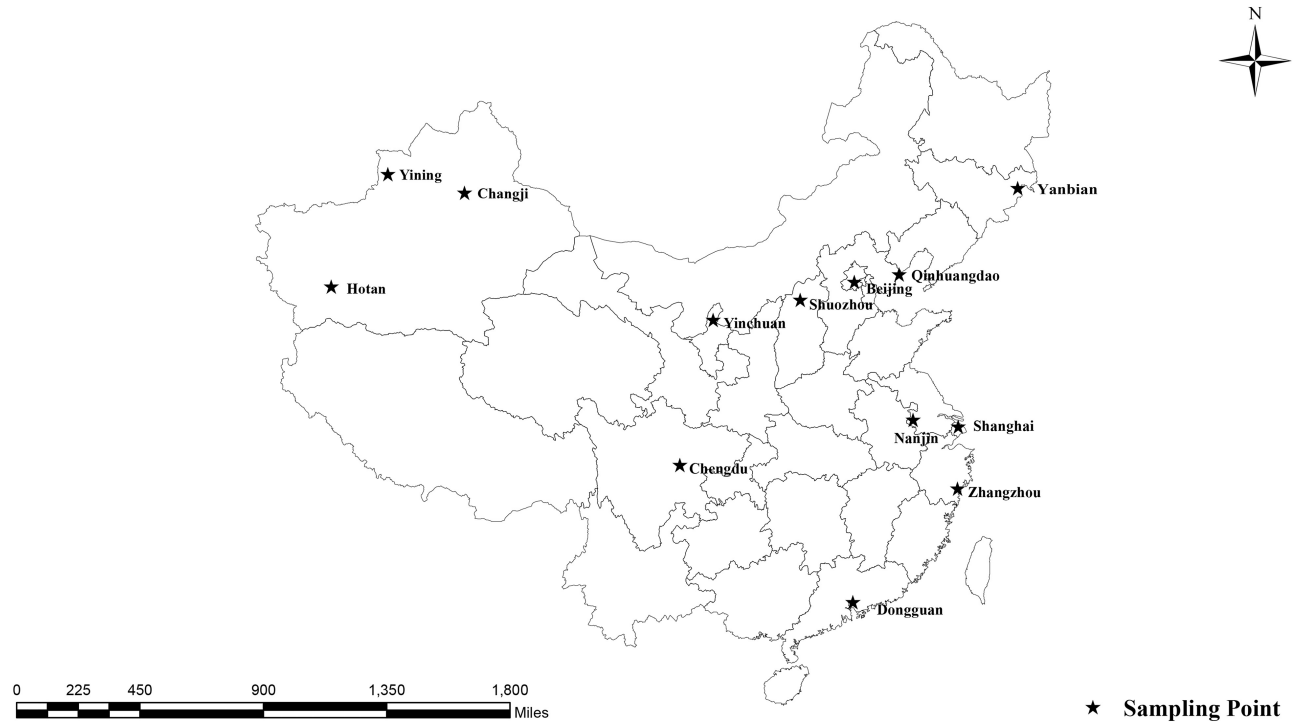

FIGURE 1 | Locations where specimens were collected in this study.

PCR Amplification and Sequence Analysis

Enterocytozoon bieneusi was detected via nested PCR amplification of the ITS region of the rRNA gene, using the primers and PCR conditions described previously by Buckholt et al. (2002). First, 12.5 μL 2 × EasyTaq PCR SuperMix (TransGene Biotech Co., Beijing, China) was used to amplify each specimen in a 25-μL reaction volume containing 10.9 μL deionized water, 0.3 μM of each primer, 1 μL genomic DNA for the primary PCR, and 1 μL primary amplification product for the secondary PCR. A positive control (DNA from dairy cattle-derived genotype I) and a negative control (distilled water) were used in each PCR run. PCR amplification was repeated twice on each specimen.

All positive secondary PCR amplicons (∼390 bp each) were sent for bidirectional sequencing at GENEWIZ (Suzhou, China). The resultant sequences were assembled using Chromas Pro, version 2.18[2] and compared with the reference sequences in the National Center for Biotechnology Information[3] database using ClustalX, version 2.1[4] to determine the *E. bieneusi* genotypes. The nucleotide sequences obtained in this study were submitted to GenBank[5] under accession numbers MK789437–MK789446.

Phylogenetic and Statistical Analyses

The sequences of the ITS regions of the *E. bieneusi* genotypes obtained in this study were compared with those previously identified in humans, other animals and the environment. Bayesian inference (BI) and Monte Carlo Markov chain methods were used to construct phylogenetic trees in MrBayes, version 3.2.6[6]. The general time reversible model (GTR + G) was the best-fit nucleotide substitution model determined by ModelTest, version 3.7[7]. The number of substitutions was set at six, with a proportion of invariable sites. Posterior probability values were calculated by running 1,000,000 generations with four simultaneous tree-building chains. Trees were saved every 1000th generation. At the end of each run, the standard deviation of the split frequencies was <0.01, and the potential scale reduction factor approached one. A 50% majority rule consensus tree was constructed for each analysis using the final 75% of the trees generated via BI. Analyses were run three times to ensure convergence and insensitivity to prior runs. The maximum clade credibility tree generated by these analyses was viewed and edited using FigTree version 1.3.1 software[8].

The Statistical Package for the Social Sciences (SPSS, version 22.0, available at https://www.ibm.com) was used for the statistical analyses, including Fisher's exact test and 95% confidence intervals. All results were considered statistically significant at $p < 0.05$.

[2]http://technelysium.com.au

[3]https://www.ncbi.nlm.nih.gov/

[4]http://clustal.org/

[5]https://www.ncbi.nlm.nih.gov/genbank/

[6]http://mrbayes.sourceforge.net/

[7]http://www.softpedia.com/get/Science-CAD/Modeltest.shtml

[8]https://www.softpedia.com/get/Science-CAD/FigTree-AR.shtml

TABLE 2 | *Enterocytozoon bieneusi* occurrence and genotype profiles in racehorses in China.

Cities	No. Positive/No. samples (%)	95% CI	χ^2	*P*-value	*E. bieneusi* genotype (n)
Beijing1	2/32 (6.3)	0–15.1			**Peru6** (2)
Beijing2	0/39				
Beijing3	3/45 (6.7)	0–14.2			**EbpC** (2), BJH-1 (1)
Baicheng	0/29				
Changji	9/34 (26.5)	10.8–42.1			horse1 (9)
Chengdu	1/34 (2.9)	0–8.9			horse1 (1)
Dongguan	1/19 (5.3)	0–16.3			**EbpA** (1)
Hotan	0/21				
Nanjing	0/9	0			
Qinhuangdao	1/136 (0.7)	0–2.2			HBH-1 (1)
Shanghai	2/84 (2.4)	0–5.7			horse1 (2)
Shuozhou	4/15 (26.7)	1.3–52.0			horse1 (3), SXH-1 (1)
Wenzhou	0/23				
Wuhan	3/20 (15.0)	0–32.1			**Peru6** (2), horse2 (1)
Yanbian	0/14				
Yinchuan	0/44				
Zhaosu	4/23 (17.4)	0.6–43.2			horse1 (1), horse2 (1), **TypeIV** (1), **CAF1** (1)
Total	30/621 (4.8)	3.1–6.5	78.464	<0.01	horse1 (16), **Peru6** (4), **EbpC** (2), horse2 (2), **EbpA** (1), **CAF1** (1), **TypeIV** (1), BJH-1 (1), HBH-1 (1), SXH-1 (1)

Genotypes detected in humans are shown in bold.

TABLE 3 | *Enterocytozoon bieneusi* occurrence and genotypes among racehorses of different ages and sex.

Ages and sex	No. Positive/No. specimens (%)	95% CI	χ^2	*P*-value	*E. bieneusi* genotype (n)
Youths	12/74 (16.2)	7.6–24.8	23.686	<0.01	horse1 (9), horse2 (1), TypeIV (1), CAF1 (1)
Adults	18/547 (3.3)	1.8–4.8			EbpA (1), EbpC (2), horse1 (7), horse2 (1), Peru6 (4), BJH-1 (1), HBH-1 (1), SXH-1 (1)
Stallion	9/186 (4.8)	1.7–8.0	1.407	>0.05	horse1 (2), horse2 (2), CAF1 (1), Peru6 (1), TypeIV (1), HBH-1 (1), BJH-1 (1)
Mare	19/350 (5.4)	3.0–7.8			horse1 (12), EbpA (1), EbpC (2), Peru6 (3), SXH-1 (1)
Castrated horse	2/85 (2.4)	0–5.6			horse1 (2)

RESULTS AND DISCUSSION

Among the 621 racehorse fecal specimens analyzed, 30 (4.8%) were positive for *E. bieneusi*, with *E. bieneusi* detected in 10 equestrian clubs (58.8%) from nine cities (60.0%). *E. bieneusi* infection rates were related to the collection sites ($\chi^2 = 78.464$, $df = 16$, $p < 0.01$; **Table 2**); the highest infection rates occurred in equestrian clubs in Shuozhou (26.7%, 4/15), Changji (26.5%, 9/34), Zhaosu (17.4%, 4/23) and Wuhan (15.0%, 3/20), with the other sampled equestrian clubs having lower infection rates. Globally, the *E. bieneusi* infection rates in horses range from 0–30.9%. Currently, two studies have reported *E. bieneusi* infections in horses in China: 30.9% (81/262) in Xinjiang (Qi et al., 2016) and 22.5% (75/333) in Sichuan and Yunnan (Deng et al., 2016b), which were higher than those in the racehorses in the present study. This discrepancy may be related to the different management systems used for the horses. Wagnerová et al. (2012) reported that the *E. bieneusi* infection rate in stabled horses (26.6%, 25/94) was higher than that in pastured horses (18.9%, 23/122) and paddocked horses (11.2%, 18/161) in the Czechia. Deng et al. (2016a) reported *E. bieneusi* infection rates in China of 29.1% (48/165) in pastured horses, 26.8% (15/56) in agricultural horses, 10.4% (5/48) in racehorses, and 9.6% (5/52) in equestrian clubs. Racehorses are selected according to their health, are well cared for, and live in good conditions, which may explain their lower *E. bieneusi* infection rates compared with those of other horses.

In the present study, the prevalence rate significantly differed by age group: 16.2% (12/74) in young racehorses and 3.3% (18/547) in adults ($\chi^2 = 23.686$, $df = 1$, $p < 0.01$; **Table 3**). Similar findings were reported in a Colombian study, with infection rates of 23.7% (18/76) in young horses and 2.5% (3/119) in adult horses (Santín et al., 2010). However, previous reports from the Czechia and Algeria and from Xinjiang, Sichuan, and Yunnan in China, showed no statistical differences among the age groups of the horses (Wagnerová et al., 2012; Laatamna et al., 2015; Deng et al., 2016b; Qi et al., 2016). Furthermore, no significant differences were found in the prevalence rates among stallions (4.8%, 9/186), mares (5.4%, 19/350) and castrated horses (2.4%, 2/85) ($\chi^2 = 1.407$, $df = 2$, $p > 0.05$; **Table 3**). This result is similar to those of previous reports conducted in China, Colombia, Algeria and the Czechia (Santín et al., 2010; Wagnerová et al., 2012; Laatamna et al., 2015; Deng et al., 2016b; Qi et al., 2016). Limited data on this topic suggest that more studies are needed to determine the relationship between age, sex and *E. bieneusi* infections in horses.

In the present study, 10 *E. bieneusi* genotypes were identified in racehorses, including seven known genotypes (EbpC, EbpA, Peru6, horse1, horse2, CAF1, and TypeIV) and three novel genotypes (HBH-1, SXH-1, and BJH-1). The three novel genotypes, HBH-1, SXH-1, and BJH-1, were closely related to genotypes BEB4, Peru6, and Henan-I, with one, two, and four single nucleotide polymorphisms, respectively. Genotype HBH-1 had one nucleotide substitution (T→C) relative to genotype BEB4. Genotype SXH-1 had two nucleotide substitutions (G→A and C→T) relative to genotype Peru6. Genotype BJH-1 had four nucleotide substitutions (G→A, G→A, T→C, and T→C) relative to genotype Henan-I. Among the ten genotypes, horse1 (53.3%, 16/30) dominated, followed by Peru6 (13.3%, 4/30), horse2 (6.7%, 2/30), EbpC (6.7%, 2/30), and each of the remaining

six genotypes (3.3%, 1/30). Our phylogenetic analysis revealed that the EbpC, EbpA, TypeIV, Peru6, CAF1, horse1, SXH-1, and BJH-1 genotypes clustered into Group 1, HBH-1 into Group 2, and horse2 into Group 6 (**Figure 2**). Among these genotypes, EbpA, EbpC, Peru6, and TypeIV have been identified in a wide range of hosts, including humans, non-human primates, pets,

FIGURE 2 | Phylogenetic tree based on Bayesian analysis of the ITS sequences. Statistically significant posterior probabilities are indicated on the branches. The specimen names include the GenBank accession numbers followed by the host and genotype designation. The *E. bieneusi* genotype CSK2 (KY706128) from the white kangaroo was used as the outlier. Known and new genotypes are indicated by hollow and filled triangles, respectively.

domestic animals and wild animals (Santín and Fayer, 2011; Wang et al., 2018). Genotype horse1 has been found in horses and non-human primates, genotype horse2 has been found in horses, black bears and squirrels, and genotype CAF1 has been found in horses, pigs, goats, deer and humans (Breton et al., 2007; Jeong et al., 2007; Wagnerová et al., 2012; Deng et al., 2016a, 2017; Qi et al., 2016; Shi et al., 2016; Zhong et al., 2017). Genotypes EbpC and Type IV have been detected in humans in several regions of China (Karim et al., 2014; Yang et al., 2014; Liu et al., 2017; Wang et al., 2017). Future studies should evaluate the molecular epidemiology of *E. bieneusi* genotypes in horses and other animals to better elucidate its transmission dynamics.

Possible genotypic differences in *E. bieneusi* dominance in horses in different geographic areas should also be determined. Dominant genotypes were observed, such as horse1 in Colombia, genotype D in the Czechia, horse2 in Sichuan and Yunnan, China, and the dominant genotypes EbpA and EbpC in Xinjiang, China (Santín et al., 2010; Wagnerová et al., 2012; Laatamna et al., 2015; Deng et al., 2016b; Qi et al., 2016; **Tables 2**, **3**). Therefore, *E. bieneusi* infections in horses likely differ regionally.

CONCLUSION

Our results revealed a relatively low occurrence of *E. bieneusi* in racehorses. Ten *E. bieneusi* genotypes were identified, with horse1 being predominant. The observations of five genotypes (EbpC, EbpA, Peru6, TypeIV, and CAF1) in humans as well as three novel genotypes (BGH-1 and SXH-1 in Group 1 and HBH-1 in Group 2) suggest the possibility that racehorses may transmit *E. bieneusi* to humans.

DATA AVAILABILITY

The datasets generated for this study can be found in the GenBank under the accession numbers MK789437–MK789446.

ETHICS STATEMENT

The Ethics Review Committee of Henan Agricultural University reviewed and approved this research under the approval number IRC-HENAU-20160225. The equestrian club owners granted permission for specimen collection. Animals were handled in accordance with the Animal Ethics Procedures and Guidelines of the People's Republic of China.

AUTHOR CONTRIBUTIONS

MQ and LZ designed the study. AZ, ZW, YP, and YnZ collected and analyzed the specimens. DL and YxZ analyzed the data. AZ, MQ, and LZ wrote the manuscript. All authors read and approved the final manuscript.

FUNDING

This work was supported in part by the National Natural Science Foundation of China (31860699 and 31660712) and the Program for Young and Middle-aged Leading Science, Technology, and Innovation of Xinjiang Production & Construction Group (2018CB034). The sponsors played no roles in the study design or in the collection, analysis, or interpretation of the data, in writing the report, or in the decision to submit the article for publication.

ACKNOWLEDGMENTS

We thank Traci Raley, MS, ELS, from Liwen Bianji, Edanz Editing China (www.liwenbianji.cn/ac), for editing a draft of this manuscript.

REFERENCES

Ben, A. L., Yang, W., Widmer, G., Cama, V., Ortega, Y., and Xiao, L. (2012). Survey and genetic characterization of wastewater in Tunisia for *Cryptosporidium* spp., *Giardia duodenalis*, *Enterocytozoon bieneusi*, *Cyclospora cayetanensis* and *Eimeria* spp. *J. Water Health* 10, 431–444. doi: 10.2166/wh.2012.204

Breitenmoser, A. C., Mathis, A., Bürgi, E., Weber, R., and Deplazes, P. (1999). High prevalence of *Enterocytozoon bieneusi* in swine with four genotypes that differ from those identified in humans. *Parasitology* 118(Pt 5), 447–453. doi: 10.1017/S0031182099004229

Breton, J., Bart-Delabesse, E., Biligui, S., Carbone, A., Seiller, X., Okome-Nkoumou, M., et al. (2007). New highly divergent rRNA sequence among biodiverse genotypes of *Enterocytozoon bieneusi* strains isolated from humans in Gabon and Cameroon. *J. Clin. Microbiol.* 45, 2580–2589. doi: 10.1128/JCM.02554-06

Buckholt, M. A., Lee, J. H., and Tzipori, S. (2002). Prevalence of *Enterocytozoon bieneusi* in swine: an 18-month survey at a slaughterhouse in Massachusetts. *Appl. Environ. Microbiol.* 68, 2595–2599. doi: 10.1128/AEM.68.5.2595-2599.2002

Decraene, V., Lebbad, M., Botero-Kleiven, S., Gustavsson, A. M., and Löfdahl, M. (2012). First reported foodborne outbreak associated with microsporidia, Sweden, October 2009. *Epidemiol. Infect.* 140, 519–527. doi: 10.1017/S095026881100077X

Deng, L., Li, W., Zhong, Z., Gong, C., Cao, X., Song, Y., et al. (2017). Multi-locus genotypes of *Enterocytozoon bieneusi* in captive Asiatic black bears in southwestern China: high genetic diversity, broad host range, and zoonotic potential. *PLoS One* 12:e0171772. doi: 10.1371/journal.pone.0171772

Deng, L., Li, W., Yu, X., Gong, C., Liu, X., Zhong, Z., et al. (2016a). First report of the human-pathogenic *Enterocytozoon bieneusi* from red-bellied tree squirrels (*Callosciurus erythraeus*) in Sichuan, China. *PLoS One* 11:e0163605. doi: 10.1371/journal.pone.0163605

Deng, L., Li, W., Zhong, Z., Gong, C., Liu, X., Huang, X., et al. (2016b). Molecular characterization and multilocus genotypes of *Enterocytozoon bieneusi* among horses in southwestern China. *Parasit. Vectors.* 9:561. doi: 10.1186/s13071-016-1844-3

Didier, E. S., and Weiss, L. M. (2006). Microsporidiosis: current status. *Curr. Opin. Infect. Dis.* 19, 485–492. doi: 10.1097/01.qco.0000244055.46382.23

Didier, E. S., Weiss, L. M., Cai, A., and Marciano-Cabral, F. (2009). Overview of the presentations on microsporidia and free-living amebae at the 10th international workshops on opportunistic protists. *Eukaryot. Cell.* 8, 441–445. doi: 10.1128/EC.00302-08

Galván, A. L., Magnet, A., Izquierdo, F., Fenoy, S., Rueda, C., Fernández Vadillo, C., et al. (2013). Molecular characterization of human-pathogenic microsporidia and *Cyclospora cayetanensis* isolated from various water sources

in Spain: a year-long longitudinal study. *Appl. Environ. Microbiol.* 79, 449–459. doi: 10.1128/AEM.02737-12

Jeong, D. K., Won, G. Y., Park, B. K., Hur, J., You, J. Y., Kang, S. J., et al. (2007). Occurrence and genotypic characteristics of *Enterocytozoon bieneusi* in pigs with diarrhea. *Parasitol. Res.* 102, 123–128. doi: 10.1007/s00436-007-0740-3

Karim, M. R., Wang, R., He, X., Zhang, L., Li, J., Rume, F. I., et al. (2014). Multilocus sequence typing of *Enterocytozoon bieneusi* in nonhuman primates in China. *Vet. Parasitol.* 200, 13–23. doi: 10.1016/j.vetpar.2013.12.004

Laatamna, A. E., Wagnerová, P., Sak, B., Kvìtoòová, D., Xiao, L., Rost, M., et al. (2015). Microsporidia and *Cryptosporidium* in horses and donkeys in Algeria: detection of a novel *Cryptosporidium hominis* subtype family (Ik) in a horse. *Vet. Parasitol.* 208, 135–142. doi: 10.1016/j.vetpar.2015.01.007

Leelayoova, S., Subrungruang, I., Suputtamongkol, Y., Worapong, J., Petmitr, P. C., and Mungthin, M. (2006). Identification of genotypes of *Enterocytozoon bieneusi* from stool samples from human immunodeficiency virus-infected patients in Thailand. *J. Clin. Microbiol.* 44, 3001–3004. doi: 10.1128/JCM.00945-06

Li, N., Xiao, L., Wang, L., Zhao, S., Zhao, X., Duan, L., et al. (2012). Molecular surveillance of *Cryptosporidium* spp., *Giardia duodenalis*, and *Enterocytozoon bieneusi* by genotyping and subtyping parasites in wastewater. *PLoS Negl. Trop. Dis.* 6:e1809. doi: 10.1371/journal.pntd.0001809

Li, W., Feng, Y., and Santin, M. (2019). Host specificity of *Enterocytozoon bieneusi* and public health implication. *Trends Parasitol.* 35, 436–451. doi: 10.1016/j.pt.2019.04.004

Li, W., and Xiao, L. (2019). Multilocus sequence typing and population genetic analysis of *Enterocytozoon bieneusi*: host specificity and its impacts on public health. *Front. Genet.* 10:307. doi: 10.3389/fgene.2019.00307

Liu, H., Jiang, Z., Yuan, Z., Yin, J., Wang, Z., Yu, B., et al. (2017). Infection by and genotype characteristics of *Enterocytozoon bieneusi* in HIV/AIDS patients from Guangxi Zhuang autonomous region, China. *BMC Infect. Dis.* 17:684. doi: 10.1186/s12879-017-2787-9

Lores, B., del Aguila, C., and Arias, C. (2002). *Enterocytozoon bieneusi* (microsporidia) in faecal samples from domestic animals from Galicia, Spain. *Mem. Inst. Oswaldo. Cruz.* 97, 941–945. doi: 10.1590/S0074-02762002000700003

Maikai, B. V., Umoh, J. U., Lawal, I. A., Kudi, A. C., Ejembi, C. L., and Xiao, L. (2012). Molecular characterizations of *Cryptosporidium*, *Giardia*, and *Enterocytozoon* in humans in Kaduna State, Nigeria. *Exp. Parasitol.* 131, 452–456. doi: 10.1016/j.exppara.2012.05.011

Qi, M., Wang, R., Wang, H., Jian, F., Li, J., Zhao, J., et al. (2016). *Enterocytozoon bieneusi* genotypes in grazing horses in China and their zoonotic transmission potential. *J. Eukaryot. Microbiol.* 63, 591–597. doi: 10.1111/jeu.12308

Sak, B., Brady, D., Pelikánová, M., Kvìtoòová, D., Rost, M., Kostka, M., et al. (2011). Unapparent microsporidial infection among immunocompetent humans in the Czech Republic. *J. Clin. Microbiol.* 49, 1064–1070. doi: 10.1128/JCM.01147-10

Santín, M., Calero-Bernal, R., Carmena, D., Mateo, M., Balseiro, A., Barral, M., et al. (2018). Molecular characterization of *Enterocytozoon bieneusi* in wild carnivores in Spain. *J. Eukaryot. Microbiol.* 65, 468–474. doi: 10.1111/jeu.12492

Santín, M., and Fayer, R. (2011). Microsporidiosis: *Enterocytozoon bieneusi* in domesticated and wild animals. *Res. Vet. Sci.* 90, 363–371. doi: 10.1016/j.rvsc.2010.07.014

Santín, M., Vecino, J. A., and Fayer, R. (2010). A zoonotic genotype of *Enterocytozoon bieneusi* in horses. *J. Parasitol.* 96, 157–161. doi: 10.1645/GE-2184.1

Shi, K., Li, M., Wang, X., Li, J., Karim, M. R., Wang, R., et al. (2016). Molecular survey of *Enterocytozoon bieneusi* in sheep and goats in China. *Parasit. Vectors* 9:23. doi: 10.1186/s13071-016-1304-0

Thellier, M., and Breton, J. (2008). *Enterocytozoon bieneusi* in human and animals, focus on laboratory identification and molecular epidemiology. *Parasite* 15, 349–358. doi: 10.1051/parasite/2008153349

Wagnerová, P., Sak, B., Kvìtoòová, D., Buòatová, Z., Civišová, H., Maršálek, M., et al. (2012). *Enterocytozoon bieneusi* and *Encephalitozoon cuniculi* in horses kept under different management systems in the Czech Republic. *Vet. Parasitol.* 190, 573–577. doi: 10.1016/j.vetpar.2012.07.013

Wagnerová, P., Sak, B., McEvoy, J., Rost, M., Sherwood, D., Holcomb, K., et al. (2016). *Cryptosporidium parvum* and *Enterocytozoon bieneusi* in American Mustangs and Chincoteague ponies. *Exp. Parasitol.* 162, 24–27. doi: 10.1016/j.exppara.2015.12.004

Wang, L., Zhang, H., Zhao, X., Zhang, L., Zhang, G., Guo, M., et al. (2013). Zoonotic *Cryptosporidium* species and *Enterocytozoon bieneusi* genotypes in HIV-positive patients on antiretroviral therapy. *J. Clin. Microbiol.* 51, 557–563. doi: 10.1128/JCM.02758-12

Wang, S., Wang, R., Fan, X., Liu, T., Zhang, L., and Zhao, G. (2018). Prevalence and genotypes of *Enterocytozoon bieneusi* in China. *Acta Trop.* 183, 142–152. doi: 10.1016/j.actatropica.2018.04.017

Wang, T., Fan, Y., Koehler, A. V., Ma, G., Li, T., Hu, M., et al. (2017). First survey of *Cryptosporidium*, *Giardia* and *Enterocytozoon* in diarrhoeic children from Wuhan, China. *Infect. Genet. Evol.* 51, 127–131. doi: 10.1016/j.meegid.2017.03.006

Yang, J., Song, M., Wan, Q., Li, Y., Lu, Y., Jiang, Y., et al. (2014). *Enterocytozoon bieneusi* genotypes in children in Northeast China and assessment of risk of zoonotic transmission. *J. Clin. Microbiol.* 52, 4363–4367. doi: 10.1128/JCM.02295-14

Zhang, Y., Koehler, A. V., Wang, T., Haydon, S. R., and Gasser, R. B. (2018). First detection and genetic characterisation of Enterocytozoon bieneusi in wild deer in Melbourne's water catchments in Australia. *Parasit. Vectors* 11:2. doi: 10.1186/s13071-017-2577-7

Zhong, Z., Li, W., Deng, L., Song, Y., Wu, K., Tian, Y., et al. (2017). Multilocus genotyping of *Enterocytozoon bieneusi* derived from nonhuman primates in southwest China. *PLoS One* 12:e0176926. doi: 10.1371/journal.pone.0176926

Conflict of Interest Statement: YP was employed by the company Equivets, China.

The remaining authors declare that the research was conducted in the absence of any commercial or financial relationships that could be construed as a potential conflict of interest.

frontiers in Public Health

BRIEF RESEARCH REPORT
published: 04 October 2019
doi: 10.3389/fpubh.2019.00275

Changing Trends in the Epidemiology and Risk Factors of *Pneumocystis* Pneumonia in Spain

Estefanía Pereira-Díaz[1], *Fidel Moreno-Verdejo*[1], *Carmen de la Horra*[2,3], *José A. Guerrero*[4], *Enrique J. Calderón*[1,2,3,5]* *and Francisco J. Medrano*[1,2,3,5]

[1] *Internal Medicine Service, Hospital Universitario Virgen del Rocío, Seville, Spain,* [2] *Area of Cardiovascular and Respiratory Diseases, Instituto de Biomedicina de Sevilla (IBiS)/CSIC, Seville, Spain,* [3] *Centro de Investigación Biomédica en Red de Epidemiología y Salud Pública, Seville, Spain,* [4] *Clinical Documentation Service, Hospital Universitario Virgen del Rocío, Seville, Spain,* [5] *Department of Medicine, Universidad de Sevilla, Seville, Spain*

Objective: The information about the epidemiology of *Pneumocystis* pneumonia (PcP) in Europe is scarce, and in Spain there are only data nationwide on patients with HIV infection. This study has been carried out with the aim of knowing in our country the current epidemiological spectrum and the risk factors of PcP.

Methods: Observational, descriptive transversal study that included all patients admitted in Spain with diagnosis upon discharge of PcP registered in the National Health System's Hospital Discharge Records Database of Spain, between 2008 and 2012.

Results: Four thousand five hundred and fifty four cases of PcP were reported, 1,204 (26.4%) in HIV-negative patients. During the study period, mean annual incidence (cases per million) was 19.4, remaining globally stable, increasing from 4.4 to 6.3 in HIV-negative patients and decreasing from 15.5 to 13.4 among HIV-infected patients. Risk factors were identified in 85.5% of HIV-negative cases, the most frequent being hematological neoplams (29%), chronic lung diseases (15.9%), and non-hematological cancers (14.9%). Mean mortality and hospitalization cost were high (25.5% and 12,000 euros, respectively).

Conclusions: The results of this first nationwide study in Spain allow a change in the misconception that, after the AIDS epidemic, PcP is an infrequent disease, showing that today it is an emerging problem in patients without HIV infection. These findings underlines the need for increased efforts toward a better characterization of risk groups to improve prophylactic strategies and reduce the burden of disease.

Keywords: pneumonia, *Pneumocystis*, epidemiology, HIV infections, Spain

OPEN ACCESS

Edited by:
Olga Matos,
New University of Lisbon, Portugal

Reviewed by:
Lin Wang,
Institut Pasteur, France
Jianming Tang,
University of Alabama at Birmingham, United States

***Correspondence:**
Enrique J. Calderón
sandube@cica.es

Specialty section:
This article was submitted to Epidemiology, a section of the journal Frontiers in Public Health

Received: *27 July 2019*
Accepted: *12 September 2019*
Published: *04 October 2019*

Citation:
Pereira-Díaz E, Moreno-Verdejo F, de la Horra C, Guerrero JA, Calderón EJ and Medrano FJ (2019) Changing Trends in the Epidemiology and Risk Factors of Pneumocystis Pneumonia in Spain. Front. Public Health 7:275. doi: 10.3389/fpubh.2019.00275

INTRODUCTION

Pneumocytis jirovecii continues to be one of the major opportunistic pathogens that affect individuals with acquired immune deficiency syndrome (AIDS) and patients with immunosuppression due to other causes, in which it causes severe pneumonia with high morbi-mortality (1–3). Until 1980, it was an uncommon disease that affected malnourished children with severe immunodeficiencies and adults with situations of intense immunosuppression, mainly associated with chemotherapy in cancer. With the emergence of the AIDS pandemic,

the prevalence of *Pneumocystis* pneumonia (PcP) increased drastically, and it became the most common AIDS-defining disease in developed countries (1, 3).

After the introduction of chemoprophylaxis with co-trimoxazole in HIV-infected patients with a $CD4^+$ lymphocyte count lower than 200 cells/mm^3 from 1989 and, above all, after the generalization of highly active antiretroviral therapy (HAART) in the mid-'90s, an important decrease in the incidence of PcP was observed in developed countries (3), which in Europe fell from 4.9 cases per 100 persons-year before 1995 to 0.3 cases per 100 persons-year after 1998 (4). Despite this, PcP continues to be a non-infrequent disease in patients with HIV infection, both in developed countries and in some areas of the third world in which HIV is endemic, where access to chemoprophylaxis and antiretroviral drugs is limited (1, 5).

Additionally, an increasing number of PcP cases are currently being described in immunosuppressed patients without HIV infection (1, 2), due to the increased use of immunosuppressive drugs and chemotherapy in people with cancer, bone marrow, or solid organ transplants and autoimmune diseases in developed countries (2, 6–8).

Specific chemoprophylaxis with trimethoprim-sulfamethoxazole, dapsone, or atovaquone is effective for preventing PcP in patients with HIV infection and also in subjects without infection (6, 7, 9), although in the latter group the circumstances associated with a greater risk of symptomatic infection are poorly defined. As such, to reduce the incidence of this disease in patients not infected with HIV, it is necessary to identify the high-risk groups, which should receive prophylaxis and/or close monitoring in order to be able to carry out an early diagnosis of the disease.

Moreover, the frequency of PcP seems to be increasing in some patient subgroups without HIV infection, such as those who have received a kidney transplant (10). These findings suggest that the clinical-epidemiological characteristics of PcP could currently be changing. However, the information about the epidemiology nationwide on the current situation of PcP in Europe is scarce (11), and in Spain there are only data on patients with HIV infection (12). Therefore, this study has been carried out with the aim of knowing in our country the current epidemiological spectrum and the risk factors of PcP.

MATERIALS AND METHODS

Design

Observational, descriptive transversal study that included patients admitted in Spain with diagnosis upon discharge of PcP registered as code 136.3 of the International Classification of Diseases, Ninth Revision, Clinical Modification (ICD-9-CM), listed in any position in the Hospitalization Minimum Data Set (CMBD), that is the National database of hospital discharge records in Spain, between 2008 and 2012. The project was approved by the Clinical Research Ethics Committee (CEIC) of the Hospital Universitario Virgen del Rocío.

Variables

First at all, an exploratory analysis of the database was carried out to identify possible outliers, duplicates, and lost values. When the same patient had several hospitalization episodes, only the variables of the first episode were included in the analysis. There was no gaps in the dataset (each calendar year was fully covered).

The data collected in the CMBD database were the discharge year, the admission date, sex, age, HIV infection diagnosis, weight of the "All Patient Refined Diagnosis-Related Groups" (APR-DGRs), cost of the process in euros, days hospitalized, death during hospitalization and re-admission within 30 days after discharge. When the same patient had several hospitalization episodes during different calendar periods, readmissions were counted only once. The annual incidence rate of PcP (per million inhabitants) was calculated considering the data of the Spanish Statistical Office (INE) of Spain (13) for the study years.

Moreover, the study researchers identified a risk category in patients without HIV infection. For the coding of this variable, the tool validated for clinical studies "Clinical Classifications Software (CCS) for ICD-9-CM" (14) was used. The CCS variables were grouped into nine mutually exclusive categories that, frequently, were as conditions or diseases associated with PCP (2, 6, 8, 9, 11, 15, 16). If there were two or more risk categories in the same patient, considering the data on incidence and/or frequency of PcP reported in the literature (8, 11, 16) the following order of preference for recording the risk category was followed: (1) active with chemotherapy, (2) hematologic malignances, (3) malignances other than hematologic, (4) any transplant, (5) autoimmune diseases, including rheumatoid arthritis, systemic lupus erythematosus, polymyositis, dermatomyositis, chronic mixed connective tissue disease, Crohn's disease, and systemic vasculitis, (6) chronic lung diseases, (7) chronic nephropathies, (8) hematologic disorders other than malignances, (9) chronic liver diseases, (10) unknown risk factor.

Two study researchers (EP and FM) reviewed all of the records independently and assigned each of the cases to one of these risk categories. The discrepancies in the categorization (which affected <5% of patients) were resolved by a third researcher (EC).

Statistical Analyses

Results are expressed as mean values ± standard deviation (SD). The chi-square test was used for assessing differences between proportions. For continuous variables, levels of significance were calculated with the one-way analysis of variance (ANOVA) test for parametric variables and with the Mann-Whitney *U*-test and the Kruskal-Wallis *H*-test for non-parametric variables. Temporal trends in the incidence of PcP were investigated by Poisson regression. The results were considered statistically significant at $p < 0.005$. Statistical analyses were performed by using the Statistical Package for Serial Studies for personal computers (IBM SPSS version 22.0, IBM Corporation, Somers, NY, USA).

RESULTS

PcP Incidence

During the 2008–2012 period, CMBD recorded a total of 4,554 cases of PcP. Of these, 1,204 (26.44%) were recorded in patients without HIV infection. Overall incidence of PcP remained stable during the observation period (mean annual rate for the period of 19.4, coefficient –0.007, $p = 0.47$). The incidence rate in patients without HIV infection increased significantly from 4.4 per million in 2008 ($n = 201$ cases) to 6.3 in 2012 ($n = 299$ cases) (coefficient 0.08, $p < 0.001$), and amongst those infected by HIV decreased from 15.5 to 13.4 per million (coefficient −0.03, $p = 0.001$) (**Table 1**).

Demographic Characteristics, Clinical Evolution, and Consumption of Resources

Compared to patients with HIV infection, patients without HIV infection had a higher mean age (58 vs. 42.1 years of age) and the proportion of men was higher (74.1 vs. 60.5%). Hospital stay (24.9 vs. 22 days), the DRG weight (2.8 vs. 2.7) and the cost of hospitalization (12,137 vs. 11,436 euros) were also higher and they had a worse clinical evolution, with higher rates of intrahospital mortality (25.5 vs. 13.6%) and re-admissions (24.9 vs. 10.8%) (**Table 2**). The annual evolution of the different variables in the study period in patients without HIV infection is displayed in **Table 3**. There were only statistically significant differences for the age variable ($p = 0.002$), the sex ($p = 0.022$) and the cost per episode of hospitalization ($p = 0.001$).

PcP Risk Factors

A PcP risk factor was observed in 85.5% of cases, with the most common being hematological cancers (29%), chronic lung diseases (15.9%), and non-hematological neoplasms (14.9%). The other risk factors are displayed in **Table 4**. The annual evolution of the different risk categories during the study period are displayed in **Figure 1**, with changes being observed in their distribution during this period, with the most important being the increase in the proportion of patients with non-hematological neoplasms from 13.4% in 2008 to 19.7% in 2012 and in subjects who receive chemotherapy from 3.5% in 2008 to 7% in 2012 and the decrease in patients with hematological neoplasms (29.9% in 2008 and 24.4% in 2012).

DISCUSSION

The present study is the first to address nationwide the epidemiology of PcP in patients with or without HIV infection in Spain. Our results indicate that PcP currently continues to be in our country a disease with a stable incidence and that its epidemiological spectrum is changing, with a decrease in the cases of patients with HIV infection and a parallel increase in subjects without this infection being observed during the study period. Furthermore, the study confirms that PcP in patients without HIV infection has a high mortality rate and healthcare cost and it has allowed the main risk groups to be identified, among which factors previously not associated with PcP such as chronic lung diseases are found.

The potential study limitations are related to the use of administrative bases as a source of information. The CDMD is an

TABLE 2 | Epidemiologic, hospitalization cost, and outcome of patients with *Pneumocystis* pneumonia, Spain, 2008–2012.

	Total *N* = 4,554	HIV-positive *N* = 3,350 (73.5%)	HIV-negative *N* = 1,204 (26.4%)	*p*
Male, No. (%)	3,212 (70.6)	2,486 (60.5)	728 (74.2)	<0.001*
Age (years), mean ± SD	46.3 ± 14.3	42.1 ± 9.3	58 ± 18.3	<0.001**
Stay (days), mean ± SD	22.7 ± 22.1	22 ± 20.4	24.9 ± 26	0.003**
APR-DRGs weight, mean ± SD	2.7 ± 2.2	2.7 ± 2	2.8 ± 2.8	<0.001**
Cost (euros), mean ± SD	11,620 ± 11,816	11,436 ± 9,969	12,137 ± 15,900	<0.001**
Re-admission, No. (%)	663 (14.6)	363 (10.8)	300 (24.9)	<0.001*
Death, No. (%)	761 (16.7)	454 (13.6)	307 (25.5)	<0.001*

*SD, standard deviation; APR-DRGs, All Patients Refined Diagnosis Related Groups; *Chi-Square test; ** Mann-Whitney U-test.*

TABLE 1 | Annual incidence rate of *Pneumocystis* pneumonia (PcP), Spain, 2008–2012.

Year	Spanish population*	Total		HIV-negative		HIV-positive	
		PcP cases	Incidence rate§ (95% CI)	PcP cases	Incidence rate§ (95% CI)	PcP cases	Incidence rate§ (95% CI)
2008	46,157,822	917	19.9 (18.6–21.2)	201	4.4 (3.8–5)	716	15.5 (14.4–16.7)
2009	46,745,807	986	21.1 (19.8–22.4)	256	5.5 (4.8–6.2)	730	15.6 (14.5–16.8)
2010	47,021,031	833	17.7 (16.5–19)	192	4.1 (3.5–4.7)	641	13.6 (12.6–14.7)
2011	47,190,493	884	18.7 (18–20)	256	5.4 (4.8–6.1)	628	13.3 (12.3–14.4)
2012	47,265,321	934	19.8 (19–21.1)	299	6.3 (5.6–7.01)	635	13.4 (12.4–15)
p (coefficient)**			0.476 (−0.007)		<0.001 (0.08)		0.001 (−0.03)

**Source: Instituto Nacional de Estadística (Spain); § per million inhabitants; CI, (confidence interval); ** Temporal trends were investigated by Poisson regression. A positive coefficient indicate an increase in the incidence and a negative value a decrease in the incidence.*

TABLE 3 | Annual change of study variables in HIV-negative cases of *Pneumocystis* pneumonia, Spain, 2008–2012.

Year	*n*	Sex (male), %	Age (years), mean ± SD	Stay (days), mean ± SD	APR-DRGs weight, mean ± SD	Cost (euros), mean ± SD	Re-admission, %	Mortality, %
2008	201	57.2	56 ± 19.9	25.5 ± 26.1	2.5 ± 1.9	10,534 ± 7,916	26.4	24.9
2009	255	60.9	55.9 ± 19.1	23.4 ± 17.2	2.5 ± 2.1	10,598 ± 8,835	22.3	19.5
2010	193	57.8	57.2 ± 17.8	26.3 ± 27.6	2.6 ± 3.5	12,567 ± 17,288	23.4	29.7
2011	256	69.1	57.8 ± 17.6	23.7 ± 20.1	2.5 ± 3.4	12,631 ± 17,143	23.8	27.7
2012	299	56.5	61.5 ± 17.2	25.8 ± 34.1	2.7 ± 4.1	13,827 ± 21,452	28.1	26.4
Mean	240.8	60.5	57.9 ± 18.3	24.9 ± 26	2.6 ± 3.2	12,138 ± 15,900	24.9	25.5
p	<0.001*	0.022*	0.002**	0.828***	0.317**	<0.001***	0.527*	0.115*

*SD, standard deviation; APR-DRGs, All Patients Refined Diagnosis Related Groups (standardized stratifier in four levels of severity whose weight increases as the severity of the patient increases); *Chi-square test; **ANOVA, *** Kruskal Wallis H-test.*

TABLE 4 | Risk category for *Pneumocystis* pneumonia (PcP) in HIV-negative patients, Spain, 2008–2012.

Risk category	No. (%)
Hematologic malignances	349 (29)
Chronic lung diseases	192 (15.9)
Malignances other than hematologic	179 (14.9)
Autoimmune diseases*	93 (7.7)
Chronic nephropathies	68 (5.6)
Treatment with chemotherapy	59 (5)
Any transplant	54 (4.5)
Hematologic disorders other than malignances	21 (1.7)
Chronic liver diseases	14 (1.2)
Unknown	176 (14.5)

**Rheumatoid arthritis, systemic lupus erythematosus, polymyositis, dermatomyositis, chronic mixed connective tissue disease, Crohn's disease, and systemic vasculitis.*

administrative record that must be completed in all hospitals in Spain. The clinical variables are obtained through the discharge report and, as such, if the coders of the different centers interpret the clinical data recorded in a different manner, there could be reliability and variability problems.

However, the coding is carried out by experts who receive specific training and use a standardized coding regulation (17), which reduces the possibility of information bias. Moreover, the CMBD database covers 98% of hospital discharges from public hospitals in Spain (18), and a significant percentage of discharges in private hospitals, which in 2012 was more than 60% (19). Therefore, taking into account that PcP is a disease treated while the patients are hospitalized, our results are representative of the epidemiology of this disease for the Spanish territory.

In our survey, the total number of patients hospitalized because of PcP in Spain between 2008 and 2012 was 4,554, with an average annual incidence of 19.4 cases per million inhabitants that, interestingly, remained stable during the study period. The incidence observed is lower than that found in previous studies carried out in the Spanish region of Andalusia in the 1988–1999 period (34 cases per million inhabitants) (20). These findings are explained by the decrease in HIV-infected patients after the generalization of the HAART treatment and are in line with other epidemiological studies carried out in Spain (21) and Europe (4, 11, 22).

26.4% of cases of PcP were recorded in patients without HIV infection with a mean annual incidence rate in this patient group of 5.1 cases per million inhabitants, which is similar to that reported in the United Kingdom in the 2006–2010 period (5.1 cases per million inhabitants) (11), which confirms that it is not an isolated phenomenon in our country.

During the study period in this group, there was a progressive increase in the incidence of the disease and a parallel increase in the percentage of cases in this group with respect to the overall amount of patients diagnosed. This trend is also in line with previous analyses carried out by our group in which the proportion of PcP cases in patients without HIV infection was 13% in a study carried out in the Spanish region of Andalusia (1998–1999 period) (20), and of the 18% in another previous nationwide study that we carried out in Spain (2003–2007 period) (23). This trend has also been observed in the United Kingdom in the 2000–2010 period, where there was an annual increase of 9% in patients not infected by HIV, and a parallel annual decrease of 7% in patients with HIV infection (11). However, the rising PcP rate is not always true, as there was a dip from 2009 to 2010.

Regarding the epidemiological and clinical presentation spectrum, independent of the cause of immunosuppression, PcP in patients without HIV infection continue to be more severe than those observed in HIV-infected patients and they have higher intrahospital mortality and re-admission rates, as was reported in previous studies (22, 24), however, in some of them, mortality rates of up to 38% (25) have been reported. This situation could be the result of the presence of underlying diseases with a worse prognosis than HIV infection, a delay in diagnosis and the start of suitable treatment for PcP due to the lower index of suspicion (20) or else, it could be secondary to a greater pulmonary inflammatory response to *Pneumocystis* in this patient group (2, 7, 9).

During the study period, in patients without HIV infection, an increase in the mean age of patients hospitalized due to PcP was observed, results that could be related to a greater survival rate of the subjects at risk of having the disease. However, the intermediate indicators related to the complexity of the patients and the management of the PcP, such as the APR-DRG weight, mean hospitalization and the re-admission rate remained stable.

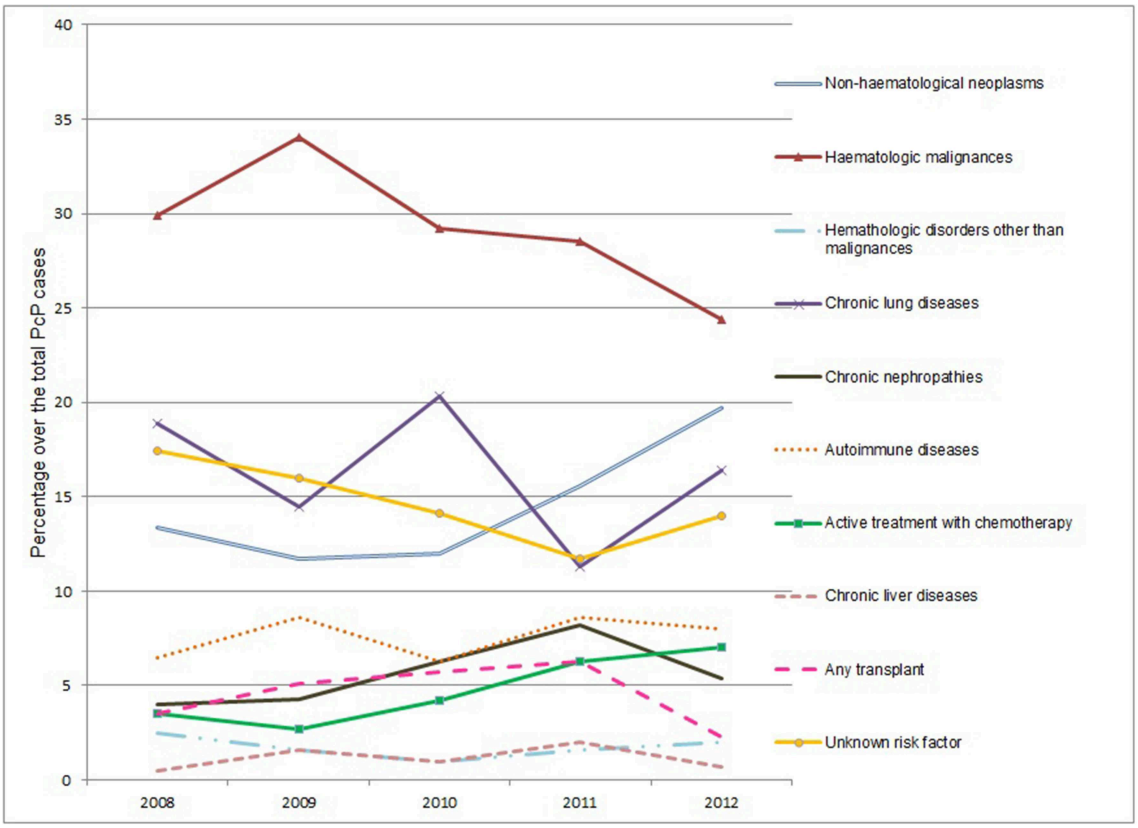

FIGURE 1 | Risk factors for *Pneumocystis* pneumonia among HIV-negative patients during the study period, Spain, 2008–2012. Changes 2012 vs. 2008 (Chi-Square test): non-hematological neoplasms ($p = 0.067$); hematologic malignances ($p = 0.177$); Hematologic disorders other than malignances ($p = 0.726$); chronic lung diseases ($p = 0.467$); chronic nephropathies ($p = 0.482$); autoimmune diseases ($p = 0.514$); active treatment with chemotherapy ($p = 0.069$); chronic liver diseases ($p = 1$); any transplant ($p = 0.307$); unknown risk factor ($p = 0.309$).

Moreover, our results show that PcP episodes have a high cost, in which we observed during the period an increase in the cost of hospitalization that is not related to the greater complexity of patients or greater mean hospitalization, and which does not allow for a decrease in re-admissions and which, simply, could be in relation to the inflation that fluctuated in this period in Spain between 4.1 and 2.4% per year (13).

With regard to PcP risk factors in patients without HIV infection, those most commonly observed in our study were hematological neoplasms (29%), as occurred in previous studies (11). The proportion of cases of this subgroup is slightly lower than that which we observed in the 2003–2007 period, which was 34% (23), probably as a result of the greater use of prophylaxis, which is a now widely accepted recommendation in patients with hematological neoplasms (26, 27).

Moreover, during the study period a rise in the proportion of cases in the category of solid neoplasms was observed, increasing from 13.4% in 2008 to 19.7% in 2012, being much higher than the reported in other series (11, 16). We would have to relate these results to the increasingly more common use of aggressive chemotherapy protocols (27). Furthermore, as in other studies (11, 28), it is confirmed that patients with chronic lung diseases are currently a new risk group, being in our study the second clinical category most commonly associated with PcP. In this regard, numerous studies have highlighted that *P. jirovecii* colonization (identification of the pathogen in respiratory samples in patients which do not have pneumonia) is a common biological phenomenon in patients with chronic obstructive pulmonary disease (40.5%), cystic fibrosis (21.5%), or interstitial lung disease (33.8%) (29–31) and, as such, this group could represent an important species-specific reservoir of *Pneumocystis* infection.

Due to all of the above, PcP could currently be considered to be an emerging disease in immunocompromised subjects without HIV infection, as a result of the growing number of patients who receive immunosuppression therapy and aggressive chemotherapy protocols for the control of neoplasms, which are known risk factors for the development of PcP described above (2, 6, 8, 9, 11, 15, 16) and for the emergence of new and unknown risk groups such as patients with chronic lung diseases in which there is a delay in diagnosis and there are no defined chemoprophylaxis guidelines.

CONCLUSION

The results show that, despite the general belief that PcP is an uncommon disease after the generalization of HAART for HIV infection, its epidemiological impact is still significant in Spain. Its incidence has increased in patients without HIV infection in whom, in addition to classic risk factors such as solid or hematological neoplasms, new emerging risk groups have been identified, such as patients with chronic lung diseases; however, in almost 15% of them it was not possible to identify the predisposing factor, which is not surprising, bearing in mind that 10% of the general population may be colonized by the disease (32). PcP mortality in patients without HIV infection continues to be high (25.5%), and an increase in the mean age and in the cost of caring for patients was observed during the study period, not related to the increase of the clinical complexity or mean hospitalization.

Our findings justify the need to carry out new studies that allow for a better characterization of PcP risk groups in patients without HIV infection and, in this manner, define more effective prevention and early diagnosis guidelines that allow the growth and mortality of this devastating illness to be halted.

DATA AVAILABILITY STATEMENT

The datasets generated for this study are available on request to the corresponding author.

ETHICS STATEMENT

The project was approved by the Clinical Research Ethics Committee (CEIC) of the Hospital Universitario Virgen del Rocío. According to Spanish law, patient consent is not required for register-based studies. No further ethical permissions are required for the analyses of these anonymized patient-level data.

AUTHOR CONTRIBUTIONS

EC and FM conceived and designed the research. EP-D and FM collected and analyzed the data and wrote the draft of the manuscript. JG performed the statistical analysis. EP-D, FM-V, CH, and FM contributed to the development of the study and interpreted the data. All authors reviewed and approved the final version of the manuscript.

FUNDING

This study was supported, in part, by the Institute of Health Carlos III, Spanish Ministry of Economy, Industry and Competitiveness (grant FIS-03/1743). Additional support for this work was provided by the Red Iberoamericana sobre Pneumocystosis in the framework of The Ibero-American Programme for Science, Technology and Development (grant CYTED 212RT0450).

ACKNOWLEDGMENTS

We acknowledge support of the publication fee by the CSIC Open Access Publication Support Initiative through its Unit of Information Resources for Research (URICI).

REFERENCES

1. Morris A, Lundgren JD, Masur H, Walzer PD, Hanson DL, Frederick T, et al. Current epidemiology of *Pneumocystis* pneumonia. *Emerg Infect Dis*. (2004) 10:1713–20. doi: 10.3201/eid1010.030985
2. Morris A, Norris KA. Colonization by *Pneumocystis jirovecii* and its role in disease. *Clin Microbiol Rev*. (2012) 25:297–317. doi: 10.1128/CMR.00013-12
3. Kaplan JE, Hanson D, Dworkin MS, Frederick T, Bertolli J, Lindegren ML, et al. Epidemiology of human immunodeficiency virus-associated opportunistic infections in the United States in the era of highly active antiretroviral therapy. *Clin Infect Dis*. (2000) 30:S5–14. doi: 10.1086/313843
4. Weverling GJ, Mocroft A, Ledergerber B, Kirk O, Gonzáles-Lahoz J, d'Arminio Monforte A, et al. Discontinuation of *Pneumocystis carinii* pneumonia prophylaxis after start of highly active antiretroviral therapy in HIV-1 infection. *EuroSIDA study group*. *Lancet*. (1999) 353:1293–8. doi: 10.1016/S0140-6736(99)03287-0
5. De Armas YR, Wissmann G, Müller AL, Pederiva MA, Brum MC, Brackmann RL, et al. *Pneumocystis jirovecii* pneumonia in developing countries. *Parasite*. (2011) 18:219–28. doi: 10.1051/parasite/2011183219
6. Calderón EJ, Gutiérrez-Rivero S, Durand-Joly I, Dei-Cas E. *Pneumocystis* infection in humans: diagnosis and treatment. *Expert Rev Anti Infect Ther*. (2010) 8:683–701. doi: 10.1586/eri.10.42
7. Varela JM, Medrano FJ, Dei-Cas E, Calderon EJ. *Pneumocystis jirovecii* pneumonia in AIDS patients. In: Zajac V, editor. *Microbes, Viruses and Parasites in AIDS Process*. Rijeka: InTech (2011). p. 113–42. Available online at: https://www.intechopen.com/books/microbes-viruses-and-parasites-in-aids-process/pneumocystis-jirovecii-pneumonia-in-aids-patients
8. Fillatre P, Decaux O, Jouneau S, Revest M, Gacouin A, Robert-Gangneux F, et al. Incidence of *Pneumocystis jiroveci* pneumonia among groups at risk in HIV-negative patients. *Am J Med*. (2014) 127:1242.e11–17. doi: 10.1016/j.amjmed.2014.07.010
9. Carmona EM, Limper AH. Update on the diagnosis and treatment of *Pneumocystis* pneumonia. *Ther Adv Respir Dis*. (2011) 5:41–59. doi: 10.1177/1753465810380102
10. Thomas S, Vivancos R, Corless C, Wood G, Beeching NJ, Beadsworth MB. Increasing frequency of *Pneumocystis jirovecii* pneumonia in renal transplant recipients in the United Kingdom: clonal variability, clusters, and geographic location. *Clin Infect Dis*. (2011) 53:307–8. doi: 10.1093/cid/cir329
11. Maini R, Henderson KL, Sheridan EA, Lamagni T, Nichols G, Delpech V, et al. Increasing *Pneumocystis* pneumonia, England, UK, 2000-2010. *Emerg Infect Dis*. (2013) 19:386–92. doi: 10.3201/eid1903.121151
12. Alvaro-Meca A, Palomares-Sancho I, Diaz A, Resino R, De Miguel AG, Resino S. *Pneumocystis* pneumonia in HIV-positive patients in Spain: epidemiology and environmental risk factors. *J Int AIDS Soc*. (2015) 18:19906. doi: 10.7448/IAS.18.1.19906
13. Spanish Statistical Office. *Instituto Nacional de Estadística de España. Índice de Precios de Consumo (IPC)*. Base 2011. Año 2012. (2018). Available online at: http://www.ine.es/jaxiT3/Datos.htm?t=2852 (accessed June 8, 2019).

14. Agency for Healthcare Research and Quality (AHRQ) through a Federal-State-Industry partnership. *Clinical Classifications Software (CCS) for ICD-9-CM*. (2018). Available online at: http://www.hcup-us.ahrq.gov/toolssoftware/ccs/ccs.jsp (accessed May 6, 2019).
15. Pagano L, Fianchi L, Mele L, Girmenia C, Offidani M, Ricci P, et al. *Pneumocystis carinii* pneumonia in patients with malignant haematological diseases: 10 years'experience of infection in GIMEMA centres. *Br J Haematol*. (2002) 117:379–86. doi: 10.1046/j.1365-2141.2002.03419.x
16. Liu Y, Su L, Jiang SJ, Qu H. Risk factors for mortality from *pneumocystis carinii* pneumonia (PCP) in non-HIV patients: a meta-analysis. *Oncotarget*. (2017) 8:59729–39. doi: 10.18632/oncotarget.19927
17. Ministry of Health, Consumption and Social Welfare of Spain. *Manual de usuario Mi CMBD*. (2014). Available online at: http://icmbd.es/docs/manualMiCMBD.pdf (accessed June 8, 2019).
18. Ministry of Health, Consumption and Social Welfare of Spain. *Hospital Discharge Records in the National Health System*. CMBD (2018). Available online at: https://pestadistico.inteligenciadegestion.mscbs.es/publicoSNS/Comun/DefaultPublico.aspx (accessed September 16, 2019).
19. Ministry of Health, Consumption and Social Welfare of Spain. *Explotación estadística del Conjunto Mínimo Básico de Datos Hospitalarios*. Norma estatal 2012. Notas Metodológicas (2012). Available online at: https://www.mscbs.gob.es/estadEstudios/estadisticas/docs/NormaGRD2012/2012_norma_estatal_not_metod.pdf (accessed June 8, 2019).
20. Calderón EJ, Varela JM, Medrano FJ, Nieto V, González-Becerra C, Respaldiza N, et al. Epidemiology of *Pneumocystis carinii* pneumonia in southern Spain. *Clin Microbiol Infect*. (2004) 10:673–6. doi: 10.1111/j.1469-0691.2004.00921.x
21. López-Sánchez C, Falcó V, Burgos J, Navarro J, Martín MT, Curran A, et al. Epidemiology and long-term survival in HIV-infected patients with *Pneumocystis jirovecii* pneumonia in the HAART era: experience in a university hospital and review of the literature. *Medicine*. (2015) 94:e681. doi: 10.1097/MD.0000000000000681
22. Roux A, Canet E, Valade S, Gangneux-Robert F, Hamane S, Lafabrie A, et al. *Pneumocystis jirovecii* pneumonia in patients with or without AIDS, France. *Emerg Infect Dis*. (2014) 20:490–7. doi: 10.3201/eid2009.131668
23. García-López A. *Clinical and epidemiological characteristics of Pneumocystis pneumonia in patients without HIV infection in Spain in the period 2003-2007* (Master's thesis). University of Seville, Seville, Spain (2014).
24. Monnet X, Vidal-Petiotm E, Osman D, Hamzaoui O, Durrbach A, Goujard C, et al. Critical care management and outcome of severe *Pneumocystis pneumonia* in patients with and without HIV infection. *Crit Care*. (2008) 12:R28. doi: 10.1186/cc6806
25. Roblot F, Godet C, Le Moal G, Garo B, Faouzi Souala M, Dary M, et al. Analysis of underlying diseases and prognosis factors associated with *Pneumocystis carinii* pneumonia in immunocompromised HIV-negative patients. *Eur J Clin Microbiol Infect Dis*. (2002) 21:523–31. doi: 10.1007/s10096-002-0758-5
26. Green H, Paul M, Vidal L, Leibovici L. Prophylaxis for *Pneumocystis* pneumonia (PCP) in non-HIV immunocompromised patients. *Cochrane Database Syst Rev*. (2014) 10:CD005590. doi: 10.1002/14651858.CD005590.pub3
27. Maertens J, Cesaro S, Maschmeyer G, Einsele H, Donnelly JP, Alanio A, et al. *ECIL guidelines for preventing Pneumocystis jirovecii pneumonia in patients with haematological malignancies and stem cell transplant recipients. J Antimicrob Chemother*. (2016) 71:2397–404. doi: 10.1093/jac/dkw157
28. Ricciardi A, Gentilotti E, Coppola L, Maffongelli G, Cerva C, Malagnino V, et al. Infectious disease ward admission positively influences *P. jiroveci* pneumonia (PjP) outcome: a retrospective analysis of 116 HIV-positive and HIV-negative immunocompromised patients. *PLoS ONE*. (2017) 12:e0176881. doi: 10.1371/journal.pone.0176881
29. Calderon EJ, Regordan C, Medrano FJ, Ollero M, Varela JM. *Pneumocystis carinii* infection in patients with chronic bronchial disease. *Lancet*. (1996) 347:977. doi: 10.1016/S0140-6736(96)91468-3
30. Probst M, Ries H, Schmidt-Wieland T, Serr A. Detection of *Pneumocystis carinii* DNA in patients with chronic lung diseases. *Eur J Clin Microbiol Infect Dis*. (2000) 19:644–5. doi: 10.1007/s100960000329
31. Gutiérrez S, Respaldiza N, Campano E, Martínez-Risquez MT, Calderón EJ, De la Horra C. *Pneumocystis jirovecii* colonization in chronic pulmonary disease. *Parasite*. (2011) 18:121–6. doi: 10.1051/parasite/2011182121
32. Medrano FJ, Montes-Cano M, Conde M, de la Horra C, Respaldiza N, Gasch A, et al. *Pneumocystis jirovecii in general population. Emerg Infect Dis*. (2005) 11:245–50. doi: 10.3201/eid1102.040487

Conflict of Interest: The authors declare that the research was conducted in the absence of any commercial or financial relationships that could be construed as a potential conflict of interest.

frontiers in Public Health

BRIEF RESEARCH REPORT
published: 15 October 2019
doi: 10.3389/fpubh.2019.00292

Genetic Polymorphisms of Superoxide Dismutase Locus of *Pneumocystis jirovecii* in Spanish Population

Rubén Morilla[1,2,3], *Amaia González-Magaña*[2,3], *Vicente Friaza*[4], *Yaxsier de Armas*[4], *Francisco J. Medrano*[2,3], *Enrique J. Calderón*[2,3]* *and Carmen de la Horra*[2,3]

[1] *Department of Nursing, Universidad de Sevilla, Seville, Spain,* [2] *Instituto de Biomedicina de Sevilla, Hospital Universitario Virgen del Rocío, Consejo Superior de Investigaciones Científicas, Universidad de Sevilla, Seville, Spain,* [3] *Centro de Investigación Biomédica en Red de Epidemiología y Salud Pública (CIBERESP), Hospital Universitario Virgen del Rocío, Seville, Spain,* [4] *Hospital Microbiology Department, Institute of Tropical Medicine "Pedro Kourí", Havana, Cuba*

Objective: *Pneumocystis* pneumonia remains a major opportunistic infection in immunocompromised patients worldwide. Colonization with *Pneumocystis jirovecii* has recently gained attention as an important issue for understanding the complete cycle of human *Pneumocystis* infection. *P. jirovecii* Superoxide Dismutase (SOD) gene could be a molecular target with high clinical relevance, but the epidemiological information about SOD genotypes distribution is scarce. The aim of this work was to provide information about the prevalence of genotypes of *Pneumocystis* SOD among Spanish patients and to describe possible differences between colonized and *Pneumocystis* pneumonia patients.

Methods: we developed a cross-sectional study analyzing broncho-alveolar lavage fluid samples from 30 *Pneumocystis* pneumonia patients, 30 colonized patients, and 20 controls using a nested PCR protocol designed to amplify the sodA gene of *P. jirovecii*. The diagnostic yield of SOD Nested PCR was evaluated against the routine practice of mtLSUrRNA Nested PCR, which is considered the gold standard.

Results: SOD locus was amplified in 90% of *Pneumocystis* pneumonia patients, 10% of colonized patients, and none of controls. Genotype SOD1 was observed in 11 cases (52.4%) and genotype SOD2 in 10 cases (47.6%). Genotype SOD2 was observed only in *Pneumocystis* pneumonia patients while the genotype SOD1 was observed in both colonized and *Pneumocystis* pneumonia patients.

Conclusions: This study provides epidemiological information about SOD genotypes distribution in Spain, showing a low genetic diversity and a predominant presence of genotype SOD1 in colonized patients. SOP Nested PCR was more sensitive and accurate assay in *Pneumocystis* pneumonia patients than in colonized individuals.

Keywords: *Pneumocystis*, molecular epidemiology, superoxide dismutase, colonization, Spain

OPEN ACCESS

Edited by:
Olga Matos,
New University of Lisbon, Portugal

Reviewed by:
Walter Mazzucco,
University of Palermo, Italy
Mengyan Wang,
Hangzhou Xixi Hospital, China

***Correspondence:**
Enrique J. Calderón
sandube@cica.es

Specialty section:
This article was submitted to Epidemiology, a section of the journal Frontiers in Public Health

Received: *27 July 2019*
Accepted: *27 September 2019*
Published: *15 October 2019*

Citation:
Morilla R, González-Magaña A, Friaza V, de Armas Y, Medrano FJ, Calderón EJ and de la Horra C (2019) Genetic Polymorphisms of Superoxide Dismutase Locus of Pneumocystis jirovecii in Spanish Population. Front. Public Health 7:292. doi: 10.3389/fpubh.2019.00292

INTRODUCTION

Pneumocystis pneumonia (PcP) remains a major opportunistic infection in HIV-infected patients in both developed and developing countries and an emerging problem in immunocompromised patients without HIV infection worldwide (1). Today, the interest in *Pneumocystis* infection goes beyond PcP because a new spectrum of disease seems to emerge in immunocompetent individuals.

The presence of *Pneumocystis jirovecii* in patients with underlying chronic diseases such as chronic obstructive pulmonary disease or interstitial lung diseases has been suggested to be a comorbidity factor (2, 3). But also, *Pneumocystis* colonization has gained attention as an important issue for understanding the complete cycle of human *Pneumocystis* infection.

For *Pneumocystis* infection diagnosis in humans, conventional or real-time PCR assays based on the amplification of the large subunit of mitochondrial ribosomal DNA (mtLSU rDNA) are the most commonly used, but many other sequences have been targeted. Among the most assessed sequences are the major surface glycoprotein, the small subunit of mitochondrial ribosomal DNA (mtSSU rDNA), the internal transcribed spacers, the thymidylate synthase, the dihydrofolate reductase, or the heat-shock protein (4).

Superoxide dismutases (SOD; EC 1.15.1.1) are ubiquitous key enzymes involved in the cellular defense against oxidative stress. These enzymes catalyse the first step of the detoxification of the superoxide anion in a metal cofactor dependent reaction and result essential in cellular protection against reactive oxygen species (ROS). There are several classed of SOD that have different cofactor metal present in the active site (5–7).

The gene encoding a manganese-dependent superoxide dismutase (MnSOD) has been characterized in *Pneumocystis* from rat, mouse, rabbit, pig, monkey, and human (8). Five genotypes have been described heretofore of which three are the most frequent: SOD1 (110C; 215T), SOD2 (110T; 215C), and SOD3 (110T, 215T) (9–11).

This gene has been used in a few epidemiological studies mainly into a multilocus approach (9–12) but the epidemiological information about SOD genotypes distribution is scarce.

The aim of this work was to provide information about the prevalence of genotypes of *Pneumocystis* SOD among Spanish patients and to describe possible differences between colonized and PcP patients.

MATERIALS AND METHODS

This study had a cross-sectional design and included 80 not selected successive male or female patients over age 18 years who were admitted to the bronchoscopy unit between 2006 and 2014 for evaluation of their disease at Virgen del Rocio University Hospital, of whom an bronchoalveolar lavage (BAL) specimen was available for analysis. Children were exclude of this study. In all cases, informed consent was obtained from the patients before obtain of BAL fluid. The study was approved by the hospital's ethics committee and it was performed according ethical principles regarding human experimentation contained in Declaration of Helsinki.

Thirty patients had AIDS-related PcP, 30 were Chronical Obstructive Pulmonary Disease (COPD) patients colonized by *P. jirovecii* without clinical or radiological signs of PcP and 20 were control patients with different lung diseases without *Pneumocystis* colonization or infection. All of them were Caucasian of Spanish origin. A single individual of control group was HIV-infected, other three were organs transplant recipients.

In all cases the presence or absence of *Pneumocystis* was confirmed by analyzing BAL samples with nested PCR amplification of the mtLSUrDNA gene of *Pneumocystis* (13). A colonized subject was defined as an individual without signs or symptoms of pneumonia from whom a respiratory sample was obtained that contained *Pneumocystis*-DNA detectable by PCR. A PcP patient was defined as an individual with a clinical pneumonia who had *P. jirovecii* in respiratory samples identified by microscopy or molecular methods without other causal agents.

The samples were separated into two aliquots of 250 μl that were cryopreserved at −20°C. DNA extraction was performed with commercial Kit NucleoSpin Tissue (Macherey-Nagel) following the manufacturer's recommendations. Extracted DNA was eluted with 55 μl of ultrapure water. Its concentration and purity (A260/A280) was determined, discarding A260/A280 values >2 and lower than 1.6, which would indicate contamination by proteins and RNA, respectively.

Samples that had been identified as positive by nested PCR of the mtLSUrRNA gene were further examined to study SOD gene. A nested PCR protocol was designed to amplify a locus of the *sodA* gene of *P. jirovecii* which included in the first amplification round, the use of the external primers MnSODFw(-5′-GGT TTA ATT AGT CTT TTA GGC AC-3′) y SODR4-(5′-CCA AGA ATA ACT TTG CCT TGA G-3′) to obtain a 584 bp fragment. The second round of amplification utilized the primers FS2-(5′-TCT TTC TCA TGA TTT GCT TGA GG-3′) and RS2-(5′-CTT TCC TAT ACC TAC CAC CAC C-3′) and yielded a 218 bp product. Rounds included 35 and 40 cycles of amplification, respectively. The PCR products were analyzed by electrophoresis on a 2% agarose gel containing ethidium bromide, and the bands were visualized by UV light. To prevent false positives due to contamination, pipette tips with filters were used at all stages. DNA extraction, preparation of the reaction mixture, PCR amplification, and detection were performed in different areas of the laboratory. In addition, a positive control was included in each reaction. To detect any cross-contamination, all PCR steps were performed with a negative control of sterile water. All experiments were repeated at least twice.

The products of positive nested PCR for SOD locus were purified by columns of Sephacryl S-400 (Amersham Pharmacia Biotech). Genetic characterization was performed by direct sequencing in the Genomics Service of the Institute of Biomedicine of Seville (IBiS), where they were injected into capillary sequencer ABI PRISM 3500 DNA Analyzer of Applied Biosystems.

The consensus SOD gene sequence was obtained from the NCBI web-page with the identification code and the polymorphisms were analyzed as previously described at position 110 (Y:C or T) and 215 (Y:C or T). Sequencing files were opened with Chromas lite 2.1.1 software and converted to FASTA format, in order to align the MEGA software vs. 6.0.

Finally, nested PCR for SOD assay was evaluated for sensitivity and specificity against the routine practice of Nested PCR for mtLSUrRNA gene, which is considered as gold standard. Specimens were considered true positive if they were positive by both PCR, and true negative if negative by both PCR. The diagnostic accuracy (ACC) was defined as follows:

TABLE 1 | Characteristics of patients in study and results of the molecular typing by subgroups.

Patients	*N*	Sex (% males)	Age ($\bar{X} \pm$ SD, years)	Sequenced/ amplified samples	Genotype SOD1 (110C; 215T)	Genotype SOD2 (110T; 215C)
PcP	30	73.3%	41.12 ± 12.05	19/27	9	10
COPD colonized	30	90.0%	66.19 ± 12.50	2/3	2	0
Non colonized	20	70.0%	47.21 ± 18.45	–	–	

$\bar{X}$, Mean; sd, standard deviation; PcP, Pneumocystis pneumonia; COPD, Chronic obstructive pulmonary disease.

TABLE 2 | Comparing characteristics and properties of SOD nested PCR as diagnostic test between PcP patients and colonized patients using mtLSU nested PCR as gold standard.

Diagnostic variable	PcP patients	Colonized COPD patients
Sensitivity, % (95% CI)	80% (62.7–90.5%)	10% (3.5–25.6%)
Specificity, % (95% CI)	100% (83.9–100%)	100% (83.9-100%)
PPV, % (95% CI)	100% (86.2–100%)	100% (43.8–100%)
NPV, %(95% CI)	76.92% (57.9–89%)	42.6% (29.5–56.7%)
FPR, %(95% CI)	0% (0–16.1%)	0% (0–16.1%)
FNR, %(95% CI)	20% (9.5–37.3%)	90% (74.4–96.5%)
Accuracy, %(95% CI)	88% (76.2–94.4%)	46% (33–59.6%)
Youden's index	0.8	0.1
Likelihood ratio (–), (95% CI)	0.2 (0.1–0.41)	0.9 (0.8–1.1)

PPV, Positive predictive value; NPV, negative predictive value; FPR, False positive rate; FNR, False negative rate; PcP, Pneumocystis pneumonia; COPD, Chronic obstructive pulmonary disease.

$ACC = (TP + TN)/(P + N)$ in which TP = true positive; TN = true negative; P = number of positive and N = number of negative. In addition, we calculated the Youden's J statistic (also called Youden's index) as a single statistic that captures the performance of a dichotomous diagnostic test.

RESULTS

Pneumocystis jirovecii SOD gene was detected 30 out of 80 patients, in 90% (27/30) of PcP patients, in 10% (3/30) of COPD colonized patients and in none on control patients.

SOD typing was possible in 19 of the 27 PcP patients and in two of the three COPD patients in which SOD gene was detected by PCR. Genotype SOD1 (110C; 215T) was identified in 11 cases and genotype SOD2 (110T; 215C) was identified in 10 cases (**Table 1**).

SOD Nested-PCR results were compared with data of Nested PCR for mtLSUrRNA gene, regarded as diagnostic gold standard, and concordances calculated among the results obtained. There were SOD Nested-PCR agreement with mtLSUrRNA Nested-PCR in 90% of PcP cases, in 10% of COPD colonized patients, and 100% of non-infected controls.

The likelihood positive ratio, sensitivity, and specificity, Predictive Negative Value, Predictive Positive Value, diagnostic accuracy and Youden's index of SOD Nested-PCR in PcP and colonized COPD patients are showed in **Table 2**.

DISCUSSION

This study provides some epidemiological information about SOD genotypes distribution in Spain and shows that there are a low genetic diversity circulating in our area.

In our study, only two (SOD1 and SOD2) of the five genotypes described in the literature has been observed. These genotypes has been described as the most prevalent in several epidemiological studies (9, 10, 12, 14–16). Similarly, they are the only ones detected in other studies (12, 15). In this sense, the genotypic distribution of this locus in our region is similar to that described in London, UK, and Harare, Zimbabwe (15, 16) and differs from whose reported in France, Cuba and Portugal, where they have also detected other genotypes (9, 10, 14). These results support the possible existence of geographic differences in the distribution of these genotypes, but further of multicentre studies covering a larger sample would be needed for confirmation.

None of the genotypes seems to be predominant over the other among the PcP patients included in our study. Nonetheless, despite appearing in only two cases, it is noteworthy that the genotype found in the colonized subjects is the SOD1 (110C, 215T). This is consistent with data that suggest a potential association between this genotype with moderate or low microorganism load, which could be related with lower virulence and have clinical implications (11). However, it needs to be taken account that these are preliminary findings to be confirmed by future studies on a larger sample of patients.

In our study, differences between the values obtained for AIDS-related PcP and COPD colonized patients are probably due to different amplification rates obtained in each group due to lower parasite burden in colonized patients than in PcP patients (17).

The difficult to identify the SOD gene is due to it is a nuclear unicopy gene, while the mtLSU gene is located in mitochondrial ribosomes and therefore multicopy (4). This would explain why in colonized individuals where the parasite load is usually quite low, SOD gene is much more difficult to detect.

This characteristic could be useful in clinical use to distinguish colonized patients of PcP patients. However, SOP Nested PCR should not use alone for clinical diagnosis because, whilst it has a good specificity (100%), it has a low sensitivity (80%). Notwithstanding the foregoing, SOP Nested PCR could be used together with more sensitive PCR as those that target multicopies genes in a multiplex PCR as an early, discriminating, and accurate tool to diagnose PcP (18).

On the other hand, the lower sensitivity of SOP Nested PCR in colonized individuals (10%) and the poor diversity of genotypes limits its usefulness in multilocus genotyping studies that include not only PcP patients but also colonized individuals.

However, these conclusions need to be taken with a degree of caution as small size of study and because the information provided by a cross-sectional design is limited. Therefore, carrying out future more comprehensive studies to further define the role of SOP nested PCR in epidemiological studies of *Pneumocystis* infection and its utility in clinical diagnosis would be desirable.

DATA AVAILABILITY STATEMENT

The sequences of polymorphisms described in our paper can be found in Genbank under accession numbers: MG010739.1; MG010730.1.

ETHICS STATEMENT

The studies involving human participants were reviewed and approved by Comité de ética de la investigación del Hospital Universitario Virgen del Rocío. The patients/participants provided their written informed consent to participate in this study.

AUTHOR CONTRIBUTIONS

EC and CH conceived and designed the research. AG-M and VF collected and analyzed the data. YA and FM performed the statistical analysis. VF, AG-M, CH, and FM contributed to the development of the study and interpreted the data. RM and EC wrote the draft of the manuscript. All authors reviewed and approved the final version of the manuscript.

FUNDING

This study was supported, in part, by the Red Iberoamericana sobre Pneumocystosis in the framework of The Ibero-American Programme for Science, Technology and Development (grant CYTED 212RT0450).

REFERENCES

1. Calderón EJ, de Armas Y, Panizo MM, Wissmann G. *Pneumocystis jirovecii* pneumonia in Latin America. A public health problem? *Expert Rev Anti Infect Ther.* (2013) 11:565–70. doi: 10.1586/eri.13.41
2. Gutiérrez S, Respaldiza N, Campano E, Martínez-Risquez MT, Calderón EJ, De la Horra C. *Pneumocystis jirovecii* colonization in chronic pulmonary disease. *Parasite.* (2011) 18:121–6. doi: 10.1051/parasite/2011182121
3. Martínez-Rísquez MT, Friaza V, de la Horra C, Martín-Juan J, Calderón EJ, Medrano FJ. *Pneumocystis jirovecii* infection in patients with acute interstitial pneumonia. *Rev Clin Esp.* (2018) 218:417–20. doi: 10.1016/j.rceng.2018.04.013
4. Calderón EJ, Gutiérrez-Rivero S, Durand-Joly I, Dei-Cas E. *Pneumocystis* infection in humans: diagnosis and treatment. *Expert Rev Anti Infect Ther.* (2010) 8:683–701. doi: 10.1586/eri.10.42
5. Valko M, Leibfritz D, Moncol J, Cronin MT, Mazur M, Telser J. Free radicals and antioxidants in normal physiological functions and human disease. *Int J Biochem Cell Biol.* (2007) 39:44–84. doi: 10.1016/j.biocel.2006.07.001
6. Brioukhanov AL, Netrusov AI, Eggen RI. The catalase and superoxide dismutase genes are transcriptionally up-regulated upon oxidative stress in the strictly anaerobic archaeon *Methanosarcina barkeri*. *Microbiology.* (2006) 152:1671–7. doi: 10.1099/mic.0.28542-0
7. Zeinali F, Homaei A, Kamrani E. Sources of marine superoxide dismutases: characteristics and applications. *Int J Biol Macromol.* (2015) 79:627–37. doi: 10.1016/j.ijbiomac.2015.05.053
8. Denis CM, Mazars E, Guyot K, Odberg-Ferragut C, Viscogliosi E, Dei-Cas E, et al. Genetic divergence at the SODA locus of six different formae speciales of *Pneumocystis carinii*. *Med Mycol.* (2000) 38:289–300. doi: 10.1080/714030952
9. Maitte C, Leterrier M, Le Pape P, Miegeville M, Morio F. Multilocus sequence typing of *Pneumocystis jirovecii* from clinical samples: how many and which loci should be used? *J Clin Microbiol.* (2013) 51:2843–9. doi: 10.1128/JCM.01073-13
10. Monroy-Vaca EX, de Armas Y, Illnait-Zaragozí MT, Diaz R, Toraño G, Vega D, et al. Genetic diversity of *Pneumocystis jirovecii* in colonized Cuban infants and toddlers. *Infect Genet Evolut.* (2014) 22:60–6. doi: 10.1016/j.meegid.2013.12.024
11. Esteves F, Gaspar J, de Sousa B, Antunes F, Mansinho K, Matos O. *Pneumocystis jirovecii* multilocus genotyping in pooled DNA samples: a new approach for clinical and epidemiological studies. *Clin Microbiol Infect.* (2012) 18:E177–84. doi: 10.1111/j.1469-0691.2012.03828.x
12. Esteves F, Gaspar J, De Sousa B, Antunes F, Mansinho K, Matos O. Clinical relevance of multiple single-nucleotide polymorphisms in *Pneumocystis jirovecii* Pneumonia: development of a multiplex PCR-single-base-extension methodology. *J Clin Microbiol.* (2011) 49:1810–5. doi: 10.1128/JCM.02303-10
13. Pederiva MA, Wissmann G, Friaza V, Morilla R, de La Horra C, Montes-Cano MA, et al. High prevalence of *Pneumocystis jirovecii* colonization in Brazilian cystic fibrosis patients. *Med Mycol.* (2012) 50:556–60. doi: 10.3109/13693786.2011.645892
14. Esteves F, Gaspar J, Tavares A, Moser I, Antunes F, Mansinho K, et al. Population structure of *Pneumocystis jirovecii* isolated from immunodeficiency virus-positive patients. *Infect Genet Evolut.* (2010) 10:192–9. doi: 10.1016/j.meegid.2009.12.007
15. Wakefield AE, Lindley AR, Ambrose HE, Denis CM, Miller RF. Limited asymptomatic carriage of *Pneumocystis jiroveci* in human immunodeficiency virus-infected patients. *J Infect Dis.* (2003) 187:901–8. doi: 10.1086/368165
16. Miller RF, Lindley AR, Malin AS, Ambrose HE, Wakefield AE. Isolates of *Pneumocystis jirovecii* from Harare show high genotypic similarity to isolates from London at the superoxide dismutase locus. *Trans R Soc Trop Med Hyg.* (2005) 99:202–6. doi: 10.1016/j.trstmh.2004.09.005
17. Fauchier T, Hasseine L, Gari-Toussaint M, Casanova V, Marty PM, Pomares C. Detection of *Pneumocystis jirovecii* by quantitative PCR to differentiate colonization and pneumonia in immunocompromised HIV-positive and HIV-negative patients. *J Clin Microbiol.* (2016) 54:1487–95. doi: 10.1128/JCM.03174-15
18. Montesinos I, Delforge ML, Ajjaham F, Brancart F, Hites M, Jacobs F, et al. Evaluation of a new commercial real-time PCR assay for diagnosis of *Pneumocystis jirovecii* pneumonia and identification of dihydropteroate synthase (DHPS) mutations. *Diagn Microbiol Infect Dis.* (2017) 87:32–6. doi: 10.1016/j.diagmicrobio.2016.10.005

Conflict of Interest: The authors declare that the research was conducted in the absence of any commercial or financial relationships that could be construed as a potential conflict of interest.

frontiers in Microbiology

ORIGINAL RESEARCH
published: 22 October 2019
doi: 10.3389/fmicb.2019.02401

Genotyping and Zoonotic Potential of *Enterocytozoon bieneusi* in Pigs in Xinjiang, China

Dong-Fang Li[1,2†], Ying Zhang[1†], Yu-Xi Jiang[1], Jin-Ming Xing[1], Da-Yong Tao[1], Ai-Yun Zhao[1], Zhao-Hui Cui[2], Bo Jing[1], Meng Qi[1] and Long-Xian Zhang[2]**

[1] College of Animal Science, Tarim University, Alar, China, [2] College of Animal Science and Veterinary Medicine, Henan Agricultural University, Zhengzhou, China

OPEN ACCESS

Edited by:
Olga Matos,
New University of Lisbon, Portugal

Reviewed by:
Fernando Izquierdo Arias,
CEU San Pablo University, Spain
Maria Luisa Lobo,
New University of Lisbon, Portugal

***Correspondence:**
Meng Qi
qimengdz@163.com
Long-Xian Zhang
zhanglx8999@henau.edu.cn

[†] These authors have contributed equally to this work

Specialty section:
This article was submitted to Infectious Diseases, a section of the journal Frontiers in Microbiology

Received: 19 August 2019
Accepted: 04 October 2019
Published: 22 October 2019

Citation:
Li D-F, Zhang Y, Jiang Y-X, Xing J-M, Tao D-Y, Zhao A-Y, Cui Z-H, Jing B, Qi M and Zhang L-X (2019) Genotyping and Zoonotic Potential of Enterocytozoon bieneusi in Pigs in Xinjiang, China. Front. Microbiol. 10:2401. doi: 10.3389/fmicb.2019.02401

Enterocytozoon bieneusi is an obligate intracellular fungus, infecting various invertebrate and vertebrate hosts, it is common in humans and causes diarrhea in the immunocompromised. In the present study, 801 fecal specimens were collected from pigs on seven large-scale pig farms in Xinjiang, China. Nested polymerase chain reaction (PCR) amplification of the internal transcribed spacer (ITS) gene showed that the overall *E. bieneus*i infection rate was 48.6% (389/801). The *E. bieneusi* infection rates differed significantly among the collection sites (20.0–73.0%) (χ^2 = 75.720, *df* = 6, $p < 0.01$). Post-weaned pigs had the highest infection rate (77.2%, 217/281), followed by fattening pigs (67.4%, 87/129) and pre-weaned suckling pigs (35.5%, 60/169). Adult pigs had the lowest infection rate (11.3%, 25/222). The *E. bieneusi* infection rates also differed significantly among age groups (χ^2 = 246.015, *df* = 3, $p < 0.01$). Fifteen genotypes were identified, including 13 known genotypes (CHC, CS-1, CS-4, CS-7, CS-9, D, EbpA, EbpC, EbpD, H, PigEb4, PigEBITS5, and WildBoar8) and two novel genotypes (XJP-II and XJP-III). Among them, six genotypes (CS-4, D, EbpA, EbpC, H, and PigEBITS5) have been reported in humans. Phylogenetic analysis showed that all the genotypes belonged to Group 1 of *E. bieneusi*. These findings suggest that pigs may play an important role in transmitting *E. bieneusi* infections to humans.

Keywords: *Enterocytozoon bieneusi*, infection rate, novel genotype, potential zoonotic, pig

INTRODUCTION

Over 1300 microsporidial species infect a variety of invertebrate and vertebrate hosts, *Enterocytozoon bieneusi* is considered the most common microsporidial species to cause opportunistic infections in humans (Sak et al., 2011; Matos et al., 2012). *E. bieneusi* infections cause diarrhea, malabsorption and possible lung pathologies, and host health status is the main influencing factor (del Aguila et al., 1997; Matos et al., 2012). *E. bieneusi* is transmitted mainly via the fecal-oral route through ingestion of contaminated water or food or accidental ingestion of spores eliminated in the feces of infected animals or humans (Stentiford et al., 2016).

Analysis of the ribosomal internal transcribed spacer (ITS) nucleotide sequence polymorphism is widely used for *E. bieneusi* molecular typing (Santín and Fayer, 2011; Zhang et al., 2011; Karim et al., 2014; Liu et al., 2017; Deng et al., 2018). Over 470 *E. bieneusi* genotypes have been identified from the ITS gene in humans, mammals, birds and water; however, this pathogen also exists in many undefined areas worldwide (Henriques-Gil et al., 2010; Li D. et al., 2019). Phylogenetic analysis has revealed high diversity and genetic variation among isolates from human and animal origins, and these isolates are clustered into 11 major genetic groups (Galván-Díaz et al., 2014; Wang et al., 2019).

Studies have identified zoonotic *E. bieneusi* genotypes from pigs in China, thus implicating pigs as dispersing agents and a potential source of human infections (Li et al., 2014a,b, 2017;

TABLE 1 | *Enterocytozoon bieneusi* occurrence and genotype distribution in pigs in Xinjiang, China.

Collection site	No. positive/No. specimens	% (95 CI)	*Enterocytozoon bieneusi* genotypes (n)
Marabishi	48/98	49.0 (38.9–59.1)	CHC5 (1), CS-7 (3), **D** (6), **EbpA** (1), ***EbpC*** (34), EbpD (1), **PigEBITS5** (2),
Alaer	19/95	20.0 (11.8–28.2)	**D** (1), ***EbpC*** (17), **H** (1)
Yarkant	63/130	48.5 (39.8–57.2)	CHC5 (1), **D** (8), ***EbpA*** (43), **EbpC** (9), **PigEBITS5** (2),
Baicheng	67/99	67.7 (58.3–77.1)	***EbpA*** (50), **EbpC** (10), **PigEBITS5** (7)
Shaya	73/100	73.0 (64.1–81.9)	CS-1 (3), CS-4 (20), CS-9 (1), ***EbpA*** (11), ***EbpC*** (11), EbpD (3), PigEb4 (12), **PigEBITS5** (6), WildBoar8 (3), XJP-II (2), XJP-III (1)
Changji	49/130	37.7 (29.3–46.1)	**EbpA** (19), ***EbpC*** (27), EbpD (1), **PigEBITS5** (2)
Ruoqiang	70/149	47.0 (38.9–55.1)	CS-1 (2), **D** (2), **EbpA** (5), ***EbpC*** *(60)*, **H** (1)
Total	389/801	48.6 (45.1–52.0)	CHC5 (2), CS-1 (5), **CS-4 (20)**, CS-7 (3), CS-9 (1), **D (17)**, **EbpA (129)**, ***EbpC (168)***, EbpD (5), **H (2)**, PigEb4 (12), **PigEBITS5 (19)**, WildBoar8 (3), XJP-II (2), XJP-III (1)

Genotypes detected in humans are in bold, and dominant genotypes are in italics.

TABLE 2 | *Enterocytozoon bieneusi* occurrence and genotype in pigs in China.

Province	No. of positive/No. of examined (%)	*Enterocytozoon bieneusi* genotypes (n)	References
Guangdong	19/72(26.4%)	EbpA[a] (1), ***EbpC*** (17), GD1 (1)	Zou et al., 2018
Heilongjiang[c]	351/641(54.8%)	CC-1 (2), CHN7/O (1), CS-1 (8), CS-1/EbpC (1), CS-2 (1), CS-3 (1), CS-3/EbpA[a] (2), CS-4 (34), CS-5 (1), CS-6 (1), CS-7 (1), CS-8 (4), CS-10 (1), D (20), EbpA[a] (37), EbpA[a]/EbpC (4), EbpA[a]/Henan-IV (1), EbpB (28), EbpB/EbpC (1), ***EbpC*** (61), EbpC/Henan-IV (1), EbpC/O (30), EbpD (1), H (18), Henan-IV (6), HLJ-I (2), HLJ-II (1), HLJ-III (1), HLJ-IV (1), LW1 (1), O (18), PigEBITS5[a]/Henan-IV (1)	Li et al., 2014a,c; Zhao et al., 2014; Wan et al., 2016
Henan[b]	744/1372(54.2%)	CHC5 (4), CM8 (11), ***EbpA***[a] (154), ***EbpC*** (278), G (10), H (14), HN-1 (6), HN-2 (2), HN-3 (1), HN-4 (1), Henan-III (1), LW1 (12), PigEBITS4[a] (24), PigEbITS5[a] (17), XZP-II (1)	Wang et al., 2018a; Li W. et al., 2019
Inner mongolia	3/8(37.5%)	CHN7 (1), EbpC (1), O (1)	Li et al., 2014a,c
Jilin[c]	145/330(43.9%)	CHN1 (4), CHN7 (11), CHN8 (1), CHN9 (1), CHN10 (2), CS-1 (3), CS-1/G (1), CS-4 (4), CS-6/EbpA[a] (1), CS-8 (1), CS-9 (1), CS-9/EbpB (6), CS-9/EbpD (1), EBITS3 (1), ***EbpA***[a] (34), EbpA[a]/EbpC (8), ***EbpC*** (30), H/EbpC (1), Henan-III (1), Henan-IV (2), LW1[a] (4), O (2)	Li et al., 2014a,b,c; Wan et al., 2016; Zhang et al., 2011
Liaoning[c]	13/73(17.4%)	EbpB/EbpC (6)	Li et al., 2014c; Wan et al., 2016
Shaanxi	442/560(78.9%)	CHC5 (31), CHG3 (1), CHN7 (1), CS-4 (1), D (1), EbpA[a] (20), H (4), Henan-IV (3), PigEB4 (3), PigEBITS4[a] (33), PigEBITS5[a] (13), SHZA1 (2), SHZC1 (1), SLTC1 (2), ***SLTC2*** (59), SLTC3 (15), SMXB1 (1), SMXC1 (1), SMXD1 (1), SMXD2 (1), SYLA1 (2), SYLA2 (1), SYLA3 (1), SYLA4 (1), ***SYLA5*** (56), SYLC1 (1), SYLD1 (1), SZZA1 (1), SZZA2 (8), SZZB1 (1), SZZC1 (3), ***SZZD1*** (81), SZZD2 (1)	Wang et al., 2018b
Sichuan	230/623(36.9%)	CHC5 (10), D (1), EbpA[a] (22), ***EbpC*** (143), Henan-IV (24), PigEBITS4[a] (12), PigEBITS5 (1), SH8[a] (6), WildBoar 7 (1), WildBoar 8[a] (7), WildBoar 11 (1), SC02 (1), SCT01 (1), SCT02 (1)	Li et al., 2017; Luo et al., 2019
Tibet	309/715(43.2%)	D (1), ***EbpC*** (302), I (2), XZP-I (1), XZP-II (3)	Li W. et al., 2019
Yunnan	59/200(29.5%)	D (1), EbpA[a] (15), ***EbpC*** (31), G (1), H (1), Henan-IV (6), PigEBITS5[a] (1), YN1 (1), YN2 (2), YN3 (1)	Zou et al., 2018
Zhejiang	47/124(37.9%)	CAF-1 (2), EbpA[a] (2), ***EbpC*** (39), PigEBITS5[a] (2), ZJ1 (1), ZJ2 (1)	Zou et al., 2018

[a]Enterocytozoon bieneusi genotypes with synonyms were amended using the nomenclature system established by Santín and Fayer, 2009: EbpA (synonyms: CHS5, F), PigEBITS4 (synonyms: CHG19, PEbD), PigEBITS5 (synonyms: PEbA), SH8 (synonyms: WildBoar 10), and WildBoar8 (synonyms: WildBoar9). [b]Partial PCR samples were selected for sequencing. [c]Partial PCR samples were not successfully sequenced. Dominant genotypes are in italics.

Li W. et al., 2019; Zhao et al., 2014; Wan et al., 2016; Wang et al., 2018a; Zou et al., 2018; Luo et al., 2019). In China, Xinjiang Uygur Autonomous Region (hereafter referred to as Xinjiang) lies in inland Eurasia and has a typical half-arid/arid climate (34°25′–48°10′ N, 73°40′–96°18′ E). It is the largest provincial-level administrative region by land area and a historically important passage of the ancient silk road. Information on the occurrence of *E. bieneusi* in pigs in Xinjiang is scarce; therefore, this study was conducted to examine the occurrence of *E. bieneusi* in pigs in Xinjiang, China, and to assess the zoonotic transmission risk of this pathogen.

MATERIALS AND METHODS

Ethics Statement

Permission was obtained from animal owners or managers before collecting specimens, and no specific permits were required for the described field studies. All work involving animals was carried out in accordance with the Regulations for the Administration of Affairs Concerning Experimental Animals. The Research Ethics Committee of Henan Agricultural University reviewed and approved our study (approval no. LVRIAEC 2017-019).

Fecal Specimen Collection, DNA Extraction, and Purification

Eight hundred one fresh fecal specimens were collected from Duroc and Landrace pigs on seven large-scale intensive pig farms in Xinjiang between September 2017 and June 2018. Each sampled farm contained 10000–80000 pigs. All farms were visited on a single occasion. A veterinarian randomly collected the fecal specimens either from the rectum or from the internal portion of a stool sample on the ground avoid possible contamination from the specimen surface touched the ground. All specimens (approximately 5–30 g) were collected using sterile disposal latex gloves; marked with the date, age, and farm; stored in insulated boxes; and transferred to the laboratory. Collected specimens included 169 fecal specimens from pre-weaned suckling pigs (<20 days old), 281 specimens from post-weaned suckling pigs (21–70 days old), 129 specimens from fattening pigs (71–180 days old), and 222 specimens from sows (>181 days old).

Genomic DNA was directly extracted from the fecal specimens (approximately 200 mg) using the E.Z.N.A.® Stool DNA Kit (Omega Biotek Inc., Norcross, GA, United States) per the manufacturer's instructions with minor modifications. The extracted DNA was stored at −20°C prior to polymerase chain reaction (PCR) analysis.

PCR Amplification and Sequence Analysis

Enterocytozoon bieneusi was identified via nested PCR amplification and sequencing of the ITS region of the rRNA gene. The primers and thermal cycle parameters used for the two PCR amplifications have been described previously (Buckholt et al., 2002). The outer primers were EBITS3 (5′-GGTCATAGGGATGAAGAG) and EBITS4 (5′-TTCGAGTTCTTTCGCGCTC), and the cycling parameters were 35 cycles of 94°C for 30 s, 57°C for 30 s, and 72°C for 40 s. The inner primers were EBITS1 (5′-GCTCTGAATATCTATGGCT) and EBITS2.4 (5′-ATCGCCGACGGATCCAAGTG), and the cycling parameters were 30 cycles of 94°C for 30 s, 55°C for 30 s, and 72°C for 40 s. The 2×EasyTaq PCR SuperMix (TransGene Biotech Co., Beijing, China) was used for PCR amplification. All PCR assays included both a positive control (DNA from dairy cattle-derived genotype I) and a negative control (distilled water). PCR amplification was repeated twice for each specimen.

Positive secondary PCR products (∼390 bp) were sequenced by GENEWIZ (Suzhou, China), and all products were sequenced in both directions to ensure accurate sequencing results. ClustalX 2.1[1] was used to align the resulting DNA sequences. Sequences obtained were aligned with reference sequences downloaded from the National Center for Biotechnology Information[2] to determine genotypes. The nucleotide sequences obtained in the present study were submitted to GenBank[3] under accession numbers MK778892–K778899 and MK778901–MK778907.

Phylogenetic and Statistical Analysis

Bayesian inference (BI) and Monte Carlo Markov chain methods were used to construct phylogenetic trees in MrBayes,

[1]http://www.clustal.org/

[2]https://www.ncbi.nlm.nih.gov/

[3]https://www.ncbi.nlm.nih.gov/genbank/

TABLE 3 | *Enterocytozoon bieneusi* occurrence and genotypes in pigs of different ages.

Age (days)	No. positive/No. specimens	% (95 CI)	*Enterocytozoon bieneusi* genotypes (n)
Pre-weaned	60/169	35.5 (28.2–42.8)	***EbpC*** (24), **EbpA** (12), **D** (11), PigEb4 (5), **PigEBITS5** (4), **CS-4** (3), WildBoar8 (1)
Post-weaned	217/281	77.2 (72.3–82.2)	***EbpC*** (105), **EbpA** (64), **PigEBITS5** (11), CS-4 (9), **D** (6), PigEb4 (5), EbpD (4), CS-1 (4), CS-7 (3), WildBoar8 (2), CHC5 (1), **H** (1), XJP-1 (2)
Fattening pigs	87/129	67.4 (59.2–75.6)	***EbpA*** (46), **EbpC** (26), **CS-4** (7), **PigEBITS5** (3), CHC5 (1), CS-1 (1), CS-9 (1), **H** (1), XJP-2 (1)
Sow	25/222	11.3 (7.1–15.5)	***EbpC*** (13), **EbpA** (7), PigEb4 (2), **CS-4** (1), EbpD (1), **PigEBITS5** (1)

Genotypes detected in humans are in bold and dominant genotypes were in italics.

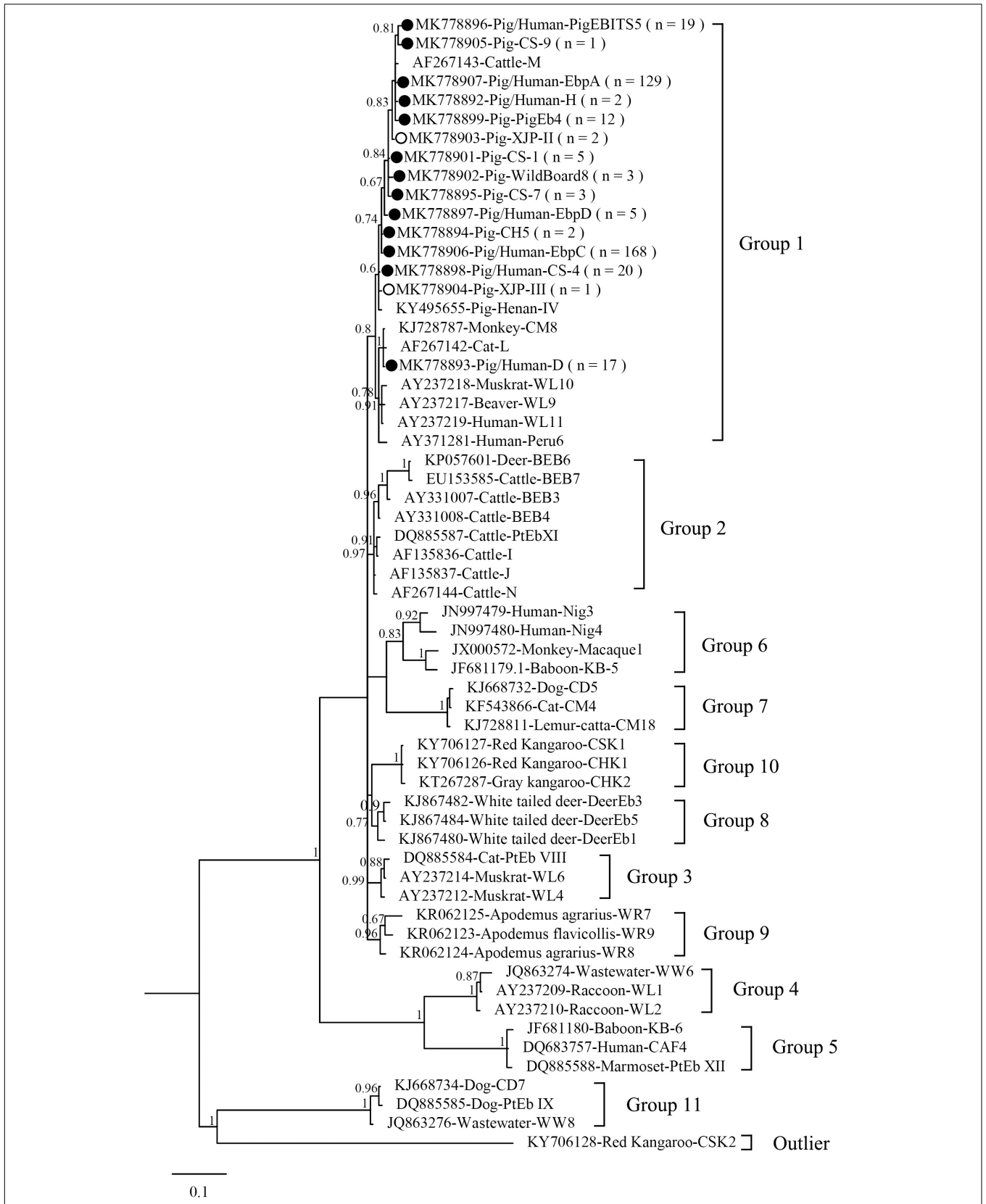

FIGURE 1 | Phylogenetic tree based on Bayesian analysis of the ITS sequences. Statistically significant posterior probabilities are indicated on the branches. Known and novel *Enterocytozoon bieneusi* genotypes identified in the present study are indicated by filled and hollow circles, respectively.

version 3.2.6[4]. The posterior probability values were calculated by running 1,000,000 generations. A 50% majority-rule consensus tree was constructed from the final 75% of the trees generated via BI. Analyses were run three times to ensure convergence and insensitivity to priors.

The Statistical Package for the Social Sciences (SPSS, version 22.0, available at https://www.ibm.com) was used for the statistical analyses, including Fisher's exact test and 95% confidence intervals. Differences with $p < 0.05$ were considered significant.

RESULTS AND DISCUSSION

In the present study, the overall *E. bieneusi* infection rate in pigs was 48.6% (389/801) (**Table 1**), which was higher than most previously reported rates from Chinese provinces, including Guangdong (26.4%, 19/72) (Zou et al., 2018), Inner Mongolia (37.5%, 3/8) (Li et al., 2014a,c), Jilin (43.9%, 145/330) (Zhang et al., 2011; Li et al., 2014a,b,c; Wan et al., 2016), Liaoning (17.4%, 13/73) (Li et al., 2014c; Wan et al., 2016), Sichuan (36.9%, 230/623) (Li et al., 2017; Luo et al., 2019), Tibet (43.2%, 309/715) (Li W. et al., 2019), Yunnan (29.5%, 59/200) and Zhejiang (37.9%, 47/124) (Zou et al., 2018), but lower than that from Shaanxi (78.9%, 442/560) (Wang et al., 2018b; **Table 2**). The differences in *E. bieneusi* infection rates may be partially attributed to differences in feeding densities, comparisons with cages that had lower pig densities, and greater opportunities for *E. bieneusi* transmission among animals in high densely packed cages (Wang et al., 2018b).

The *E. bieneusi* infection rates significantly differed among the collection sites ($\chi^2 = 75.720$, $df = 6$, $p < 0.01$). The highest infection rate was found on a farm from Shaya (73.0%, 73/100) (**Table 1**). The *E. bieneusi* infection rate also differed significantly among age groups ($\chi^2 = 246.015$, $df = 3$, $p < 0.01$). Post-weaned pigs had the highest infection rate (77.2%, 217/281), while adult pigs (sows) had the lowest infection rate (11.3%, 25/222) (**Table 3**). Most previous studies included information on *E. bieneusi* for different age groups of pigs in China. High *E. bieneusi* infection rates were found in pre-weaned and post-weaned pigs from Heilongjiang (78.4%, 87/111; 70.4%, 50/71), Jilin (68.8%, 22/32; 74.6%, 53/71), Zhejiang (54.7%, 76/139), and Henan Provinces (54.2%, 137/253) (Li et al., 2014b, Li W. et al., 2019; Wan et al., 2016; Zou et al., 2018). The higher prevalence among post-weaned pigs may have been due to lower immunity and stress from early wean (Wang et al., 2018b). However, high *E. bieneusi* infection rates were found in fattening pigs from Liaoning (100%, 3/3), Jilin (35.7%, 20/56), Tibet (75.5%, 173/229) and Yunnan Provinces (21%, 42/200) (Wan et al., 2016; Zou et al., 2018; Li W. et al., 2019). The differences in *E. bieneusi* infection rates in these age groups may be partially attributed to differences in geoecology, rearing conditions, animal husbandry, and feeding densities.

From 389 positive specimens, 15 *E. bieneusi* genotypes were identified from nucleotide sequences via ITS-PCR. These included 13 known genotypes (CHC5, CS-1, CS-4, CS-9, CS-7, D, EbpA, EbpC, EbpD, H, PigEb4, PigEBITS5, and WildBoard8) and 2 novel genotypes (named XJP-II and XJP-III; **Table 1**). EbpC (43.2%, 168/389) and EbpA (33.2%, 129/389) were the predominant genotypes in pigs in Xinjiang (**Table 1**). The dominant genotypes also varied across sample regions. Genotype EbpC was dominant in Marabishi, Alaer, Changji, and Ruoqiang; genotype EbpA was dominant in Yarkant and Baicheng; and genotype CS-4 was dominant and identified only in Shaya (**Table 1**). In addition, the *E. bieneusi* genotype distribution differed among ages. Genotype EbpC was predominant in pre-weaned, post-weaned, and adult pigs, while EbpA predominated in fattening pigs. These results were similar to those reported for Guangdong, Henan, Jilin, Sichuan, Tibet, Yunnan and Zhejiang Provinces in China, where reported genotypes EbpC and EbpA were predominant in pigs (Li et al., 2014a,b, 2017, Li W. et al., 2019; Zhao et al., 2014; Wan et al., 2016; Wang et al., 2018a; Zou et al., 2018; Luo et al., 2019; **Table 2**).

Of the 120 *E. bieneusi* genotypes reported in pigs worldwide (Sak et al., 2008; Němejc et al., 2014; Fiuza et al., 2015; Prasertbun et al., 2017; Wang et al., 2018a,b), over 80 have been reported in pigs in China (Wan et al., 2016; Wang et al., 2018b,c; Li W. et al., 2019). Fifteen genotypes were identified in the present study, of which, six (CS-4, D, EbpA, EbpC, H and PigEBITS5) have been identified in humans. Genotypes CS-4, D, EbpA, EbpC, and H were identified in children and HIV/AIDS patients from China (Wang et al., 2013; Yang et al., 2014; Liu et al., 2017). These results suggest that pigs play an important role in transmitting *E. bieneusi* to humans and other animals.

Figure 1 shows the phylogeny of the ITS sequences from the 15 genotypes identified in the present study, and all genotypes identified were classified in Group 1. Accumulating evidence suggests that genotypes in Group 1 have significant zoonotic importance but no strong host specificity (Wan et al., 2016; Li and Xiao, 2019; Li W. et al., 2019). Although direct evidence linking human infections to *E. bieneusi* of animal origin is lacking, direct contact with pigs or with a water supply contaminated by pig waste are considered significant risk factors for zoonotic transmission (Cama et al., 2007).

CONCLUSION

This study revealed that *E. bieneusi* is common in pigs in Xinjiang, China. Thirteen known genotypes and two novel genotypes (XIP-II and XIP-III) were classified in Group 1, and showed six of the 15 identified genotypes have been found in humans, indicating that pigs may be reservoirs for zoonotic transmission of human microsporidiosis. These findings extend the knowledge of the *E. bieneusi* distribution among pigs in China.

DATA AVAILABILITY STATEMENT

The datasets generated for this study can be found in GenBank under the accession numbers MK778892–K778899 and MK778901–MK778907.

[4]http://mrbayes.sourceforge.net/

ETHICS STATEMENT

Permission was obtained from animal owners or managers before collecting specimens, and no specific permits were required for the described field studies. All work involving animals was carried out in accordance with the Regulations for the Administration of Affairs Concerning Experimental Animals. The Research Ethics Committee of Henan Agricultural University reviewed and approved our study (approval no. LVRIAEC 2017-019).

AUTHOR CONTRIBUTIONS

MQ and L-XZ designed the study. YZ, Y-XJ, J-MX, D-YT, A-YZ, and BJ collected and analyzed the specimens. D-FL and Z-HC analyzed the data. D-FL, MQ, and L-XZ wrote the manuscript. All authors read and approved the final manuscript.

FUNDING

This work was supported in part by the National Natural Science Foundation of China (31860699, 31702227, and 31660712) and the Program for Young and Middle-aged Leading Science, Technology, and Innovation of Xinjiang Production & Construction Group (2018CB034). The sponsors played no roles in the study design or in the collection, analysis, or interpretation of the data, in writing the report, or in the decision to submit the article for publication.

ACKNOWLEDGMENTS

We thank Traci Raley, MS, ELS, from Liwen Bianji, Edanz Editing China (www.liwenbianji.cn/ac) for editing a draft of this manuscript.

REFERENCES

Buckholt, M. A., Lee, J. H., and Tzipori, S. (2002). Prevalence of *Enterocytozoon bieneusi* in swine: an 18-month survey at a slaughterhouse in Massachusetts. *Appl. Environ. Microbiol.* 68, 2595–2599. doi: 10.1128/AEM.68.5.2595-2599.2002

Cama, V. A., Pearson, J., Cabrera, L., Pacheco, L., Gilman, R., Meyer, S., et al. (2007). Transmission of *Enterocytozoon bieneusi* between a child and guinea pigs. *J. Clin. Microbiol.* 45, 2708–2710. doi: 10.1128/JCM.00725-07

del Aguila, C., Lopez-Velez, R., Fenoy, S., Turrientes, C., Cobo, J., Navajas, R., et al. (1997). Identification of *Enterocytozoon bieneusi* spores in respiratory samples from an AIDS patient with a 2-year history of intestinal microsporidiosis. *J. Clin. Microbiol.* 35, 1862–1866.

Deng, L., Li, W., Zhong, Z., Chai, Y., Yang, L., Zheng, H., et al. (2018). Molecular characterization and new genotypes of *Enterocytozoon bieneusi* in pet chipmunks (*Eutamias asiaticus*) in Sichuan province, China. *BMC Microbiol.* 18:37. doi: 10.1186/s12866-018-1175-y

Fiuza, V. R. S., Oliveira, F. C. R., Fayer, R., and Santín, M. (2015). First report of *Enterocytozoon bieneusi* in pigs in Brazil. *Parasitol. Int.* 64, 18–23. doi: 10.1016/j.parint.2015.01.002

Galván-Díaz, A. L., Magnet, A., Fenoy, S., Henriques-Gil, N., Haro, M., Gordo, F. P., et al. (2014). Microsporidia detection and genotyping study of human pathogenic *E. bieneusi* in animals from Spain. *PLoS One* 9:e92289. doi: 10.1371/journal.pone.0092289

Henriques-Gil, N., Haro, M., Izquierdo, F., Fenoy, S., and del Águila, C. (2010). Phylogenetic approach to the variability of the microsporidian *Enterocytozoon bieneusi* and its implications for inter- and intrahost transmission. *Appl. Environ. Microbiol.* 76, 3333–3342. doi: 10.1128/AEM.03026-09

Karim, M. R., Wang, R., Dong, H., Zhang, L., Li, J., Zhang, S., et al. (2014). Genetic polymorphism and zoonotic potential of *Enterocytozoon bieneusi* from nonhuman primates in China. *Appl. Environ. Microbiol.* 80, 1893–1898. doi: 10.1128/AEM.03845-13

Li, W., Deng, L., Wu, K., Huang, X., Song, Y., and Su, H. (2017). Presence of zoonotic *Cryptosporidium* scrofarum, *Giardia duodenalis* assemblage A and *Enterocytozoon bieneusi* genotypes in captive Eurasian wild boars (*Sus scrofa*) in China: potential for zoonotic transmission. *Parasit Vect.* 10:10. doi: 10.1186/s13071-016-1942-2

Li, W., Diao, R., Yang, J., Xiao, L., Lu, Y., Li, Y., et al. (2014a). High diversity of human-pathogenic *Enterocytozoon bieneusi* genotypes in swine in northeast China. *Parasitol. Res.* 113, 1147–1153. doi: 10.1007/s00436-014-3752-9

Li, W., Li, Y., Li, W., Yang, J., Song, M., Diao, R., et al. (2014b). Genotypes of *Enterocytozoon bieneusi* in livestock in China: high prevalence and zoonotic potential. *PLoS One* 9:e97623. doi: 10.1371/journal.pone.0097623

Li, W., Tao, W., Jiang, Y., Diao, R., Yang, J., and Xiao, L. (2014c). Genotypic distribution and phylogenetic characterization of *Enterocytozoon bieneusi* in diarrheic chickens and pigs in multiple cities, China: potential zoonotic transmission. *PLoS One* 9:e108279. doi: 10.1371/journal.pone.0108279

Li, W., Feng, Y., and Santin, M. (2019). Host specificity of *Enterocytozoon bieneusi* and public health implications. *Trends Parasitol.* 35, 436–451. doi: 10.1016/j.pt.2019.04.004

Li, D., Zheng, S., Zhou, C., Karim, M. R., Wang, L., Wang, H., et al. (2019). Multilocus typing of *Enterocytozoon bieneusi* in pig reveals the high prevalence, zoonotic potential, host adaptation and geographical segregation in China. *J. Eukaryot. Microbiol.* 66, 707–718. doi: 10.1111/jeu.12715

Li, W., and Xiao, L. (2019). Multilocus sequence typing and population genetic analysis of *Enterocytozoon bieneusi*: host specificity and its impacts on public health. *Front. Genet.* 10:307. doi: 10.3389/fgene.2019.00307

Liu, H., Jiang, Z., Yuan, Z., Yin, J., Wang, Z., Yu, B., et al. (2017). Infection by and genotype characteristics of *Enterocytozoon bieneusi* in HIV/AIDS patients from Guangxi Zhuang autonomous region, China. *BMC Infect. Dis.* 17:684. doi: 10.1186/s12879-017-2787-9

Luo, R., Xiang, L., Liu, H., Zhong, Z., Liu, L., Deng, L., et al. (2019). First report and multilocus genotyping of *Enterocytozoon bieneusi* from Tibetan pigs in southwestern China. *Parasite* 26:24. doi: 10.1051/parasite/2019021

Matos, O., Lobo, M. L., and Xiao, L. (2012). Epidemiology of *Enterocytozoon bieneusi* infection in humans. *J. Parasitol. Res.* 2012:981424. doi: 10.1155/2012/981424

Němejc, K., Sak, B., Květoňová, D., Hanzal, V., Janiszewski, P., Forejtek, P., et al. (2014). Prevalence and diversity of *Encephalitozoon* spp. and *Enterocytozoon bieneusi* in wild boars (Sus scrofa) in Central Europe. *Parasitol. Res.* 113, 761–767. doi: 10.1007/s00436-013-3707-6

Prasertbun, R., Mori, H., Pintong, A. R., Sanyanusin, S., Popruk, S., Komalamisra, C., et al. (2017). Zoonotic potential of *Enterocytozoon* genotypes in humans and pigs in Thailand. *Vet. Parasitol.* 233, 73–79. doi: 10.1016/j.vetpar.2016.12.002

Sak, B., Kvác, M., Hanzlíková, D., and Cama, V. (2008). First report of *Enterocytozoon bieneusi* infection on a pig farm in the Czech Republic. *Vet. Parasitol.* 153, 220–224. doi: 10.1016/j.vetpar.2008.01.043

Sak, B., Kváč, M., Kučerová, Z., Květoňová, D., and Saková, K. (2011). Latent microsporidial infection in immunocompetent individuals-a longitudinal study. *PLoS Negl. Trop. Dis.* 5:e1162. doi: 10.1371/journal.pntd.0001162

Santín, M. and Fayer, R. (2009). *Enterocytozoon bieneusi* genotype nomenclature based on the internal transcribed spacer sequence: a consensus. *J. Eukaryot. Microbiol.* 56, 34–38. doi: 10.1111/j.1550-7408.2008.00380.x

Santín, M., and Fayer, R. (2011). Microsporidiosis: *Enterocytozoon bieneusi* in domesticated and wild animals. *Res. Vet. Sci.* 90, 363–371. doi: 10.1016/j.rvsc.2010.07.014

Stentiford, G. D., Becner, J. J., Weiss, L. M., Keeling, P. J., Didier, E. S., Williams, B. A. P., et al. (2016). Microsporidia-emergent pathogens in the global food chain. *Trends Parasitol.* 32:657. doi: 10.1016/j.pt.2016.06.002

Wan, Q., Lin, Y., Mao, Y., Yang, Y., Li, Q., Zhang, S., et al. (2016). High prevalence and widespread distribution of zoonotic *Enterocytozoon bieneusi* genotypes in

swine in Northeast China: implications for public health. *J. Eukaryot. Microbiol.* 63, 162–170. doi: 10.1111/jeu.12264

Wang, H., Zhang, Y., Wu, Y., Li, J., Qi, M., Li, T., et al. (2018a). Occurrence, molecular characterization, and assessment of zoonotic risk of *Cryptosporidium* spp., *Giardia duodenalis*, and *Enterocytozoon bieneusi* in Pigs in Henan, Central China. *J. Eukaryot. Microbiol.* 65, 893–901. doi: 10.1111/jeu.12634

Wang, S. S., Li, J. Q., Li, Y. H., Wang, X. W., Fan, X. C., Liu, X., et al. (2018b). Novel genotypes and multilocus genotypes of *Enterocytozoon bieneusi* in pigs in northwestern China: a public health concern. *Infect. Genet. Evol.* 63, 89–94. doi: 10.1016/j.meegid.2018.05.015

Wang, S. S., Wang, R. J., Fan, X. C., Liu, T. L., Zhang, L. X., and Zhao, G. H. (2018c). Prevalence and genotypes of *Enterocytozoon bieneusi* in China. *Acta Trop.* 183, 142–152. doi: 10.1016/j.actatropica.2018.04.017

Wang, H. Y., Qi, M., Sun, M. F., Li, D. F., Wang, R. J., Zhang, S. M., et al. (2019). Prevalence and population genetics analysis of *Enterocytozoon bieneusi* in dairy cattle in China. *Front. Microbiol.* 10:1399. doi: 10.3389/fmicb.2019.01399

Wang, L., Xiao, L., Duan, L., Ye, J., Guo, Y., Guo, M., et al. (2013). Concurrent infections of *Giardia duodenalis*, *Enterocytozoon bieneusi*, and *Clostridium difficile* in children during a cryptosporidiosis outbreak in a pediatric hospital in China. *PLoS Negl. Trop. Dis.* 7:e2437. doi: 10.1371/journal.pntd.0002437

Yang, J., Song, M., Wan, Q., Li, Y., Lu, Y., Jiang, Y., et al. (2014). *Enterocytozoon bieneusi* genotypes in children in Northeast China and assessment of risk of zoonotic transmission. *J. Clin. Microbiol.* 52, 4363–4367. doi: 10.1128/JCM.02295-14

Zhang, X., Wang, Z., Su, Y., Liang, X., Sun, X., Peng, S., et al. (2011). Identification and genotyping of *Enterocytozoon bieneusi* in China. *J. Clin. Microbiol.* 49, 2006–2008. doi: 10.1128/JCM.00372-11

Zhao, W., Zhang, W., Yang, F., Cao, J., Liu, H., Yang, D., et al. (2014). High prevalence of *Enterocytozoon bieneusi* in asymptomatic pigs and assessment of zoonotic risk at the genotype level. *Appl. Environ. Microbiol.* 80, 3699–3707. doi: 10.1128/aem.00807-14

Zou, Y., Hou, J. L., Li, F. C., Zou, F. C., Lin, R. Q., Ma, J. G., et al. (2018). Prevalence and genotypes of *Enterocytozoon bieneusi* in pigs in southern China. *Infect. Genet. Evol.* 66, 52–56. doi: 10.1016/j.meegid.2018.09.006

Conflict of Interest: The authors declare that the research was conducted in the absence of any commercial or financial relationships that could be construed as a potential conflict of interest.

frontiers in Microbiology

ORIGINAL RESEARCH
published: 19 December 2019
doi: 10.3389/fmicb.2019.02917

Development of a Gold Nanoparticle-Based Lateral-Flow Immunoassay for *Pneumocystis* Pneumonia Serological Diagnosis at Point-of-Care

Ana Luísa Tomás[1,2], Miguel P. de Almeida[3], Fernando Cardoso[1], Mafalda Pinto[2], Eulália Pereira[3], Ricardo Franco[2] and Olga Matos[1]**

[1] Medical Parasitology Unit, Group of Opportunistic Protozoa/HIV and Other Protozoa, Global Health and Tropical Medicine, Instituto de Higiene e Medicina Tropical, Universidade NOVA de Lisboa, Lisbon, Portugal, [2] UCIBIO, REQUIMTE, Departamento de Química, Faculdade de Ciências e Tecnologia, Universidade NOVA de Lisboa, Caparica, Portugal, [3] REQUIMTE/LAQV, Departamento de Química e Bioquímica, Faculdade de Ciências da Universidade do Porto, Porto, Portugal

OPEN ACCESS

Edited by:
Jae-Hyuk Yu,
University of Wisconsin-Madison,
United States

Reviewed by:
Jon Woods,
University of Wisconsin-Madison,
United States
Soo Chan Lee,
University of Texas at San Antonio,
United States

***Correspondence:**
Ricardo Franco
ricardo.franco@fct.unl.pt
Olga Matos
omatos@ihmt.unl.pt

Specialty section:
This article was submitted to Fungi and Their Interactions, a section of the journal Frontiers in Microbiology

Received: 04 November 2019
Accepted: 03 December 2019
Published: 19 December 2019

Citation:
Tomás AL, de Almeida MP, Cardoso F, Pinto M, Pereira E, Franco R and Matos O (2019) Development of a Gold Nanoparticle-Based Lateral-Flow Immunoassay for Pneumocystis Pneumonia Serological Diagnosis at Point-of-Care. Front. Microbiol. 10:2917. doi: 10.3389/fmicb.2019.02917

Pneumocystis jirovecii pneumonia (PcP) is a major human immunodeficiency virus (HIV)-related illness, rising among immunocompromised non-HIV patients and in developing countries. Presently, the diagnosis requires respiratory specimens obtained through invasive and costly techniques that are difficult to perform in all patients or implement in all economic settings. Therefore, the development of a faster, cost-effective, non-invasive and field-friendly test to diagnose PcP would be a significant advance. In this study, recombinant synthetic antigens (RSA) of *P. jirovecii*'s major surface glycoprotein (Msg) and kexin-like serine protease (Kex1) were produced and purified. These RSA were applied as antigenic tools in immunoenzymatic assays for detection of specific anti-*P. jirovecii* antibodies (IgG and IgM) in sera of patients with (n = 48) and without (n = 28) PcP. Results showed that only IgM anti-*P. jirovecii* levels were significantly increased in patients with PcP compared with patients without *P. jirovecii* infection ($p \leq 0.001$ with both RSA). Thus, two strip lateral flow immunoassays (LFIA), based on the detection of specific IgM anti-*P. jirovecii* antibodies in human sera samples, were developed using the innovative association of *P. jirovecii*'s RSA with spherical gold nanoparticles (AuNPs). For that, alkanethiol-functionalized spherical AuNPs with ca. ˜40 nm in diameter were synthetized and conjugated with the two RSA (Msg or Kex1) produced. These AuNP-RSA conjugates were characterized by agarose gel electrophoresis (AGE) and optimized to improve their ability to interact specifically with serum IgM anti-*P. jirovecii* antibodies. Finally, two LFIA prototypes were developed and tested with pools of sera from patients with (positive sample) and without (negative sample) PcP. Both LFIA had the expected performance, namely, the presence of a test and control red colored lines with the positive sample, and only a control red colored line with the negative sample. These results provide valuable insights into the possibility

of PcP serodiagnosis at point-of-care. The optimization, validation and implementation of this strip-based approach may help to reduce the high cost of medical diagnosis and subsequent treatment of PcP both in industrialized and low-income regions, helping to manage the disease all around the world.

Keywords: *Pneumocystis* pneumonia, gold nanoparticles, point-of-care, lateral-flow immunoassay, serological diagnosis, major surface glycoprotein, kexin-like serine protease 1, synthetic recombinant antigens

INTRODUCTION

The fungus *Pneumocystis jirovecii* is a pathogen able to cause a fatal pneumonia (PcP) in immunocompromised patients worldwide (Barry and Johnson, 2001; Huang et al., 2011; Esteves et al., 2014; Matos et al., 2017). In industrialized countries, the incidence of PcP has decreased with the widespread use of chemoprophylaxis and the introduction of combination antiretroviral therapy, but it still remains a serious clinical problem for human immunodeficiency virus (HIV)-infected patients (Huang et al., 2011; Esteves et al., 2014; Matos et al., 2017; European Centre for Disease Prevention and Control (ECDC)/WHO Regional Office for Europe, 2018). Likewise, the rising number of immunocompromised non-HIV-infected patients susceptible to *P. jirovecii* infection in these countries, warrants the need for improved diagnostic and treatment strategies (Hughes, 2005; Roux et al., 2014). In developing countries, where there is a lack of diagnostic resources and expertise, the number of PcP cases reported have been increasing significantly as more sensitive/specific laboratory methods are being used (Chakaya et al., 2003; van Oosterhout et al., 2007; Huang et al., 2011; Matos, 2012; Esteves et al., 2014; Morrow et al., 2014).

Despite all the advances in understanding *P. jirovecii* infection over the last years, in the twenty-first century the standard diagnosis of this disease still depends on the detection of *P. jirovecii* organisms through expensive and laborious technologies (cytochemical or immunofluorescent staining and/or PCR) applied to respiratory specimens obtained by invasive techniques, such as bronchoscopy (Alanio et al., 2016; Matos and Esteves, 2016; Matos et al., 2017; Tomás and Matos, 2018). These standard diagnosis methods, besides being difficult to implement in all economic settings, are not always possible to perform in patients with respiratory failure or in children (Alanio et al., 2016; Matos and Esteves, 2016; Matos et al., 2017; Tomás and Matos, 2018). Therefore, to improve disease management worldwide, there is a need to develop and implement an alternative approach for the diagnosis of PcP that can reduce associated costs, the need for invasive procedures, and also improves response time and specificity.

Lateral flow immunoassays (LFIA) offer an easy solution to these limitations as they are a simple, rapid and user friendly technique, that do not require time-consuming instrumental methods or technical expertise, allowing a low-cost point-of-care alternative (Chan et al., 2013; Pöhlmann et al., 2014; Li et al., 2015; Singh et al., 2015). Although LFIA is a well-recognized technique, a specific serological biomarker for PcP diagnosis has not been established (Morris and Masur, 2011; Esteves et al., 2015; Matos and Esteves, 2016). Yet, reports of protection against acquisition of infection by passive transfer of immune sera in mice (Gigliotti et al., 2002) and by vaccination in immunosuppressed non-human primates (Kling and Norris, 2016), triggers interest in serum antibodies as serological biomarkers of the disease. In addition, the suggestion that the IgM isotype has a predominant role in shaping the earliest steps in recognition and clearance of *Pneumocystis* infection both in mice (Rapaka et al., 2010) and in humans (Djawe et al., 2010; Tomás et al., 2016), not only support the role of antibodies in disease protection, but also highlights the idea that a serological test for PcP diagnosis is viable.

As *P. jirovecii*'s major surface glycoproteins (Msg) are characteristic of this microorganism and highly immunogenic, containing both B and T cell protective epitopes (Stringer and Keely, 2001), they are the obvious candidate to study serological responses. In fact, promising studies using recombinant antigens of this protein and antibody immunodetection techniques, have shown that patients with PcP or previous episodes of PcP present higher serum levels of anti-*P. jirovecii* antibodies than patients without *P. jirovecii* infection or without previous PcP events (Daly et al., 2004; Djawe et al., 2010; Gingo et al., 2011; Blount et al., 2012; Tomás et al., 2016). However, as Msg presents antigenic variation during infection as an evasion mechanism (Kling and Norris, 2016; Hauser, 2019), other antigenic candidates began to been explored. *Pneumocystis* kexin-like serine protease 1 (Kex1) is one of them, because it holds an antigenically stable active site peptide sequence coded by a nuclear single-copy gene (Kutty and Kovacs, 2003; Esteves et al., 2009), which avoids possible genetic variation. Therefore, recombinant Kex1 antigens were also used to study the humoral response to *P. jirovecii*, and the results suggest that a high humoral response to this protein can be detected and correlates with disease protection (Gingo et al., 2011; Kling and Norris, 2016).

Taking this into consideration and knowing that measuring the presence of biomarkers becomes quicker, more sensitive and more flexible when nanoparticles are put to work as tags or labels (Baptista et al., 2008; Baptista et al., 2011; Almeida et al., 2014), led to the idea to develop an immunonanodiagnostic platform for PcP diagnosis at point-of-care. Gold nanoparticles (AuNPs) are the nanomaterial most commonly used in the development of nanotechnology approaches for clinical diagnosis because of their ability to form conjugates with biomolecules (e.g., proteins and oligonucleotides) and due to their high surface area, stability and intense color (Nagatani et al., 2006; Baptista et al., 2008; Wilson, 2008; Franco and Pereira, 2013; O'Farrel, 2013; Almeida et al., 2014). Thus, in this study, a bionanodiagnostic platform for PcP diagnosis was developed associating recombinant synthetic

antigens of *P. jirovecii*'s Msg and Kex1 with functionalized gold nanoparticles, in order to improve detection of specific anti-*P. jirovecii* antibodies in human sera samples.

This platform, illustrated in **Figure 1**, was developed using AuNP-RSA conjugates to detect IgM anti-*P. jirovecii* antibodies in patients sera, reactive to either of the RSA, in order to allow less invasive biological specimens to be used in the diagnosis of this infectious disease. These LFIA prototypes intends to be specific, sensitive and accurate for PcP diagnosis, making a highly relevant contribution to public health and economy in industrialized countries and in communities with low-income and lack of technology, helping to manage the disease worldwide.

MATERIALS AND METHODS

Production of *P. jirovecii*'s Recombinant Synthetic Antigens (RSA) and Anti-RSA Antibodies

RSA Production and Expression

The Msg RSA was designed as previously described (Tomás et al., 2016) and Kex1 RSA followed the same procedure, studying the immunogenicity of the *P. jirovecii*'s KEX1 longest gene sequences available (GenBank: AY130996.1 and AY127566.1) (Kutty and Kovacs, 2003). The putative reactive epitopes were selected using bioinformatic tools to analyze electrochemical properties, secondary structure prediction, polarity, relative position to the membrane and hydrophobicity profile of the specific polypeptides at the online software ExPASy – ProtScale and CBS – TMHMM – version 2.0 (Dai et al., 2012, 2013; Tomás et al., 2016). Only specific and conserved regions of *Pneumocystis* KEX1 genes, presenting high similarity with the sequences previously reported in GenBank for *Pneumocystis*' Kex1 protein were considered for the final selection of the RSA composition, through the NCBI blast tool. Regions with high-predicted antigenicity and reactivity were chosen and DNA oligonucleotides coding these regions (connected by pentaglycine residues) were synthesized and cloned into the plasmid pHTP0 (Nzytech®). The insert sequences were confirmed by sequencing (Stabvida®). After synthesis, each RSA was cloned into the expression vector pLATE 31 (#K1261, Thermo Scientific®), following manufacturer's instructions. This process enabled the synthetic production of both RSA with a polyhistidine tail end (6xHis), allowing their purification by immobilized metal ion affinity chromatography (IMAC). These vectors were used to clone $CaCl_2$ competent *E. coli XJb (DE3)* cells by heat shock. Cell pellets from 15 mL of IPTG-induced cultures were re-suspended in 6 mL of lysis buffer (10 mM Tris-HCl, 50 mM KCl, 1 mM EDTA, 0.2 mM PMSF, 500 mM NaCl, 1% Triton X-100, 0.5% CHAPS, 2 mM $CaCl_2$ and 0.02 $\mu g.mL^{-1}$ DNAse I) and subjected to three cycles of a freeze-thaw method. The supernatants were removed and the pellets were re-suspended in 6 mL of 8 M Urea. An IMAC purification system (HiTrap columns, GE Healthcare®) packed with a histidine chelating resin (Ni Sepharose™ 6 FastFlow, GE Healthcare®) was used. The column was balanced with 10 mL ligation buffer [20 mM Na_2HPO_4, 500 mM NaCl, 20 mM Imidazole (pH = 7.4)], then the sample containing the RSA was applied. The column was washed with 10 mL of ligation buffer, and the RSA were eluted with 20 mL of elution buffer [20 mM Na_2HPO_4, 500 mM NaCl, 500 mM Imidazole, 5% (v/v) glycerol (pH = 7.4)]. The eluted proteins were desalted with a desalting membrane (D-0655, Sigma-Aldrich®) into a new buffer [20 mM Na_2HPO_4, 20 mM NaCl, 2% (v/v) glycerol (pH = 7.4)], analyzed by sodium dodecyl sulfate-polyacrylamide gel electrophoresis (SDS-PAGE) on 15% acrylamide gels and by indirect ELISA using anti-polyhistidine antibodies. Their final concentrations were determined (NanoDrop 1000, Thermo Scientific®) before use.

Polyclonal Anti-RSA Antibodies Production

In order to produce antibodies able to recognize the RSA produced, ascitic fluids containing polyclonal anti-RSA antibodies were produced following the protocol of Ou et al. (1993), with modifications. Briefly, after RSA purification, 50 μg of each RSA were emulsified in incomplete Freund's adjuvant plus peptide adjuvant and the emulsion was injected intraperitoneally into five 5–6 weeks old BALB/c male mice for each RSA. Subsequent immunizations with 50 μg of RSA emulsified in incomplete Freund's adjuvant, took place at 2–3 weeks interval. After four inoculations, a test-bleed (0.5 mL per animal) was tested by ELISA for titration. When serum titers against the RSA were greater or equal to 1:1000, an intraperitoneal injection of 1×10^6 cells of sarcoma 180 cell line was performed in each mouse, to obtain high titer polyclonal ascitic fluids. When a 20–25% increase in body weight of each mouse was recorded (caused by the ascite), they were euthanized and the ascitic fluids were collected and quantified (NanoDrop 1000, Thermo Scientific®). These fluids will be referred throughout this work as "AuNP-RSA antibodies."

All animals used in the study were housed and cared for under the guidelines set forth in the Guide for the Care and Use of Laboratory Animals. Good animal handling practices were used and all European Directives were followed, namely the Portuguese DL 113/2013. Experiments were conducted by people certified by the Portuguese national body for experimental animal manipulations "Direcção Geral de Alimentação e Veterinária" (DGAV). The facilities at Instituto de Higiene e Medicina Tropical/Universidade Nova de Lisboa (IHMT/UNL) animal house, procedures for maintenance and care of animals as well the experimental scheme used (immunization, blood collection, spleen removal, and euthanasia procedures) are accredited by the Portuguese DGAV and in accordance with relevant guidelines and regulations of the ethical committee of IHMT/UNL.

Human Serum Specimens

This study retrospectively analyzed sera from 76 HIV-infected patients with respiratory symptoms attending hospitals in the Lisbon area, between 2010 and 2018. Their bronchoalveolar lavage (BAL) specimens were submitted to the Group of Opportunistic Protozoa/HIV and Other Protozoa of Instituto

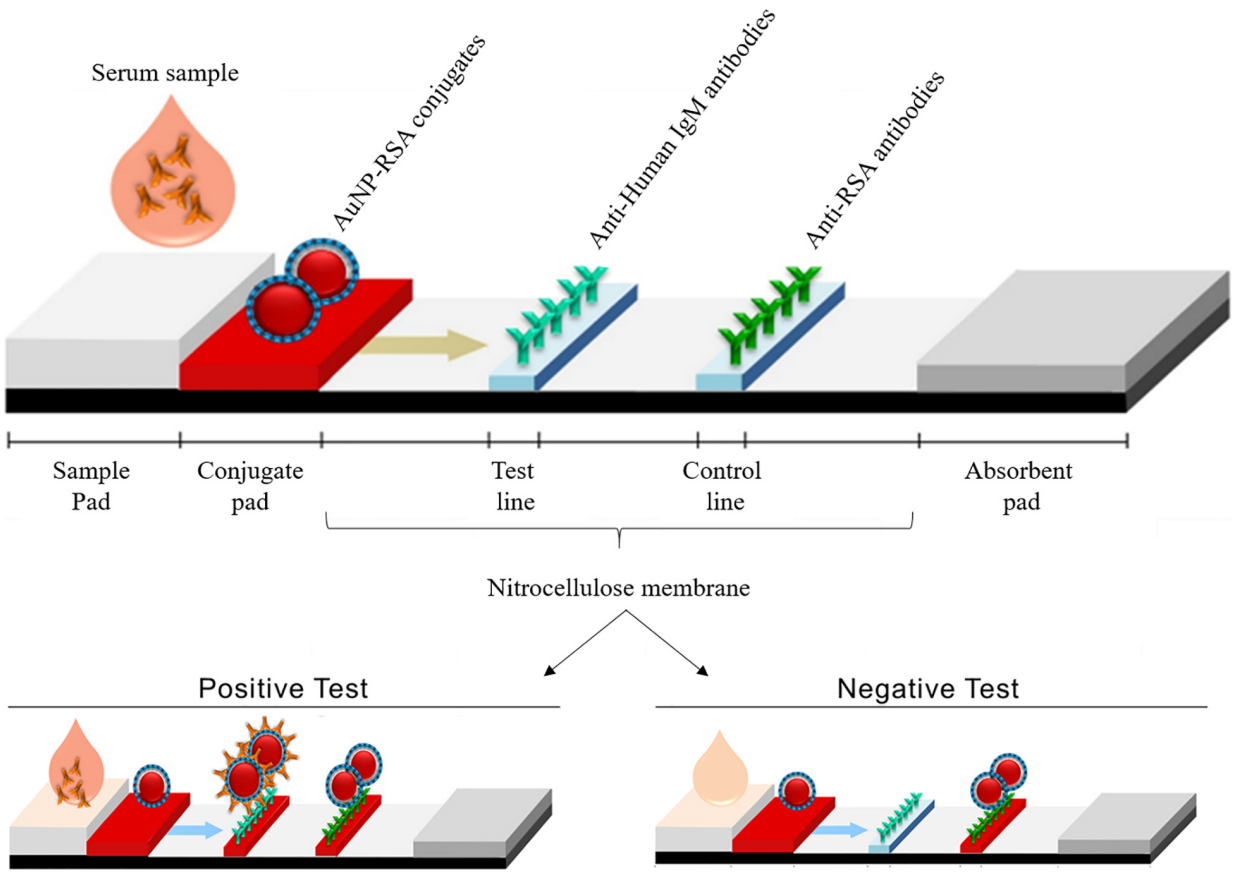

FIGURE 1 | Illustration of LFIA strips developed in this study, showing its various components and the expected results in positive and negative tests. In a positive test, AuNP-RSA conjugates will bind to IgM anti-*P. jirovecii* antibodies present in the serum of infected patients, forming a complex that is captured by the immobilized anti-human IgM in the test line that becomes red colored. AuNP-RSA conjugates in excess will continue to migrate from the test line to the control line, where immobilized anti-RSA antibodies will capture them, giving rise to a second red line. In the negative test, as IgM anti-*P. jirovecii* antibodies are absent in the patient's serum, no complex is formed with AuNP-RSA conjugates, which precludes the interaction with anti-human IgM antibodies, preventing the color formation at the test line (no color). In the control line, the AuNP-RSA conjugates will be captured by the immobilized anti-RSA antibodies, giving rise to a red line.

de Higiene e Medicina Tropical (Lisboa, Portugal) with the purpose of routine diagnosis of PcP with the patients' informed consent and according to the routine institutional procedures. The diagnosis of PcP was confirmed in 48 patients by visualization of the organism in BAL specimens using indirect immunofluorescence with monoclonal antibodies (IF/MAb) (MONOFLUO *Pneumocystis jirovecii*, BioRad®) and/or by *P. jirovecii*'s DNA detection through nested-PCR (nPCR) from the locus *mtLSUrRNA*, after DNA extraction (QIAamp, QIAGEN®). Twenty-eight patients whose specimens were negative for *P. jirovecii* were considered not infected (without PcP). All patients' demographic data were kept confidential and coded for the research team.

All selected patient's sera samples were analyzed through indirect ELISA for detection of circulation anti-*P. jirovecii* antibodies. Then, the optimization of AuNP-RSA conjugates interaction with anti-*P. jirovecii* antibodies was performed creating a pool of positive sera (positive sample) and a pool of negative sera (negative sample) using five serum specimens from patients with and without *P. jirovecii* infection, respectively.

The Instituto de Higiene e Medicina Tropical (Lisboa, Portugal) ethics committee approved the study's protocol and waived informed consent as a retrospective observational study.

ELISA for Detection of Anti-*P. jirovecii*'s Antibodies

The purified RSA were applied individually as antigenic tools in indirect ELISA to detect IgG and IgM anti-*P. jirovecii* in patient's sera. Odd (test) column wells of the microtiter plate were coated overnight at 4°C with 50 μL of the RSA diluted to 5 $\mu g.mL^{-1}$ in 0.05 M carbonate buffer (pH = 8.4). Even (blank) columns wells were coated in the same conditions with PBS 1x. After coating, the wells were washed once with PBS and blocked with 70 μL of 1% polyvinyl alcohol (PVA) for 1 h at room temperature (20–25°C). After blocking, PVA was removed from the plate without washing. Duplicates of each serum sample were analyzed in a test and blank well, under conditions (dilution, incubation time and temperature) determined by the Ig class to be detected and the RSA used as antigenic tool, being the specific protocols presented

at **Table 1**. Finally, the optical densities (OD) were measured at 405nm and the mean OD of the blank wells was deducted to the mean OD of the test wells to obtain the final OD value for each sample.

Mann-Whitney-U non-parametric tests were used to examine the differences between the distribution of antibody titers in different patient categories with a significance level of 0.05, using the Statistical Package for Social Sciences (SPSS) version 20.0.

Synthesis and Functionalization of Spherical Gold Nanoparticles

For synthesis and functionalization of gold nanospheres, all glassware was washed with aqua regia and rinsed thoroughly with deionized water followed by ultrapure water (18.2 $M\Omega \cdot cm^{-1}$) before use.

Citrate capped spherical gold nanoparticles (AuNPs) were synthesized following a method previously described (Bastús et al., 2011). Briefly, 150 mL of a 2.2 mM citrate solution (1.06448, Merck®) was heated using an oil bath, under stirring. After the reflux was stablished, 1 mL of a 25 mM gold (III) chloride solution (484385, Sigma®) was added to the reaction vessel and let to react for 10 min. After these steps, a seeds suspension was obtained. Then, the resultant suspension was cooled down to 90°C, keeping the condenser fitted and the stirring conditions. An extra 1 mL of the same gold (III) solution was added and let to react for 30 min. After this period, this last step was repeated.

Later, the citrate capping was replaced by functionalization of the AuNPs with 11-mercaptoundecanoic acid (11-MUA, 450561, Aldrich®). This step involved adding 10 mM 11-MUA ethanolic solution, to attain a 11-MUA:AuNP ratio of 30,000. After an overnight incubation, the AuNPs were washed (3000 *g* for 30 min) to remove free 11-MUA in solution. The highest volume possible of supernatant was discarded and the pellet was resuspended in ultrapure water up to ∼5% of the initial volume. The final suspension was stored in the dark until use.

AuNPs were characterized by ultraviolet-visible spectroscopy (UV-Vis) before and after functionalization and by dynamic light scattering (DLS), electrophoretic light scattering (ELS) and nanoparticle tracking analysis (NTA) after the functionalization process. UV-Vis was performed in a Varian Cary 50 Bio spectrophotometer, using a quartz cell, with the suspension at an appropriate dilution. DLS and ELS measurements were performed three times for the same sample at 25°C, with light detection at 273° (DLS) and at 17° using the backscatter mode (ELS) of the Malvern Zetasizer NanoZS equipment. NTA was performed in a Malvern Nanosight NS300 (with a 642 nm laser module), with the analysis of 5 videos of 1 min each, captured in 5 different portions of the sample (still mode). These measurements were then merged in a single size distribution.

Conjugation of AuNPs With the RSA

The antigen concentration to use in the conjugation process to guarantee the maximum coverage of the AuNPs surface but also the colloidal stability of the AuNP-RSA conjugates was optimized. For that purpose, AuNP-Msg and AuNP-Kex1 conjugates were formed through electrostatic interactions established between increased molar ratios of each RSA and the AuNPs in solution, as described previously (Guirgis et al., 2012; Cavadas et al., 2016; Almeida et al., 2018). A solution of 0.06nM AuNPs was incubated overnight (≈15 h) at 4°C with molar ratios ranging from 0 to 5000 of Msg and Kex1 stock solutions of 0.16 and 0.11 $mg.mL^{-1}$, respectively. After conjugation, non-bound RSA were removed by centrifugation (5800 g for 5 min), separating the pellets containing the AuNP-RSA from the supernatant, to perform agarose gel electrophoresis (AGE). Agarose gels (0.3%) were prepared by heating agarose in TAE buffer (0.125 × pH = 8.4), and allowing the gel to form at room temperature. The AuNP-RSA conjugates pelleted after centrifugation were re-suspended in 13.5 μL of phosphate buffer (5 mM Na_2HPO_4, pH = 7.4) and 1.5 μL of glycerol (99%, Nzytech®) prior to loading. The gels were run at constant voltage of 180 V with a 21 cm electrode spacing for 20 min in TAE 0.125 × using the E865 CONSORT power supply. Digital pictures were acquired (WAS-LX1A Huawei P10 Lite camera) and processed through eReuss software (a gel analysis application freely available at https://github.com/lkrippahl/eReuss), providing an accurate measurement of the red bands migration in agarose, which allows the calculation of their electrophoretic mobility (Ferard, 1994; Almeida et al., 2018). Electrophoretic mobility [μ (μm.cm/V.s)] is defined as the observed rate of migration of a component [ν (μm/s)] divided by the electric field strength [*E* (V/cm)] in a given medium. In the case of AGE, a solid support medium, only apparent values can be determined (Ferard, 1994). Thus, the molar ratio in which the AuNP-RSA electrophoretic mobility reaches a plateau, corresponding to saturation of the AuNP surface with each RSA, was selected through duplicate experiments.

Analysis of Human Sera Interaction With AuNP-RSA by Agarose Gel Electrophoresis

To avoid unspecific antibody binding to the AuNP-Msg and AuNP-Kex1 conjugates, bovine serum albumin (BSA) (AppliChem®) and Casein (Sigma®) were studied as blocking agents. A BSA and Casein stock solution at 1 $mg.mL^{-1}$ were added to 0.06 nM AuNP-RSA conjugates in solution at increased molar ratios ranging from 0 to 10 with AuNP-Kex1 conjugates and from 0 to 50 with AuNP-Msg conjugates, producing AuNP-RSA-BSA and AuNP-RSA-Casein conjugates. The incubation was performed during 90 min at 4°C, the non-bound blocking agents were removed by centrifugation (5800 g for 5 min) and the pellets prepared for agarose gel electrophoresis. Similarly to what was done with the AuNP-RSA conjugates, the molar ratio plateau was selected through duplicate experiments for each blocking agent.

An optimal molar ratio of human serum was established in the same way, incubating 0.06 nM solutions of AuNP-RSA-Casein and AuNP-RSA-BSA conjugates with molar ratios ranging from 0 to 7.5 of the positive sera pool (80 $mg.mL^{-1}$). The molar ratio in which the optimal coverage of the conjugate was obtained, was selected.

These serum molar ratios were applied in an AGE assay, where 0.06 nM AuNP-RSA solutions and 0.06nM AuNP-RSA-BSA

TABLE 1 | ELISA protocols and conditions for detection of IgG and IgM anti-*P. jirovecii* antibodies reactive against the RSA produced.

Protocol	RSA applied as antigenic tool			
	Kex1		Msg	
Application of 50 μL of serum diluted in PBS with 0.05% tween-20 and 5% BSA	1/20	1/40	1/60	1/140
Incubation	1 h at 37°C			
Washing	4x with PBS with 0.05% tween-20 1x with distilled water			
Application of 50 μL of anti-human immunoglobulin M (A2189, sigma§) diluted in PBS with 0.05% tween-20	1/1000		1/4000	
Application of 50 μL of anti-human immunoglobulin G (A2064, sigma§) diluted in PBS with 0.05% tween-20		1/3000		1/4000
Incubation	1 h at 37°C			
Washing	4x with PBS with 0.05% tween-20 1x with distilled water			
Application of 50 μL of substrate	4-nitrophenylphosphate sodium salt (1 $mg.mL^{-1}$)			
Incubation	Overnight at 4°C	Overnight at 4°C	Overnight at 4°C	2 h at 37°C

and AuNP-RSA-Casein conjugates solutions were incubated for 90 min at 4°C with and without the human positive and negative sera pools. After incubation, the non-bound serum was discarded after centrifugation (5800g for 5 min) and the electrophoretic mobility of each conjugate was established. This assay was performed in triplicate and the analysis of the differences between the electrophoretic mobility of each conjugate formed was evaluated and used to established the optimal conjugate (AuNP-RSA or AuNP-RSA-BSA or AuNP-RSA-Casein) to be used in the LFIA development.

Assembly of LFIA Strips for Detection of IgM Anti-*P. jirovecii* Antibodies in Human Sera

For LFIA development, a starter kit from Advanced Microdevices, Ambala Cantt, India, was used. This kit offers: two types of cellulose fiber absorbent pads with different thickness (AP-045 with 0.4 mm and AP-080 with 0.8 mm); three types of nitrocellulose membranes (NM) fixed on a plastic backing, with different protein binding capacities (type CNPF, a low protein binding membrane with pore sizes of 8 and 10 μm; type CNPC, a high protein binding membrane with pore sizes of 12 and 15 μm; and type CNPH, the highest protein binding membrane with wicking times of 70, 90, 150, and 200 s); two glass fiber sample pads, one without any specific pre-treatment (GFB-R4) and a second one pre-treated with buffers and detergents to help prevent non-specific binding of sample components to the pad (GFB-R7L); and two conjugate pads, a polyester matrix without any specific pre-treatment (PT-R5) and another one pre-treated with buffers for uniform movement of gold nanoparticle conjugates (PT-R7).

Absorbent Pad and Membrane Selection

To perform this selection, dipsticks composed by the nitrocellulose membrane (NM) and the absorbent pad were tested. Membranes were manually cut into 6 × 0.5 cm sections. The control and test lines were spotted manually, in a circle or in a line, by depositing 0.03 $mg.mL^{-1}$ of anti-RSA antibodies (anti-Msg or anti-Kex1, depending on the RSA present in the conjugate) and 0.001 $mg.mL^{-1}$ of anti-human IgM antibodies (I-0759, Sigma®), respectively. Different dilutions in Tris buffer (10 mM Tris-HCl, pH = 7) for the control antibodies, ranging from 0 to 1/4, and for the test antibodies, ranging from 0 to 1/10, were studied. The membranes dried for 30 min at room temperature before use. A blocking process of the membranes was also tested with an additional step of 30 min incubation at room temperature with skin milk (2%, Sigma®), followed by three washes with PBS with 0.05% Tween-20 and dried at 37°C during 30 min. At the top of the membrane, a 3 × 0.5 cm section of absorbent pad (AP-045 or AP-080) was attached with 1–2 mm overlapping with the membrane. A solution of 0.72 nM AuNP-RSA-Caseín conjugates was incubated with appropriate molar ratio of positive serum for 90 min at 4°C and then, the dipsticks composed by the NM and the absorbent pad were immersed into 50 μL of this solution in a tube, with the absorbent pad side up for 2 min. Driven by capillary forces, the liquid migrated up the membrane into the absorbent pad. The selection of the optimal set of membrane/absorbent pad was based on visually inspection of test and control line results.

Conjugate Pad, Sample Pad and Sample Buffer and Dilution Selection

To perform this selection, full LFIA strips were assembled and tested. Conjugate release pads available were manually cut into 1 × 0.5 cm sections and tested with and without pre-treatment with PBS containing 5% sucrose, 1% BSA and 0.5% Tween 20. Then, they were saturated with 15 μL of conjugate concentrations ranging from 0.2 to 4.6 nM. These conjugate pads dried for 2 h at 37°C before assembling to the membrane/absorbent pad set (see above) and then attached to the bottom of the strip (at

the origin of the sample flow), with 1–2 mm overlapping with the membrane. The sample pads were also manually cut into 3 × 0.5 cm sections and tested with and without prior saturation with 0.03% anti-human immunoglobulin G (2040-04, Sigma®) and dried overnight at room temperature, before assembling at the bottom of the strip, overlapping almost completely with the conjugate pad. After the whole LFIA strip was assembled, 200 μL of positive serum diluted from 0 to 1/100 into phosphate buffer (5 mM Na_2HPO_4, pH = 7.4), phosphate buffer with 0.05% BSA and 0.05% Tween-20, phosphate buffer with 1% BSA and 1% Tween-20 or PBS with 0.05% Triton-X-100, was added to the sample pad. Driven by capillary force, the sample migrated up the sample pad to the conjugate pad and to the membrane into the absorbent pad. After 10 min, the selection of the optimal set of conjugate pad/sample pad and optimal sample buffer/dilution conditions was based on a visually inspection of test and control line results, on the manufacturer's recommendation for the uniform movement of gold nanoparticles conjugates and on quantification of color intensity in test and control lines.

Quantification of Color Intensity

The quantification of color intensity in test and control lines was made in strips tested before and after pre-treatment of conjugate/sample pads, in strips tested with different positive sample dilutions and in strips tested with the final optimal conditions. Digital pictures of the optimized strips were acquired (WAS-LX1A Huawei P10 Lite camera) and eReuss (a gel analysis application freely available at https://github.com/lkrippahl/eReuss) parameters were adapted for color intensity quantification. To set the image processing, in the band color droplist of the software, the average color of the test and control lines was selected, forcing the software to ignore the color channel in which the lines have a light intensity closer to the background. This step ensures that the intensity value given by the software for each line results from the previous elimination of the background. Then, in the image clipping set, the NM region with both test and control lines results was selected for processing. The software, for each defined vertical strip, sums the color intensity of the pixels in horizontal sections giving a plot with the heights of each point per line. In band profiling step, the conditions in which we intend to measure the peaks of color intensity in the different control/test lines were set. Two Gaussians were fitted per strip, one for each test or control line, with a minimum height value of 5% of the image brightness range, to set the cut-off value of intensity. The remaining parameters were left with the default settings. The software identified the peaks by iteratively fitting a Gaussian distribution to the maximum intensity value in the curve, subtracting that distribution and repeating until either the number of Gaussians was reached or the maximum value falls below the minimum height parameter. A final report with the summarized results was obtained and analyzed for selection of the optimal sample dilution and the need for sample/conjugate pad pre-treatments.

LFIA Strips Testing With Clinical Samples

The viability of the prepared immunochromatographic strips as tools for detection of anti-*P. jirovecii* antibodies was tested, in triplicate experiments, by loading human serum pools from patients with and without PcP.

In the case of strips in which the conjugates were composed by AuNP-Msg-Casein, 200 μL of positive/negative human serum pools, diluted 1:50 in phosphate buffer with 0.05% BSA and 0.05% Tween-20, were added to the sample pad. In strips with adsorbed AuNP-Kex1-Casein conjugates, 200 μL of positive/negative human serum pools, diluted 1:20 in phosphate buffer with 0.05% BSA and 0.05% Tween-20, were used instead. Driven by capillary forces, the samples migrated up the conjugate pad to the membrane into the absorbent pad and, during 10 min, the test results were evaluated visually. Further quantification of color intensity in test and control lines of each strip was performed using the eReuss software.

RESULTS

Design, Expression, and Purification of Msg and Kex1 RSA

The Msg RSA was designed as previously described (Tomás et al., 2016).

The Kex1 RSA consists of 110 amino acids composed by three regions with high-predicted antigenicity and reactivity from *P. jirovecii*'s Kex1 entire sequence (see **Supplementary Figures S1–S6**), that were chosen and synthesized interconnected by two "linkers" of five glycine residues and expressed with a tail of six residues of histidine. In this RSA, epitope 1 is coded by $Kex1_{104-134}$ amino acids, epitope 2 by $Kex1_{467-501}$ amino acids and epitope 3 by $Kex1_{725-758}$ amino acids, according to GenBank accession numbers AAN12365.1 and AAM97495.1 (see **Supplementary Figure S7**; Kutty and Kovacs, 2003).

The SDS-PAGE analysis showed that both RSA were expressed with their predicted molecular sizes (16.7 kDa for Msg RSA and 22 kDa for Kex1 RSA) after IPTG induction (**Figures 2A,B**) and that they were successfully purified by immobilized metal-ion affinity chromatography (IMAC) (**Figure 2C**). Indirect ELISA using anti-polyhistidine antibodies were performed to optimize the purification process, ensuring that the RSA were detected during the elution phase and not during column washing after sample application (see **Supplementary Figure S8**).

Detection of Serum Anti-*P. jirovecii* Antibodies

Two different IgG and IgM ELISA were developed, according to the protocols presented in **Table 1**, using Kex1 RSA and Msg RSA as coating antigens. The results of the distribution of the IgG and IgM anti-*P. jirovecii* levels across patients with PcP and without *P. jirovecii* infection are represented in **Figure 3**.

Both RSA showed applicability in the detection of specific IgG and IgM anti-*P. jirovecii* antibodies. However, IgG ELISA showed inability to distinguish patients with PcP from patients without *P. jirovecii* infection as the median levels of the Igs detected in these patient's groups were not statistically different ($p > 0.05$). Yet, IgM ELISA with both Kex1 RSA and Msg RSA demonstrated ability to distinguish patients with the disease

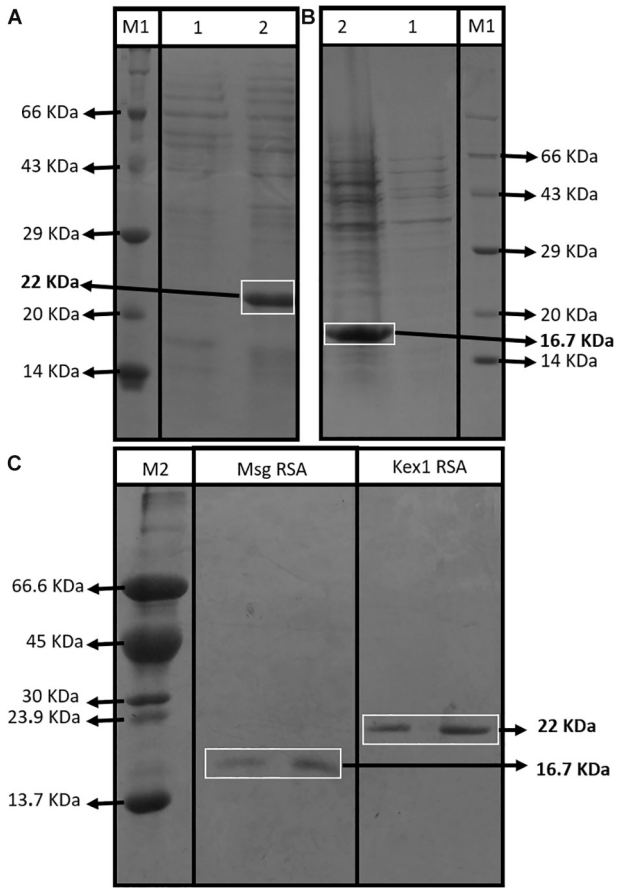

FIGURE 2 | Assessment of the RSA expression and purification process. SDS-PAGE profiles of non-induced (1) and induced (2) *E. coli XJb (DE3)* cells transformed with the expression vector with the Kex1 RSA **(A)** and the Msg RSA **(B)**; and SDS-PAGE profiles of purification products of the Msg RSA and Kex1 RSA, after IMAC protocol **(C)**. Two different protein molecular weight standards were used, the Roti[§] -Mark standard from Carl-Roth[§] (M1) and one produced "in house" (M2). The bands of interest and their theoretical molecular weight are highlighted (16.7 kDa for Msg RSA and 22 kDa for Kex1 RSA).

from patients without *P. jirovecii* infection. With the Kex1 RSA, the median levels of IgM anti-*P. jirovecii* detected by ELISA was 0.3871 in patients with PPc and 0.0997 in patients without *P. jirovecii* infection, which were considered statistically different ($p < 0.002$). With the Msg RSA, the differences between the median levels of IgM anti-*P. jirovecii* detected by ELISA in patients with and without the disease were also considered statistically significant ($p = 0.001$), and the values were 0.6076 in patients with PPc and 0.4195 in patients without *P. jirovecii* infection.

Characterization of Gold Nanoparticles

Gold nanoparticles were characterized by UV-Vis, DLS, ELS, and NTA.

The UV-Vis spectrum of the citrate-capped AuNPs (as synthesized) shows a localized surface plasmon resonance (LSPR) band with its maximum at 526 nm. From the UV-Vis spectrum data (Abs_{LSPR} and Abs_{450}), it was determined that the batch of AuNPs had a concentration of 0.2 nM with an average size of 39 nm (Haiss et al., 2007). After functionalization with 11-MUA (see **Supplementary Figure S9A**) the hydrodynamic size data obtained from DLS showed a Z-Average of 46.2 ± 0.2 nm. The zeta-potential value obtained by ELS was -36 ± 1 mV, indicating a high colloidal stability. The hydrodynamic diameter distribution obtained by NTA (see **Supplementary Figure S9B**), presented an average of 51.0 ± 3.8 nm and a mode of 41.7 ± 2.9 nm. The mode is down shifted by 9.3 nm compared to the average, since the aggregates (especially noticeable in the distribution between 60 and 90 nm) contribute for the mean value.

Gold Nanoparticle-*P. jirovecii*'s RSA Conjugates (AuNP-RSA)

The functionalized AuNPs produced were conjugated to Msg (AuNP-Msg) or Kex1 (AuNP-Kex1) RSA of *P. jirovecii,* in order to synthesize probes for the detection of IgM anti-*P. jirovecii* antibodies in sera of patients with PcP. Agarose gel electrophoresis assays were used to characterize the AuNPs before and after conjugation with the RSA (Guirgis et al., 2012; Cavadas et al., 2016; Kim et al., 2016; Almeida et al., 2018). As shown in **Figures 4A,C**, the migration distance of the RSA-conjugated particles (AuNP-Msg and AuNP-Kex1), compared to the non-conjugated AuNPs, decreases as the RSA:AuNP ratio increases. However, when the amount of RSA reached 175.5 nM (ratio 2925:1), the addition of more RSA no longer decreased significantly the mobility of the conjugates and a plateau began to form. Therefore, a RSA:AuNP ratio of 2925:1 was stablished as the optimum to produce AuNP-RSA conjugates in which RSA molecules fully cover the AuNPs. For these RSA:AuNP ratios of 2925:1, the difference between the calculated electrophoretic mobility ($\Delta\mu$) of AuNP alone and AuNP-RSA conjugates was 0.46 ± 0.01 μm.cm/V.s for AuNP-Msg conjugates and 0.42 ± 0.02 μm.cm/V.s for AuNP-Kex1 conjugates (**Figures 4B,D**).

Blocking of AuNP-RSA Conjugates for Reaction With Human Sera

In order to avoid unspecific interactions with human sera, increasing the specificity of the interaction between the conjugates and the target antibodies, blocking of the AuNP-RSA conjugates was assessed with BSA or with casein, two well know proteins used routinely for this purpose in immunoassays (Binder and Isler, 2013). The electrophoretic mobility of AuNP-Msg conjugates incubated with increasing ratios of BSA or casein was determined by AGE (see **Supplementary Figure S10**). A plateau was observed for a BSA:AuNP-Msg ratio of 20, so that value was chosen for future experiments. In the case of AuNP-Kex1 conjugates, since there is no observable interaction of the blocking agents with these conjugates, no particular BSA:AuNP-Kex1 and Casein:AuNP-Kex1 ratios were found (see **Supplementary Figure S11**). However, to evaluate the interaction of human sera with conjugates with and without blocking agent, a ratio of 2:1 of casein to AuNP-Kex1 was used.

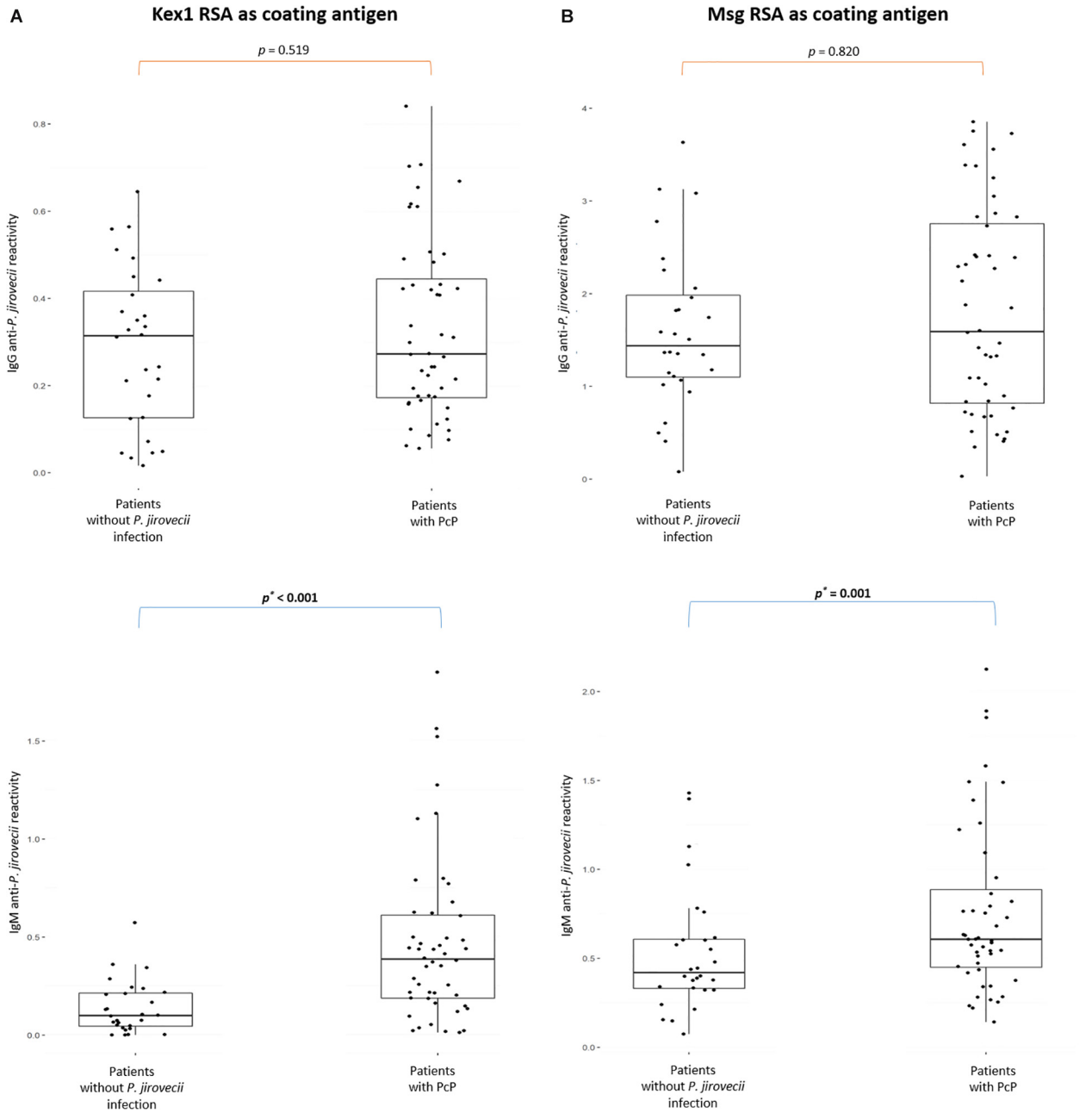

FIGURE 3 | Boxplots with IgG and IgM anti-*P. jirovecii* levels results across patients with PcP and patients without *P. jirovecii* infection. Simple boxplots showing the reactivity levels (OD at 405 nm) of IgG and IgM anti-*P. jirovecii* antibodies detected by ELISA protocols applied with the Kex1 RSA **(A)** and Msg RSA **(B)** as coating antigens, in all sera specimens of patients analyzed in the study. The statistic values (*p*) representing the statistical significant difference from Mann Whitney-U tests performed between patient's groups are presented.

The blocked and unblocked AuNP-RSA conjugates were further assessed by AGE to characterize their ability to interact with human sera from patients with and without *P. jirovecii* infection. Based on the same type of AGE experiments, in which several molar ratios of the positive human serum pool to blocked AuNP-RSA conjugates were evaluated, a human serum ratio of 4.55 was selected for further experiments (see **Supplementary Figures S12, S13**).

AuNP-RSA, AuNP-RSA-BSA, and AuNP-RSA-Casein conjugates were incubated with and without positive (PosSerum) and negative (NegSerum) serum pools at the selected ratio and then assessed by AGE (see **Supplementary Figure S14**). Results suggest that there were still free spaces on the surface of the AuNP-Msg conjugates that were blocked by casein and by BSA, causing a decrease in the electrophoretic mobility of the conjugates in the absence

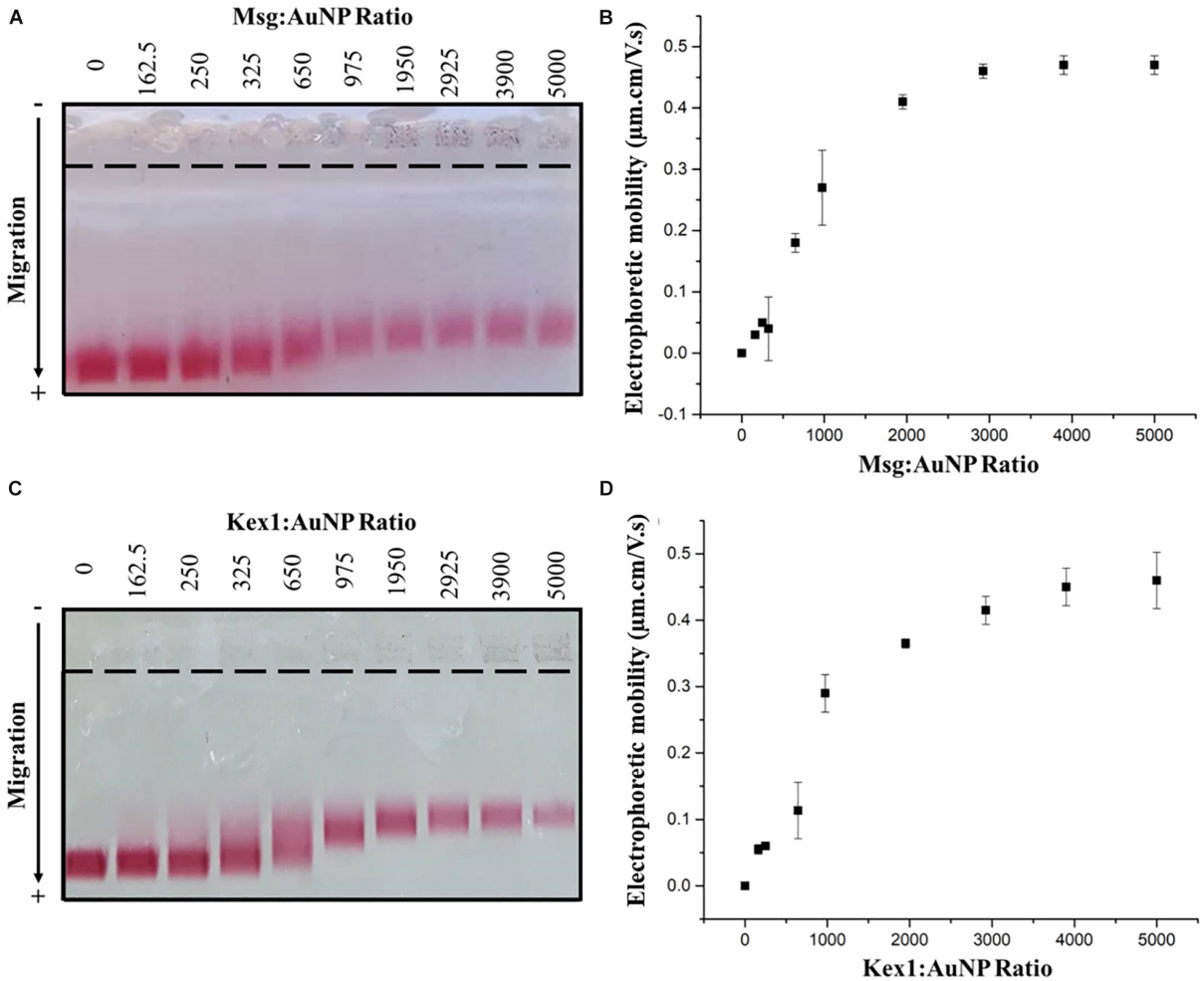

FIGURE 4 | AuNP-RSA conjugates formation. Agarose gel electrophoresis at increasing ratios of Msg RSA to AuNPs **(A)** and Kex1 RSA to AuNPs **(C)**, showing the migration of each conjugate bands toward the positive electrode. Differences between the electrophoretic mobility of the AuNPs alone and AuNP-Msg **(B)** or AuNP-Kex1 **(D)** conjugates at increasing ratios, calculated from the migration distances in gel. The nine ratios (162.5–5000) correspond to protein concentrations of 9.75, 15, 19.5, 39, 58.5, 117, 175.5, 234, and 300 nM. Standard deviation bars correspond to duplicate experiments.

of serum (see **Supplementary Figures S14A,B**). However, in the case of AuNP-Kex1 conjugates (see **Supplementary Figures S14C,D**), the electrophoretic mobility of the conjugates before serum interaction, is very similar in the presence or absence of any blocking agent, which reinforces the idea that the blocking step is not as crucial for these AuNP-Kex1 conjugates as it is for the AuNP-Msg conjugates, as previously observed (see **Supplementary Figures S10, S11**). Nevertheless, the blocking step was maintained for both AuNP-RSA conjugates, in order to avoid the event of non-specific interactions with human sera components. For this purpose, casein appeared to be more effective, as non-specific interactions between the negative serum and the conjugates were lower in the presence of this blocking agent than in the presence of BSA. That can be verified by a decrease in the migration shift between the blocked conjugates, before and after interaction with the negative serum (see **Supplementary Figure S14**: a shift of 0.13 µm.cm/V.s in AuNP-Msg-Casein conjugates against a shift of 0.42 µm.cm/V.s in AuNP-Msg-BSA conjugates; a shif of 0.23 µm.cm/V.s in AuNP-Kex1-conjugates against a shift of 0.39 µm.cm/V.s in AuNP-Kex1-BSA conjugates).

Interaction Between Human Sera and AuNP-RSA-Casein Conjugates

The interaction between AuNP-RSA-Casein conjugates and human sera from patients with and without *P. jirovecii* infection was assessed by AGE and is represented in **Figure 5**. Results shows a consistent detection of a migration shift between AuNP-RSA-Casein conjugates that interacted with sera from PcP patients and conjugates that interacted with sera from patients without *P. jirovecii* infection (0.31 µm.cm/V.s in the case of AuNP-Msg-casein conjugates and 0.79 µm.cm/V.s in the case of AuNP-Kex1-casein conjugates). The presence of these shifts in AGE assays are a proof-of-concept for the LFIA to be developed:

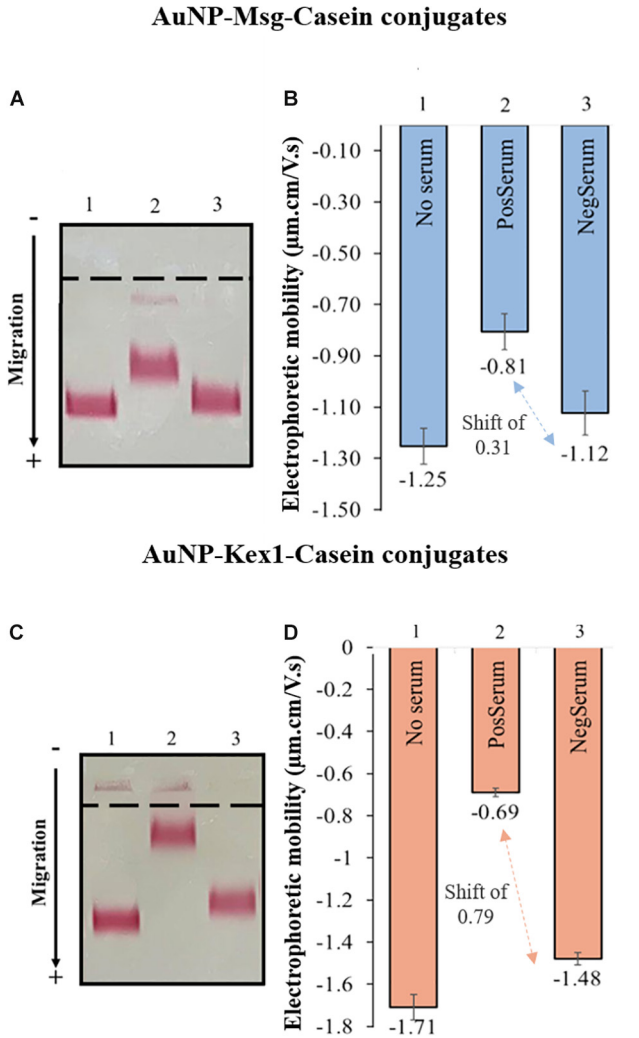

FIGURE 5 | Interaction of AuNP-Msg-Casein **(A,B)** and AuNP-Kex1-Casein conjugates **(C,D)** with sera pools from patients with and without *P. jirovecii* infection. **(A,C)** Agarose gel electrophoresis of AuNP-RSA-Casein conjugates before interaction with serum (1) and after interaction with positive (2) and negative (3) serum samples. **(B)** Electrophoretic mobility of the AuNP-RSA-Casein conjugates before interaction with human sera (No Serum) and after interaction with the positive human sera (PosSerum) and negative human sera (NegSerum). Shifts (µm.cm/V.s) between blocked conjugates with positive and with negative sera are indicated, evidencing the binding of antibodies present in the positive serum. Standard deviation bars correspond to triplicate experiments.

in fact, anti-*P. jirovecii* antibodies present in PcP patient's sera specifically interact with both RSA, binding to the AuNP-RSA-Casein conjugates and decreasing their migration distance in the gel. Additionally, no significant interactions between AuNP-RSA-Casein conjugates and non-infected patient's sera occur, since the migration distance of these conjugates before and after contact with the negative sample is similar, considering all the experiments performed.

Results also show that the distance migration shift between conjugates that interact with the positive sera and conjugates that interact with negative sera is bigger in the presence of AuNP-Kex1 conjugates (up to 2.5x), suggesting that this RSA is a better antigenic tool for anti-*P. jirovecii* antibodies detection than the Msg RSA.

Assembly and Optimization of LFIA Strips Using AuNP-RSA-Casein Conjugates

For LFIA strips development, a commercial starter kit was used (see section Materials and Methods for a detailed description of the components). LFIA's components selection was based on manufacturer's advices and visual inspection of test and control lines results (data not shown).

Absorbent Pad and Membrane Selection and Optimization

By visual inspection, it was observed that all NM can be used successfully without a previous blocking step. Additionally, the signal in the control and test lines appeared to increased proportionally with pore diameter and the wicking time of the NM. However, as membranes type CNPH are presented by the manufacturer as the NM with the highest protein binding capacity, the one with the longest wicking time (200 s) was the one chosen for the LFIA development.

No visual differences were noted in CNPH200 NM dipsticks results using one or the other absorbent pad available in the kit. However, as absorbent pad 045 is thinner, it allows a slower migration along the NM, which may improve the number of interactions in the control and test lines. Therefore, it was the absorbent pad selected for LFIA development.

The selection of the control and test antibodies dilutions was made in order to obtain uniform signals in both lines. By visual inspection (data not shown), a dilution of 1/2 in Tris buffer for the control antibodies and no dilution for the test antibodies were selected.

Conjugate and Sample Pad Selection and Optimization

In the case of conjugate pads available, as the manufacturer states that the PT-R7 pad was pre-treated for uniform movement of gold nanoparticles conjugates, unlike the PT-R5 pad, the PT-R7 pad was the one selected. Concerning the AuNP-RSA-Casein conjugates concentration to be used, a colloidal solution of 2.4 nM was stablished as sufficient to provide a visual interpretation of the test results (data not shown).

Regarding the sample pad selection, as GFB-R7L pads were pre-treated by the manufacturer with detergents and buffers that decreased sera non-specific binding to the pad, they allowed better visual interpretation of the results than the GFB-R4 untreated pad, and that's why GFB-R7L pad was the one chosen.

To improve signal intensity on both test and control lines, pre-treatments of the selected conjugate pad (with a buffer containing sucrose, BSA and Tween 20) and sample pad (with anti-human immunoglobulin G) were performed. The color intensity of test/control lines in strips before and after treatment was assessed visually and quantified by the eReuss software, and the results are presented in **Figure 6**. Results show that pre-treatments

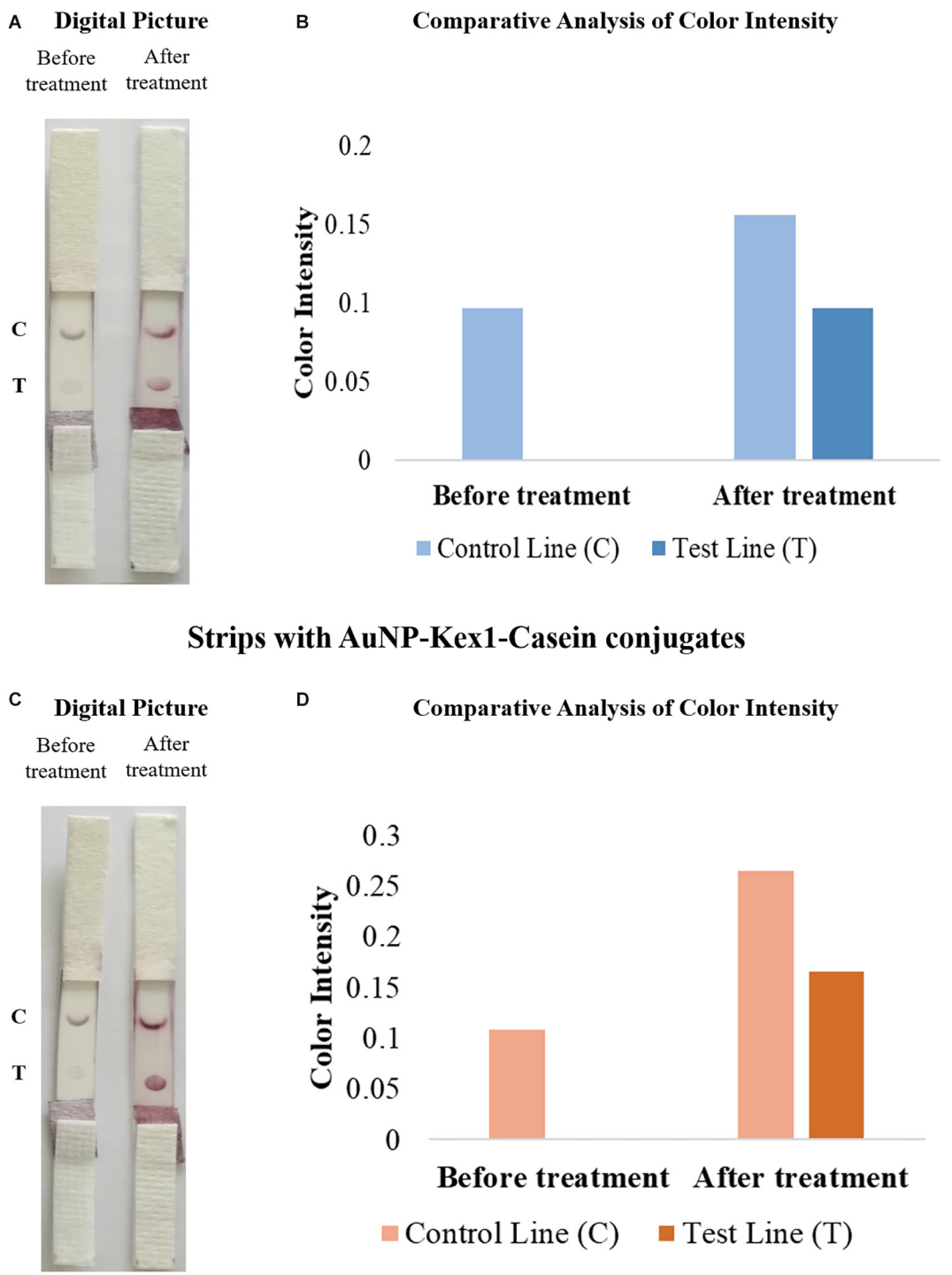

FIGURE 6 | Comparative analysis of the results from LFIA strips containing AuNP-Msg-Casein conjugates **(A,B)** and AuNP-Kex1-Casein conjugates **(C,D)** in the presence (after treatment) and absence (before treatment) of conjugate and sample pad pre-treatments. **(A,C)** Digital pictures of strips before and after conjugate pad treatment with a buffer (5% sucrose, 1% BSA and 0.5% Tween 20) and sample pad treatment with 0.03% anti-human immunoglobulin G. From bottom to top, strips were composed by the sample pad, the conjugate pad, the nitrocellulose membrane with the test (T) and control (C) lines and the absorbent pad. **(B,D)** Quantification of color intensity of the control and test lines, where the intensity shown in each line corresponds to the maximum height of the Gaussian line fitted by eReuss software.

steps enhanced visual signal of both test and control lines (**Figures 6A,C**), which was confirmed by color quantification, showing higher peaks of color intensity in both lines after these treatments (**Figures 6B,D**).

Sample Buffer and Dilution Selection

By visual inspection of strip results (data not shown), phosphate buffer with 0.05% BSA and 0.05% Tween-20 was selected as the optimal sample buffer. Then, final dilutions of 1:50 and 1:20 of sera samples were established as optimal for LFIA with AuNP-Msg-Casein conjugates and AuNP-Kex1-Casein conjugates, respectively, through visual inspection and color intensity quantification of strip test results, represented in **Figure 7**. Although higher color intensities were expected at lower sample dilutions, these results were reproducible and may be associated with an agglutination phenomenon, further addressed in the Discussion section.

Optimized LFIA Strips Testing With Human Sera Pools

After optimization, LFIA strips were tested with sera pools from patients with (positive sample) and without (negative sample) PcP, in triplicate experiments (see **Supplementary Figure S15**). Visually, 3 min after sample addition it was already possible to detect the presence of a colored line in the control zone on strips with the negative sample and two colored lines, in the control and test zones, on strips with the positive sample. The results remained invariable 10 min after the end of the elution process, i.e., solvent reaching the absorbent pad (**Figures 8A,C**).

The software used for color intensity analysis was unable to detect color on the test lines of the strips with negative samples, and detect similar color intensity for the control and test lines on the strips with positive samples (**Figures 8B,D**).

DISCUSSION

Nowadays, there is a demand to find point-of-care diagnostic tests that enable fast and inexpensive screening/diagnosis of infectious diseases, to improve disease control and retrenchment of healthcare systems costs worldwide. In the case of *Pneumocystis* pneumonia, in which there are no specific clinical, radiologic or gasometric findings and none of the serologic biomarkers studied until now showed to be highly-specific of the disease (Morris and Masur, 2011; Esteves et al., 2015; Matos and Esteves, 2016; Tomás and Matos, 2018), this has been a challenge. Thus, current diagnosis techniques depend on the direct or indirect detection of the pathogen in respiratory specimens, which makes them dependent on costly and invasive procedures.

Recently, studies showed that a technology based on synthetic amino acid sequences, designed to hold more than one reactive region of the selected antigens, could enhance the immunological diagnosis of *Toxoplasma gondii* (Dai et al., 2012, 2013). Therefore, in our previous study, this research group designed a recombinant synthetic antigen (RSA) with three antigenic regions of the Msg protein, in order to standardize and enhance the detection of reactive antibodies against *P. jirovecii* (Tomás et al., 2016). In this single antigenic tool, several proven reactive and conserved fragments of the Msg were used, improving its immunogenic power and consequently its application as an anti-*P. jirovecii* antibody detection tool (Tomás et al., 2016). In the present study, this RSA was used in combination with a new RSA, produced based on the immunogenic behavior of *P. jirovecii* Kex1 protein. This second RSA was also designed to hold more than one reactive region of *P. jirovecii* Kex1 protein, in order to increase the sensitivity and specificity of the serological approach. The idea of using this new protein (Kex1), encoded by a single copy gene (Kutty and Kovacs, 2003), emanate from the recent reports that support its role in the protection of PcP (Gingo et al., 2011; Kling and Norris, 2016) and to counteract the genetic variation that the Msg protein may present during infection (Hauser, 2019).

Both RSA were obtained with high purity (**Figure 2C**), and were applied as antigenic tools in different ELISA assays (**Table 1**) to assess whether specific anti-*P. jirovecii* antibodies can be detected in human sera at the time of patient's presentation with symptomatology compatible with PcP. Thus, 76 serum specimens collected at the time of patient's BAL procedure for PcP routine diagnosis were analyzed by these optimized indirect ELISA with both RSA, for detection of IgG and IgM anti-*P. jirovecii* antibodies. IgG ELISA results showed that, even though IgG response is detected with both RSA, it is not possible to distinguish patients with PcP from patients without *P. jirovecii* infection by their IgG levels (**Figure 3**). That may be explained by previous PcP events or by the reports of *P. jirovecii* colonization in patients presenting diverse levels of immunodeficiency, primary respiratory disorders, or even in the immunocompetent general population (Wakefield et al., 2003; Medrano et al., 2005; Morris and Norris, 2012), which could lead to the production of memory cells that could induce IgG antibodies production throughout the individual's life.

Yet, IgM ELISA using each RSA as a coating antigen (**Figure 3**), showed successful application in the serodiagnosis of PcP, as anti-*P. jirovecii* levels detected, unlike IgG levels, were significantly different between patients with and without the disease ($p \leq 0.001$). These results corroborate what had previously been verified in studies with mice, where it was suggested that the IgM isotype has a predominant role in shaping the earliest steps in recognition and clearance of *P. jirovecii* infection, since IgM-deficient mice showed to be more susceptible to PcP progression (Rapaka et al., 2010). These results suggest that IgM anti-*P. jirovecii* antibodies seems to be a possible serological biomarker for active PcP diagnosis, which could provide a major improvement over the current diagnosis standards.

Taking this into consideration, the innovative character of the present study stems from the use of these RSA in association with gold nanoparticles with tunable bright colors, to design a point-of-care platform for PcP diagnosis based on a solid-phase (strip-based) test. The LFIA developed relies on the ability of AuNPs to interact with the RSA to form conjugates that are used as recognition tools capable of interacting with IgM anti-*P. jirovecii* antibodies present in the serum of patients with PcP

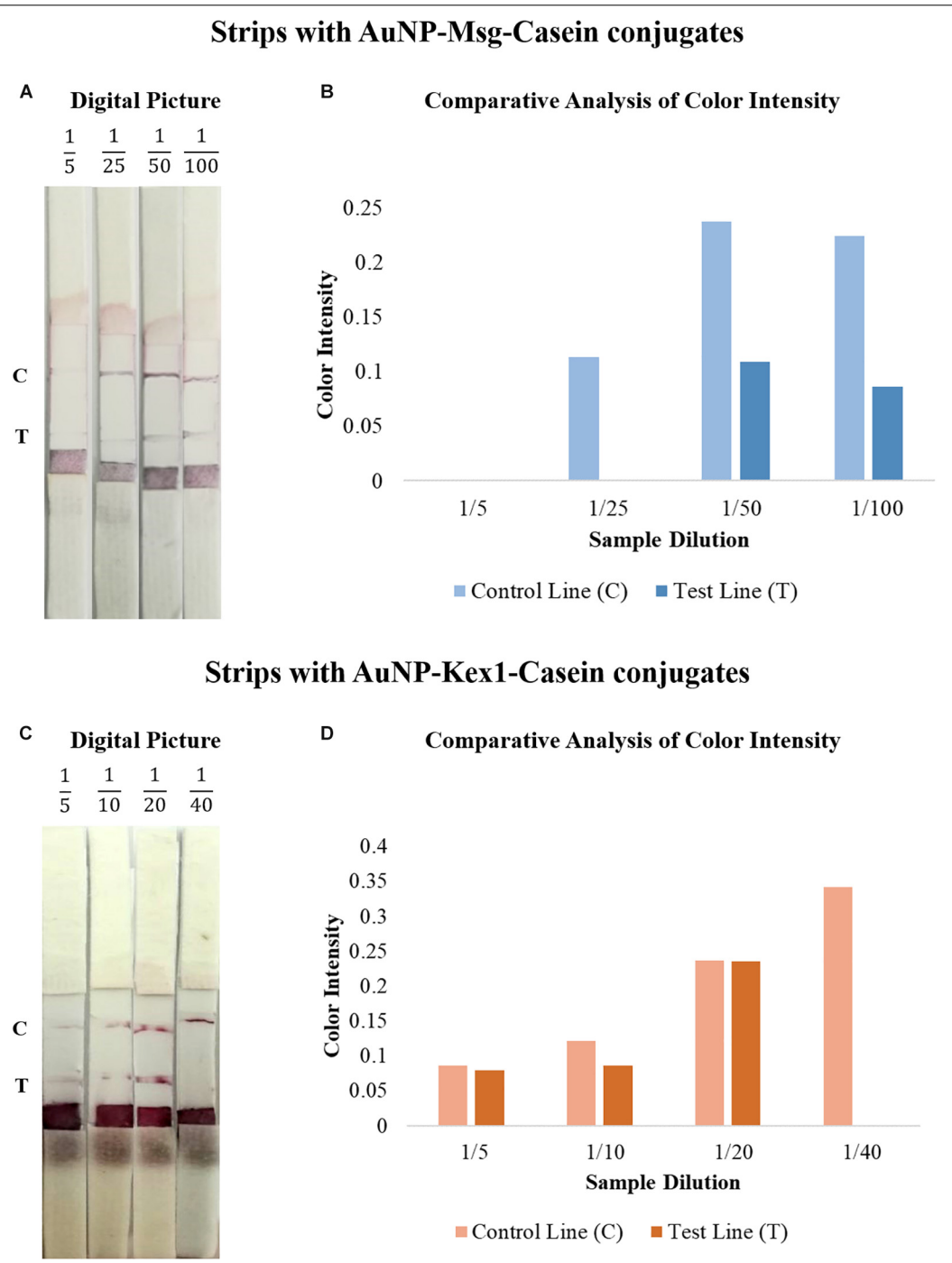

FIGURE 7 | Comparative analysis of the results from LFIA strips containing AuNP-Msg-Casein conjugates **(A,B)** and AuNP-Kex1-Casein conjugates **(C,D)**, after applying the positive sample in different dilutions. **(A,C)** Digital pictures of LFIA strip results with sample dilutions ranging from 1:5 to 1:100 in Msg LFIA strips and ranging from 1:5 to 1:40 in Kex1 strips. From bottom to top, strips were composed by the sample pad, the conjugate pad, the nitrocellulose membrane with the test (T) and control (C) lines and the absorbent pad. **(B)** Quantification of color intensity of the control and test lines, where the intensity shown in each line corresponds to the maximum height of the Gaussian line fitted by eReuss software.

(**Figure 1**). Although the traditional LFIA schemes for antibody detection uses AuNPs conjugated with an immunoglobulin-binding protein and the pathogen's antigen immobilized in the analytical zone (test line), some studies have shown that a less conventional scheme using AuNPs directly conjugated with pathogen's antigen molecules for detection of serum antibodies can achieve greater diagnostic sensitivity (Sotnikov et al., 2015, 2018). This increase in sensitivity is achieved by targeting the

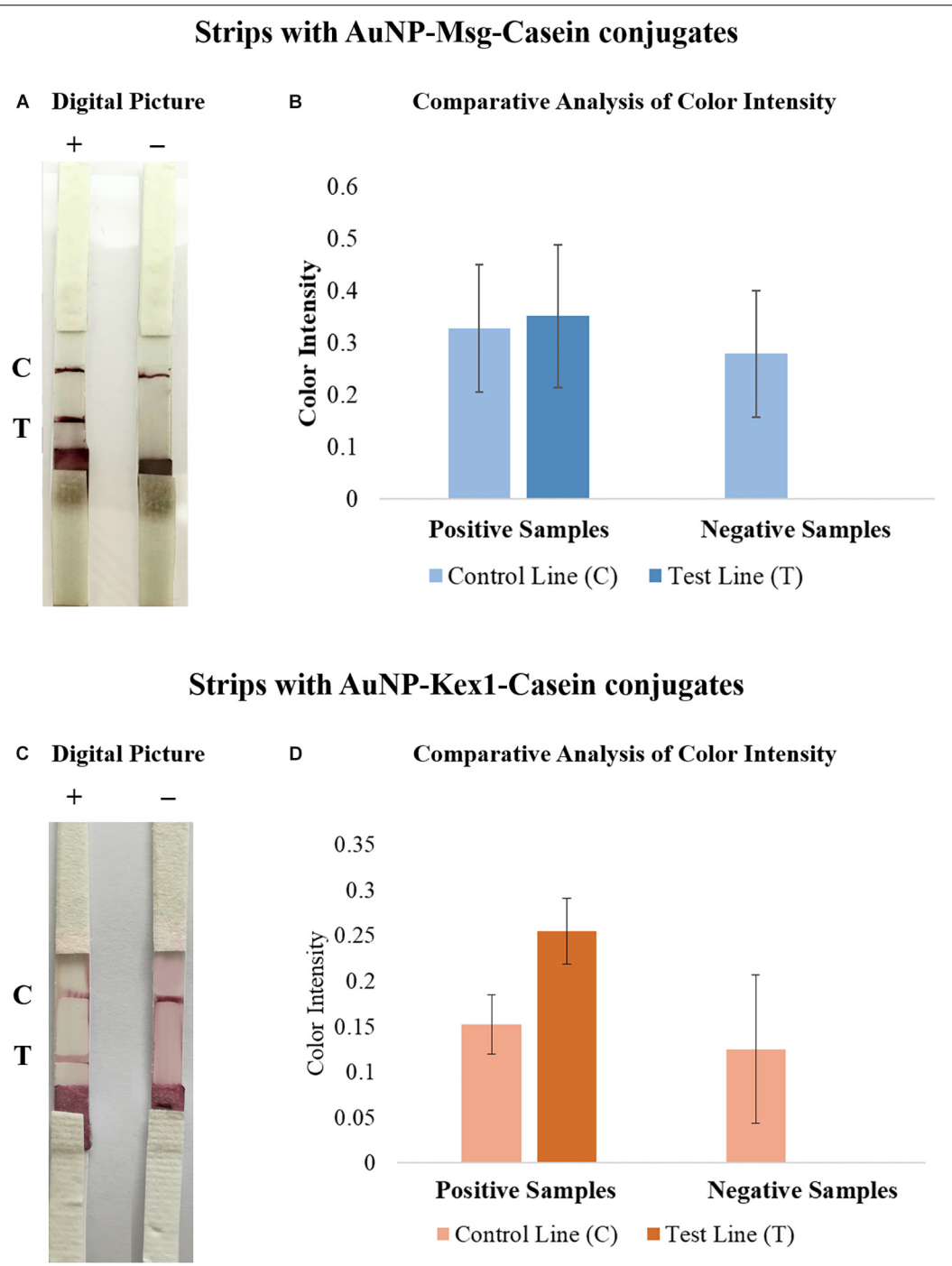

FIGURE 8 | Comparative analysis of the results from LFIA strips containing AuNP-Msg-Casein conjugates **(A,B)** and AuNP-Kex1-Casein conjugates **(C,D)**, after elution of a positive (+) or a negative (-) sample. **(A,C)** Digital pictures of LFIA strip results. From bottom to top, strips were composed by the sample pad, the conjugate pad, the nitrocellulose membrane with the test (T) and control (C) lines and the absorbent pad. **(B,D)** Quantification of color intensity of the control and test lines present in all replicates, where the intensity shown in each line corresponds to the maximum height of the Gaussian line fitted by eReuss software and the error bars represent the standard deviation values.

capture of the antibodies of interest in the conjugation process, due to the specific interaction of those antibodies with the corresponding antigens present in the conjugates. Thus, as in this study we sought to detect IgM, a class of immunoglobulins whose serum levels remain elevated for a short period of time during infection, less conventional AuNP-antigen conjugates were chosen for LFIA development. Additionally, ELISA results have shown that both Msg and Kex1 RSA are able to interact

specifically with anti-*P. jirovecii* IgM antibodies in patient's sera samples. Then, two LFIA strips for the detection of anti-*P. jirovecii* antibodies in human sera were developed, based on AuNP-Msg and AuNP-Kex1 conjugates.

Lateral flow technology is well suited to point-of-care diagnostics because it is robust and inexpensive, not requiring power, a cold chain for storage and transport, or specialized reagents (O'Farrel, 2013). This is possible because all necessary materials and reagents are prepared to be stable and ready to use at the time of sample application and the use of AuNPs ensures a visual interpretation of the results, without the need for any detection instrument.

Therefore, in this study, we synthetized MUA-capped AuNPs with a large diameter (≈40 nm, see **Supplementary Figure S9**) to obtain higher color intensity in the test/control lines with lower AuNPs concentrations (Haiss et al., 2007; Santra et al., 2017), which also helps to guarantee the low cost of the test. Additionally, the 11-MUA ligand is known to favor electrostatic protein conjugation with AuNPs (Gomes et al., 2012), which helped AuNPs conjugation with the *P. jirovecii*'s RSA and the formation of AuNP-Msg and AuNP-Kex1 conjugates.

These AuNP-RSA conjugates were characterized and optimized through AGE assays which allow the separation of the conjugates according to their differences in size and surface charge (Guirgis et al., 2012; Franco and Pereira, 2013; Cavadas et al., 2016; Kim et al., 2016; Almeida et al., 2018). Analysis of AuNP-RSA conjugates with increasing RSA:AuNP molar ratios after electrophoresis (**Figures 4A,C**) showed that as more RSA is adsorbed at the AuNPs surface, the formed conjugate migrates less in the agarose gel. This is consistent with increases in size, which decreases their electrophoretic mobility, and decreases in negative charge due to shielding induced by RSA coverage of the AuNPs, decreasing their ability to migrate toward the positive electrode. It was possible to define a plateau for the mobility of the AuNP-RSA conjugates (**Figures 4B,D**), considering the standard deviation values, that corresponds to saturation of the AuNPs surface with the RSA. So, these assays confirmed the formation of a persistent RSA corona around the AuNPs and allowed the selection of an optimal molar ratio of ca. 3000 RSA per AuNP for coverage of AuNPs with both RSA.

The ability of AuNP-RSA conjugates to interact with specific anti-*P. jirovecii* antibodies from human sera was also evaluated by AGE. The purpose of these assays was to establish a proof-of-concept for the LFIA test, demonstrating that these conjugates are indeed capable of functioning as anti-*P. jirovecii* antibody recognition tools. To achieve this goal, AuNP-RSA conjugates were incubated with human serum before and after treatment with BSA and casein (see **Supplementary Figure S14**), which are two non-antibody-reactive blocking agents that are usually applied as immunoassay blockers (Binder and Isler, 2013). This step was performed to ensure blockage of non-specific binding sites available on the surface of AuNPs after saturation with the RSA, so that non-specific interactions between AuNPs and serum proteins were minimized. For both AuNP-RSA conjugates, casein proved to be the most effective blocking agent, reducing non-specific interactions between human sera and those conjugates (see **Supplementary Figure S14**). However, even in the presence of a pre-blocking step with casein, there is some residual interaction between the negative serum and the conjugates (**Figure 5**). This event can be due to the presence of IgG anti-*P. jirovecii* antibodies in sera of patients with previous contact with *P. jirovecii*, which is supported by reports of high seropositivity for *P. jirovecii* in healthy individuals (Morris and Norris, 2012). Yet, the presence of these type of interactions does not impair the LFIA concept to be developed for two main reasons. The first one is based on the fact that these interactions will not be detected in the LFIA strip test because the search is directed to the presence of IgM anti-*P. jirovecii* antibodies, as this Ig class was the only one showing applicability in distinction of patients with active disease from not infected patients, with the ELISA results. The second reason is the consistent presence of a migration shift in the AGE assay resulting from different electrophoretic mobility's of AuNP-RSA-Casein conjugates after interaction with the positive and negative samples (**Figure 5**). These shifts result from specific interactions between anti-*P. jirovecii* antibodies present in the sera of PcP patients and the RSA, which leads to a decrease in the migration of the AuNP-RSA-Casein conjugates after contact with the positive sample, functioning as a proof-of-concept for the LFIA to be developed. It's important to notice that a more significant shift was achieved when using the Kex1 RSA. Although this was theoretically unexpected, since Kex1, unlike Msg, is not a specific or multicopy *P. jirovecii* surface antigen, it was consistent with our ELISA results that showed more significant differences between PcP and no PcP patient's IgM levels with the Kex1 RSA than with the Msg RSA. Together, these results suggest that this antigen will provide better diagnostic performance to the LFIA test than the Msg RSA.

Even so, the next step was the assembly of the two LFIA strips for detection of IgM anti-*P. jirovecii* antibodies in human sera. For that, components from a commercial starter kit were tested. Based on the visual interpretation of the strip results and on the manufacturer's recommendations for the development of LFIA with AuNP conjugates, the final components were selected. Then, the LFIA results were optimized to meet the following criteria: the appearance of color in the test and control lines within a reasonably short time (up to 10 min); presentation of a positive and negative result easily distinguished by the naked eye and confirmed by color quantification; minimum consumption of reagents for cost control. Taking this into consideration, pre-treatment steps were performed in the selected conjugate and sample pads. During the optimization process, it was noted that after adsorption, it was difficult to elute the AuNP-RSA-Casein conjugates from the conjugate pad (data not shown). Thus, as previously described by other authors that developed colloidal gold-based lateral-flow immunoassays (Kolosova et al., 2007; Li et al., 2015), we pre-treated the conjugate pad with a buffer containing 5% sucrose, 1% BSA and 0.5% Tween 20, to improve conjugates stability and re-solubilization. On the other hand, since the LFIA assay is only intended for the detection of IgM class antibodies and since AGE assays have shown that other immunoglobulins (probably IgG) can interact with our conjugates, we considered adding a preliminary

step to eliminate some of the patient's IgG antibodies before serum contact with the conjugates. For this purpose, a pre-treatment of the sample pad with anti-human IgG antibodies was made, as suggested by other authors which developed LFIA for detection of IgM antibodies (Li et al., 2015). The aim of this step was to increase the sensitivity of the test by decreasing the percentage of anti-*P. jirovecii* IgG antibodies that reach the conjugate pad, in order for the conjugates to be more available to interact with the target IgM anti-*P. jirovecii* antibodies.

The results from **Figures 6A,C** show that visually the test and control lines became easier to see with the naked eye and the results from **Figures 6B,D** confirmed this by color quantification. The comparative analysis of color intensity between strips before and after treatment, showed that the color intensity of both control and test lines has increased after treatment and that the software was not able to recognize the visible signal on the test line before treatment with the cut-off established. These results confirm that the pre-treatment steps improve the interpretation of the results, demonstrating that these steps are crucial to increase the assay sensitivity. On the other hand, the results showed a more intense color in the control line than in the test line. However, as the signal in the control line is suffering from drying effect ("coffee-ring"), we decided to make the following optimizations dispensing the control and test antibodies in a line instead of in a circle.

After, the sample dilution was also optimized (**Figure 7**). The intensity of the signals in the control and test lines increased with the dilution of the sample up to 1:50 in LFIA with the AuNP-Msg conjugates and up to 1:20 in LFIA with the AuNP-Kex1conjugates. Although signal weakening at higher dilutions was expected due to excessive sample dilution, the lack of test signals or the presence of a weaker signal at low dilutions, with both AuNP-RSA-Casein conjugates, was not expected. This is especially relevant for AuNP-Msg-Casein conjugates. We speculate that excessive levels of anti-*P. jirovecii* antibodies in the samples might lead to the formation of conjugate-antibody aggregates, preventing their free movement along the elution profile. The need for higher dilutions for conjugates with the Msg RSA than for conjugates with the Kex1 RSA was anticipated and consistent with our ELISA results, which demonstrated that serum levels of anti-Msg antibodies are higher than serum levels of anti-Kex1 antibodies. Taken together, these results demonstrate that sample dilution and sample pad pre-treatment are key factors that influence LFIA performance, and should be reevaluated when validating these LFIA in a large cohort study, before their implementation in the clinical practice.

Finally, triplicates of the optimized LFIA strips (see **Supplementary Figure S15**) were tested with a pool of serum specimens from patients with PcP (positive sample) and a pool of serum specimens from patients without *P. jirovecii* infection (negative sample) in the selected dilutions (**Figure 8**). During these assays, it was established that 3 min are enough for the sample to elute completely until the absorbing pad, giving a LFIA final result. The digital pictures (**Figures 8A,C**) and the color intensity analysis (**Figures 8B,D**) of the final results showed that in strips tested with the negative pool, only a colored line was visible on the control zone and detected by the color quantification software in all replicates. Additionally, in strips tested with the positive sample, a colored line was visible and detected by the software in both test and control zones as expected in all replicates, in both Msg and Kex1 LFIA strips.

However, these results also show that further optimization processes are needed. On the one hand, the variability between the assays (represented by the error bars in **Figure 8**), which may be justified by the lack of standardization of reagent application and strips assembly, should be minimized through automatic manufacturing processes. On the other hand, the results show that the color intensity in the control line is higher in strips tested with negative samples than in strips tested with positive samples. Although this could be explained by a higher number of free AuNP-RSA-Casein conjugates in strips tested with negative samples, it should be addressed in further optimizations by improving the conjugates:control antibodies ratio used. Finally, the results from Msg LFIA strips, showed that the conjugates seem to have formed aggregates. Although this did not impair the performance of the test, future optimization should focus on maintaining the stability of these conjugates after adsorption to the conjugate matrix, in order to obtain equally intense red lines in the LFIA strips.

CONCLUSION

In conclusion, this study provides a proof-of-concept that a point of care diagnostic test for PcP can be developed and that both LFIA developed allow the detection of IgM anti-*P. jirovecii* reactive against both RSA. This is important because in our previous study (Tomás et al., 2016) and in this study, we verified that IgM levels could be used as a serological biomarker of *P. jirovecii* active infection. However, future work is needed in order to optimize and validate this diagnostic approach in a large prospective study with patients from different clinical groups, in order to assess the sensitivity, specificity and accuracy of the two LFIA strips proposed, individually and combined. Only with these results, it will be possible to confirm the need to study the reactivity against more than one RSA in parallel and then optimize a diagnostic kit, for implementation in the clinical practice. If both AuNP-RSA conjugates prove useful in PcP diagnosis, a multiplex strategy, based in the use of two conjugate pads for the simultaneous detection of two proteins (Zhu et al., 2013), could be adapted for the present LFIA strips.

The technology proposed in this study reveals to the scientific community how these less conventional conjugates can be used in the development of an alternative approach to the conventional diagnosis of PcP, reducing the need for the current invasive procedures used in the collection of respiratory specimens, as well as reducing time response and costs associated with PcP diagnosis. Ultimately, this study will help in the management of PcP in industrialized countries, also having a major impact on

developing countries with low income and lack of technology, where PcP is an emerging disease with high prevalence and poorly controlled.

DATA AVAILABILITY STATEMENT

The raw data supporting the conclusions of this article will be made available by the authors, without undue reservation, to any qualified researcher.

ETHICS STATEMENT

The studies involving human participants were reviewed and approved by the Instituto de Higiene e Medicina Tropical, Lisboa, Portugal. Written informed consent for participation was not required for this study in accordance with the national legislation and the institutional requirements. The animal study was reviewed and approved by the Instituto de Higiene e Medicina Tropical, Lisbon, Portugal.

AUTHOR CONTRIBUTIONS

AT, RF, and OM were responsible for the study design. AT wrote the manuscript. AT, MA, FC, and MP performed the experiments. OM, EP, and RF were responsible for reagents, materials, and analysis tools supplies. All authors contributed to the approval of the final version of the manuscript.

FUNDING

This work was supported by grants from Fundação para a Ciência e a Tecnologia (MCTES funds, Portugal) and European Union (European Social Fund and European Regional Development Fund): UID/Multi/04378/2019 and POCI-01-0145-FEDER-007728 (UCIBIO-REQUIMTE); UID/QUI/50006/2019 and POCI-01-0145-FEDER-007265 (LAQV-REQUIMTE); UID/Multi/04413/2013 (GHTM); SFRH/BD/95983/2013 (to MA); and SFRH/BD/108433/2015 (to AT). Partially funded by a Gilead GÉNESE grant (PGG/001/2014). The authors declare that funding sources had no role in the study design, data collection, data interpretation or, writing of the report.

ACKNOWLEDGMENTS

We are grateful to Prof. Ludwig Krippahl (NOVA LINCS, Faculdade de Ciências e Tecnologia, Universidade NOVA de Lisboa, Portugal), for developing the gel analysis application eReuss, and to Carlos Costa for the help with the eReuss software application in quantitative analyzes.

SUPPLEMENTARY MATERIAL

The Supplementary Material for this article can be found online at: https://www.frontiersin.org/articles/10.3389/fmicb.2019.02917/full#supplementary-material

REFERENCES

Alanio, A., Hauser, P. M., Lagrou, K., Melchers, W. J., Helweg-Larsen, J., Matos, O., et al. (2016). ECIL guidelines for the diagnosis of *Pneumocystis jirovecii* pneumonia in patients with haematological malignancies and stem cell transplant recipients. *J. Antimicrob. Chemother.* 71, 2386–2396. doi: 10.1093/jac/dkw156

Almeida, M. P., Pereira, E., Baptista, P. V., Gomes, I., Figueiredo, S., Soares, L., et al. (2014). "Gold nanoparticles in analytical chemistry," in *Comprehensive Analytical Chemistry*, 1st Edn, eds M. Valcárcel, and A. I. López-Lorente (Amsterdam: Elsevier), 529–567.

Almeida, M. P., Quaresma, P., Sousa, S., Couto, C., Gomes, I., Krippahl, L., et al. (2018). Measurement of adsorption constants of laccase on gold nanoparticles to evaluate the enhancement in enzyme activity of adsorbed laccase. *Phys. Chem. Chem. Phys.* 20, 16761–16769. doi: 10.1039/C8CP03116A

Baptista, P. V., Doria, G., Quaresma, P., Cavadas, M., Neves, C. S., Gomes, I., et al. (2011). Nanoparticles in molecular diagnostics. *Prog. Mol. Biol. Transl. Sci.* 104, 427–488. doi: 10.1016/B978-0-12-416020-0.00011-5

Baptista, P. V., Pereira, E., Eaton, P., Doria, G., Miranda, A., Gomes, I., et al. (2008). Gold nanoparticles for the development of clinical diagnosis methods. *Anal. Bioanal. Chem.* 391, 943–950.

Barry, S. M., and Johnson, M. A. (2001). Pneumocystis carinii pneumonia: a review of current issues in diagnosis and management. *HIV Med.* 2, 123–132.

Bastús, N. G., Comenge, J., and Puntes, V. (2011). Kinetically controlled seeded growth synthesis of citrate-stabilized gold nanoparticles of up to 200 nm: size focusing versus Ostwald ripening. *Langmuir* 27, 11098–11105. doi: 10.1021/la201938u

Binder, S., and Isler, J. A. (2013). "Detection of antibodies relevant to infectious disease," in *The Immunoassay Handbook*, ed. D. Wild (Oxford: Elsevier), 149–155.

Blount, R. J., Jarlsberg, L. G., Daly, K. R., Worodria, W., Davis, J. L., Cattamanchi, A., et al. (2012). Serologic responses to recombinant *Pneumocystis jirovecii* major surface glycoprotein among Uganda patients with respiratory symptoms. *PLoS One* 7:e51545. doi: 10.1371/journal.pone.0051545

Cavadas, M. A. S., Monopoli, M. P., Cunha, C. S. E., Prudêncio, M., Pereira, E., Lynch, I., et al. (2016). Unravelling malaria antigen binding to antibody-gold nanoparticle conjugates. *Part. Part. Syst. Charact.* 33, 906–915. doi: 10.1002/ppsc.201600187

Chakaya, J. M., Bii, C., Amukoye, E., Ouko, T., Muita, L., Gathua, S., et al. (2003). Pneumocystis carinii pneumonia in HIV/AIDS patients at an urban district hospital in Kenya. *East Afr. Med. J.* 80, 30–35.

Chan, C. P., Mak, W. C., Cheung, K. Y., Sin, K. K., Yu, C. M., Rainer, T. H., et al. (2013). Evidence-based point-of-care diagnostics: current status and emerging technologies. *Annu. Rev. Anal. Chem.* 6, 191-211. doi: 10.1146/annurev-anchem-062012-092641

Dai, J., Jiang, M., Wang, Y., Qu, L., Gong, R., and Si, J. (2012). Evaluation of a recombinant multiepitope peptide for serodiagnosis of *Toxoplasma gondii* infection. *Clin. Vaccine Immunol.* 19, 338–342. doi: 10.1128/CVI.05553-11

Dai, J. F., Jiang, M., Qu, L. L., Sun, L., Wang, Y. Y., Gong, L. L., et al. (2013). *Toxoplasma gondii*: enzyme-linked immunosorbent assay based on a recombinant multi-epitope peptide for distinguishing recent from past infection in human sera. *Exp. Parasitol.* 133, 95–100. doi: 10.1016/j.exppara.2012.10.016

Daly, K. R., Koch, J., Levin, L., and Walzer, P. D. (2004). Enzyme-linked immunosorbent assay and serologic responses to *Pneumocystis jirovecii*. *Emerg. Infect. Dis.* 2004, 848–854. doi: 10.3201/eid1005.030497

Djawe, K., Huang, L., Daly, K. R., Levin, L., Koch, J., Schwartzman, A., et al. (2010). Serum antibody levels to the *Pneumocystis jirovecii* major surface glycoprotein

in the diagnosis of *P. jirovecii* pneumonia in HIV+ patients. *PLoS One* 5:e14259. doi: 10.1371/journal.pone.0014259

Esteves, F., Calé, S. S., Badura, R., De Boer, M. G., Maltez, F., Calderon, E. J., et al. (2015). Diagnosis of Pneumocystis pneumonia: evaluation of four serologic biomarkers. *Clin. Microbiol. Infect.* 21:379.e1–e10. doi: 10.1016/j.cmi.2014.11.025

Esteves, F., Medrano, F. J., de Armas, Y., Wissmann, G., Calderón, E. J., and Matos, O. (2014). Pneumocystis and Pneumocystosis: first meeting of experts from Latin-American and Portuguese-speaking countries - a minireview. *Expert Rev. Anti. Infect. Ther.* 12, 545–548. doi: 10.1586/14787210.2014.894883

Esteves, F., Tavares, A., Costa, M. C., Gaspar, J., Antunes, F., and Matos, O. (2009). Genetic characterization of the UCS and Kex1 loci of *Pneumocystis jirovecii*. *Eur. J. Clin. Microbiol. Infect. Dis.* 28, 175–178. doi: 10.1007/s10096-008-0596-1

European Centre for Disease Prevention, and Control (ECDC)/WHO Regional Office for Europe, (2018). *HIV/AIDS Surveillance in Europe 2018 –. (2017) Data*. Copenhagen: WHO Regional Office for Europe.

Ferard, G. (1994). Quantities and units for electrophoresis in the clinical laboratory (IUPAC Recommendations 1994). *Pure Appl. Chem.* 66, 891–896. doi: 10.1351/pac199466040891

Franco, R., and Pereira, E. (2013). "Gold nanoparticles and proteins, interaction," in *Encyclopedia of Metalloproteins*, eds R. H. Kretsinger, V. N. Uversky, and E. A. Permyakov (New York, NY: Springer), 908–915.

Gigliotti, F., Haidaris, C. G., Wright, T. W., and Harmsen, A. G. (2002). Passive intranasal monoclonal antibody prophylaxis against murine Pneumocystis carinii pneumonia. *Infect. Immun.* 70, 1069–1074.

Gingo, M. R., Lucht, L., Daly, K. R., Djawe, K., Palella, F. J., Abraham, A. G., et al. (2011). Serologic responses to Pneumocystis proteins in human immunodeficiency virus patients with and without *Pneumocystis jirovecii* pneumonia. *J. Acquir. Immune Defic. Syndr.* 57, 190–196. doi: 10.1097/QAI.0b013e3182167516

Gomes, I., Feio, M. J., Santos, N. C., Eaton, P., Serro, A. P., Saramago, B., et al. (2012). Controlled adsorption of cytochrome c to nanostructured gold surfaces. *J. Nanopart Res.* 14:1321. doi: 10.1007/s11051-012-1321-7

Guirgis, B., Sáe Cunha, C., Gomes, I., Cavadas, M., Silva, I., Doria, G., et al. (2012). Gold nanoparticle-based fluorescence immunoassay for malaria antigen detection. *Anal. Bioanal. Chem.* 402, 1019–1027. doi: 10.1007/s00216-011-5489-y

Haiss, W., Thanh, N. T. K., Aveyard, J., and Fernig, D. G. (2007). Determination of size and concentration of gold nanoparticles from UV-Vis spectra. *Anal. Chem.* 79, 4215–4221. doi: 10.1021/ac0702084

Hauser, P. M. (2019). Is the unique camouflage strategy of Pneumocystis associated with its particular niche within host lungs? *PLoS Pathog.* 15:e1007480. doi: 10.1371/journal.ppat.1007480

Huang, L., Cattamanchi, A., Davis, J. L., den Boon, S., Kovacs, J., Meshnick, S., et al. (2011). International HIV-associated opportunistic pneumonias (IHOP) study; lung HIV study. HIV associated pneumocystis pneumonia. *Proc. Am. Thorac. Soc.* 8, 294–300. doi: 10.1513/pats.201009-062WR

Hughes, W. T. (2005). "Pneumocystis pneumonitis in non-HIV-infected patients: update," in *Pneumocystis Pneumonia*, 3rd Edn, eds P. D. Walzer, and M. T. Cushion (New York, NY: Marcel Dekker, Inc.), 407–434.

Kim, S., Wark, A. W., and Lee, H. J. (2016). Gel electrophoretic analysis of differently shaped interacting and non-interacting bioconjugated nanoparticles. *RSC Adv.* 6, 109613–109619.

Kling, H. M., and Norris, K. A. (2016). Vaccine-induced immunogenicity and protection against Pneumocystis pneumonia in a nonhuman primate model of HIV and Pneumocystis coinfection. *J. Infect. Dis.* 213, 1586–1595. doi: 10.1093/infdis/jiw032

Kolosova, A. Y., De Saeger, S., Sibanda, L., Verheijen, R., and Van Peteghem, C. (2007). Development of a colloidal gold-based lateral-flow immunoassay for the rapid simultaneous detection of zearalenone and deoxynivalenol. *Anal. Bioanal. Chem.* 389, 2103–2107.

Kutty, G., and Kovacs, J. A. (2003). A single-copy gene encodes Kex1, a serine endoprotease of *Pneumocystis jiroveci*. *Infect. Immun.* 71, 571–574.

Li, X., Zhang, Q., Hou, P., Chen, M., Hui, W., Vermorken, A., et al. (2015). Gold magnetic nanoparticle conjugate-based lateral flow assay for the detection of IgM class antibodies related to TORCH infections. *Int. J. Mol. Med.* 36, 1319–1326. doi: 10.3892/ijmm.2015.2333

Matos, O. (2012). Pneumocystis jirovecii pneumonia in Africa: impact and implications of highly sensitive diagnostic technologies. *N. Am. J. Med. Sci.* 4, 486–487.

Matos, O., and Esteves, F. (2016). "Laboratory diagnosis of *Pneumocystis jirovecii* pneumonia," in *Microbiology of Respiratory System Infection*, eds K. Kon, and M. Rai (Amsterdam: Elsevier), 185–210.

Matos, O., Tomás, A. L., and Antunes, F. (2017). "*Pneumocystis jirovecii* and PcP," in *Current Progress in Medical Mycology*, eds H. M. M. Montes, and L. M. Lopes-Bezerra (Cham: Springer International Publishing), 215–254.

Medrano, F. J., Montes-Cano, M., Conde, M., De La Horra, C., Respaldiza, N., Gasch, A., et al. (2005). Pneumocystis jirovecii in general population. *Emerg. Infect. Dis.* 11, 245–250.

Morris, A., and Norris, K. A. (2012). Colonization by *Pneumocystis jirovecii* and its role in disease. *Clin. Microbiol. Rev.* 25, 297–317. doi: 10.1128/CMR.00013-12

Morris, A. M., and Masur, H. (2011). A serologic test to diagnose Pneumocystis pneumonia: are we there yet? *Clin. Infect. Dis.* 53, 203–204. doi: 10.1093/cid/cir348

Morrow, B. M., Samuel, C. M., Zampoli, M., Whitelaw, A., and Zar, H. J. (2014). Pneumocystis pneumonia in South African children diagnosed by molecular methods. *BMC Res. Notes* 7:26. doi: 10.1186/1756-0500-7-26

Nagatani, N., Tanaka, R., Yuhi, T., Endo, T., Kerman, K., Takamura, Y., et al. (2006). Gold nanoparticle-based novel enhancement method for the development of highly sensitive immunochromatographic test strips. *Sci. Technol. Adv. Mater.* 7, 270–275.

O'Farrel, B. (2013). "Lateral flow immunoassay systems: evolution from the current state of the art to the next generation of highly sensitive, quantitative rapid assays," in *The Immunoassay Handbook*, ed. D. Wild (Oxford: Elsevier), 89–107.

Ou, S. K., Hwang, J. M., and Patterson, P. H. (1993). A modified method for obtaining large amounts of high titer polyclonal ascites fluid. *J. Immunol. Methods* 165, 75–80. doi: 10.1016/0022-1759(93)90108-J

Pöhlmann, C., Dieser, I., and Sprinzl, M. (2014). A lateral flow assay for identification of *Escherichia coli* by ribosomal RNA hybridisation. *Analyst* 139, 1063–1071. doi: 10.1039/c3an02059b

Rapaka, R. R., Ricks, D. M., Alcorn, J. F., Cehn, K., Khader, S. A., Zheng, M., et al. (2010). Conserved natural IgM antibodies mediate innate and adaptive immunity against the opportunistic fungus Pneumocystis murina. *J. Exp. Med.* 207, 2907–2919. doi: 10.1084/jem.20100034

Roux, A., Gonzalez, F., Roux, M., Mehrad, M., Menotti, J., Zahar, J. R., et al. (2014). Update on pulmonary *Pneumocystis jirovecii* infection in non-HIV patients. *Med. Mal. Infect.* 44, 185–198. doi: 10.1016/j.medmal.2014.01.007

Santra, B., Shneider, M. N., and Car, R. (2017). In situ characterization of nanoparticles using Rayleigh scattering. *Sci. Rep.* 7:40230. doi: 10.1038/srep40230

Singh, J., Sharma, S., and Nara, S. (2015). Nanogold based lateral flow assay for the detection of *Salmonella* typhi in environmental water samples. *Anal. Methods* 7, 9281–9288.

Sotnikov, D. V., Zherdev, A. V., Avdienko, V. G., and Dzantiev, B. B. (2015). Immunochromatographic assay for serodiagnosis of tuberculosis using an antigen-colloidal gold conjugate. *Appl. Biochem. Microbiol.* 51, 834–839.

Sotnikov, D. V., Zherdev, A. V., and Dzantiev, B. B. (2018). Theoretical and experimental comparison of different formats of immunochromatographic serodiagnostics. *Sensors* 18:36. doi: 10.3390/s18010036

Stringer, J. R., and Keely, S. P. (2001). Genetics of surface antigen expression in Pneumocystis carinii. *Infect. Immun.* 69, 627–639.

Tomás, A. L., Cardoso, F., Esteves, F., and Matos, O. (2016). Serological diagnosis of pneumocystosis: production of a synthetic recombinant antigen for immunodetection of *Pneumocystis jirovecii*. *Sci. Rep.* 6:36287. doi: 10.1038/srep36287

Tomás, A. L., and Matos, O. (2018). Current advances in laboratory diagnosis. *OBM Genet.* 2, 1–24. doi: 10.21926/obm.genet.1804049

van Oosterhout, J. J., Laufer, M. K., Perez, M. A., Graham, S. M., Chimbiya, N., Thesing, P. C., et al. (2007). Pneumocystis pneumonia in HIV-positive adults, Malawi. *Emerg. Infect. Dis.* 13, 325–328.

Wakefield, A. E., Lindley, A. R., Ambrose, H. E., Denis, C. M., and Miller, R. F. (2003). Limited asymptomatic carriage of *Pneumocystis jiroveci* in human immunodeficiency virus–infected patients. *J. Infect. Dis.* 187, 901–908.

Wilson, R. (2008). The use of gold nanoparticles in diagnostics and detection. *Chem. Soc. Rev.* 37, 2028–2045. doi: 10.1039/b712179m

Zhu, J., Zou, N., Mao, H., Wang, P., Zhu, D., Ji, H., et al. (2013). Evaluation of a modified lateral flow immunoassay for detection of high-sensitivity cardiac troponin I and myoglobin. *Biosens. Bioelectron.* 42, 522–525. doi: 10.1016/j.bios.2012.10.016

Conflict of Interest: AT, FC, and OM have a patent PT109078 pending to Instituto de Higiene e Medicina Tropical (Lisbon, Portugal) related to the Msg RSA used in this study.

The remaining authors declare that the research was conducted in the absence of any commercial or financial relationships that could be construed as a potential conflict of interest.

frontiers in Microbiology

ORIGINAL RESEARCH
published: 07 February 2020
doi: 10.3389/fmicb.2020.00127

Pneumocystis jirovecii Diversity in Réunion, an Overseas French Island in Indian Ocean

Solène Le Gal[1,2], Gautier Hoarau[3], Antoine Bertolotti[4], Steven Negri[1], Nathan Le Nan[1], Jean-Philippe Bouchara[1], Nicolas Papon[1], Denis Blanchet[5,6], Magalie Demar[5,6] and Gilles Nevez[1,2]**

[1] Groupe d'Étude des Interactions Hôte-Pathogène (GEIHP) EA 3142, Université d'Angers-Université de Brest, Angers, France, [2] Laboratory of Mycology and Parasitology, CHRU de Brest, Brest, France, [3] Department of Microbiology, CHU La Réunion, Saint Pierre, France, [4] Department of Infectious Diseases, CHU La Réunion, Saint Pierre, France, [5] Laboratory of Mycology and Parasitology, Andrée Rosemon Hospital, Cayenne, French Guiana, [6] Equipe EA3593 - Ecosystèmes Amazoniens et Pathologie Tropicale, Université de Guyane, Cayenne, French Guiana

Data on *Pneumocystis jirovecii* characteristics from the overseas French territories are still scarce whereas numerous data on *P. jirovecii* genotypes are available for metropolitan France. The main objective of the present study was to identify *P. jirovecii* multilocus genotypes in patients living in Réunion and to compare them with those identified using the same method in metropolitan France and in French Guiana. Archival *P. jirovecii* specimens from immunosuppressed patients, 16 living in Réunion (a French island of the Indian ocean), six living in French Guiana (a South-American French territory), and 24 living in Brest (Brittany, metropolitan France) were examined at the large subunit rRNA (mtLSUrRNA) genes, cytochrome *b* (*CYB*), and superoxide dismutase (*SOD*) genes using PCR assays and direct sequencing. A total of 23 multi-locus genotypes (MLG) were identified combining mtLSUrRNA, *CYB,* and *SOD* alleles, i.e., six in Reunionese patients, three in Guianese patients, and 15 in Brest patients. Only one MLG (mtLSU1-*CYB*1-*SOD*2) was shared by Reunionese and Guianese patients (one patient from each region) whereas none of the 22 remaining MLG were shared by the 3 patient groups. A total of eight MLG were newly identified, three in Réunion and five in Brest. These results that were obtained through a retrospective investigation of a relatively low number of *P. jirovecii* specimens, provides original and first data on genetic diversity of *P. jirovecii* in Réunion island. The results suggest that *P. jirovecii* organisms from Réunion present specific characteristics compared to other *P. jirovecii* organisms from metropolitan France and French Guiana.

Keywords: *Pneumocystis jirovecii*, genotypes, Réunion, *Pneumocystis* pneumonia, multilocus sequence typing (MLST), French Guiana, France

OPEN ACCESS

Edited by:
Olga Matos,
New University of Lisbon, Portugal

Reviewed by:
Francisco Esteves,
Universidade Nova de Lisboa, Portugal
Magali Chabé,
Université de Lille, France

****Correspondence:***
Solène Le Gal
solene.legal@chu-brest.fr
Gilles Nevez
gilles.nevez@chu-brest.fr

Specialty section:
This article was submitted to Fungi and Their Interactions, a section of the journal Frontiers in Microbiology

Received: *18 October 2019*
Accepted: *20 January 2020*
Published: *07 February 2020*

Citation:
Le Gal S, Hoarau G, Bertolotti A, Negri S, Le Nan N, Bouchara J-P, Papon N, Blanchet D, Demar M and Nevez G (2020) Pneumocystis jirovecii Diversity in Réunion, an Overseas French Island in Indian Ocean. Front. Microbiol. 11:127. doi: 10.3389/fmicb.2020.00127

INTRODUCTION

Pneumocystis jirovecii is an opportunistic and transmissible fungus responsible for severe pneumonia *Pneumocystis* pneumonia (PCP) in immunocompromised patients. PCP remains the most frequent AIDS-defining illness in human immunodeficiency virus (HIV)-infected patients in metropolitan France (Cazein et al., 2015) and the West French Indies (Martinique and Guadeloupe)

whereas in French Guiana, another French region of Americas, PCP occupies the fifth position of AIDS causes. PCP is also the most frequent AIDS-defining illness in Réunion, a French island of the Indian Ocean, located close to Capricorn tropic, 600 km from east coast of Madagascar (Cire Océan Indien, 2015). HIV-infection incidence is higher in the French regions of Americas than in metropolitan France whereas its incidence is lower in Réunion (Cazein et al., 2015). PCP is also a severe disease in other immunosuppressed patients who are not infected with HIV, such as patients treated with immunosuppressive and/or cytostatic therapies (Roux et al., 2014).

Data on *P. jirovecii* characteristics from the overseas French territories are still scarce. Indeed, there is only one report on this topic, which concerned *P. jirovecii* genotypes in French Guiana (Le Gal et al., 2015) located 7,000 km from metropolitan France whereas there are no data on genomic characteristics of *P. jirovecii* from Réunion, located 9,300 km from metropolitan France and 12,000 km from French Guiana (**Figure 1**). Conversely, numerous data on *P. jirovecii* genotypes are available for metropolitan France (Nevez et al., 2003; Totet et al., 2003; Le Gal et al., 2013; Maitte et al., 2013; Gits-Muselli et al., 2015; Alanio et al., 2016; Desoubeaux et al., 2016; Charpentier et al., 2017; Vindrios et al., 2017). In this context, the main objective of the present study was to identify *P. jirovecii* multilocus genotypes in patients living in Réunion and to compare these genotypes with those identified using the same method in patients living in metropolitan France or French Guiana.

MATERIALS AND METHODS

Pneumocystis jirovecii Specimens and Patients

Seventeen *P. jirovecii* specimens from 16 patients [sex ratio M/F 13/3, median age 52 years (limits, 30–72 years)] who developed PCP and who were monitored at South Réunion Island University Hospital, were retrospectively studied. The 16 patients were diagnosed with PCP from March 2015 through June 2017. Ten patients had hematological malignancies, five patients were HIV-infected, and one patient had non-X histiocytosis.

Six *P. jirovecii* specimens from six patients [sex ratio M/F 1/5; median age 33 years (range, 30–57)] monitored at Andrée Rosemon Hospital, Cayenne, French Guiana, were also studied retrospectively. The six patients were HIV-infected and developed PCP from November 2011 through October 2012.

Twenty-four *P. jirovecii* specimens from 24 patients [sex ratio M/F 16/8, median age 64 years (limits, 33–84 years)] monitored at Brest University Hospital, Brest, Brittany, metropolitan France, were also analyzed retrospectively. These 24 patients were diagnosed with PCP from January 2013 through June 2017. Clinical and biological data of the three patient groups are summarized in **Table 1** and detailed in **Supplementary Table S1**. Data on Guianese patients were previously published elsewhere (Le Gal et al., 2015). Data on Brest patients were previously published in part elsewhere (Nevez et al., 2020).

Patients of the three groups had undergone a bronchoalveolar lavage (BAL) or induced sputum procedure to investigate pulmonary symptoms and/or fever. *P. jirovecii* had initially been detected in specimens by microscopy using Musto stain, Wright Giemsa stain, and/or an indirect immunofluorescence assay (MonofluoKit *Pneumocystis*, Bio-Rad, Marnes-La-Coquette, France), and/or PCR assays amplifying the mtLSUrRNA gene as described elsewhere (Hoarau et al., 2017; Le Gal et al., 2017). Extracted DNAs from the three patient groups were stored at −80°C until typing.

The study was non-interventional, and therefore did not require inform consents and ethical approval according to French laws and regulations (CSP Art L1121e1.1).

Pneumocystis jirovecii Typing

Extracted DNAs of BAL and induced sputum samples were examined for *Pneumocystis* genotyping based on unilocus and multilocus sequence typing (MLST) methods. Three loci, mtLSUrRNA, cytochrome *b* (*CYB*) and superoxide dismutase (*SOD*) genes were analyzed, as we previously described, using direct sequencing (Vindrios et al., 2017). Consensus sequences were aligned with reference sequences [GenBank accession numbers M58605 (mtLSUrRNA), AF074871 (*CYB*) and KT592355 (*SOD*)] (Sinclair et al., 1991; Walker et al., 1998; Singh et al., 2017) using the BioEdit software with the Clustal® W program. MtLSUrRNA alleles were named using the nomenclature described previously by Beard et al. (2000), *CYB* and *SOD* alleles were named using the nomenclature described previously by Esteves et al. (2010) and Maitte et al. (2013). According to Struelens (1996), the discriminatory power which was determined using Hunter index (H) (Hunter, 1990) was considered good if higher than 0.95. To avoid contamination, each step of the PCR assays was performed in different areas of the laboratory with different sets of micropipettes. Mix reagents were prepared in a laminar flow cabinet. To monitor for possible contamination, negative controls were included in each experiment and PCR round.

The Maximum Likelihood method implemented in MEGA (version 7.0.26) was used to reconstruct a phylogenetic tree based on the Hasegawa-Kishino-Yano model (Kumar et al., 2016). Substitution model was determined by Bayesian Information Criterion in jModelTest 0.1.1 (Posada, 2008). Bootstrap values for internal branches were generated from 1,000 replicates. MtLSUrRNA (209 bp), *CYB* (563 bp) and *SOD* (380 bp) sequences were concatenated and aligned to a reference sequence (SeqRef mtLSU CYB SOD). This reference sequence corresponds to a 209-bp portion of mtLSUrRNA reference sequence (M58605) concatenated with a 563-bp portion of *CYB* reference sequence (AF074871) and a 380-bp portion of *SOD* reference sequence (KT592355) (Sinclair et al., 1991; Walker et al., 1998; Singh et al., 2017).

Relatedness between *Pneumocystis* MLGs was evaluated with the minimum spanning tree (MST) method using GrapeTree, a free web browser application implementing Kruskal's algorithm and Edmonds' algorithm (Zhou et al., 2018). MLGs were treated as multistate categories based on an infinite allele model, i.e., all changes are equally likely.

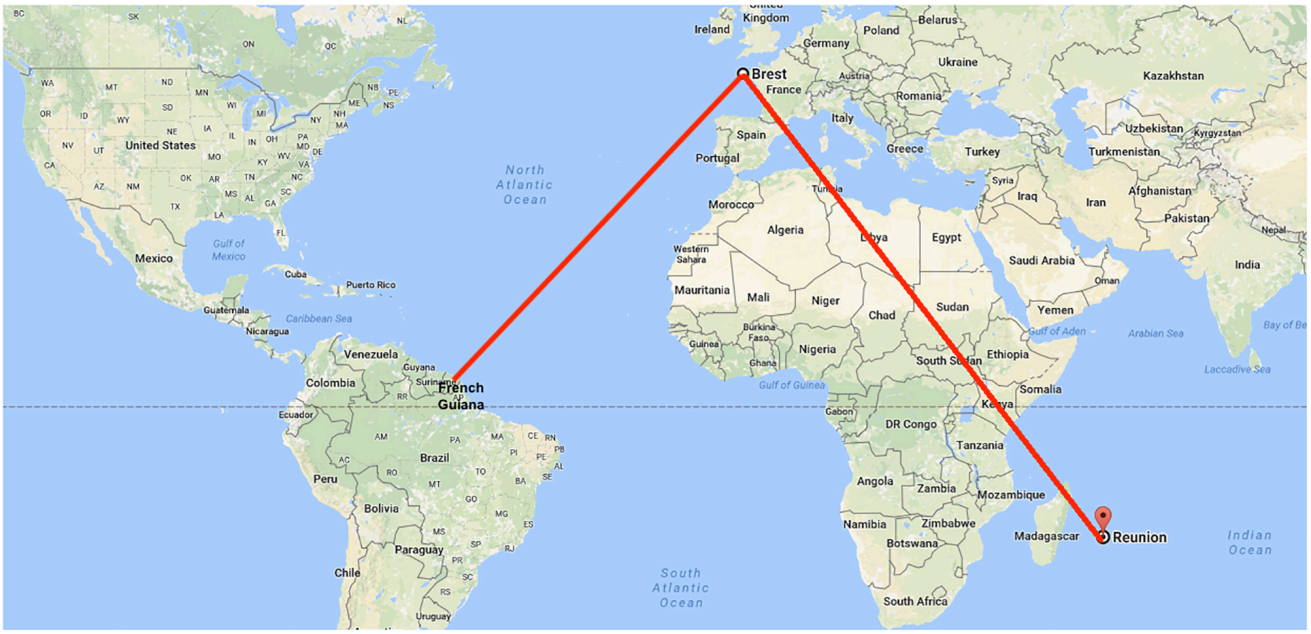

FIGURE 1 | Geographical locations of Reunion Island, French Guiana and Brest.

TABLE 1 | Characteristics of the three groups of patients from whom *Pneumocystis jirovecii* specimens were genotyped.

	La Réunion	French Guiana	Brest (metropolitan France)
No. of patients	16	6	24
Sex ratio (M/F)	13/3	1/5	16/8
Median age (range)	52 (30–72)	33 (30–57)	64 (33–84)
Period of PCP diagnosis (mo/yr)	03/2015–06/2017	11/2011–10/2012	01/2013–06/2017
Presentation of *Pneumocystis* infection (No. of patients)	PCP (16)	PCP (6)	PCP (24)
Techniques of *Pneumocystis* detection in pulmonary specimens (No. of patients)	Musto stain (7), PCR (16)[a]	Wright-Giemsa (5), IFA (4)[b]	IFA (15), PCR (24)[c]
Risk factors for *Pneumocystis* infection (No. of patients)	Hematological malignancy (10), HIV infection (5), non-X histiocytosis (1)	HIV infection (6)	Cancer (7), HIV infection (6), hematological malignancy (5), renal transplantation (2), immunosuppressive treatment (2), lymphopenia (2)

F, female; HIV, Human Immunodeficiency Virus; IFA, immunofluorescence assay (MonofluoKit Pneumocystis, Bio-Rad, Marnes-La-Coquette, France); M, male; PCP, Pneumocystis pneumonia; PCR, polymerase chain reaction. [a]*The PCR assay was performed as described by Hoarau et al. (2017). All specimens were positive for P. jirovecii detection using PCR whereas only 7 out 16 were positive using Musto stain.* [b]*5 out of 6 specimens were positive for P. jirovecii detection using Wright – Giemsa stain whereas 4 out of 6 were positive using IFA.* [c]*The PCR assay was performed as described by Le Gal et al. (2017). All specimens were positive for P. jirovecii detection using PCR whereas only 15 were positive using IFA.*

Nucleotide Sequence Accession Numbers

The nucleotide sequences of the new *CYB* allele sequences with changes at scoring positions have been deposited in GenBank under accession numbers MN602710 and MN602711.

RESULTS

Pneumocystis genotyping results are detailed in **Table 2**. MtLSUrRNA sequences were obtained for the 16 Reunionese patients (17 samples), the six Guianese patients, and the 24 Brest patients. Five alleles were identified, considering the mtLSU alleles previously described elsewhere (Beard et al., 2000; Esteves et al., 2010; **Table 2**). MtLSU1 was the most frequent allele in Reunionese patients (7 patients; 43.7%). MtLSU3 was the most frequent allele in Guianese patients (3 patients; 50%). MtLSU1, mtLSU2 and mtLSU3 were the most frequent alleles in Brest patients, these three genotypes being equally detected (seven patients each; 29.2%). MtLSU1, mtLSU2 and mtLSU3 were shared by the three patients' groups while mtLSU4 was shared by Reunionese and Brest patients. MtLSU5 was identified only in one Reunionese patients (6.2%). The presence of more than one allele was observed in seven Reunionese patients

TABLE 2 | Genotypes of *Pneumocystis jirovecii* identified in patients developing *Pneumocystis* pneumonia from Réunion, French Guiana and Brest.

Patient code	Underlying conditions	mtLSU allele	*CYB* allele	*SOD* allele	Multilocus genotype
R1	ALL	mtLSU1 + mtLSU2	*CYB*8 + *CYB*10	Mixed	Mixed
R2	HIV infection	mtLSU1 + mtLSU4	*CYB*3 + *CYB*1	Mixed	Mixed
R3	AML	mtLSU2 + mtLSU3	*CYB*5	*SOD*1	Mixed
R4	AML	mtLSU1	ND	ND	ND
R5	Myeloma	mtLSU4	*CYB*11	*SOD*2	mtLSU4-*CYB*11-*SOD*2
R6	Non-X histiocytosis	mtLSU4	*CYB*6	*SOD*1	mtLSU4-*CYB*6-*SOD*1
R7	ALL	mtLSU4	*CYB*11	*SOD*2	mtLSU4-*CYB*11-*SOD*2
R8	HIV infection	mtLSU1 + mtLSU2 + mtLSU3	*CYB*1	Mixed	Mixed
R9	Polycythemia vera	mtLSU1 + mtLSU2	*CYB*1 + *CYB*8	*SOD*1	Mixed
R10	HIV infection	mtLSU4	*CYB*1	ND	ND
		mtLSU1 + mtLSU4	*CYB*1	Mixed	Mixed
R11	Myeloma	mtLSU3	*CYB*10	*SOD*1	mtLSU3-*CYB*10-*SOD*1
R12	Lymphoma	mtLSU2	*CYB*1	ND	ND
R13	AML	mtLSU5	*CYB*3	ND	ND
R14	HIV infection	Mixed	Mixed	*SOD*1 + *SOD*4	ND
R15	ALL	mtLSU3	*CYB*1	*SOD*4	mtLSU3-*CYB*1-*SOD*4
R16	HIV infection	mtLSU1	*CYB*1 + *CYB*6	*SOD*2	mtLSU1-*CYB*1-*SOD*2 + mtLSU1-*CYB*6-*SOD*2
G1	HIV infection	mtLSU2	*CYB*1	*SOD*2	mtLSU2-*CYB*1-*SOD*2
G2	HIV infection	Mixed	Mixed	Mixed	Mixed
G3	HIV infection	mtLSU1 + mtLSU3	*CYB*1	*SOD*2	mtLSU1-*CYB*1-*SOD*2 + mtLSU3-*CYB*1-*SOD*2
G4	HIV infection	mtLSU3	*CYB*1	*SOD*2	mtLSU3-*CYB*1-*SOD*2
G5	HIV infection	mtLSU2	*CYB*1	*SOD*2	mtLSU2-*CYB*1-*SOD*2
G6	HIV infection	mtLSU3	*CYB*1	*SOD*2	mtLSU3-*CYB*1-*SOD*2
B1	HIV infection	mtLSU2	*CYB*2	*SOD*1	mtLSU2-*CYB*2-*SOD*1
B2	Cancer	mtLSU4	*CYB*1	*SOD*1	mtLSU4-*CYB*1-*SOD*1
B3	Cancer	mtLSU1	*CYB*5 + *CYB*8	*SOD*2	mtLSU1-*CYB*5-*SOD*2 + mtLSU1-*CYB*8-*SOD*2
B4	Immunosuppressive treatment	mtLSU1	*CYB*2	*SOD*2	mtLSU1-*CYB*2-*SOD*2
B5	HIV infection	mtLSU1 + mtLSU4	*CYB*2	*SOD*1	mtLSU1-*CYB*2-*SOD*1 + mtLSU4-*CYB*2-*SOD*1
B6	AML	mtLSU1	*CYB*8	*SOD*2	mtLSU1-*CYB*8-*SOD*2
B7	Lymphopenia	mtLSU2	Mixed	Mixed	Mixed
B8	Lymphopenia	mtLSU2	*CYB*8	*SOD*1	mtLSU2-*CYB*8-*SOD*1
B9	Myeloma	mtLSU2	*CYB*7 + *CYB*1	Mixed	Mixed
B10	Lymphoma	mtLSU3	*CYB*1	*SOD*1	mtLSU3-*CYB*1-*SOD*1
B11	Myeloma	mtLSU4	*CYB*1	*SOD*1	mtLSU4-*CYB*1-*SOD*1
B12	Renal Transplant Recipient	mtLSU4	*CYB*2	*SOD*1	mtLSU4-*CYB*2-*SOD*1
B13	Cancer	Mixed	*CYB*1 + *CYB*2	*SOD*2	Mixed
B14	Cancer	mtLSU1	*CYB*1	Mixed	Mixed
B15	HIV infection	mtLSU3	*CYB*6	*SOD*1	mtLSU3-*CYB*6-*SOD*1
B16	Immunosuppressive treatment	Mixed	*CYB*1 + *CYB*6	*SOD*2	Mixed
B17	HIV infection	mtLSU1 + mtLSU3	*CYB*1	*SOD*1 + *SOD*4	Mixed
B18	Cancer	mtLSU2	*CYB*1	Mixed	Mixed
B19	Lymphoma	mtLSU2	*CYB*2	Mixed	Mixed
B20	Cancer	mtLSU1 + mtLSU3	*CYB*1	*SOD*1	mtLSU1-*CYB*1-*SOD*1 + mtLSU3-*CYB*1-*SOD*1
B21	HIV infection	mtLSU3	*CYB*5	*SOD*1	mtLSU3-*CYB*5-*SOD*1
B22	Cancer	mtLSU3	ND	*SOD*2	ND
B23	Renal Transplant Recipient	mtLSU4	*CYB*2	*SOD*1	mtLSU4-*CYB*2-*SOD*1
B24	HIV infection	mtLSU2 + mtLSU3	*CYB*2	*SOD*2	mtLSU2-*CYB*2-*SOD*2 + mtLSU3-*CYB*2-*SOD*2

F, female; HIV, Human Immunodeficiency Virus; M, male; ALL, acute lymphoblastic leukemia; AML, acute myeloblastic leukemia; mtLSUrRNA, mitochondrial large subunit ribosomal RNA; CYB, cytochrome b; SOD, superoxide dismutase; mixed, allele mix due to the presence of several different alleles that could not be identified; ND, not determined. Patients and samples are identified with a letter (R for Reunionese patients, G for Guianese patients and B for Brest patients) followed by a number.

(43.7%), two Guianese patients (33.3%) and six patients from Brest (25%). The Hunter index for mtLSU genotyping was evaluated to 0.76.

CYB sequences were obtained from 15 out of 16 Reunionese patients (16 samples), as well as from the 6 Guianese patients and 23 out of 24 patients from Brest. Considering the *CYB*

alleles previously described elsewhere (Esteves et al., 2010; Maitte et al., 2013), seven already known alleles (*CYB*1, *CYB*2, *CYB*3, and *CYB*5 to *CYB*8) and two new alleles (*CYB*10 and *CYB*11) were identified (**Table 2**), *CYB*1 being the most frequent in the three patient groups [seven Reunionese patients (46.7%), five Guianese patients (83.3%), 10 Brest patients (43.5%)]. The new *CYB*10 allele differs from *CYB*2 by a change from C to T residue at scoring position 279, and the new *CYB*11 allele differs from *CYB*1 by a change from C to T residue at scoring position 742. *CYB*1 was shared by the three populations. In contrast, *CYB*3, *CYB*10, and *CYB*11 were identified only in Reunionese patients [three (20%), three (20%) and two (13.3%) patients, respectively] while *CYB*2 and *CYB*7 were detected only in Brest patients [eight (37.8%) patients and one (4.3%) patient, respectively]. The presence of more than one allele was observed in five Reunionese patients (33.3%), one Guianese patient (16.7%) and five patients from Brest (21.7%). The Hunter index for *CYB* genotyping was evaluated to 0.76.

SOD sequences were obtained from 13 out of the 16 Reunionese patients, as well as from the six Guianese patients and the 24 patients from Brest. Considering the *SOD* alleles previously described elsewhere (Esteves et al., 2010; Maitte et al., 2013), three alleles were identified (**Table 2**), *SOD*1 being the most frequent in Reunionese and Brest patients (five (38.5%) and 12 (50%) patients, respectively) and *SOD*2 the most frequent in Guianese patients [five patients (83.3%)]. *SOD*2 was identified in the three patient groups. The presence of more than one allele was observed in five Reunionese patients (38.5%), one Guianese patient (16.7%) and six patients from Brest (25%). The Hunter index for *SOD* genotyping was evaluated to 0.59.

Combining mtLSUrRNA, *CYB,* and *SOD* alleles, 23 multilocus genotypes (MLG) were identified (**Table 2**). MtLSU4-*CYB*11-*SOD*2, mtLSU3-*CYB*1-*SOD*2, and mtLSU4-*CYB*2-*SOD*1 were the most frequent MLG in Reunionese patients (two patients, 16.7%), Guianese patients (three patients, 50%), and Brest patients (three patients, 13%), respectively. Only one MLG (mtLSU1-*CYB*1-*SOD*2) was shared by the Reunionese and the Guianese patients (one patient from each region, 8.3 and 16.7% respectively) whereas the 22 remaining MLG were not shared by the three patient groups. The presence of more than one genotype was observed in seven Reunionese patients (58.3%), two Guianese patients (33.3%) and 12 patients from Brest (52.2%). The Hunter index for MLST was evaluated to 0.978.

The phylogenetic tree was generated based on sequence analysis of mtLSUrRNA, *CYB*, and *SOD* alleles through the MLST approach (**Figure 2**). The analysis showed that some genotypes detected in patients from metropolitan France and the Réunion island were close despite the rarity of MLST genotype sharing. Nonetheless, the bootstrap values were low (<50).

As well, MST analysis revealed that most of *Pneumocystis* isolates from the three geographic regions were close and belonged to the same genetic cluster since they had a single allelic mismatch with at least one other isolate (**Figure 3**). However, two isolates from Réunion who shared the same MLG (mtLSU4-*CYB*11-*SOD*2) were more distant from the other isolates since they had two allelic mismatches with the closest isolate.

DISCUSSION

In this study, the first data on *P. jirovecii* genotypes in patients from Réunion, a French region in the Indian Ocean, were obtained. Using an unilocus approach, we identified mtLSUrRNA, *CYB*, and *SOD* common alleles in the three patient populations (Réunion, French Guiana, and Brest), suggesting that *P. jirovecii* organisms from Réunion, French Guiana and Metropolitan France share common characteristics. Nonetheless, some alleles were identified only from one patient population, e.g., mtLSU5, *CYB*10, and *CYB*11 were identified only from Reunionese patients.

We chose to analyze mtLSUrRNA, *CYB*, and *SOD* loci because this MLST scheme is highly discriminant as described by Maitte et al. (2013). Indeed, in the present study, the discriminatory power of our technique, based on the Hunter index, was evaluated to 0.978, which is considered to be good, i.e., >0.95, one criterion of those described by the ESCMID to validate a typing method (Struelens, 1996). The sequencing was performed using Sanger method, which is easy to be performed. However, it could be less sensitive to detect and identify alleles in a mixture than PCR-SSCP or high-throughput methods, such as ultra-deep sequencing or multiplex PCR-Single-Base-Extension (Hauser et al., 2001; Esteves et al., 2011, 2016; Alanio et al., 2016; Charpentier et al., 2017). In the present study mixed alleles were identified in 15 out of 46 patients (32.6%) for mtLSUrRNA, in 11 out of 44 patients (25%) for CYB, and in 12 out of 43 patients (27.9%) for SOD. Considering MLG analysis, mixed MLGs were identified in 21 out of 42 patients (50%). These rates are lower than those observed in studies using PCR-SSCP (Hauser et al., 2001) or molecular high-throughput methods, such as ultra-deep sequencing (Alanio et al., 2016; Charpentier et al., 2017), in which rates of mixed genotypes may reach 85% for nuclear loci and even 92% for mitochondrial loci. However, this potential weakness of our method should not question our analysis based on major genotypes. Moreover, the method we used is suitable for examining samples with low fungal loads (Vindrios et al., 2017; Nevez et al., 2018, 2020).

The alleles *CYB*10 and *CYB*11 identified in Reunionese patients were newly described in this study. Allele *CYB*10 differs from allele *CYB*2 described by Esteves et al. (2010) by the substitution from C to T residue at position 279, which is a silent mutation. However, this allele corresponds to haplotype 13 as described by Charpentier et al. (2017) using another nomenclature. It was identified in two patients from Grenoble, metropolitan France. Allele *CYB*11 differs from allele *CYB*1 by having a T residue at position 742. This substitution from C to T represents a non-synonymous mutation leading to the substitution from leucyl to phenylalanyl residue at position 275 (L275F). This mutation located at the quinol oxidation (Qo) site of the mitochondrial cytochrome bc1 may induce potential atovaquone resistance of *P. jirovecii.* Indeed, atovaquone which is used as second line treatment of PCP or PCP prophylaxis, is an analog of ubiquinone that binds the Qo site. This mutation, but not this allele, has previously been described by Kazanjian et al. (2001) among *P. jirovecii* isolates from patients with past history of atovaquone exposure. It is noteworthy that the two Reunionese

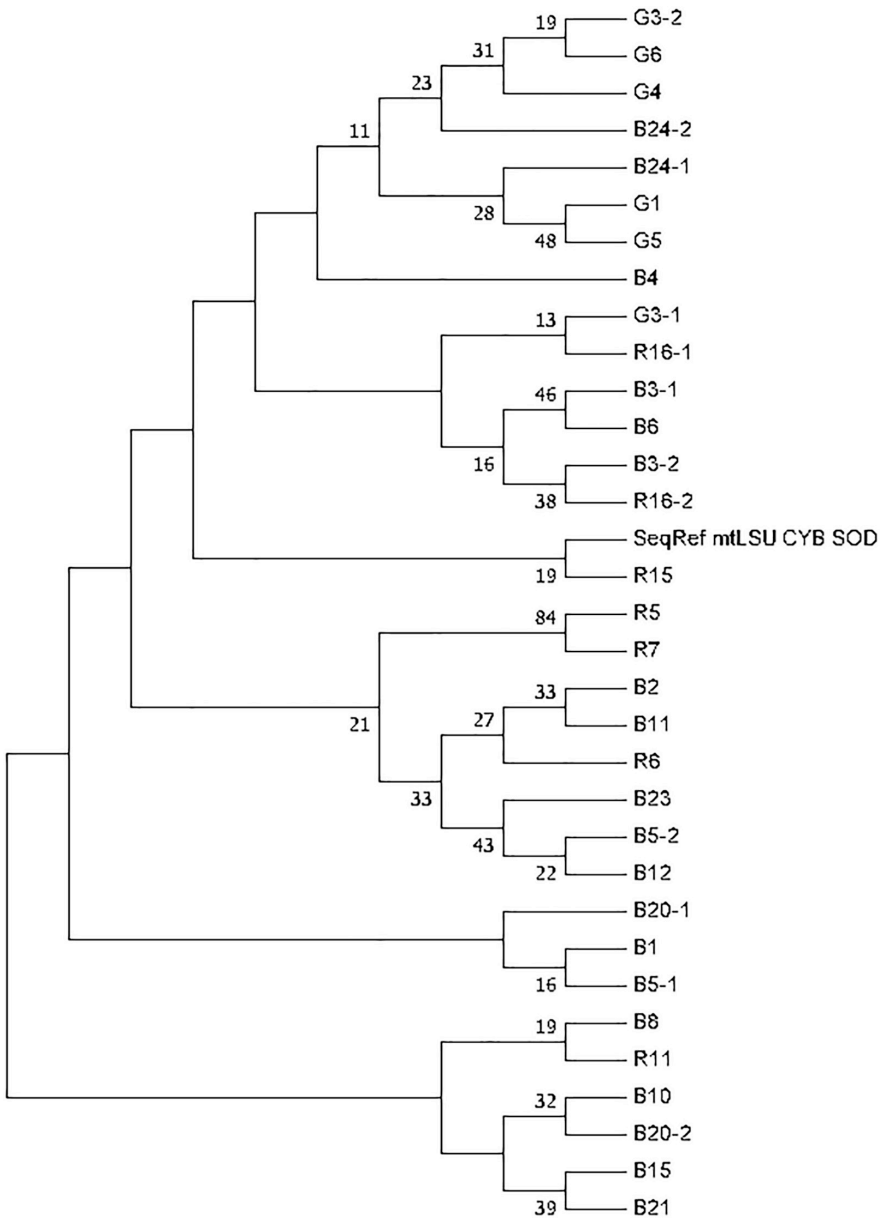

FIGURE 2 | Phylogenetic tree generated based on *Pneumocystis jirovecii* MLST genotypes. The tree was constructed on the basis of concatenated loci (mtLSUrRNA, *CYB*, and *SOD*). Phylogenetic analysis used the Maximum Likelihood method based on the Hasegawa-Kishino-Yano model. The bootstrap consensus tree was inferred from 1,000 replicates. Branches corresponding to partitions reproduced in less than 50% bootstrap replicates are collapsed. The percentage of replicate trees in which the associated taxa clustered together in the bootstrap test are shown next to the branches. Only bootstrap values >10% are shown. Initial tree(s) for the heuristic search were obtained automatically by applying Neighbor-Join and BioNJ algorithms to a matrix of pairwise distances estimated using the Maximum Composite Likelihood (MCL) approach, and then selecting the topology with superior log likelihood value. The analysis involved 33 nucleotide sequences. There were a total of 1152 positions in the final dataset. Evolutionary analyses were conducted in MEGA7. Patients and samples are identified with a letter (R for Reunionese patients, G for Guianese patients and B for Brest patients) followed by a number.

patients, who were infected with cytochrome *b* mutant *P. jirovecii* organisms, were effectively subjected to atovaquone prophylaxis in a context of hematological malignancy (myeloma for one patient, and T-cell acute lymphoblastic leukemia for the other), at the time of PCP diagnosis. This observation was consistent with that we recently reported concerning the selection of cytochrome *b* mutants in heart transplant recipients in a context of PCP case clusters and the use of atovaquone prophylaxis (Argy et al., 2018).

In this study, allele mtLSU5 was identified only from one Reunionese patient. This infrequent allele has been previously identified in metropolitan patients from Brest and Lille (de Armas et al., 2012; Le Gal et al., 2015) and in a Guianese patient (patient G2 in the present study) (Le Gal et al., 2015) using cloning instead

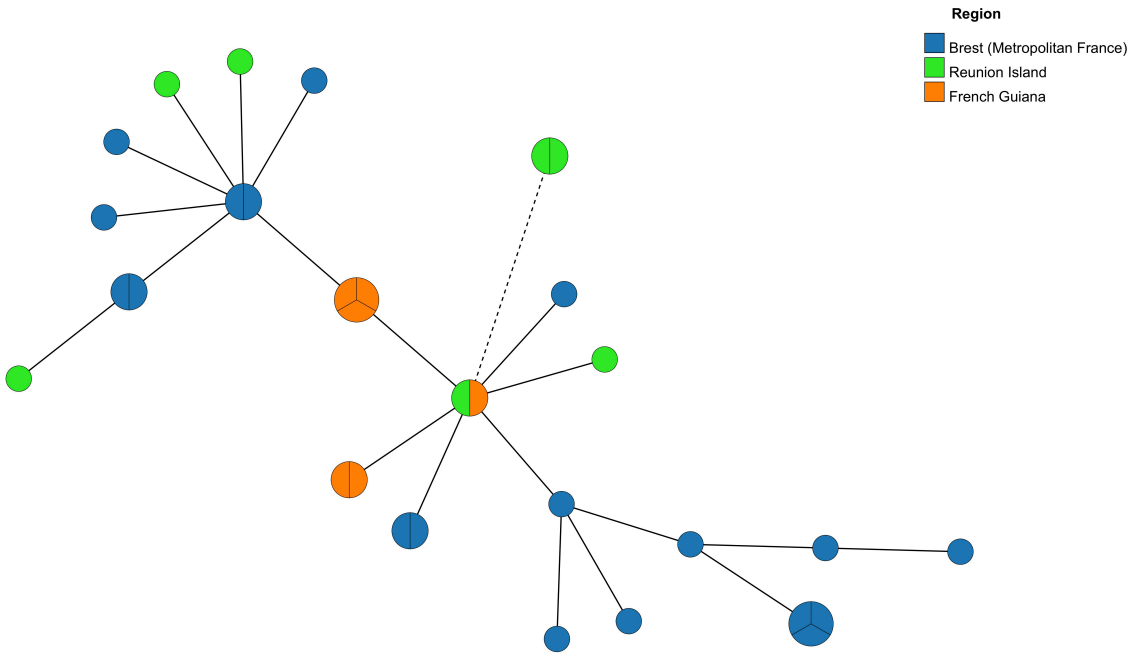

FIGURE 3 | Minimum Spanning Tree analysis of *Pneumocystis* isolates from six Reunionese patients, five Guianese patients and 15 Brest (Metropolitan France) patients harboring one multilocus genotype (MLG) (one allele per locus) or two MLGs (two alleles for one locus). Each circle corresponds to one MLG. The size of the circles is correlated with the number of isolates possessing the corresponding MLG. The color of the circles indicates the origin region of the *Pneumocystis* isolates. A continuous connecting line corresponds to one different allele separating two MLGs. A dashed connecting line corresponds to two different alleles separating two MLGs.

of direct sequencing of the mtLSUrRNA sequences. Thus, this allele does not represent a specific characteristic of *P. jirovecii* organisms from Réunion island.

There are available data on genotyping of *P. jirovecii* isolates from adult patients or children who lived in Zimbabwe or Mozambique (Africa), two countries relatively close to Réunion and from other adults or children who lived in Cuba (West Indies), a country relatively close to French Guiana (Miller et al., 2003, 2005; de Armas et al., 2012; Monroy-Vaca et al., 2014; Esteves et al., 2016). This geographical proximity deserves *P. jirovecii* genotype comparison. Considering the results of unilocus typing, mtLSU3 allele is the most frequent allele in adults from Cuba as well as in adults from French Guiana (de Armas et al., 2012), whereas mtLSU2 is the most frequent allele in children from Cuba (Monroy-Vaca et al., 2014). To the best of our knowledge, no information on *SOD* and *CYB* alleles in adults from Cuba is available. Conversely, in children, *CYB*1 and *SOD*1 are the most frequent alleles in Cuba whereas alleles *CYB*1 and *SOD*2 are the most frequent alleles in adults in French Guiana. No data on *P. jirovecii* genotyping in children from French Guiana are available.

MtLSU3 and mtLSU1 are the most frequent alleles in adults from Zimbabwe and Reunion respectively (Miller et al., 2003). In the same patient population, *SOD*2 and *SOD*1 are the most frequent alleles in Zimbabwe and Reunion respectively (Miller et al., 2003). Conversely, in children from Mozambique the most frequent allele is mtLSU2 and/or mtLSU5 (considering that information on scoring nucleotide position 248 is lacking) (Esteves et al., 2016). No data on *CYB* alleles from Zimbabwe and Mozambique, whichever patient population, are available.

Finally, due to differences in characteristics of the studied patient populations (adults vs. children, numbers of patients) and analyzed loci, it remains difficult to draw a conclusive analysis of this genotype comparison.

A total of 23 MLG were identified. It is noteworthy that 22 were not shared by the three patient group whereas only one MLG was shared by two of the three patient groups. Thus, the results of MLG analysis, due to the high discriminatory power of the method (Hunter index, 0.978), allow to discriminate *P. jirovecii* isolates into three different groups according to the geographic origin of the patients. Nonetheless, among the five MLG identified only in Reunionese patients, two (mtLSU1-*CYB*6-*SOD*2 and mtLSU3-*CYB*1-*SOD*4) has already been reported in patients from metropolitan France and Portugal (Esteves et al., 2010; Maitte et al., 2013). Conversely, the three other MLG (mtLSU3-*CYB*10-*SOD*1, mtLSU4-*CYB*11-*SOD*2, and mtLSU4-*CYB*6-*SOD*1) were reported for the first time in the present study. It is noteworthy that the MLG mtLSU4-*CYB*11-*SOD*2 consists in the combination of mtLSU4 allele, *SOD*2 allele and the newly described allele *CYB*11 which might have been selected in the course of atovaquone prophylaxis. Be that as it may, taken together, these results suggest that *P. jirovecii* organisms from Réunion island may present specific characteristics.

Three MLG were identified in Guianese patients; all of them have already been reported in patients from metropolitan

France or Portugal (Esteves et al., 2010; Maitte et al., 2013; Desoubeaux et al., 2016; Charpentier et al., 2017). These results are not consistent with those previously obtained using another genotyping method (Le Gal et al., 2015), which suggested that specific genotypes and consequent specific characteristics of *P. jirovecii* organisms may exist in French Guiana. This could be explained by the fact that more data are available in literature on MLG combining mtLSUrRNA, *CYB*, and *SOD* alleles than on MLG combining ITS, *DHPS*, and mtLSUrRNA alleles, the method we used previously.

Fifteen MLG were identified in Brest patients, of which ten have already been reported in patients from metropolitan France and Portugal (Esteves et al., 2010; Maitte et al., 2013; Desoubeaux et al., 2016; Charpentier et al., 2017; Vindrios et al., 2017) whereas five were reported for the first time. These five MLG (mtLSU1-*CYB*2-*SOD*2, mtLSU1-*CYB*3-*SOD*1, mtLSU1-*CYB*5-*SOD*2, mtLSU2-*CYB*2-*SOD*2, and mtLSU3-*CYB*2-*SOD*2) may represent specific characteristics of *P. jirovecii* organisms in Brittany, western France. Likewise, the three MLG identified in Réunion island may represent specific characteristics of *P. jirovecii* organisms in this French overseas island. However, the results of the MST suggest that *P. jirovecii* organisms from the three French regions are closely related and belong to the same genetic cluster, excepting two isolates from Réunion. These two isolates share the same new MLG (mtLSU4-*CYB*11-*SOD*2) (see above).

Finally, a total of eight MLG were newly identified, three in Réunion and five in Brest, suggesting that specific characteristics in these two French regions, located 9,300 km apart may exist. However, genotyping results should not be too conclusive considering the low number of patients for whom MLG were identified in this study (six Reunionese patients, five Guianese patients, 15 patients from Brest). Moreover, the dates of *P. jirovecii* sampling in the three geographical regions were not identical, which may represent a bias of enrolment. Likewise, the underlying diseases of the patients were not strictly similar since Guianese patients were all HIV-infected contrary to Reunionese patients and patients from Brest, these disparities representing a bias as well. Furthermore, available data on MLG combining mtLSUrRNA, *CYB*, and *SOD* alleles are still limited since only four studies from France and one from Portugal were based on these sequences (Esteves et al., 2010; Maitte et al., 2013; Desoubeaux et al., 2016; Charpentier et al., 2017; Vindrios et al., 2017). Moreover, the results of phylogenetic tree and MST analysis are poorly informative. Be that as it may, despite these possible limitations, the present study brings original and first data on genetic diversity of *P. jirovecii* organisms from Réunion island and its comparison with other very distant French regions.

DATA AVAILABILITY STATEMENT

The datasets generated for this study can be found in the GenBank database (accession numbers: MN602710 and MN602711).

ETHICS STATEMENT

Ethical review and approval was not required for the study on human participants in accordance with the local legislation and institutional requirements. Written informed consent for participation was not required for this study in accordance with the national legislation and the institutional requirements.

AUTHOR CONTRIBUTIONS

SL and GN analyzed the DNA sequences and wrote the manuscript. GH and AB performed *P. jirovecii* detection, provided *P. jirovecii* specimens from Réunion, and analyzed patients' characteristics. SN and NL performed in part the genotyping. J-PB and NP contributed to the discussion and correction of the manuscript. DB and MD performed *P. jirovecii* detection and provided *P. jirovecii* specimens, and analyzed patients' characteristics from French Guiana.

SUPPLEMENTARY MATERIAL

The Supplementary Material for this article can be found online at: https://www.frontiersin.org/articles/10.3389/fmicb.2020.00127/full#supplementary-material

REFERENCES

Alanio, A., Gits-Muselli, M., Mercier-Delarue, S., Dromer, F., and Bretagne, S. (2016). Diversity of *Pneumocystis jirovecii* during infection revealed by ultra-deep pyrosequencing. *Front. Microbiol.* 7:733. doi: 10.3389/fmicb.2016.00733

Argy, N., Le Gal, S., Coppee, R., Song, Z., Vindrios, W., Massias, L., et al. (2018). Pneumocystis cytochrome B mutants associated with atovaquone prophylaxis failure as the cause of *Pneumocystis* infection outbreak among heart transplant recipients. *Clin. Infect. Dis.* 67, 913–919. doi: 10.1093/cid/ciy154

Beard, C. B., Carter, J. L., Keely, S. P., Huang, L., Pieniazek, N. J., Moura, I. N., et al. (2000). Genetic variation in *Pneumocystis carinii* isolates from different geographic regions: implications for transmission. *Emerg. Infect. Dis.* 6, 265–272. doi: 10.3201/eid0603.000306

Cazein, F., Pillonel, J., Le Strat, Y., Pinget, R., Le Vu, S., Brunet, S., et al. (2015). Découvertes de séropositivité VIH et de SIDA, France, 2003-2013. *Bull. Epidemiol. Hebd.* 9- 10, 152–161.

Charpentier, E., Garnaud, C., Wintenberger, C., Bailly, S., Murat, J. B., Rendu, J., et al. (2017). Added value of next-generation sequencing for multilocus sequence typing analysis of a *Pneumocystis jirovecii* pneumonia outbreak1. *Emerg. Infect. Dis.* 23, 1237–1245. doi: 10.3201/eid2308.161295

Cire Océan Indien (2015). Surveillance des infections à VIH et Sida à la Réunion et Mayotte, région océan Indien de 2003 à 2014, données actualisées au 31/12/2014. *Bull. Veille Sanitaire* 29, 2–7.

de Armas, Y., Friaza, V., Capo, V., Durand-Joly, I., Govin, A., de la Horra, C., et al. (2012). Low genetic diversity of *Pneumocystis jirovecii* among Cuban population based on two-locus mitochondrial typing. *Med. Mycol.* 50, 417–420. doi: 10.3109/13693786.2011.607474

Desoubeaux, G., Dominique, M., Morio, F., Thepault, R. A., Franck-Martel, C., Tellier, A. C., et al. (2016). Epidemiological outbreaks of *Pneumocystis jirovecii* pneumonia are not limited to kidney transplant recipients: genotyping confirms common source of transmission in a liver transplantation unit. *J. Clin. Microbiol.* 54, 1314–1320. doi: 10.1128/JCM.00133-16

Esteves, F., Gaspar, J., De Sousa, B., Antunes, F., Mansinho, K., and Matos, O. (2011). Clinical relevance of multiple single-nucleotide polymorphisms in *Pneumocystis jirovecii* Pneumonia: development of a multiplex PCR-single-base-extension methodology. *J Clin Microbiol.* 49, 1810–1815. doi: 10.1128/JCM.02303-10

Esteves, F., Gaspar, J., Tavares, A., Moser, I., Antunes, F., Mansinho, K., et al. (2010). Population structure of *Pneumocystis jirovecii* isolated from immunodeficiency virus-positive patients. *Infect., Genet. Evol.* 10, 192–199. doi: 10.1016/j.meegid.2009.12.007

Esteves, F., de Sousa, B., Calderon, E. J., Huang, L., Badura, R., Maltez, F., et al. (2016). Multicentre study highlighting clinical relevance of new high-throughput methodologies in molecular epidemiology of *Pneumocystis jirovecii* pneumonia. *Clin. Microbiol. Infect.* 22:e569.e9–e566.e19. doi: 10.1016/j.cmi.2016.03.013

Gits-Muselli, M., Peraldi, M. N., de Castro, N., Delcey, V., Menotti, J., Guigue, N., et al. (2015). New short tandem repeat-based molecular typing method for *Pneumocystis jirovecii* reveals intrahospital transmission between patients from different wards. *PloS One* 10:e0125763. doi: 10.1371/journal.pone.0125763

Hauser, P., Blanc, D. S., Sudre, P., Senggen Manoloff, E., Nahimana, A., Bille, J., et al. (2001). Genetic diversity of *Pneumocystis carinii* in HIV-positive and -negative patients as revealed by PCR-SSCP typing. *AIDS* 15, 461–466. doi: 10.1097/00002030-200103090-00004

Hoarau, G., Le Gal, S., Zunic, P., Poubeau, P., Antok, E., Jaubert, J., et al. (2017). Evaluation of quantitative FTD-*Pneumocystis jirovecii* kit for *Pneumocystis* infection diagnosis. *Diagn. Microbiol. Infect. Dis.* 89, 212–217. doi: 10.1016/j.diagmicrobio.2017.08.001

Hunter, P. R. (1990). Reproducibility and indices of discriminatory power of microbial typing methods. *J. Clin. Microbiol.* 28, 1903–1905. doi: 10.1128/jcm.28.9.1903-1905.1990

Kazanjian, P., Armstrong, W., Hossler, P. A., Lee, C. H., Huang, L., Beard, C. B., et al. (2001). *Pneumocystis carinii* cytochrome b mutations are associated with atovaquone exposure in patients with AIDS. *J. Infect. Dis.* 183, 819–822. doi: 10.1086/318835

Kumar, S., Stecher, G., and Tamura, K. (2016). MEGA7: molecular Evolutionary Genetics Analysis version 7.0 *for bigger datasets*. *Mol. Biol. Evol.* 33, 1870–1874. doi: 10.1093/molbev/msw054

Le Gal, S., Blanchet, D., Damiani, C., Gueguen, P., Virmaux, M., Abboud, P., et al. (2015). AIDS-related *Pneumocystis jirovecii* genotypes in French Guiana. *Infect. Genet. Evol.* 29, 60–67. doi: 10.1016/j.meegid.2014.10.021

Le Gal, S., Robert-Gangneux, F., Pepino, Y., Belaz, S., Damiani, C., Gueguen, P., et al. (2017). A misleading false-negative result of *Pneumocystis* real-time PCR assay due to a rare punctual mutation: a French multicenter study. *Med. Mycol.* 55, 180–184. doi: 10.1093/mmy/myw051

Le Gal, S., Rouille, A., Gueguen, P., Virmaux, M., Berthou, C., Guillerm, G., et al. (2013). *Pneumocystis jirovecii* haplotypes at the internal transcribed spacers of the rRNA operon in French HIV-negative patients with diverse clinical presentations of *Pneumocystis* infections. *Med. Mycol.* 51, 851–862. doi: 10.3109/13693786.2013.824123

Maitte, C., Leterrier, M., Le Pape, P., Miegeville, M., and Morio, F. (2013). Multilocus sequence typing of *Pneumocystis jirovecii* from clinical samples: how many and which loci should be used? *J. Clin. Microbiol.* 51, 2843–2849. doi: 10.1128/JCM.01073-13

Miller, R. F., Lindley, A. R., Ambrose, H. E., Malin, A. S., and Wakefield, A. E. (2003). Genotypes of Pneumocystis jiroveci isolates obtained in Harare, Zimbabwe, and London, United Kingdom. *Antimicrob. Agents Chemother.* 47, 3979–3981. doi: 10.1128/aac.47.12.3979-3981.2003

Miller, R. F., Lindley, A. R., Malin, A. S., Ambrose, H. E., and Wakefield, A. E. (2005). Isolates of *Pneumocystis jirovecii* from Harare show high genotypic similarity to isolates from London at the superoxide dismutase locus. *Trans. R. Soc. Trop. Med. Hyg.* 99, 202–206. doi: 10.1016/j.trstmh.2004.09.005

Monroy-Vaca, E. X., De Armas, Y., Illnait-Zaragozi, M. T., Diaz, R., Torano, G., Vega, D., et al. (2014). Genetic diversity of *Pneumocystis jirovecii* in colonized Cuban infants and toddlers. *Infect. Genet. Evol.* 22, 60–66. doi: 10.1016/j.meegid.2013.12.024

Nevez, G., Le Gal, S., Noel, N., Wynckel, A., Huguenin, A., Le Govic, Y., et al. (2018). Investigation of nosocomial pneumocystis infections: usefulness of longitudinal screening of epidemic and post-epidemic pneumocystis genotypes. *J. Hosp. Infect.* 99, 332–345. doi: 10.1016/j.jhin.2017.09.015

Nevez, G., Totet, A., Jounieaux, V., Schmit, J. L., Dei-Cas, E., and Raccurt, C. (2003). *Pneumocystis jiroveci* internal transcribed spacer types in patients colonized by the fungus and in patients with pneumocystosis from the same French geographic region. *J. Clin. Microbiol.* 41, 181–186. doi: 10.1128/jcm.41.1.181-186.2003

Nevez, G., Guillaud-Saumur, T., Cros, P., Papon, N., Vallet, S., Quinio, D., et al. (2020). *Pneumocystis* primary infection in infancy: additional french data and review of the literature. *Med. Mycol.* 58, 163–171. doi: 10.1093/mmy/myz040

Posada, D. (2008). JModelTest: phylogenetic model averaging. *Mol. Biol. Evol.* 25, 1253–1256. doi: 10.1093/molbev/msn083

Roux, A., Canet, E., Valade, S., Gangneux-Robert, F., Hamane, S., Lafabrie, A., et al. (2014). *Pneumocystis jirovecii* pneumonia in patients with or without AIDS, France. *Emerg. Infect. Dis.* 20, 1490–1497. doi: 10.3201/eid2009.131668

Sinclair, K., Wakefield, A. E., Banerji, S., and Hopkin, J. M. (1991). Pneumocystis carinii organisms derived from rat and human hosts are genetically distinct. *Mol Biochem Parasitol.* 45, 183–184. doi: 10.1016/0166-6851(91)90042-5

Singh, Y., Mirdha, B. R., Guleria, R., Khalil, S., Panda, A., Chaudhry, R., et al. (2017). Circulating genotypes of *Pneumocystis* jirovecii and its clinical correlation in patients from a single tertiary center in India. *Eur. J. Clin. Microbiol. Infect. Dis.* 36, 1635–1641. doi: 10.1007/s10096-017-2977-9

Struelens, M. J. (1996). Consensus guidelines for appropriate use and evaluation of microbial epidemiologic typing systems. *Clin. Microbiol. Infect.* 2, 2–11. doi: 10.1111/j.1469-0691.1996.tb00193.x

Totet, A., Pautard, J. C., Raccurt, C., Roux, P., and Nevez, G. (2003). Genotypes at the internal transcribed spacers of the nuclear rRNA operon of *Pneumocystis jirovecii* in nonimmunosuppressed infants without severe pneumonia. *J. Clin. Microbiol.* 41, 1173–1180. doi: 10.1128/jcm.41.3.1173-1180.2003

Vindrios, W., Argy, N., Le Gal, S., Lescure, F. X., Massias, L., Le, M. P., et al. (2017). Outbreak of *Pneumocystis jirovecii* infection among heart transplant recipients: molecular investigation and management of an interhuman transmission. *Clin. Infect. Dis.* 65, 1120–1126. doi: 10.1093/cid/cix495

Walker, D. J., Wakefield, A. E., Dohn, M. N., Miller, R. F., Baughman, R. P., Hossler, P. A., et al. (1998). Sequence polymorphisms in the Pneumocystis carinii cytochrome b gene and their association with atovaquone prophylaxis failure. *J Infect Dis.* 178, 1767–1775.

Zhou, Z., Alikhan, N. F., Sergeant, M. J., Luhmann, N., Vaz, C., Francisco, A. P., et al. (2018). GrapeTree: visualization of core genomic relationships among 100,000 bacterial pathogens. *Genome Res.* 28, 1395–1404. doi: 10.1101/gr.232397.117

Conflict of Interest: The authors declare that the research was conducted in the absence of any commercial or financial relationships that could be construed as a potential conflict of interest.

frontiers in Microbiology

REVIEW
published: 18 February 2020
doi: 10.3389/fmicb.2020.00172

Invasion of Host Cells by Microsporidia

Bing Han[1,2], *Peter M. Takvorian*[1,3] *and Louis M. Weiss*[1,4]*

[1] Department of Pathology, Albert Einstein College of Medicine, New York, NY, United States, [2] Department of Pathogenic Biology, School of Basic Medical Sciences, Shandong University, Jinan, China, [3] Department of Biological Sciences, Rutgers University, Newark, NJ, United States, [4] Department of Medicine, Albert Einstein College of Medicine, New York, NY, United States

Microsporidia are found worldwide and both vertebrates and invertebrates can serve as hosts for these organisms. While microsporidiosis in humans can occur in both immune competent and immune compromised hosts, it has most often been seen in the immune suppressed population, e.g., patients with advanced HIV infection, patients who have had organ transplantation, those undergoing chemotherapy, or patients using other immune suppressive agents. Infection can be associated with either focal infection in a specific organ (e.g., keratoconjunctivitis, cerebritis, or hepatitis) or with disseminated disease. The most common presentation of microsporidiosis being gastrointestinal infection with chronic diarrhea and wasting syndrome. In the setting of advanced HIV infection or other cases of profound immune deficiency microsporidiosis can be extremely debilitating and carries a significant mortality risk. Microsporidia are transmitted as spores which invade host cells by a specialized invasion apparatus the polar tube (PT). This review summarizes recent studies that have provided information on the composition of the spore wall and PT, as well as insights into the mechanism of invasion and interaction of the PT and spore wall with host cells during infection.

Keywords: microsporidia, invasion apparatus, polar tube, spore wall, sporoplasm, cell–host interaction

OPEN ACCESS

Edited by:
Olga Matos,
New University of Lisbon, Portugal

Reviewed by:
Gira Bhabha,
New York University, United States
Paul Dean,
Teesside University, United Kingdom
Mahrukh Usmani,
New York University, United States,
in collaboration with reviewer GB

***Correspondence:**
Louis M. Weiss
louis.weiss@einsteinmed.org

Specialty section:
This article was submitted to Infectious Diseases, a section of the journal Frontiers in Microbiology

Received: *05 November 2019*
Accepted: *24 January 2020*
Published: *18 February 2020*

Citation:
Han B, Takvorian PM and Weiss LM (2020) Invasion of Host Cells by Microsporidia. Front. Microbiol. 11:172. doi: 10.3389/fmicb.2020.00172

INTRODUCTION

Microsporidia are a diverse group of unicellular obligate intracellular spore-forming eukaryote parasites that were identified more than 150 years ago with the identification of *Nosema bombycis* (Naegeli, 1857) as the etiologic agent of Pébrine (pepper disease) in silkworms. Microsporidia are widely distributed in nature and there are over 200 genera and 1400 species which have been characterized (Cali et al., 2017). Phylogenetic analysis of microsporidia have demonstrated that they are related to the Fungi, either as a basal branch of the Fungi or as a sister group (Weiss et al., 1998; Lee et al., 2008; Capella-Gutiérrez et al., 2012), and that they are most likely related to the Cryptomycota (Corsaro et al., 2014; Keeling, 2014).

As parasites, they can infect a wide variety of hosts ranging from invertebrates to vertebrates and have been reported from every major group of animals from protists to mammals, including man. They can be found environmentally in terrestrial, marine, and freshwater ecosystems (Cali and Takvorian, 2004). Infection by microsporidia in economically important invertebrate hosts such as silkworm, honeybee, and shrimp as well as vertebrates such as fish can cause significant economic losses (Stentiford et al., 2016). Microsporidia infections in daphnia, nematode, locust, honeybee,

and mosquito play important roles in the regulation of the population size of their hosts (Brambilla, 1983; Higes et al., 2010; Pan et al., 2018).

There are multiple routes of transmission for microsporidia to spread in nature. The most common of these being vertical transmission (the direct transfer of infection from parent to progeny) and horizontal transmission (the transmission of the pathogens from one individual to another of the same generation by oral transmission of spores through contaminated food and water) (Steinhaus and Martignoni, 1970; Fine, 1975; Goertz et al., 2007; Becnel et al., 2014). In humans the majority of infections by microsporidia are thought to be zoonotic and transmitted by the ingestion of spores in food or water (Fayer and Santin, 2014).

Since the 1980s, microsporidia have been identified as significant opportunistic parasites of humans (Cali and Owen, 1988; Weber et al., 1994; Didier and Weiss, 2011; Weiss and Becnel, 2014) with only a few reports prior to that time (Strano et al., 1976). Currently, 9 genera and 17 species have been reported to infect humans (Weiss and Becnel, 2014). Microsporidia are important pathogens in patients with advanced AIDS, bone marrow transplantation, organ transplantation, and patients using new antibody based immune modulatory agents (Didier and Khan, 2014). Infection is also being increasingly recognized in the elderly and pediatric population as well as travelers (Gumbo et al., 1999; Ghoshal et al., 2015).

While Microsporidia are a diverse group of unicellular parasites, they all form a diagnostic spore containing a coiled polar filament surrounding the nucleus or diplokaryon and its associated cytoplasmic organelles, the sporoplasm (**Figure 1**). The resistant spore can persist in the environment for months and in some cases, for years under the right conditions (Kramer, 1970). This highly resistant spore is the only microsporidial form that is extracellular and is the infective stage (Vavra and Larsson, 1999, 2014; Cali and Takvorian, 2014). The spores of microsporidia are generally small, oval- or pyriform- shaped, resistant structures that vary in length from approximately 1 to 12 μm (Sprague and Vavra, 1977; Canning and Lom, 1986; Olson et al., 1994). Those infecting mammals are generally 1 to 4 μm in length (Bryan et al., 1991; Weber et al., 1994).

The typical mature microsporidian spore has an electron-dense outer spore coat overlying an inner thicker lucent coat followed by a membrane surrounding the spore contents. Diagnostic for the microsporidia is a polar filament, anteriorly attached to an anchoring disk (AD) with the straight part of the polar filament immediately following and encompassed by a membranous sheath. Projecting from the anterior portion of the sheath are a series of tightly packed array of membrane, the lamellar polaroplast, which is followed by clusters of wider tubules, the tubular polaroplast. The central portion of the spore contains a nucleus or pair of abutted nuclei (diplokaryon), in cytoplasm with tightly packed ribosomes. The posterior of most spores contain a highly variable structure referred to as the posterior vacuole. Surrounding the nuclear and cytoplasmic central region of the spore is the coiled polar filament [i.e., polar tube (PT)]. There may be few to many dozens of cross sections

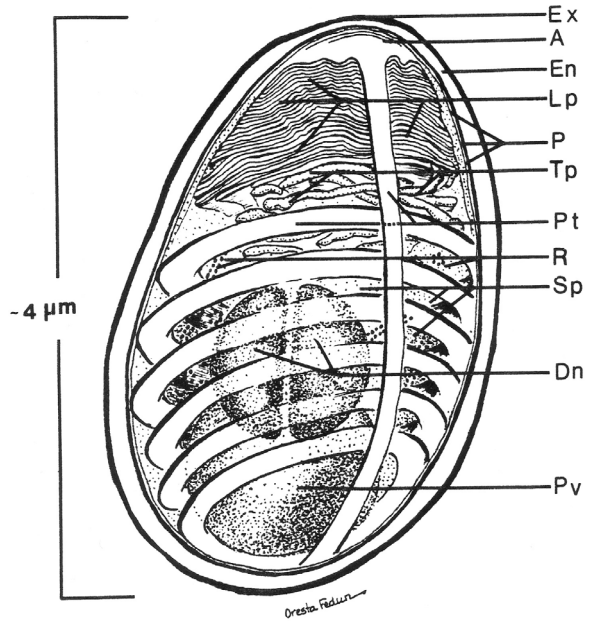

FIGURE 1 | Diagram of the internal structure of a microsporidian spore. The spore coat has an outer electron dense region called the exospore (Ex) and an inner thicker electron lucent region, endospore (En). A unit membrane (P) separates the spore coat from the spore contents. The extrusion apparatus, anchoring disc (A), polar tubule (Pt), lamellar polaroplast (lp), and tubular polaroplast (Tp) dominate the spore contents and is diagnostic for microsporidian identification. The posterior vacuole (Pv) is a membrane-bound vesicle that sometimes contains a "membrane whirl" or "glomerular like" structure or flocculent material or some combination of these structures. The spore cytoplasm is dense and contains ribosomes (R) in tightly coiled helical array. The nucleation may consist of a single nucleus or a pair of abutted nuclei, diplokaryon (D). The size of the spore depends on the particular species and can vary from less than one micron to over 10 microns. The number of polar tubule coils is also variable from a few to thirty or more, again depending on the species. Reprinted with the permission of the publisher (Cali and Takvorian, 2014).

of the polar filament coil, arranged in a single or multiple rows, depending on the organism (Cali and Takvorian, 2014).

Microsporidia infect host cells by employing a unique, highly specialized invasion process that involves the spore wall (SW), PT, and the infectious sporoplasm (SP). This germination event which results in the transfer of the infective sporoplasm into a susceptible host cell requires a series of complex events, which include environmental changes necessary to activate the spore (Leitch et al., 1993; Leitch and Ceballos, 2008). An activated spore undergoes a progression of changes to both the spore coat and spore contents (**Figure 2**). An initial change consists of a bulge of the apical end of the spore accompanied by a narrowing of the endospore coat in that region. The apical attachment complex of the polar filament, its associated membranes, and the filament proper of the inactive spore, all become reoriented upon activation. Additionally, the apical complex everts, forming a collar-like structure as the polar filament, now termed the PT exits from the spore-wall (Cali et al., 2002; Takvorian et al., 2005; Cali and Takvorian, 2014). The extruded PT serves as a conduit

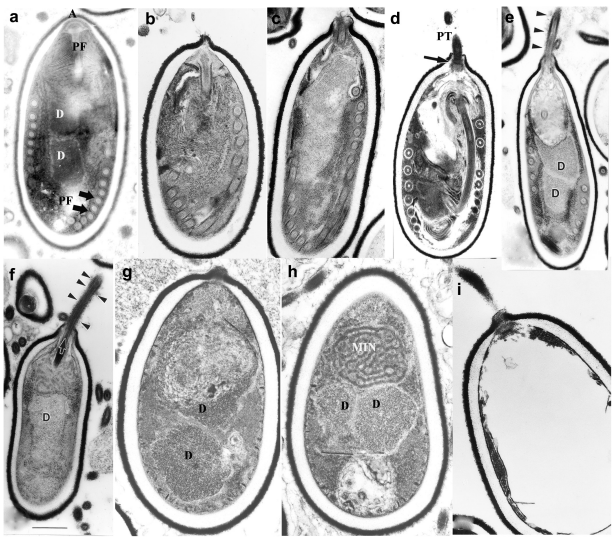

FIGURE 2 | Germination of microsporidian spore. *Anncaliia algerae* spores incubated in germination buffer and processed for TEM. The sequence of images illustrates the events that occur in the germination process. **(a)** Typical *A. algerae* spore; **(b)** spore coat bulging; **(c)** spore coat rupture and polaroplast expanded; **(d)** early eversion and translocation of polar tube (PT); **(e)** majority of PT extruded, nuclear and cytoplasmic structures still in spore; **(f)** no PT coils remain in spore but sporoplasm still present; **(g)** spore "membrane channels" visible immediately below endospore; **(h)** posterior vacuole, diplokaryon and MIN (sporoplasm) the last structures exiting the spore shell; **(i)** empty spore shell with PT still attached. Reprinted with the permission of the publisher (Cali and Takvorian, 2014).

for the sporoplasm to transfer from the spore into a new host (Cali et al., 2002; Cali and Takvorian, 2014; Takvorian et al., 2019). Non-activated spores may also be phagocytized by a host cell and eventually discharge their PTs, depositing the sporoplasm into the host cytoplasm (Franzen, 2004, 2005; Franzen et al., 2005). On occasion, discharged sporoplasms have been observed interacting with the host cell plasmalemma and being taken into the cell by endocytosis/phagocytosis (Takvorian et al., 2013).

The PT upon discharge then interacts with the host cell forming an invagination in the host cell membrane, thereby creating a microenvironment, which we have termed the invasion synapse (**Figure 3**). The proteins [polar tube proteins (PTPs), sporoplasm surface proteins, and host cell receptors] that participate in the formation of the invasion synapse remain to be fully characterized. Within this protected microenvironment, the sporoplasm which has traveled down the PT into this synapse is delivered to the host cell and invasion occurs (Han et al., 2017). The exact mechanism of entry of microsporidia into their host cells is unknown. It is possible that the PT either pierces the host cell membrane in this synapse delivering the sporoplasm directly into the host cells, or that the sporoplasm itself may interact with the host cell membrane during invasion (Takvorian et al., 2013; Han et al., 2017). Based on observations on the Encephalitozoonidae (Han et al., 2017, 2019), we hypothesize that that the sporoplasm interacts with the host cell membrane and an invasion vacuole is formed (**Figure 3**). Once the infectious sporoplasm enters the host cell it undergoes development into meronts (proliferative forms), sporonts, sporoblasts (developing spore) and finally mature spores (Visvesvara, 2002).

SPORE WALL PROTEINS (SWPs)

The spore wall contains three layers: an electron-dense, proteinaceous exospore, an electron lucent endospore, and an underlying plasma membrane (Vávra, 1976; Canning and Lom, 1986; Cali and Owen, 1988). This spore wall maintains the morphology of the spore and protects the organism from harsh environmental conditions before it infects the host (Shadduck and Polley, 1978). It has been demonstrated that the spore wall contains chitin as well as numerous spore wall proteins (SWPs) (Vávra, 1976). In addition, to protecting the spore from the environment, the spore wall also interacts with the environment and host cell and is involved in the process of activating PT germination (Yang et al., 2018). SWPs that localize to the exospore are exposed directly to the host cells and environment. These SWPs are in all probability involved in the process of host cell binding, signaling, or enzymatic interactions (Hayman et al., 2005; Southern et al., 2007). For example, some SWPs have been demonstrated to bind to mucin and proteoglycans (Hayman et al., 2005; Southern et al., 2007), which would enable spores to bind the mucin layer in the gastrointestinal tract, thereby, facilitating invasion of intestinal epithelial cells by the PT on germination (Weiss et al., 2014). Endosporal SWPs are also in all likelihood involved in the processes of the endospore formation, PT interaction, and spore germination.

According to several studies on the composition of the spore wall, there are multiple SWPs present in both the exospore and endospore (**Table 1**). The identification of these SWPs has primarily focused on the Encephalitozoonidae, *Encephalitozoon cuniculi* (Ec), *E. hellem* (Eh) and *E. intestinalis* (Ei), which infect humans as well as other mammalian hosts, and *Nosema bombycis* (Nb), which can infect silkworms (Yang et al., 2018). Several SWPs have been identified from the Encephalitozoonidae of which EcSWP1, EiSWP1, EiSWP2, EhSWP1a, and EhSWP1b are localized to exospore and EcEnP1, EiEnP1, EcEnP2, EcSWP3 and EcCDA which are localized to the endospore (Bohne et al., 2000; Hayman et al., 2001; Brosson et al., 2005; Peuvel-Fanget et al., 2006; Xu et al., 2006; Southern et al., 2007). With the availability of genome data for the Encephalitozoonidae as well as many other microsporidia on MicrosporidiadB.org (part of EuPathdB.org) homologs of these SWPs have been found in most of the Encephalitozoonidae as well as in the other microsporidia genomes found on MicrosporidiadB (such as microsporidia that infect invertebrates) (Weiss et al., 2014). Examples of such homologs include, *Antonospora locustae* SWP2 (AlocSWP2) and *Enterocytozoon hepatopenaei* SWP1 (EHSWP1) (Chen et al., 2017; Jaroenlak et al., 2018).

Nosema bombycis which infects the silkworm *Bombyx mori*, has been studied as a model microsporidian for decades [since it was first identified by Louis Pasteur (Pasteur, 1870)]. Fourteen hypothetical SWPs were identified by proteomic analysis from *Nosema bombycis* (Wu et al., 2008). While some

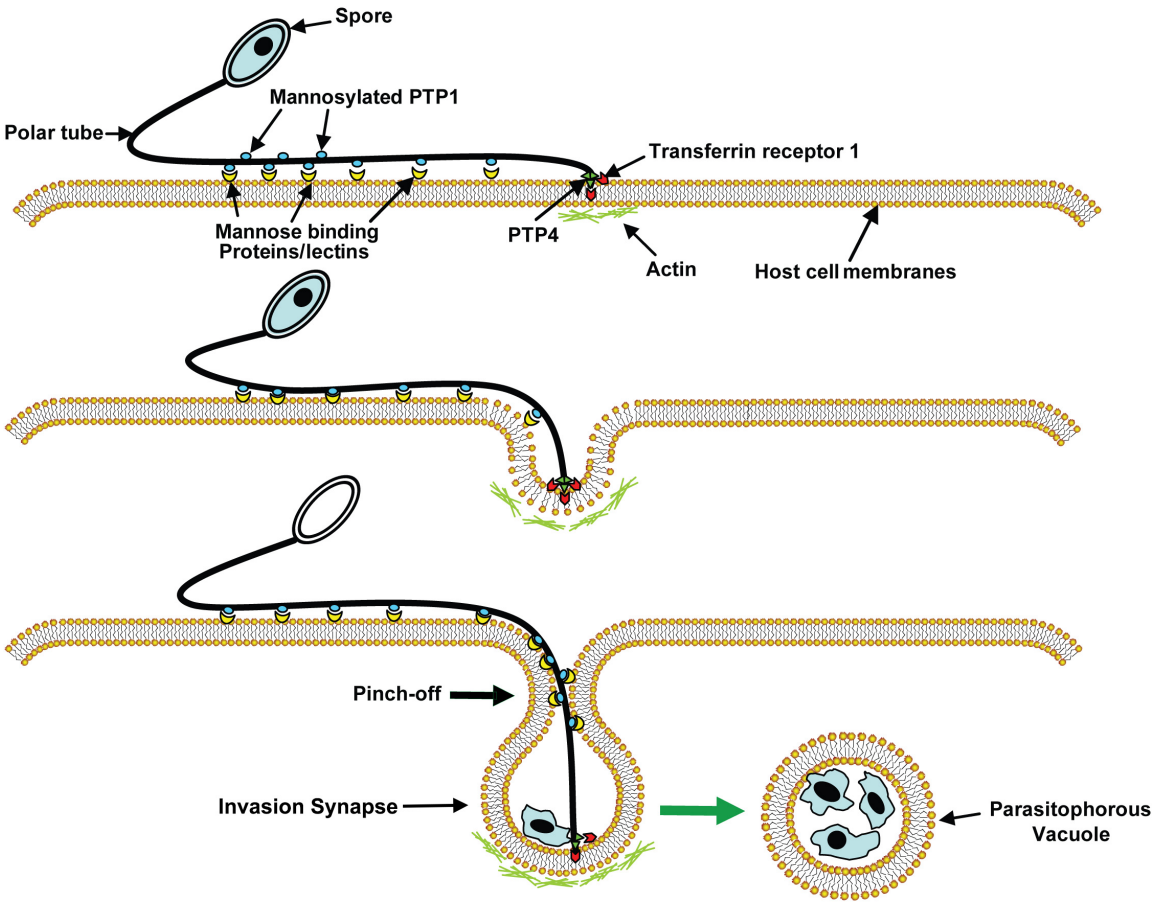

FIGURE 3 | A model of microsporidia invasion of a host cell. Polar tube protein 1 (PTP1) interacts with mannose binding proteins (MBPs) on the host surface adhering the PT to the host surface allowing the PT to form an invasion synapse by pushing into the host cell membrane. Interactions of PTP1 (and possibly PTP4) with the host cell membrane in the invasion synapse exclude the external environment from the invasion synapse creating a protected microenvironment for the extruded microsporidian sporoplasm. Polar tube protein 4 (PTP4) epitopes at the tip of PT interact with Transferrin receptor 1 (TfR1) or other host cell interacting proteins (HCIPs) on the host cell surface triggering signaling events such as clathrin-mediated endocytosis and the involvement of host cell actin in the final invasion event with formation of a parasitophorous vacuole. Reprinted with permission of the publisher (Han et al., 2017).

of these have homologs in the other microsporidia genomes on MicrosporidiadB.org, many of them have only been identified in *Nosema bombycis*. According to immunoelectron microscopy studies of these hypothetical SWPs, NbSWP5, NbSWP16 and NbSWP32 are located in the exospore and NbSWP25, NbSWP30, EOB14572 are located in the endospore (Wu et al., 2008, 2009; Li et al., 2012; Wang et al., 2015, 2017). NbSWP7 and NbSWP9 were found to be present in both the spore wall and PT (Yang et al., 2015, 2017). NbSWP11 was found on the membranous structures of the sporoblast and mature spore (Yang et al., 2014). NbSWP12 was located both inside and outside of the spore wall (Chen et al., 2013). NbSWP26 was expressed largely in endospore and plasma membrane during endospore development, but sparsely distributed in the exospore of mature spores (Li et al., 2009).

Chitin is the main component of the endospore, and chitin has been reported to be the major component of fibrils that form bridges across the endospore and to be part of the fibrillary system of the exospores, which is essential in maintaining spore cell structure and function (Erickson and Blanquet, 1969; Han and Weiss, 2018). The presence of chitin in the spore wall is useful as a target of diagnosis as it can be stained by fluorescence dyes such as Calcofluor white or Uvitex 2B. These fluorescent brighteners are widely used for identifying microsporidia in clinical and environmental samples (Vavra and Chalupsky, 1982; Ghosh and Weiss, 2009).

POLAR TUBE PROTEINS (PTPs)

All microsporidial spores possess a unique, highly specialized invasion apparatus consisting of the polar filament, which coils inside of the spore and connects to a mushroom-shaped AD at the anterior end of the spore (Vávra, 1976; Takvorian and Cali, 1986). Upon appropriate environmental stimulation, the PT will be rapidly extruded from the spore and then serve as a conduit for the nucleus and sporoplasm passage into the host cell, the entire process taking less than 2 seconds (Weidner, 1972; Frixione et al., 1992). Although it has been over 125 years since

TABLE 1 | The identified spore wall proteins of Microsporidia.

	Protein	Subcellular location	Function domain	Mw (kDa)	Amino acids/GenBank ID	References
Encephalitozoon cuniculi	EcSWP1	Exospore	–	45.9	450 aa ECU10_1660	Bohne et al., 2000
	EcEnP1	Endospore	HBM	40.6	357 aa ECU01_0820	Peuvel-Fanget et al., 2006
	EcEnP2/EcSWP3	Endospore	Transmembrane	22.5	221 aa ECU01_1270	Peuvel-Fanget et al., 2006; Xu et al., 2006
	EcCDA	Endospore and plasma membrane	Glycoside hydrolase and deacetylase	28.1	254 aa ECU11_0510	Brosson et al., 2005
Encephalitozoon intestinalis	EiSWP1	Exospore	–	41.5	388 aa AF355750.1	Hayman et al., 2001
	EiSWP2	Exospore	–	107.2	1002 aa AF355749.1	Hayman et al., 2001
	EiEnP1	Exospore and endospore and polar membrane layer	HBM	39.1	348 aa EF539266	Southern et al., 2007
Encephalitozoon hellem	EhSWP1a	Exospore	–	54.9	509 aa FJ870923	Polonais et al., 2010
	EhSWP1b	Exospore	–	57.9	533 aa FJ870924	Polonais et al., 2010
Nosema bombycis	NbSWP5	Endospore and polar tube	–	20.3	186 aa EF683105	Li et al., 2012
	NbSWP7	Exospore and endospore	–	32.8	287 aa EOB13707.1	Yang et al., 2015
	NbSWP9	Exospore, endospore and polar tube	Transmembrane helix region (TMHMM)	42.8	367 aa EOB13793.1	Yang et al., 2015
	NbSWP11	Exospore and endospore	DnaJ domain	52.3	446 aa EF683111	Yang et al., 2014
	NbSWP12	Exospore and endospore	BAR-2 domain	26.6	228 aa EF683112	Chen et al., 2013
	NbSWP16	Exospore	HBM	44.0	221 aa EOB14338	Wang et al., 2015
	NbSWP25	Endospore	HBM	30.7	268 aa EF683102	Wu et al., 2009
	NbSWP26	Exospore, endospore and plasma membrane	HBM	25.7	223 aa EU677842	Li et al., 2009
	NbSWP30	Endospore	–	32.1	278 aa EF683101	Wu et al., 2008
	NbSWP32	Exospore	–	37.4	316 aa EF683103	Wu et al., 2008
	EOB14572	Endospore and polar tube	Four tandem repeats	37.0	316 aa NBO_24g0018	Wang et al., 2017
Enterocytozoon hepatopenaei	EHSWP1	Exospore and endospore	HBM, BAR-2	27.0	228 aa MG015710	Jaroenlak et al., 2018
Antonospora locustae	AlocSWP2	Exospore and endospore	GPI, HBM	25.0	222 aa KX255658	Chen et al., 2017

the first reports of the existence of the PT by light microscopy (Thelohan, 1894), and more than 50 years since the first use of electron microscopy to image the polar filament inside of the spore (Huger, 1960), this structure, its protein composition, the mechanism of PT extrusion, and sporoplasm transport within the tube are still enigmatic.

The mechanism and chemical factors necessary for spore germination are poorly understood. Various stimuli (pH, cations, and anions) have been identified to trigger germination, some of which appear to be microsporidian species specific (**Table 2**). Swelling of the polaroplast and posterior vacuole presumably due to the increasing of osmotic pressure inside of the spore, probably involving aquaporins (Ghosh et al., 2006), has been observed in many microsporidia during the germination process (Thelohan, 1894; Ohshima, 1937; Lom and Vavra, 1963). A study of trehalase function in *Anncaliia (Nosema) algerae* demonstrated that the cleavage of the disaccharide trehalose into glucose by trehalase could rapidly increase the intrasporal hydrostatic pressure inside of the spore and that this increase in hydrostatic pressure could trigger spore germination (Undeen, 1990; Undeen and Meer, 1994). This increase in intrasporal osmotic pressure from the breakdown of trehalose has been postulated to induce germination in aquatic microsporidia (Undeen and Vander Meer, 1999). This may, however, not be the

TABLE 2 | Conditions for activation and discharge of polar tubes.

Organism	*In vitro* method of PT germination	References
Amblyospora sp.	1.6M sucrose plus 0.2M KCl, pH 9	Undeen and Avery, 1984
Edhazardia aedis	0.1M KCl, pH 10.5	Frixione et al., 1992
Encephalitozoon hellem	140 mM NaCl, 5 mM KCl, 1 mM $CaCl_2$, 1 mM MgCl 2, pH 9.5 or 7.5 with and without 5% H_2O_2	Leitch et al., 1993 He et al., 1996
Encephalitozoon hellem	140 mM NaCl, 1 mM $CaCl_2$, 1 mM $MgCl_2$, 5 mM KCl, pH 7.5 for 15min then 5% H_2O_2 for another 15 min	Han et al., 2019
Encephalitozoon intestinalis	140 mM NaCl, 5 mM KCl, 1 mM $CaCl_2$, 1 mM $MgCl_2$, pH 9.5 or 7.5 with and without 5% H_2O_2	He et al., 1996
Encephalitozoon intestinalis	Spores from urine resuspended in 0.025 N NaOH in phosphate buffered saline	Beckers et al., 1996
Glugea fumiferanae	Chlorides of alkali metal ions at pH 10.8: CsCl, RbCl, KCl, NaCl, or LiCl	Ishihara, 1967
Glugea hertwigi	Calcium ionophore A-23187	Weidner, 1982
	pH shift from neutral (7.0) to alkaline (9.5) in 150 mM phosphate buffer	
	50 mM sodium citrate in 100 mM glycylglycine buffer pH 9.5	
	150 mM phosphate buffer in 100 mM glycylglycine buffer pH 9.5	
Gurleya sp.	Dessication followed by rehydration with normal saline	Gibbs, 1953
Nosema sp.	3% 40-volume H_2O_2	Walters, 1958
Nosema algerae	$KHCO_3$-K_2CO_3 buffer pH 8.8	Vavra and Undeen, 1970
Nosema algerae	KCl, NaCl, RbCl, CsCl, or NaF, pH 9.5; $KHCO_3$, pH 9.0 (0.1 to 0.3M solutions) requires pretreatment in distilled H_2O	Undeen, 1978
Nosema algerae	0. 05M halogen anion Br^-, Cl^-, or I^- in combination with Na^+ or K^+ pH 9.5; or 0.05M F^- in combination with Na^+ or K^+ pH 5.5	Undeen and Avery, 1988
Nosema algerae	0.1M NaCl buffered at pH 9.5 with 20 mM glycine-NaOH or borate-NaOH	Undeen and Avery, 1988, Undeen and Frixione, 1991
Nosema algerae	0.1M NaCl buffered at pH 9.5 with 20 mM Tris-borate	Frixione et al., 1992
Nosema algerae	Alkali metal cations in 0.1M NaCl or KCl, pH 9.5 or 0.1M $NaNO_2$, pH 9.5 or Na^+ ionophore monesin in 0.04M NaCl pH 9.5	Frixione et al., 1994
Nosema apis	Dehydration in air, followed by rehydration with neutral distilled H_2O	Kramer, 1960
Nosema apis	Dehydration in air, followed by rehydration in phosphate buffered saline, pH 7.1	Olsen et al., 1986
Nosema apis	0.5M NaCl with 0.5M $NaHCO_3$, pH 6	de Graaf et al., 1993
Nosema bombycis	30% H_2O_2 or 30% H_2O_2 with 1% $NaHCO_3$	Kudo, 1918
Nosema bombycis	Boiled digestive fluid of silkworm or 3% H_2O_2	Ohshima, 1927
Nosema bombycis	Digestive fluid of silkworm or liver extract medium pH > 8.0	Trager, 1937
Nosema bombycis	NaOH (N/10 to N/160) pH 11–13 neutralized with HCl to pH 6.0–9.0	Ohshima, 1937
Nosema bombycis	KOH (N/7 to N/640) neutralized with HCl to pH 6.5–8.0	Ohshima, 1964a
Nosema bombycis	0.375M KCl, 0.05M Glycine, 0.05M KOH pH 9.4–10.0	Ohshima, 1964b
Nosema bombycis	1.5 to 3% H_2O_2	Ohshima, 1966
Nosema bombycis	0.1N KOH followed by preheated silkworm hemolymph	Ishihara, 1968
Nosema bombycis	0.05M Glycine, 0.05M KOH, and 0.375M KCl, pH 10.5	Liu et al., 2016
Nosema costelytrae	Pretreatment with 0.2M KCl pH 12 followed by 0.2M KCl pH 7	Malone, 1990
Nosema heliothidis	Pretreatment with 0.15M cation (K, Na, Li, Rb, or Cs) at pH 11, followed by 0.15M cation (K), pH 7	Undeen, 1978
Nosema helminthorum	Mechanical pressure	Dissanaike, 1955
Nosema locustae	Dehydration with 2.5M sucrose or 5% polyethylene glycol followed by 0.1M Tris-HCl, 0.1M NaCl or 0.1M glycine-NaOH, 0.1M NaCl pH 9–10	Undeen, 1990
Nosema locustae	Dehydration in air followed by rehydration in 0.1M Tris-HCl, pH 9.2, 37°C	Whitlock and Johnson, 1990
Nosema michaelis	Pretreatment in veronal acetate buffer, pH 10, followed by tissue culture medium 199	Weidner, 1972
Nosema pulicis	Weak acetic acid/iodine water	Korke, 1916
Nosema whitei	Dehydration in air, followed by rehydration with neutral distilled H_2O	Kramer, 1960
Nosema furnacalis	0.17M KCl, 10 mM Na_2EDTA, 25 mM *N,N-bis*(2-hydroxyethyl) glycine (Bicine), 30 mM glucose, pH 8.0	Sagers et al., 1996
Perezia pyraustae	Dehydration in air, followed by rehydration with neutral distilled H_2O	Kramer, 1960
Plistophora anguillarum	0.1M Potassium citrate-HCl pH 3 to 4 or 0.01M KHCO 3-K_2CO_3 pH 10 or 0.5 to 50% H_2O_2	Hashimoto et al., 1976
Plistophora hyphessobryconis	5% H_2O_2	Lom and Vavra, 1963
Spraguea lophii (Glugea americanus)	pH shift from acid/neutral to alkaline (pH 9.0) in 0.5M glycylglycine or 0.5M carbonate buffer containing 2% mucin or 0.5M poly-D-glutamic acid	Pleshinger and Weidner, 1985
Spraguea lophii (Glugea americanus)	Calcium ionophore A-23187	Pleshinger and Weidner, 1985

(Continued)

TABLE 2 | Continued

Organism	*In vitro* method of PT germination	References
Spraguea lophii (Glugea americanus)	Phosphate buffered saline pH 8.5–9.0 containing 0.1–0.5% porcine mucin.	Weidner et al., 1984
Spraguea lophii (Glugea americanus)	Storage in 0.05M Hepes, retreatment in 10^{-5} M Ca^{2+} pH 7, followed by Hepes pH 9.5 containing 2% mucin.	Weidner et al., 1995
Thelohania californica	Mechanical pressure	Kudo and Daniels, 1963
Thelohania magna	Mechanical pressure	Kudo, 1916, 1920
Vairimorpha necatrix	Pretreatment with 0.15M cation (K, Li, Rb, or Cs), pH 10.5, followed by 0.15M cation (Na or K), pH 9.4	Undeen, 1978
Vairimorpha plodiae	Pretreatment with 0.1 or 1M KCl, pH 11, followed by 0.1 or 1M KCl, pH 8.0	Malone, 1984
Vavraia culicis	0.2M KCl, pH 6.5 (one isolate) pH 7.0–9.0 (another isolate)	Undeen, 1983
Vavraia oncoperae	Pretreatment with 3 mM EDTA followed by 0.2M KCl pH 11	Malone, 1990

mechanism in other microsporidia as a study of the germination kinetics of individual *Nosema bombycis* spores, which belong to the terrestrial microsporidia, using laser tweezers Raman spectroscopy and phase-contrast microscopy imaging revealed a different germination mechanism (Miao et al., 2018). The dynamics of imaging intensity of individual spore germination detected by phase-contrast microscopy revealing that the germination speed and the germination rates are different with different germination methods, but the length of germination time was relatively constant, showing the homogeneity of *Nosema bombycis* spore germination. The actual change of intracellular macromolecules such as trehalose, nucleic acid, and protein were tracked by the single-cell Raman spectroscopy, and this demonstrated that there was no change in the intensities of trehalose peaks prior to germination, nor were new peaks of saccharides observed, indicating that spore germination in this related microsporidia is probably not due to the action of trehalase on trehalose (Miao et al., 2018).

A study using Cryo-Transmission Electron Microscopy (CTEM) to examine the structure of extruded PTs of *Anncaliia algerae* has shown that the PT is composed of various structures containing masses of tightly folded or stacked membranes (**Figure 4**) (Takvorian et al., 2019). This study illustrated that the "sperm head" shaped sporoplasm traverses the PT as a fully intact membrane bound cellular entity. The PT surface was shown to be covered with fine fibrillary material which was interpreted to be modified glycoproteins on the surface of PT (**Figure 4A**). Furthermore, the CTEM image of the PT terminus revealed that the distal end of the PT (**Figure 4B**), has a closed tip that can form a terminal sac before the PT tip is forced to open (Takvorian et al., 2019).

The everting PT, and the PT within the intact spore, is not empty, but has been shown by several authors to be filled with electron-dense materials (Cali et al., 2002; Vavra and Larsson, 2014; Takvorian et al., 2019) which are thought by some to be unpolymerized PTPs and perhaps membranes (Kudo and Daniels, 1963; Weidner, 1972, 1976). According to several ultrastructural observations eversion of the PT has been likened to a tube sliding within a tube (or a glove finger being turned inside out) and it has been further hypothesized that PTPs polymerize on the forming tube when they exit at the distal tip of the PT (Weidner, 1982; Weidner et al., 1995). Currently, however, there is no data demonstrating polymerization of cloned PTPs into tube-like structures.

Studies conducted to date on the composition of the PT have resulted in the identification of five distinct PTPs (Weiss et al., 2014). These studies used various Encephalitozoonidae, but genomic data from MicrosporidiadB.org indicates that these five PTPs are also found in other microsporidia such as *A. locustae, T. hominis,* and *A. algerae* (**Table 3**).

The unusual solubility properties of PTs, which resist dissociation in 1% SDS and 9M urea but dissociate in various concentrations of 2-mercaptoethanol (2-ME) or dithiothreitol (DTT), has been used to produce PTP preparations for proteomic analysis (Keohane et al., 1994, 1996). Using this approach, polar tube protein 1 (PTP1) was first isolated from microsporidia by treating glass bead disrupted spores with SDS and Urea to remove most of the proteins and then solubilizing the residual PTs with DTT. This was followed by further purification of the DTT solubilized PTs by the use of reverse-phase high-performance liquid chromatography (HPLC) (Keohane et al., 1994, 1996). Amino acid analysis of the major protein that was purified, named PTP1, demonstrated that it is proline rich, which would contribute to the high tensile strength and elasticity of PTP1. These properties are probably important for the discharge and passage of sporoplasm through the PT (Keohane et al., 1996, 1998; Delbac et al., 2001). Further analysis of PTP1 demonstrated that it is a mannosylated protein with a significant number of O-linked mannosylation modification sites which make it possible for PTP1 to interact with mannose binding receptors on the surface of host cells and enables the PT to bind to the cell surface during infection (Xu et al., 2003, 2004; Bouzahzah and Weiss, 2010; Bouzahzah et al., 2010). Interestingly, PTP1 has been found to be quite divergent in the microsporidia, in particular the central repeating region differs significantly between the various Encephalitozoonidae (MicrosporidiaDb.org). This region has been suggested to function as an immunological masking region during infection, but there are no experimental data to support this hypothesis (Xu and Weiss, 2005; Bouzahzah et al., 2010; Weiss et al., 2014). The C and N terminal regions have more conservation, especially with regard to cysteine content (the presence of disulfide bridges in the assembly of the PT is supported by the ability of DTT and other reducing agents to solubilize the tube).

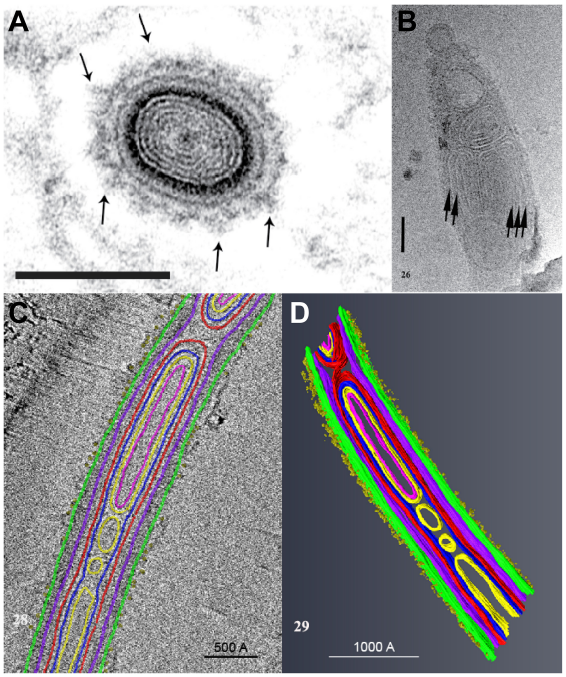

FIGURE 4 | An ultrastructural study of the extruded PT of *Anncaliia algerae*. **(A)** Light and transmission electron microscopy (TEM) showed the cross section of an extruded PT from spores. The lumen of the tube is filled with about eight alternating concentric thin ED and electron lucent (EL) rings of material. The outer wall of the PT is enclosed by a relatively thick ED wall which is in turn covered by additional rings of material. The outermost PT surface is a ring of medium dense fibrous material with tufts of fibers projecting outward (arrows). Bar is 100 nm. **(B)** CTEM of the distal end of PTs showed that end of the PT containing multiple tightly packed membranes (short arrows) that will give rise to the sporoplasm membrane "terminal sac." Note the closed tip of the tube. Bar is 50 nm. **(C)** Tomogram of a portion of PT containing cargo and membranes, and its surface is covered with tufts of fibrillar material. The different PT structures are color coded to the various densities visible in the stacks of images and identified by color. **(D)** The tomogram was segmented and 3D models generated from it using Amira software. Reprinted with the permission of the publisher (Takvorian et al., 2019).

Four additional PTPs (PTP2 through PTP5) have been identified and characterized using proteomic and antibody-based approaches, and proteomic data suggests that there are additional PTPs in the PT (Peuvel et al., 2002; Bouzahzah et al., 2010; Weiss and Becnel, 2014; Weiss et al., 2014; Han et al., 2017, 2019). PTP2 is found at the same genomic locus as PTP1. The PTP2 from various microsporidia are more conserved in their properties such as molecular weight, basic isoelectric point (pI), high lysine content and cysteine residues when compared with PTP1 conservation (Delbac et al., 2001). PTP3 was found to be solubilized in the presence of SDS without adding a reducing reagent such as DTT, indicating it is not involved in disulfide bonding with other PTPs. It has also been suggested that PTP3 might be a scaffolding protein that plays an important role during the formation of the PT by interaction with other PTPs (Peuvel et al., 2002; Bouzahzah et al., 2010). When cross linking agents are used, a complex containing PTP1, PTP2, and PTP3 is obtained from intact PTs, indicating that these proteins do indeed interact (Peuvel et al., 2002; Bouzahzah et al., 2010). Similar to the genomic locus of PTP1/PTP2, the genes of PTP4 and PTP5 were also found to cluster together in many microsporidia genomes (Weiss et al., 2014).

A PTP4 monoclonal antibody which only stained the extruded tip of PT was identified, suggesting that a specific epitope of PTP4 could be important during the interaction of the PT with its host cell (Han et al., 2017). Using an immunoprecipitation assay followed by proteomic analysis a host cell receptor protein [Transferrin 1 (TfR1)] was identified that interacted with PTP4 (Han et al., 2017). In addition, it was found that PTP4 interacted with TfR-1 in the invasion synapse and that interference with the association of PTP4 and TfR-1 decreased the ability of *E. hellem* to invade its mammalian host cell (Han et al., 2017). As the sporoplasm forms a droplet at the tip of PT during germination we hypothesized that PTPs might be able to interact with sporoplasm proteins during the process of invasion. This concept is supported by the finding that a recently identified sporoplasm surface protein (SSP1) from *E. hellem* interacts with PTP4 in a yeast-two hybrid assay (Han et al., 2019).

OBSERVATIONS ON THE SPOROPLASM

During infection of host cells by microsporidia, the infectious sporoplasm is transported from spores via the PT, resulting in the transmission of the infection (Takvorian et al., 2005; Vavra and Larsson, 2014). During this process, the sporoplasm flows through the PT, appears as a droplet at the distal end of the PT and remains attached to the PT for several minutes (Korke, 1916; Ohshima, 1937; Gibbs, 1953; Lom, 1972; Weidner, 1972; Frixione et al., 1992; Han et al., 2017). It is likely that the sporoplasm interacts with the host cell within the protected environment of the invasion synapse during invasion. After the entrance of a sporoplasm into the host cell, it starts a reproduction cycle which includes meronts (proliferative forms), sporonts, sporoblasts, and terminates with the mature spores (Cali and Takvorian, 2014; Han and Weiss, 2017). The sporoplasm is tightly associated with the PT throughout spore germination and host cell invasion (Cali and Takvorian, 2014). The sporoplasm is very sensitive to osmotic stress and the formation of the invasion synapse is probably critical to its survival when it exits the PT (Weiss et al., 2014; Han et al., 2017).

Purification of the microsporidial sporoplasm has been very difficult and, up till now, only a few proteins have been localized and characterized in the sporoplasm plasma membrane. An ATP-binding cassette (ABC) transporter subfamily protein NoboABCG1.1 was identified from silkworm pathogen *Nosema bombycis*, the IFA and IEM analysis showed that NoboABCG1.1 is a membrane protein that is located on the sporoplasm, meront, and mature spore. Knocking down NoboABCG1.1 using an RNAi approach leads to a significant reduction in the growth of *Nosema bombycis* suggesting that this transporter was important for acquisition of essential nutrients for this organism (He et al., 2019). Four nucleotide transport proteins (NTT1-4) have been identified from other species of microsporidia (*Encephalitozoon cuniculi* and *Trachipleistophora hominis*) which were believed to

TABLE 3 | Polar tube proteins PTP1 to PTP5 in microsporidia.

	PTP1	PTP2	PTP3	PTP4	PTP5
Encephalitozoon cuniculi	395 aa ECU06_0250	277 aa ECU06_0240	1256 aa ECU11_1440	276 aa ECU07_1090	251 aa ECU07_1080
Encephalitozoon intestinalis	371 aa Eint_060150	275 aa Eint_060140	1256 aa Eint_111330	279 aa Eint_071050	252 aa Eint_071040
Encephalitozoon hellem	453 aa 413 (EhATCC) EHEL_060170	272 aa EHEL_060160	1284 aa EHEL_111330	278 aa EHEL_071080	251 aa EHEL_071070
Encephalitozoon romalae	380 aa EROM_060160	274 aa EROM_060150	1254 aa EROM_111330	280 aa EROM_071050	251 aa EROM_071040
Antonospora locustae	355 aa ORF1050*	287 aa ORF1048* 568 aa (PTP2b) ORF1712* 599 aa (PTP2c) ORF1329*	Partial sequence	381 aa ORF969*	242 aa ORF968*
Paranosema grylli	351 aa	287 aa	Partial sequence	381 aa	Partial sequence
Enterocytozoon bieneusi	nd	283 aa EBI_26400	1219 aa EBI_22552	nd	nd
Trachipleistophora. hominis	nd	291 aa THOM_1756	1518 aa THOM_1479	Partial sequence THOM_1575	259 aa THOM_1161
Nosema ceranae	456 aa NCER_101591	275 aa NCER_101590	1414 aa NCER_100083	208 aa NCER_100526	268 aa NCER_100527
*Nosema bombycis***	409 aa NBO_7g0016	277 aa AEK69415	1370 aa AEF33802	222 aa ACJZ01000169 (3927–4595)	271 aa ACJZ01002324 (213–1028)
Anncaliia algerae	407 aa KI0ABA33YN06FM1	3 partial sequences	1203 aa KI0APB23YG12FM1	254 aa KI0ANB26YM04FM1	240 aa KI0AGA10AA09FM1
Vittaforma cornae	nd	293 aa VICG_01748	Partial sequence VICG_01948	254 aa VICG_01195	204 aa VICG_01807
Vavraia culicis floridensis	nd	291 aa VCUG_00650	1864 aa VCUG_02017	372 aa VCUG_02471	356 aa VCUG_02366
Edhazardia aedis	nd	307 aa EDEG_00335	1447 aa EDEG_03869 1284 aa EDEG_03429	465 aa EDEG_03857	252 aa EDEG_03856
Nosema parisii	nd	251 aa NEQG_02488	1177 aa NEQG_00122	nd	nd
Octosporea bayeri	nd	nd	Partial sequence ACSZ01010190	Partial sequence ACSZ01005588	212 aa ACSZ01000826

*nd, not determined, probably because of high sequence divergence or incomplete assembly of the genome. For PTP1 there are also some differences in the number of aa for the different strains of both E. cuniculi and E. hellem (Peuvel et al., 2000). *A. locustae https://www.ncbi.nlm.nih.gov/assembly/GCA_007674295.1/. **Nosema bombycis (annotated sequences of Nosema bombycis and Nosema antheraeae are deposited in Genbank as the following accession numbers: ACJZ01000001-ACJZ01003558). O.bayeri from Broad Institute (https://microsporidiadb.org/micro/; https://www.broadinstitute.org/fungal-genome-initiative/microsporidia-genome-sequencing).*

be obtained from bacteria by horizontal gene transfer during the microsporidia evolution (Tsaousis et al., 2008; Heinz et al., 2014; Dean et al., 2018). Three of these NTTs have been shown to be in the sporoplasm membrane and all of these NTTs were demonstrated to be able to transport ATP, GTP, NAD^+, and purine nucleotides from the host cytoplasm (Tsaousis et al., 2008; Heinz et al., 2014; Dean et al., 2018). The microsporidia have a highly reduced genome which contains ∼3000 protein coding genes, they lack functional mitochondria, and lack almost all of the genes for ATP generation other than glycolysis, therefore, these NTTs which are expressed on the parasite surface are thought to be critical strategies for microsporidia to acquire ATP and other purine nucleotides for energy and biosynthesis from their host (Katinka et al., 2001; Keeling et al., 2010; Heinz et al., 2012; Dean et al., 2016). A recent study demonstrated that another sporoplasm surface located protein family, the Microsporidia major facilitator superfamily (MFS) transport proteins are used as a second set of transporters to acquire energy and nucleotides from host cells. Four MFS proteins were identified from *Trachipleistophora hominis* (ThMFS1-4) and ThMFS1 and ThMFS3 were demonstrated to be located in the sporoplasm plasma membrane during infection (3 to

96 h post infection in cell culture). Further study revealed that all four ThMFS can transport ATP, GTP, and purine; thus they have a similar function to the NTTs (Major et al., 2019). However, neither NTTs nor ThMFS can transport the pyrimidine nucleotides suggesting that microsporidia have a yet unknown pyrimidine nucleotide import system (Heinz et al., 2014; Dean et al., 2018; Major et al., 2019).

While microsporidia were originally believed to not have mitochondria, it has been discovered that they have a highly reduced mitochondria termed a mitosome that has lost its mitochondrial genome and capacity for ATP generation (Williams et al., 2002; Goldberg et al., 2008). Mitosomes are double-membrane-bounded organelles which have been found in several species of parasites such as Microsporidia, Diplomonads, Amoebozoa, and Apicomplexa (Tovar et al., 1999, 2003; Williams et al., 2002; Keithly et al., 2005). Compared to mitochondria the mitosomes are morphologically smaller, lack cristae, and lack their own DNA (making them completely reliant on importing nuclear encoded proteins for their functions and organelle maintenance) (Burri et al., 2006; Hans-Peter Braun, 2009; Tachezy, 2019). Microsporidian mitosomes have lost their capacity for ATP production through oxidative phosphorylation, even though they can use glycolysis for energy generation, but this pathway, while active in spores, appears to not be active during the stage of intracellular growth and replication inside of host cytosol (Dolgikh et al., 2011; Heinz et al., 2012; Williams et al., 2014). Microsporidia can use glycolysis for energy generation, but this pathway, while active in spores, appears to not be active during the stage of intracellular growth and replication inside of the host cytosol (Dolgikh et al., 2011; Heinz et al., 2012; Williams et al., 2014). Thus, microsporidia depend on their host cells for energy and mitochondria accumulate around the microsporidia [this is clearly observable in Encephalitozoonidae residing in a parasitophorous vacuole within their host cells (Han et al., 2019)].

The molecular mechanism of mitochondria and microsporidia association is still unknown. A recent study revealed that *E. hellem* sporoplasm surface protein 1 (EhSSP1), a protein expressed on the surface of the sporoplasm, is involved in the interaction of microsporidia with host cell mitochondria. EhSSP1 was demonstrated to interact with all three forms of voltage-dependent anion selective channels (VDAC1-3), which are mainly expressed in the cytoplasm of the outer mitochondrial membrane. Inhibiting this interaction decreased the association of mitochondria with the microsporidian parasitophorous vacuole (Han et al., 2019). Interaction of EhSSP1 with VDAC probably facilitates energy acquisition by the microsporidia in its host cell (Han et al., 2019). Interestingly, EhSSP1 also interacted with an unidentified host cell protein in the invasion synapse, and might also have another role during invasion.

MICROSPORIDIA INVASION

Microsporidia infection of host cells involves the rapid extrusion of the PT and transfer of the sporoplasm into the host cell (Weidner, 1972; Frixione et al., 1992; Takvorian et al., 2005; Han et al., 2017). Generally, the adherence of microsporidian spores to host cells or to the vicinity of the host cells is the first step in the infection process (Weidner, 1972; Han et al., 2017). Spore wall proteins SWPs probably play a crucial role during the interaction of microsporidia and host cells (Southern et al., 2007). Several SWPs which can interact with host cells by binding to the heparin-binding motif (HBM) and host cell surface sulfated glycosaminoglycans (GAGs) have been identified from *Nosema bombycis, Encephalitozoon spp*., and *Antonospora locustae* (Hayman et al., 2001; Hayman et al., 2005; Southern et al., 2007; Li et al., 2009; Wu et al., 2009; Chen et al., 2017). Besides the interaction of HBM with GAGs during spore adherence to host cells, a separate study reported that host cell integrin is also involved in *E. intestinalis* adherence and infection of its host cells (Leonard and Hayman, 2017). Analysis of the *E. intestinalis* genome demonstrated numerous hypothetical proteins that were predicted to contain the canonical integrin-binding motif arginine-glycine-aspartic acid (RGD), which is the binding motif involved in the interaction of extracellular matrix (ECM) proteins with host cell integrins. Proteins that interact with host cell integrins have been found in many pathogenic microbes that adhere to host cells including viruses, bacteria and parasites (Patti et al., 1994; Finlay and Falkow, 1997; Rostand and Esko, 1997; Bartlett and Park, 2010). Incubation of host cells with RGD-peptides or recombinant alpha3 beta1 and alpha 5 beta 1 human integrin proteins inhibited microsporidia spore adherence and host cell infection (Leonard and Hayman, 2017). This suggests that spore adherence is important in the germination and subsequent invasion of host cells (**Figure 5**).

In addition to binding to GAGs, analysis of NbSWP26 from *Nosema bombycis* also demonstrated that it could interact with the turtle-like protein (BmTLP) of the silkworm *Bombyx mori* (Zhu et al., 2013). BmTLP is a lgSF member protein which is a cytokine receptor, cell surface antigen receptor and cell adhesion molecules that are involved in antigen presentation to vertebrate lymphocytes, co-receptors and co-stimulatory molecules of the immune system (Barclay, 2003). This interaction of NbSWP26 with BmTLP suggests that it might act as a receptor that facilitates spore invasion of silkworm cells (Zhu et al., 2013).

It has been shown that attached spores (**Figure 5**) may be phagocytosed by both professional and non-professional phagocytes via an actin based mechanism (Weidner and Sibley, 1985; Couzinet et al., 2000; Foucault and Drancourt, 2000; Hayman et al., 2005; Leitch et al., 2005). Interestingly, NbSWP5 from *Nosema bombycis* can protect spores from phagocytic uptake by cultured insect cells revealing that it may function both for structural integrity and in modulating host cell invasion (Cai et al., 2011). Phagocytosed spores will be transferred to endosomal and eventually to lysosomal compartments; however, phagocytosed spores have been shown to germinate resulting in infection of either the host cell that phagocytized the spore or adjacent cells (Franzen, 2004, 2005; Franzen et al., 2005).

The interaction of PT and sporoplasm with host cell during microsporidia infection is not fully understood. After germination of the polar tube, PTP1 (a mannosylated protein with a significant number of O-linked mannosylation

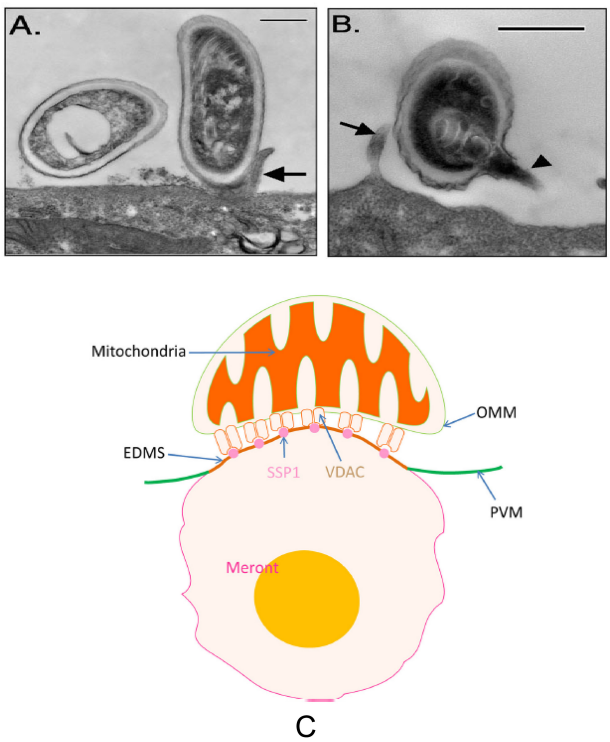

FIGURE 5 | Transmission electron microscopy of *E. intestinalis* spores attached to Caco-2 cell surfaces. The attached spores appear to be in direct contact with the cell surface or microvilli and have either intact, unextruded polar filaments **(A)** or extruded PTs **(B).** Bar is 500 nm. Arrows show host cell microvilli, and the arrowhead points to the *E. intestinalis* PT. Reprinted with permission of the author (JR Hayman) and the publisher (Hayman et al., 2005). **(C)** A model of the binding of mitochondria with the parasitophorous vacuole via the interaction of VDAC on the out mitochondria membrane with SSP1 on the surface of meronts. Reprinted with permission of the publisher (Han et al., 2019).

modification sites) can interact with mannose binding receptors on the host cell surface, thereby, attaching the PT to the host cell (Xu et al., 2003, 2004). As the PT pushes into the host cell it creates an invagination in the host cell creating a microenvironment which we have termed the invasion synapse (**Figure 3**). Within this protected environment the sporoplasm exits the PT, it is not known if the PT penetrates the host cell membrane delivering the sporoplasm into the host cytosol or if the sporoplasm penetrates directly into the host cell within this invasion synapse. For microsporidia that reside in a parasitophorous vacuole we believe, based on our published data (Han et al., 2017, 2019), that the second hypothesis is probable and that interactions of PTPs and the sporoplasm membrane with the host cell membrane are important during invasion. To this end, polar tube protein 4 (PTP4) has been demonstrated to have a specific epitope on the tip of the PT and this epitope was shown to interact with host cell transferrin receptor (TfR1) (Han et al., 2017). TfR1 is the main receptor for most cells that take up iron and is involved in iron uptake via cathrin-mediated endocytosis (Qian et al., 2002). Several viruses have been demonstrated to utilize the TfR1 pathway for binding and subsequent invasion of their host cells. The PTP4 TfR1 interaction may trigger the clathrin-mediated endocytosis pathway and could help to facilitate the process of invasion within the invasion synapse (Han et al., 2017).

After the sporoplasm invades or is transported into the host cell cytoplasm, it enters the proliferative phase of the life cycle marked by extensive multiplication via merogony. The location of this developmental stage within the host cell varies by genus (Cali and Takvorian, 2014); it can occur either in direct contact with the host cell cytoplasm (e.g., *Nosema, Enterocytozoon)*, in a parasitophorous vacuole lined by a host-produced single membrane (e.g., *Encephalitozoon*), in a parasite-secreted amorphous coat (e.g., *Pleistophora, Trachipleistophora, Thelohania)*, or surrounded by endoplasmic reticulum of the host (e.g., *Endoreticulatus, Vittaforma*) (Sprague et al., 1992; Martinez et al., 1993; Bigliardi and Sacchi, 2001; Cali and Takvorian, 2003, 2014). The interactions of various microsporidial developmental stage-specific surface proteins with host cell cytoplasm proteins or organelles (e.g., mitochondria and endoplasmic reticulum) during the process described above remains to be determined.

Host VDACs have been shown to be concentrated at the interface of host cell mitochondrial and microsporidia parasitophorous vacuole membrane (PVM) (Hacker et al., 2014). The function of VDACs which mainly locate at the outer membrane of mitochondria as channel proteins is to control the movement of adenine nucleotides, NADH, and other metabolites across the membrane (Blachly-Dyson and Forte, 2001; Cesura et al., 2003; Rostovtseva et al., 2005). The association of VDACs to the PVM has been hypothesized to be a strategy used by microsporidia to maximize its ATP supply from its host cells (Hacker et al., 2014). However, the interaction target of VDACs in microsporidia was not identified until recently when EhSSP1 was identified from *Encephalitozoon hellem* (Han et al., 2019). Studies of EhSSP1 demonstrated that the microsporidia tether the host mitochondria to its PVM during intracellular development by hijacking VDACs using EhSSP1, which is probably critical for energy uptake by the replicative forms of this organism (Han et al., 2019) (**Figure 5**).

After replication, many microsporidia appear to exit the host cell by lysis and/or apoptosis of the infected cell, however, in cell culture and in some animal models one can see adjacent foci of infection suggestive of cell to cell spread of these pathogens (Weiss and Becnel, 2014; Balla et al., 2016). There has been very limited study on the molecular pathways which provide the major modes for egress of microsporidia from host cells. A study on *Nematocida parisii* has shown that microsporidia escape from intestinal cells by co-opting the host vesicle trafficking system and escaping into the lumen (Szumowski et al., 2014). A host small GTPase protein called RAB-11, which apically localizes in many polarized epithelial cells was required for spore-containing compartments to fuse with the apical plasma membrane and direct microsporidian exocytosis (Szumowski et al., 2014). Moreover, during the process of exiting, an intestinal-specific isoform of *C. elegans* actin-5 can form coats around the membrane

compartments which contain the exocytosing spores after fusion with the apical membrane and the smGTPases rab-5, rab-11, cdc-42, and ced-10/Rac 1 promote the formation of actin coats during this process (Szumowski et al., 2016).

CONCLUSION

Microsporidia are opportunistic pathogens of immune suppressed patients and the clinical spectrum of diseases they cause is expanding with the introduction of new immune modulatory therapies. Furthermore, they are important pathogens of economically important insects and animals. The mechanism of invasion used by these pathogens is unique with a highly specialized invasion apparatus which despite its description over 125 years ago is still not understood. Progress, however, has been made in understanding the proteins in this invasion apparatus and the interaction of these proteins with some host cell proteins. Nonetheless, the mechanism of how microsporidia enter host cells and establish host pathogen relationships seen in the various microsporidia species has not been determined. In addition, the egress of microsporidia from its host cell when it has completed its replicative cycle is another area that deserves study. Understanding how microsporidia use host cell proteins in both invasion and egress will provide insight into their impact on hosts and enhance our current understanding of the transmission dynamics of this pathogen. In addition, understanding these processes will provide information needed for new therapeutic approaches to control these pathogenic protists.

AUTHOR CONTRIBUTIONS

BH, PT, and LW composed the manuscript, compiled information from the literature, and designed the figures and tables. LW edited the final manuscript.

FUNDING

This work was supported by R01 AI124753 (LW).

REFERENCES

Balla, K. M., Luallen, R. J., Bakowski, M. A., and Troemel, E. R. (2016). Cell-to-cell spread of microsporidia causes *Caenorhabditis elegans* organs to form syncytia. *Nat. Microbiol.* 1:16144. doi: 10.1038/nmicrobiol.2016.144

Barclay, A. N. (2003). Membrane proteins with immunoglobulin-like domains—a master superfamily of interaction molecules. *Sem. Immunol.* 15, 215–223. doi: 10.1016/s1044-5323(03)00047-2

Bartlett, A. H., and Park, P. W. (2010). Proteoglycans in host–pathogen interactions: molecular mechanisms and therapeutic implications. *Expert Rev. Mol. Med.* 12:e5. doi: 10.1017/S1462399409001367

Beckers, P. J., Derks, G. T., Rietveld, F. J., and Sauerwein, R. W. (1996). Encephalocytozoon intestinalis-specific monoclonal antibodies for laboratory diagnosis of microsporidiosis. *J. Clin. Microbiol.* 34, 282–285. doi: 10.1128/jcm.34.2.282-285.1996

Becnel, J. J., Andreadis, T. G., Wittner, M., and Weiss, L. (2014). "Microsporidia in insects," in *Microsporidia: Pathogens of Opportunity*, 1st Edn, eds J. J. Becnel, and L. M. Weiss (Oxford: Wiley Blackwell), 521–570. doi: 10.1002/9781118395264.ch21

Bigliardi, E., and Sacchi, L. (2001). Cell biology and invasion of the microsporidia. *Microbes Infect.* 3, 373–379. doi: 10.1016/s1286-4579(01)01393-4

Blachly-Dyson, E., and Forte, M. (2001). VDAC channels. *IUBMB Life* 52, 113–118.

Bohne, W., Ferguson, D. J., Kohler, K., and Gross, U. (2000). Developmental expression of a tandemly repeated, glycine-and serine-rich spore wall protein in the microsporidian pathogen *Encephalitozoon cuniculi*. *Infect. Immun.* 68, 2268–2275. doi: 10.1128/iai.68.4.2268-2275.2000

Bouzahzah, B., Nagajyothi, F., Ghosh, K., Takvorian, P. M., Cali, A., Tanowitz, H. B., et al. (2010). Interactions of *Encephalitozoon cuniculi* polar tube proteins. *Infect. Immun.* 78, 2745–2753. doi: 10.1128/IAI.01205-09

Bouzahzah, B., and Weiss, L. M. (2010). Glycosylation of the major polar tube protein of *Encephalitozoon cuniculi*. *Parasitol. Res.* 107, 761–764. doi: 10.1007/s00436-010-1950-7

Brambilla, D. J. (1983). Microsporidiosis in a *Daphnia pulex* population. *Hydrobiologia* 99, 175–188. doi: 10.1007/bf00008769

Brosson, D., Kuhn, L., Prensier, G., Vivares, C. P., and Texier, C. (2005). The putative chitin deacetylase of *Encephalitozoon cuniculi*: a surface protein implicated in microsporidian spore-wall formation. *FEMS Microbiol. Lett.* 247, 81–90. doi: 10.1016/j.femsle.2005.04.031

Bryan, R. T., Cali, A., Owen, R. L., and Spencer, H. C. (1991). Microsporidia: opportunistic pathogens in patients with AIDS," in *Progress in Clinical Parasitology* Vol. 2, *Trans. Tsieh Sun.* (New York, NY: Field & Wood Medical Publishers).

Burri, L., Williams, B. A., Bursac, D., Lithgow, T., and Keeling, P. J. (2006). Microsporidian mitosomes retain elements of the general mitochondrial targeting system. *Proc. Natl. Acad. Sci. U.S.A.* 103, 15916–15920. doi: 10.1073/pnas.0604109103

Cai, S., Lu, X., Qiu, H., Li, M., and Feng, Z. (2011). Identification of a *Nosema bombycis* (Microsporidia) spore wall protein corresponding to spore phagocytosis. *Parasitology* 138, 1102–1109. doi: 10.1017/S0031182011000801

Cali, A., Becnel, J. J., and Takvorian, P. M. (2017). "Microsporidia," in *Handbook of the Protists Ebook*, eds J. M. Archibald, A. G. B. Simpson, C. H. Slamovits, L. Margulis, M. Melkonian, D. J. Chapman, et al. (Berlin: Springer International Publishing).

Cali, A., and Owen, R. L. (1988). "Microsporidiosis," in *Laboratory Diagnosis of Infectious Diseases*, eds A. Balows, W. J. Hausler, M. Ohashi, Jr., A. Turano, and E. H. Lennete (Berlin: Springer), 929–950.

Cali, A., and Takvorian, P. M. (2003). Ultrastructure and development of Pleistophora Ronneafiei N. Sp., a *Microsporidium* (Protista) in the skeletal muscle of an immune-compromised individual. *J. Euk. Microbiol.* 50, 77–85. doi: 10.1111/j.1550-7408.2003.tb00237.x

Cali, A., and Takvorian, P. M. (2004). The Microsporidia: pathology in man and occurrence in nature. *SE Asian J. Trop. Med Pub. Health* 35, 58–64.

Cali, A., and Takvorian, P. M. (2014). "Developmental morphology and life cycles of the Microsporidia," in *Microsporidia-Pathogens of Opportunity*, eds L. M. Weiss, and J. J. Becnel (Hoboken, NJ: Wiley Blackwell Press), 71–133. doi: 10.1002/9781118395264.ch2

Cali, A., Weiss, L. M., and Takvorian, P. M. (2002). Brachiola algerae spore membrane systems, their activity during extrusion, and a new structural entity, the multilayered interlaced network, associated with the polar Tube and the Sporoplasm. *J. Euk. Microbiol.* 49, 164–174. doi: 10.1111/j.1550-7408.2002.tb00361.x

Canning, E. U., and Lom, J. (1986). *The Microsporidia of Vertebrates. Microsporidia of Vertebrates*. London: Academic Press.

Capella-Gutiérrez, S., Marcet-Houben, M., and Gabaldón, T. (2012). Phylogenomics supports microsporidia as the earliest diverging clade of sequenced fungi. *BMC Biol.* 10:1. doi: 10.1186/1741-7007-10-47

Cesura, A. M., Pinard, E., Schubenel, R., Goetschy, V., Friedlein, A., Langen, H., et al. (2003). The voltage-dependent anion channel is the target for a new class of inhibitors of the mitochondrial permeability transition pore. *J. Biol. Chem.* 278, 49812–49818. doi: 10.1074/jbc.m304748200

Chen, J., Geng, L., Long, M., Li, T., Li, Z., Yang, D., et al. (2013). Identification of a novel chitin-binding spore wall protein (NbSWP12) with a BAR-2 domain from *Nosema bombycis* (microsporidia). *Parasitology* 140, 1394–1402. doi: 10.1017/S0031182013000875

Chen, L., Li, R., You, Y., Zhang, K., and Zhang, L. (2017). A novel spore wall protein from *Antonospora locustae* (Microsporidia: Nosematidae) contributes to sporulation. *J. Eukaryot. Microbiol.* 64, 779–791. doi: 10.1111/jeu.12410

Corsaro, D., Walochnik, J., Venditti, D., Steinmann, J., Müller, K. D., and Michel, R. (2014). Microsporidia-like parasites of amoebae belong to the early fungal lineage Rozellomycota. *Parasitol. Res.* 113, 1909–1918. doi: 10.1007/s00436-014-3838-4

Couzinet, S., Cejas, E., Schittny, J., Deplazes, P., Weber, R., and Zimmerli, S. (2000). Phagocytic uptake of *Encephalitozoon cuniculi* by nonprofessional phagocytes. *Infect. Immun.* 68, 6939–6945. doi: 10.1128/iai.68.12.6939-6945.2000

de Graaf, D. C., Masschelein, G., Vandergeynst, F., De Brabander, H. F., and Jacobs, F. J. (1993). In vitro germination of *Nosema apis* (Microspora: Nosematidae) spores and its effect on their αα-trehalose/D-glucose ratio. *J. Invert. Pathol.* 62, 220–225. doi: 10.1006/jipa.1993.1103

Dean, P., Hirt, R. P., and Embley, T. M. (2016). Microsporidia: why make nucleotides if you can steal them? *PLoS Pathog.* 12:e1005870. doi: 10.1371/journal.ppat.1005870

Dean, P., Sendra, K., Williams, T., Watson, A., Major, P., Nakjang, S., et al. (2018). Transporter gene acquisition and innovation in the evolution of Microsporidia intracellular parasites. *Nat. Commun.* 9:1709. doi: 10.1038/s41467-018-03923-4

Delbac, F., Peuvel, I., Metenier, G., Peyretaillade, E., and Vivares, C. P. (2001). Microsporidian invasion apparatus: identification of a novel polar tube protein and evidence for clustering of ptp1 and ptp2 genes in three *Encephalitozoon* species. *Infect. Immun.* 69, 1016–1024. doi: 10.1128/iai.69.2.1016-1024.2001

Didier, E. S., and Khan, I. (2014). "The immunology of microsporidia in mammals," in *Microsporidia: Pathogens of Opportunity*, eds L. M. Weiss, and J. J. Becnel (Oxford: Wiley Blackwel Press), 307–326.

Didier, E. S., and Weiss, L. M. (2011). Microsporidiosis: not just in AIDS patients. *Curr. Opin. Infect. Dis.* 24, 490–495. doi: 10.1097/QCO.0b013e32834aa152

Dissanaike, A. (1955). Emergence of the sporoplasm in *Nosema helminthorum*. *Nature* 175, 1002–1003. doi: 10.1038/1751002a0

Dolgikh, V. V., Senderskiy, I. V., Pavlova, O. A., Naumov, A. M., and Beznoussenko, G. V. (2011). Immunolocalization of an alternative respiratory chain in *Antonospora* (Paranosema) locustae spores: mitosomes retain their role in microsporidial energy metabolism. *Eukaryot. Cell* 10, 588–593. doi: 10.1128/EC.00283-10

Erickson, B. W., and Blanquet, R. S. (1969). The occurrence of chitin in the spore wall of *Glugea weissenbergi*. *J. Invert. Path.* 14, 358–364. doi: 10.1016/0022-2011(69)90162-1

Fayer, R., and Santin, M. (2014). "Epidemiology of microsporidia in human infections," in *Microsporidia: Pathogens of Opportunity*, eds L. M. Weiss, and J. J. Becnel (Oxford: Wiley Blackwel Press), 135–164. doi: 10.1002/9781118395264.ch3

Fine, P. E. (1975). Vectors and vertical transmission: an epidemiologic perspective. *Ann. N. Y. Acad. Sci.* 266, 173–194. doi: 10.1111/j.1749-6632.1975.tb35099.x

Finlay, B. B., and Falkow, S. (1997). Common themes in microbial pathogenicity revisited. *Microbiol. Mol. Biol. Rev.* 61, 136–169. doi: 10.1128/.61.2.136-169.1997

Foucault, C., and Drancourt, M. (2000). Actin mediates *Encephalitozoon intestinalis* entry into the human enterocyte-like cell line, Caco-2. *Microb. Pathog.* 28, 51–58. doi: 10.1006/mpat.1999.0329

Franzen, C. (2004). Microsporidia: how can they invade other cells? *Trends Parasitol.* 20, 276–279.

Franzen, C. (2005). How do microsporidia invade cells? *Folia Parasitol.* 52, 36–40. doi: 10.14411/fp.2005.005

Franzen, C., Muller, A., Hartmann, P., and Salzberger, B. (2005). Cell invasion and intracellular fate of *Encephalitozoon cuniculi* (Microsporidia). *Parasitology* 130, 285–292. doi: 10.1017/s003118200400633x

Frixione, E., Ruiz, L., Santillán, M., De Vargas, L. V., Tejero, J. M., and Undeen, A. H. (1992). Dynamics of polar filament discharge and sporoplasm expulsion by microsporidian spores. *Cell Motil. Cyto* 22, 38–50. doi: 10.1002/cm.970220105

Frixione, E., Ruiz, L., and Undeen, A. H. (1994). Monovalent cations induce microsporidian spore germination in vitro. *J. Eukaryot. Microbiol.* 41, 464–468. doi: 10.1111/j.1550-7408.1994.tb06043.x

Ghosh, K., Cappiello, C. D., McBride, S. M., Occi, J. L., Cali, A., Takvorian, P. M., et al. (2006). Functional characterization of a putative aquaporin from *Encephalitozoon cuniculi*, a microsporidia pathogenic to humans. *Int. J. Parasitol.* 36, 57–62. doi: 10.1016/j.ijpara.2005.08.013

Ghosh, K., and Weiss, L. M. (2009). Molecular diagnostic tests for microsporidia. *Interdisc. Perspect. Infect. Dis.* 2009, 926521. doi: 10.1155/2009/926521

Ghoshal, U., Khanduja, S., Pant, P., Prasad, K., Dhole, T., Sharma, R., et al. (2015). Intestinal microsporidiosis in renal transplant recipients: prevalence, predictors of occurrence and genetic characterization. *Indian J. Med. Microbiol.* 33, 357–363. doi: 10.4103/0255-0857.158551

Gibbs, A. J. (1953). *Gurleya* sp. (Microsporidia) found in the gut tissue of Trachea secalis (Lepidoptera). *Parasitology* 43, 143–147. doi: 10.1017/s0031182000018424

Goertz, D., Solter, L. F., and Linde, A. (2007). Horizontal and vertical transmission of a *Nosema* sp.(Microsporidia) from Lymantria dispar (L.)(Lepidoptera: Lymantriidae). *J. Invert. Path.* 95, 9–16. doi: 10.1016/j.jip.2006.11.003

Goldberg, A. V., Molik, S., Tsaousis, A. D., Neumann, K., Kuhnke, G., Delbac, F., et al. (2008). Localization and functionality of microsporidian iron–sulphur cluster assembly proteins. *Nature* 452, 624–628. doi: 10.1038/nature06606

Gumbo, T., Hobbs, R. E., Carlyn, C., Hall, G., and Isada, C. M. (1999). Microsporidia infection in transplant patients. *Transplantation* 67, 482–484. doi: 10.1097/00007890-199902150-00024

Hacker, C., Howell, M., Bhella, D., and Lucocq, J. (2014). Strategies for maximizing ATP supply in the microsporidian *Encephalitozoon cuniculi*: direct binding of mitochondria to the parasitophorous vacuole and clustering of the mitochondrial porin VDAC. *Cell Microbiol.* 16, 565–579. doi: 10.1111/cmi.12240

Han, B., Ma, Y., Tu, V., Tomita, T., Mayoral, J., Williams, T., et al. (2019). Microsporidia interact with host cell mitochondria via voltage-dependent anion channels using sporoplasm surface protein 1. *mBio* 10:e001944-19. doi: 10.1128/mBio.01944-19

Han, B., Polonais, V., Sugi, T., Yakubu, R., Takvorian, P. M., Cali, A., et al. (2017). The role of microsporidian polar tube protein 4 (PTP4) in host cell infection. *PLoS Pathog.* 13:e1006341. doi: 10.1371/journal.ppat.1006341

Han, B., and Weiss, L. M. (2017). Microsporidia: obligate intracellular pathogens within the fungal kingdom. *Microbiol. Spectr.* 5, 97–113.

Han, B., and Weiss, L. M. (2018). Therapeutic targets for the treatment of microsporidiosis in humans. *Expert Opin. Ther. Targets* 22, 903–915. doi: 10.1080/14728222.2018.1538360

Hans-Peter Braun, R. B. (2009). Mitochondria. By *Immo E.* scheffler. *Q. Rev. Biol.* 84, 103–103. doi: 10.1086/598289

Hashimoto, K., Sasaki, Y., and Takinami, K. (1976). Conditions for extrusion of the polar filament of the spore of *Plistophora anguillarum*, a microsporidian parasite in *Anguilla japonica*. *Bull. Jpn. Soc. Sci. Fish.* 42, 837–845. doi: 10.2331/suisan.42.837

Hayman, J. R., Hayes, S. F., Amon, J., and Nash, T. E. (2001). Developmental expression of two spore wall proteins during maturation of the microsporidian *Encephalitozoon intestinalis*. *Infect. Immun.* 69, 7057–7066. doi: 10.1128/iai.69.11.7057-7066.2001

Hayman, J. R., Southern, T. R., and Nash, T. E. (2005). Role of sulfated glycans in adherence of the microsporidian *Encephalitozoon intestinalis* to host cells in vitro. *Infect. Immun.* 73, 841–848. doi: 10.1128/iai.73.2.841-848.2005

He, Q., Leitch, G. J., Visvesvara, G. S., and Wallace, S. (1996). Effects of nifedipine, metronidazole, and nitric oxide donors on spore germination and cell culture infection of the microsporidia *Encephalitozoon hellem* and *Encephalitozoon intestinalis*. *Antimicrob. Agents Chemother.* 40, 179–185. doi: 10.1128/aac.40.1.179

He, Q., Vossbrinck, C. R., Yang, Q., Meng, X.-Z., Luo, J., Pan, G.-Q., et al. (2019). Evolutionary and functional studies on microsporidian ATP-binding cassettes: insights into the adaptation of microsporidia to obligated intracellular parasitism. *Infect. Gen. Evol.* 68, 136–144. doi: 10.1016/j.meegid.2018.12.022

Heinz, E., Hacker, C., Dean, P., Mifsud, J., Goldberg, A. V., Williams, T. A., et al. (2014). Plasma membrane-located purine nucleotide transport proteins are key components for host exploitation by microsporidian intracellular parasites. *PLoS Pathog.* 10:e1004547. doi: 10.1371/journal.ppat.1004547

Heinz, E., Williams, T. A., Nakjang, S., Noël, C. J., Swan, D. C., Goldberg, A. V., et al. (2012). The genome of the obligate intracellular parasite Trachipleistophora hominis: new insights into microsporidian genome dynamics and reductive evolution. *PLoS Pathog.* 8:e1002979. doi: 10.1371/journal.ppat.1002979

Higes, M., Martin-Hernandez, R., and Meana, A. (2010). *Nosema ceranae* in Europe: an emergent nosemosis type C. *Apidologie* 41, 375–392. doi: 10.1111/j.1758-2229.2010.00186.x

Huger, A. (1960). Electron microscope study on the cytology of a microsporidian spore by means of ultrathin sectioning. *J. Insect Pathol.* 2, 84–105.

Ishihara, R. (1967). Stimuli causing extrusion of polar filaments of *Glugea fumiferanae* spores. *Can. J. Microbiol.* 13, 1321–1332. doi: 10.1139/m67-178

Ishihara, R. (1968). Some observations on the fine structure of sporoplasm discharged from spores of a microsporidian, *Nosema bombycis*. *J. Invertebr. Pathol.* 12, 245–258. doi: 10.1016/0022-2011(68)90323-6

Jaroenlak, P., Boakye, D. W., Vanichviriyakit, R., Williams, B. A., Sritunyalucksana, K., and Itsathitphaisarn, O. (2018). Identification, characterization and heparin binding capacity of a spore-wall, virulence protein from the shrimp microsporidian. *Enterocytozoon hepatopenaei* (EHP). *Parasit. Vectors* 11:177. doi: 10.1186/s13071-018-2758-z

Katinka, M. L. D., Duprat, S., Cornillot, E., Méténier, G., Thomarat, F., Prensier, G. R., et al. (2001). Genome sequence and gene compaction of the eukaryote parasite *Encephalitozoon cuniculi*. *Nature* 414, 450–453. doi: 10.1038/35106579

Keeling, P. J. (2014). "Phylogenetic place of Microsporidia in the tree of eukaryotes," in *Microsporidia: Pathogens of Opportunity*, 1st Edn, eds J. J. Becnel, and L. M. Weiss (Hoboken, NJ: Wiley Blackwell), 195–220.

Keeling, P. J., Corradi, N., Morrison, H. G., Haag, K. L., Ebert, D., Weiss, L. M., et al. (2010). The reduced genome of the parasitic microsporidian Enterocytozoon bieneusi lacks genes for core carbon metabolism. *Gen. Biol. Evol.* 2, 304–309. doi: 10.1093/gbe/evq022

Keithly, J. S., Langreth, S. G., Buttle, K. F., and Mannella, C. A. (2005). Electron tomographic and ultrastructural analysis of the *Cryptosporidium parvum* relict mitochondrion, its associated membranes, and organelles. *J. Eukaryot. Microbiol.* 52, 132–140. doi: 10.1111/j.1550-7408.2005.04-3317.x

Keohane, E., Takvorian, P., Cali, A., Tanowitz, H., Wittner, M., and Weiss, L. M. (1994). The identification and characterization of a polar tube reactive monoclonal antibody. *J. Eukaryot. Microbiol.* 41, 48S–48S.

Keohane, E. M., Orr, G. A., Takvorian, P. M., Cali, A., Tanowitz, H. B., Wittner, M., et al. (1996). Purification and characterization of a microsporidian polar tube proteins. *J. Eukaryot. Microbiol.* 43:100S. doi: 10.1111/j.1550-7408.1996.tb05023.x

Keohane, E. M., Orr, G. A., Zhang, H. S., Takvorian, P. M., Cali, A., Tanowitz, H. B., et al. (1998). The molecular characterization of the major polar tube protein gene from *Encephalitozoon hellem*, a microsporidian parasite of humans. *Mol. Biochem. Parasitol.* 94, 227–236. doi: 10.1016/s0166-6851(98)00071-1

Korke, V. (1916). On a *Nosema* (*Nosema pulicis*, ns) parasitic in the dog flea (*Ctenocephalus felis*). *Indian J. Med. Res.* 3, 725–730.

Kramer, J. P. (1960). Observations on the emergence of the microsporidian sporoplasm. *J. Insect Pathol.* 2, 433–439.

Kramer, J. P. (1970). Longevity of microsporidian spores with special reference to *Octosporea muscaedomesticae* Flu. *Acta Protozool.* 8, 217–224.

Kudo, R. (1916). Contributions to the study of parasitic protozoa. I. On the structure and life history of *Nosema bombycis* Nägeli. *Bull. Imp. Seric. Exp. Sta. Jpn.* 1, 31–51.

Kudo, R. (1918). Experiments on the extrusion of polar filaments of cnidosporidian spores. *J. Parasitol.* 4, 141–147.

Kudo, R. (1920). On the structure of some microsporidian spores. *J. Parasitol.* 6, 178–182.

Kudo, R., and Daniels, E. W. (1963). An electron microscope study of the spore of a microsporidian, *Thelohania californica*. *J. Protozool.* 10, 112–120. doi: 10.1111/j.1550-7408.1963.tb01645.x

Lee, S. C., Corradi, N., Byrnes, E. J., Torresmartinez, S., Dietrich, F. S., Keeling, P. J., et al. (2008). Microsporidia evolved from ancestral sexual fungi. *Curr. Biol.* 18, 1675–1679. doi: 10.1016/j.cub.2008.09.030

Leitch, G., Ward, T., Shaw, A., and Newman, G. (2005). Apical spore phagocytosis is not a significant route of infection of differentiated enterocytes by *Encephalitozoon intestinalis*. *Infect. Immun.* 73, 7697–7704. doi: 10.1128/iai.73.11.7697-7704.2005

Leitch, G. J., He, Q., Wallace, S., and Visvesvara, G. S. (1993). Inhibition of the spore polar filament extrusion of the Microsporidium, *Encephalitozoon hellem*, isolated from an aids patient. *J. Euk. Microbiol.* 40, 711–717. doi: 10.1111/j.1550-7408.1993.tb04463.x

Leitch, J. G., and Ceballos, C. (2008). Effects of host temperature and gastric and duodenal environments on microsporidia spore germination and infectivity of intestinal epithelial cells. *Parasitol. Res.* 104, 35–42. doi: 10.1007/s00436-008-1156-4

Leonard, C. A., and Hayman, J. R. (2017). Role of host cell integrins in the microsporidium *Encephalitozoon intestinalis* adherence and infection in vitro. *FEMS Microbiol. Lett.* 364:fnx169. doi: 10.1093/femsle/fnx169

Li, Y., Wu, Z., Pan, G., He, W., Zhang, R., Hu, J., et al. (2009). Identification of a novel spore wall protein (SWP26) from microsporidia *Nosema bombycis*. *Int. J. Parasitol.* 39, 391–398. doi: 10.1016/j.ijpara.2008.08.011

Li, Z., Pan, G., Li, T., Huang, W., Chen, J., Geng, L., et al. (2012). SWP5, a spore wall protein, interacts with polar tube proteins in the parasitic microsporidian *Nosema bombycis*. *Eukaryot. Cell* 11, 229–237. doi: 10.1128/EC.05127-11

Liu, H., Chen, B., Hu, S., Liang, X., Lu, X., and Shao, Y. (2016). Quantitative proteomic analysis of germination of *Nosema bombycis* spores under extremely alkaline conditions. *Front. Microbiol.* 7:1459. doi: 10.3389/fmicb.2016.01459

Lom, J. (1972). On the structure of the extruded microsporidian polar filament. *Parasitol. Res.* 38, 200–213. doi: 10.1007/bf00329598

Lom, J., and Vavra, J. (1963). The mode of sporoplasm extrusion in microsporidian spores. *Acta Protozool.* 1, 81–89.

Major, P., Sendra, K. M., Dean, P., Williams, T. A., Watson, A. K., Thwaites, D. T., et al. (2019). A new family of cell surface located purine transporters in Microsporidia and related fungal endoparasites. *eLife* 8:e47037. doi: 10.7554/eLife.47037

Malone, L. A. (1984). Factors controlling in vitro hatching of Vairimorpha plodiae (Microspora) spores and their infectivity to Plodia interpunctella, Heliothis virescens, and Pieris brassicae. *J. Invertebr. Pathol.* 44, 192–197. doi: 10.1016/0022-2011(84)90012-0

Malone, L. A. (1990). In vitro spore hatching of two microsporidia, *Nosema costelytrae* and *Vavraia oncoperae*, from New Zealand pasture insects. *J. Invert. Pathol.* 55, 441–443. doi: 10.1016/0022-2011(90)90091-j

Martinez, M. A., Vivares, C. P., and Bouix, G. (1993). Ultrastructural study of *Endoreticulatus durforti* N. Sp., a new Microsporidian parasite of the intestinal *Epithelium* of *Artemia* (Crustacea, Anostraca). *J. Eukaryot. Microbiol.* 40, 677–687. doi: 10.1111/j.1550-7408.1993.tb06126.x

Miao, Z., Zhang, Y., Zhang, P., Wang, X., Liu, J., and Wang, G. (2018). "Characterization of the germination kinetics of individual *Nosema bombycis* spores using phase contrast microscopy imaging and Raman spectroscopy," in *Optics in Health Care and Biomedical Optics VIII*, eds Q. Luo, X. Li, Y. Gu, Y. Tang, and D. Zhu (Washington, DC: International Society for Optics and Photonics), 108202Z.

Naegeli, C. (1857). Uber die neue krankheit der seidenraupe und verwandte organismen. *Bot. Zeit.* 15, 760–761.

Ohshima, K. (1927). A preliminary note on the structure of the polar filament of *Nosema bombycis* and its functional significance. *Annot. Zool. Jpn.* 11, 235–243.

Ohshima, K. (1937). On the function of the polar filament of *Nosema bombycis*. *Parasitology* 29, 220–224. doi: 10.1017/s0031182000024768

Ohshima, K. (1964a). Effect of potassium ion on filament evagination of spores of *Nosema bombycis* as studied by neutralization method. *Annot. Zool. Jpn.* 37, 102–103.

Ohshima, K. (1964b). Stimulative or inhibitive substance to evaginate the filament of *Nosema bombycis* NÄGELI. I. The case of artificial buffer solution. *Jpn. J. Zool.* 14, 209–229.

Ohshima, K. (1966). Emergence mechanism of sporoplasm from the spore of *Nosema bombycis* and the action of filament during evagination. *Jpn. J. Zool.* 15, 203–220.

Olsen, P., Rice, W., and Liu, T. (1986). In vitro germination of *Nosema apis* spores under conditions favorable for the generation and maintenance of sporoplasms. *J. Invert. Pathol.* 47, 65–73. doi: 10.1016/0022-2011(86)90164-3

Olson, R. E., Tiekotter, K. L., and Reno, P. W. (1994). *Nadelspora canceri* n. g., n. sp., an unusual microsporidian parasite of the dungeness crab, *Cancer magister*. *J. Protozool.* 41, 349–359. doi: 10.1111/j.1550-7408.1994.tb06089.x

Pan, G., Bao, J., Ma, Z., Song, Y., Han, B., Ran, M., et al. (2018). Invertebrate host responses to microsporidia infections. *Dev. Commun. Immun.* 83, 104–113. doi: 10.1016/j.dci.2018.02.004

Pasteur, L. (1870). *Études Sur la Maladie des vers à soie [M]*. Paris: Gauthier-Villars, successeur de Mallet-Bachelier Vol 1870, 148–168.

Patti, J. M., Allen, B. L., Mcgavin, M. J., and Höök, M. (1994). MSCRAMM-mediated adherence of microorganisms to host tissues. *Ann. Rev. Microbiol.* 48, 585–617. doi: 10.1146/annurev.mi.48.100194.003101

Peuvel, I., Delbac, F., Metenier, G., Peyret, P., and Vivares, C. P. (2000). Polymorphism of the gene encoding a major polar tube protein PTP1 in two microsporidia of the genus Encephalitozoon. *Parasitology* 121(Pt 6), 581–587.

Peuvel, I., Peyret, P., Metenier, G., Vivares, C. P., and Delbac, F. (2002). The microsporidian polar tube: evidence for a third polar tube protein (PTP3) in *Encephalitozoon cuniculi*. *Mol. Biochem. Parasitol.* 122, 69–80. doi: 10.1016/s0166-6851(02)00073-7

Peuvel-Fanget, I., Polonais, V., Brosson, D., Texier, C., Kuhn, L., Peyret, P., et al. (2006). EnP1 and EnP2, two proteins associated with the *Encephalitozoon cuniculi* endospore, the chitin-rich inner layer of the microsporidian spore wall. *Int. J. Parasitol.* 36, 309–318. doi: 10.1016/j.ijpara.2005.10.005

Pleshinger, J., and Weidner, E. (1985). The microsporidian spore invasion tube. IV. Discharge activation begins with pH-triggered Ca2+ influx. *J. Cell Biol.* 100, 1834–1838. doi: 10.1083/jcb.100.6.1834

Polonais, V., Mazet, M., Wawrzyniak, I., Texier, C., Blot, N., El Alaoui, H., et al. (2010). The human microsporidian *Encephalitozoon hellem* synthesizes two spore wall polymorphic proteins useful for epidemiological studies. *Infect. Immun.* 78, 2221–2230. doi: 10.1128/IAI.01225-09

Qian, Z. M., Li, H., Sun, H., and Ho, K. (2002). Targeted drug delivery via the transferrin receptor-mediated endocytosis pathway. *Pharmacol. Rev.* 54, 561–587. doi: 10.1124/pr.54.4.561

Rostand, K. S., and Esko, J. D. (1997). Microbial adherence to and invasion through proteoglycans. *Infect. Immun.* 65:1. doi: 10.1128/iai.65.1.1-8.1997

Rostovtseva, T. K., Tan, W., and Colombini, M. (2005). On the role of VDAC in apoptosis: fact and fiction. *J. Bioenerg. Biomembran.* 37, 129–142. doi: 10.1007/s10863-005-6566-8

Sagers, J. B., Munderloh, U. G., and Kurtti, T. J. (1996). Early events in the infection of a *Helicoverpa zea* cell line by *Nosema furnacalis* and *Nosema pyrausta* (Microspora: Nosematidae). *J. Invertebr. Pathol.* 67, 28–34.

Shadduck, J. A., and Polley, M. B. (1978). Some factors influencing the in vitro infectivity and replication of *Encephalitozoon cuniculi*. *J. Protoc.* 25, 491–496. doi: 10.1111/j.1550-7408.1978.tb04174.x

Southern, T. R., Jolly, C. E., Lester, M. E., and Hayman, J. R. (2007). EnP1, a microsporidian spore wall protein that enables spores to adhere to and infect host cells in vitro. *Eukaryot. Cell* 6, 1354–1362. doi: 10.1128/ec.00113-07

Sprague, V., Becnel, J. J., and Hazard, E. I. (1992). Taxonomy of phylum Microspora. *Crit. Rev. Microbiol.* 18, 285–395. doi: 10.3109/10408419209113519

Sprague, V., and Vavra, J. (1977). "Systematics of the microsporidia," in *Comparative Pathobiology*, eds L. A. Bulla and T. C. Cheng (New York, NY: Plenum Press), 1–510.

Steinhaus, E. A., and Martignoni, M. E. (1970). *abridged Glossary of Terms Used in Invertebrate Pathology*. Oregon: U.S. Pacific Northwest Forest and Range Experiment Station.

Stentiford, G. D., Becnel, J., Weiss, L. M., Keeling, P. J., Didier, E. S., Williams, B. P., et al. (2016). Microsporidia - emergent pathogens in the global food chain. *Trends Parasitol.* 32, 336–348. doi: 10.1016/j.pt.2015.12.004

Strano, A., Cali, A., and Neafie, R. (1976). "Microsporidiosis, Protozoa - Section 7," in *Pathology of Tropical and Extraordinary Diseases*, 2nd Edn, eds C. H. Binford, and D. H. Connor (Washington, DC: Armed Forces Institute of Pathology Press), 336–339.

Szumowski, S. C., Botts, M. R., Popovich, J. J., Smelkinson, M. G., and Troemel, E. R. (2014). The small GTPase RAB-11 directs polarized exocytosis of the intracellular pathogen *N. parisii* for fecal-oral transmission from *C. elegans*. *PNAS* 111, 8215–8220. doi: 10.1073/pnas.1400696111

Szumowski, S. C., Estes, K. A., Popovich, J. J., Botts, M. R., Sek, G., and Troemel, E. R. (2016). Small GTPases promote actin coat formation on microsporidian pathogens traversing the apical membrane of *Caenorhabditis elegans* intestinal cells.for fecal-oral transmission from *C. elegans*. *Cell Microbiol.* 18, 30–45. doi: 10.1111/cmi.12481

Tachezy, J. (2019). *Hydrogenosomes and Mitosomes: Mitochondria of Anaerobic Eukaryotes*. Berlin: Springer.

Takvorian, P. M., Buttle, K. F., Mankus, D., Mannella, C. A., Weiss, L. M., and Cali, A. (2013). The Multilayered Interlaced Network (Min) in the sporoplasm of the microsporidium anncaliia algerae is derived from golgi. *J. Euk. Microbiol.* 60, 166–178. doi: 10.1111/jeu.12019

Takvorian, P. M., and Cali, A. (1986). The ultrastructure of spores (Protozoa: Microspora) from lophius americanus, the angler fish. *J. Protozool.* 33, 570–575. doi: 10.1111/j.1550-7408.1986.tb05664.x

Takvorian, P. M., Han, B., Cali, A., Rice, W. J., Gunther, L., Macaluso, F., et al. (2019). An ultrastructural study of the extruded polar tubes of *Anncaliia algerae* (Microsporidia). *J. Euk. Microbiol.* 67, 1–17. doi: 10.1111/jeu.12751

Takvorian, P., Weiss, L., and Cali, A. (2005). The early events of brachiola algerae (Microsporidia) infection: spore germination, sporoplasm structure, and development within host cells. *Folia Parasitol.* 52, 118–129. doi: 10.14411/fp.2005.015

Thelohan, P. (1894). Sur la presence d'une capsule a filament dans les spores des microsporidies. *CR Acad. Sci.* 118, 1425–1427.

Tovar, J., Fischer, A., and Clark, C. G. (1999). The mitosome, a novel organelle related to mitochondria in the amitochondrial parasite *Entamoeba histolytica*. *Mol. Microbiol.* 32, 1013–1021. doi: 10.1046/j.1365-2958.1999.01414.x

Tovar, J., León-Avila, G., Sánchez, L. B., Sutak, R., Tachezy, J., Van Der Giezen, M., et al. (2003). Mitochondrial remnant organelles of Giardia function in iron-sulphur protein maturation. *Nature* 426:172. doi: 10.1038/nature01945

Trager, W. (1937). The hatching of spores of *Nosema bombycis* Nägeli and the partial development of the organism in tissue cultures. *J. Parasitol.* 23, 226–227.

Tsaousis, A. D., Kunji, E. R., Goldberg, A. V., Lucocq, J. M., Hirt, R. P., and Embley, T. M. (2008). A novel route for ATP acquisition by the remnant mitochondria of *Encephalitozoon cuniculi*. *Nature* 453:553. doi: 10.1038/nature06903

Undeen, A. (1978). "Spore-hatching processes in some *Nosema* species with particular reference to *N. algerae* vavra and undeen," in *Selected Topics on the Genus Nosema (Microsporida)*, ed. W. M. Brooks (Washington, DC: Miscellaneous Publications of the Entomological Society of America), 29–49.

Undeen, A. H. (1983). The germination of *Vavraia culicis* spores. *J. Protozool.* 30, 274–277.

Undeen, A. H. (1990). A proposed mechanism for the germination of microsporidian (Protozoa: Microspora) spores. *J. Theoretl. Biol.* 142, 223–235. doi: 10.1016/s0022-5193(05)80223-1

Undeen, A., and Avery, S. (1984). Germination of experimentally nontransmissible microsporidia. *J. Invertebr. Pathol.* 43, 299–301. doi: 10.1016/0022-2011(84)90156-3

Undeen, A., and Avery, S. (1988). Effect of anions on the germination of *Nosema algerae* (Microspora: Nosematidae) spores. *J. Invertebr. Pathol.* 52, 84–89. doi: 10.1016/0022-2011(88)90106-1

Undeen, A. H., and Frixione, E. (1991). Structural alteration of the plasma membrane in spores of the Microsporidium *Nosema algerae* on germination. *J. Eukaryot. Microbiol.* 38, 511–518.

Undeen, A. H., and Meer, R. K. V. (1994). Conversion of intrasporal trehalose into reducing sugars during germination of *Nosema algerae* (Protista: Microspora) spores: a quantitative study. *J. Eukaryot. Microbiol.* 41, 129–132. doi: 10.1111/j.1550-7408.1994.tb01485.x

Undeen, A. H., and Vander Meer, R. K. (1999). Microsporidian intrasporal sugars and their role in germination. *J. Invertebr. Pathol.* 73, 294–302. doi: 10.1006/jipa.1998.4834

Vávra, J. (1976). *Structure of the Microsporidia*. New York, NY: Springer.

Vavra, J., and And Larsson, J. I. R. (1999). "Structure of the microsporidia," in *The Microsporidia and Microsporidiosis*, eds M. Wittner, and L. M. Weiss (Washington, DC: ASM Press), 7–84. doi: 10.1128/9781555818227.ch2

Vavra, J., and Chalupsky, J. (1982). Fluorescence staining of microsporidian spores with the brightener "Calcofluor White M2k". *J. Protozool.* 29:503.

Vavra, J., and Larsson, J. I. R. (2014). "Structure of the Microsporidia," in *Microsporidia Pathogens of Opportunity*, eds L. M. Becnel, and J. J. Weiss (Oxford: Wiley Blackwell), 1–70. doi: 10.1002/9781118395264.ch1

Vavra, J., and Undeen, A. H. (1970). *Nosema algerae* n. sp. (Cnidospora, Microsporida) a pathogen in a laboratory colony of *Anopheles stephensi* Liston (Diptera, Culicidae). *J. Protozool.* 17, 240–249. doi: 10.1111/j.1550-7408.1970.tb02365.x

Visvesvara, G. S. (2002). In vitro cultivation of microsporidia of clinical importance. *Clin. Microbiol. Rev.* 15:401. doi: 10.1128/cmr.15.3.401-413.2002

Walters, V. A. (1958). Structure, hatching and size variation of the spores in a species of *Nosema* (Microsporidia) found in *Hyalophora cecropia* (Lepidoptera). *Parasitology* 48, 113–120. doi: 10.1017/s0031182000021107

Wang, Y., Dang, X., Ma, Q., Liu, F., Pan, G., Li, T., et al. (2015). Characterization of a novel spore wall protein NbSWP16 with proline-rich tandem repeats from *Nosema bombycis* (microsporidia). *Parasitology* 142, 534–542. doi: 10.1017/S0031182014001565

Wang, Y., Geng, H., Dang, X., Xiang, H., Li, T., Pan, G., et al. (2017). Comparative analysis of the proteins with tandem repeats from 8 microsporidia and characterization of a novel endospore wall protein colocalizing with Polar Tube from *Nosema bombycis*. *J. Eukaryot. Microbiol.* 64, 707–715. doi: 10.1111/jeu.12412

Weber, R., Bryan, R. T., Schwartz, D. A., and Owen, R. L. (1994). Human microsporidial infections. *Clin. Microbiol. Rev.* 7, 426–461. doi: 10.1128/cmr.7.4.426

Weidner, E. (1972). Ultrastructural study of microsporidian invasion into cells. *Zeitschrift Parasitenkunde* 40, 227–242.

Weidner, E. (1976). The microsporidian spore invasion tube. The ultrastructure, isolation, and characterization of the protein comprising the tube. *J. Cell Biol.* 71, 23–34. doi: 10.1083/jcb.71.1.23

Weidner, E. (1982). The microsporidian spore invasion tube. III. Tube extrusion and assembly. *J. Cell Biol.* 93, 976–979. doi: 10.1083/jcb.93.3.976

Weidner, E., Byrd, W., Scarborough, A., Pleshinger, J., and Sibley, D. (1984). Microsporidian spore discharge and the transfer of polaroplast organelle membrane into plasma membrane. *J. Protozool.* 31, 195–198. doi: 10.1111/j.1550-7408.1984.tb02948.x

Weidner, E., Manale, S. B., and Halonen Sklynn, J. W. (1995). Protein-membrane interaction is essential to normal assembly of the microsporidian spore Invasion tube. *Biol. Bull.* 188, 128–135. doi: 10.2307/1542078

Weidner, E., and Sibley, L. D. (1985). Phagocytized intracellular microsporidian blocks phagosome acidification and phagosome-lysosome fusion. *J. Protozool.* 32, 311–317. doi: 10.1111/j.1550-7408.1985.tb03056.x

Weiss, L. M., and Becnel, J. J. (2014). *Microsporidia: Pathogens of Opportunity*. Oxford: Wiley Blackwel Press.

Weiss, L. M., Delbac, F., Russell Hayman, J., Pan, G., Dang, X., and Zhou, Z. (2014). "The microsporidian polar tube and spore wall," in *Microsporidia: Pathogens of Opportunity*, 1st Edn, eds L. M. Weiss, and J. J. Becnel (Oxford: Wiley Blackwell), 261–306. doi: 10.1002/9781118395264.ch10

Weiss, L. M., Edlind, T. D., Vossbrinck, C. R., and Hashimoto, T. (1998). Microsporidian molecular phylogeny: the fungal connection. *J. Eukaryot. Microbiol.* 46, 17S–18S.

Whitlock, V., and Johnson, S. (1990). Stimuli for the in vitro germination and inhibition of *Nosema locusta* (Microspora: Nosematidae) spores. *J. Invertebr. Pathol.* 56, 57–62. doi: 10.1016/0022-2011(90)90144-u

Williams, B. A., Dolgikh, V. V., and Sokolova, Y. Y. (2014). "Microsporidian biochemistry and physiology," in *Microsporidia: Pathogens of Opportunity*, eds L. M. Weiss, and J. J. Becnel (Hoboken, NJ: Wiley Blackwell), 245–260. doi: 10.1002/9781118395264.ch9

Williams, B. A. P., Hirt, R. P., Lucocq, J. M., and Embley, T. M. (2002). A mitochondrial remnant in the microsporidian *Trachipleistophora hominis*. *Nature* 418, 865. doi: 10.1038/nature00949

Wu, Z., Li, Y., Pan, G., Tan, X., Hu, J., Zhou, Z., et al. (2008). Proteomic analysis of spore wall proteins and identification of two spore wall proteins from *Nosema bombycis* (Microsporidia). *Proteomics* 8, 2447–2461. doi: 10.1002/pmic.200700584

Wu, Z., Li, Y., Pan, G., Zhou, Z., and Xiang, Z. (2009). SWP25, a novel protein associated with the *Nosema bombycis* endospore. *J. Eukaryot. Microbiol.* 56, 113–118. doi: 10.1111/j.1550-7408.2008.00375.x

Xu, Y., Takvorian, P., Cali, A., Wang, F., Zhang, H., Orr, G., et al. (2006). Identification of a new spore wall protein from *Encephalitozoon cuniculi*. *Infect. Immun.* 74, 239–247. doi: 10.1128/iai.74.1.239-247.2006

Xu, Y., Takvorian, P., Cali, A., and Weiss, L. M. (2003). Lectin binding of the major polar tube protein (PTP1) and its role in invasion. *J. Eukaryot. Microbiol.* 50, 600–601. doi: 10.1111/j.1550-7408.2003.tb00644.x

Xu, Y., Takvorian, P. M., Cali, A., Orr, G., and Weiss, L. M. (2004). Glycosylation of the major polar tube protein of *Encephalitozoon hellem*, a microsporidian parasite that infects humans. *Infect. Immun.* 72, 6341–6350. doi: 10.1128/iai.72.11.6341-6350.2004

Xu, Y., and Weiss, L. M. (2005). The microsporidian polar tube: a highly specialised invasion organelle. *Int. J. Parasitol.* 35, 941–953. doi: 10.1016/j.ijpara.2005.04.003

Yang, D., Dang, X., Peng, P., Long, M., Ma, C., Qin, J. J. G., et al. (2014). NbHSWP11, a microsporidia *Nosema bombycis* protein, localizing in the spore wall and membranes, reduces spore adherence to host cell BME. *J. Parasit.* 100, 623–633. doi: 10.1645/13-286.1

Yang, D., Pan, G., Dang, X., Shi, Y., Li, C., Peng, P., et al. (2015). Interaction and assembly of two novel proteins in the spore wall of the microsporidian species *Nosema bombycis* and their roles in adherence to and infection of host cells. *Infect. Immun.* 83, 1715–1731. doi: 10.1128/IAI.03155-14

Yang, D., Pan, L., Chen, Z., Du, H., Luo, B., Luo, J., et al. (2018). The roles of microsporidia spore wall proteins in the spore wall formation and polar tube anchorage to spore wall during development and infection processes. *Exp. Parasitol.* 187, 93–100. doi: 10.1016/j.exppara.2018.03.007

Yang, D., Pan, L., Peng, P., Dang, X., Li, C., Li, T., et al. (2017). Interaction between SWP9 and polar tube proteins of the microsporidian *Nosema bombycis* and SWP9 as a scaffolding protein contributes to the polar tube tethering to spore wall. *Infect. Immun.* 85:e00872-16.

Zhu, F., Shen, Z., Hou, J., Zhang, J., Geng, T., Tang, X., et al. (2013). Identification of a protein interacting with the spore wall protein SWP26 of *Nosema bombycis* in a cultured BmN cell line of silkworm. *Infect. Genet. Evol.* 17C, 38–45. doi: 10.1016/j.meegid.2013.03.029

Conflict of Interest: The authors declare that the research was conducted in the absence of any commercial or financial relationships that could be construed as a potential conflict of interest.

frontiers in Microbiology

ORIGINAL RESEARCH
published: 25 February 2020
doi: 10.3389/fmicb.2020.00288

Exploring Micro-Eukaryotic Diversity in the Gut: Co-occurrence of *Blastocystis* Subtypes and Other Protists in Zoo Animals

Emma L. Betts[1], Eleni Gentekaki[2,3] and Anastasios D. Tsaousis[1]**

[1] Laboratory of Molecular and Evolutionary Parasitology, RAPID Group, School of Biosciences, University of Kent, Canterbury, United Kingdom, [2] School of Science, Mae Fah Luang University, Chiang Rai, Thailand, [3] Gut Microbiome Research Group, Mae Fah Luang University, Chiang Rai, Thailand

Blastocystis is a genetically diverse microbial eukaryote thriving in the gut of humans and other animals. While *Blastocystis* has been linked with gastrointestinal disorders, its pathogenicity remains controversial. Previous reports have suggested that one out of six humans could be carrying *Blastocystis* in their gut, while the numbers could be even higher in animals. Most studies on *Blastocystis* are either exclusively targeting the organism itself and/or the associated prokaryotic microbiome, while co-occurrence of other microbial eukaryotes has been mainly ignored. Herein, we aimed to explore presence and genetic diversity of *Blastocystis* along with the commonly occurring eukaryotes *Cryptosporidium*, *Eimeria*, *Entamoeba* and *Giardia* in the gut of asymptomatic animals from two conservation parks in the United Kingdom. Building upon a previous study, a total of 231 fecal samples were collected from 38 vertebrates, which included 12 carnivorous and 26 non-carnivorous species. None of the animals examined herein showed gastrointestinal symptoms. The barcoding region of the small subunit ribosomal RNA was used for subtyping of *Blastocystis*. Overall, 47% of animal species were positive for *Blastocystis*. Twenty six percent of samples carried more than one subtypes, including the newly identified hosts Scottish wildcat, bongo and lynx. Fifty three percent of samples carried at least another microbial eukaryote. Herewith, we discuss potential implications of these findings and the increasingly blurred definition of microbial parasites.

Keywords: *Blastocystis*, genetic diversity, subtyping, co-occurrence, phylogeny, micro-eukaryome

OPEN ACCESS

Edited by:
Christen Rune Stensvold, Statens Serum Institut (SSI), Denmark

Reviewed by:
Hamed Mirjalali, Shahid Beheshti University of Medical Sciences, Iran
Guillaume Desoubeaux, Université de Tours, France
Longxian Zhang, Henan Agricultural University, China

****Correspondence:***
Eleni Gentekaki
gentekaki.ele@mfu.ac.th
Anastasios D. Tsaousis
A.Tsaousis@kent.ac.uk;
tsaousis.anastasios@gmail.com

Specialty section:
This article was submitted to Infectious Diseases, a section of the journal Frontiers in Microbiology

Received: *02 October 2019*
Accepted: *10 February 2020*
Published: *25 February 2020*

Citation:
Betts EL, Gentekaki E and Tsaousis AD (2020) Exploring Micro-Eukaryotic Diversity in the Gut: Co-occurrence of Blastocystis Subtypes and Other Protists in Zoo Animals. Front. Microbiol. 11:288. doi: 10.3389/fmicb.2020.00288

INTRODUCTION

The gut microbiome comprises the collective genomes of microbial symbionts and is composed of bacteria, fungi, viruses and protists within the gastrointestinal (GI) tract of a host (Blaser, 2014). Though literature associated with bacterial microbiota is increasing, studies on the rest of the microbiome components are just beginning to surface. Historically, presence of protists in the gut has been considered as parasitism, thus these microbial eukaryotes have been subject to rigorous elimination in both humans and other animals (Parfrey et al., 2011). Despite this, current data demonstrates that some protists are more common than previously thought, raising the possibility

of commensalistic or even mutualistic roles in the gut ecosystem (Lukes et al., 2015; Chudnovskiy et al., 2016). In this regard, no other protist has been studied more extensively than the anaerobic stramenopile *Blastocystis*. Its prevalence in humans has been estimated to a staggering one billion (Stensvold, 2012). Though a similar estimation for animals is not available, data from numerous animal studies covering broad range of hosts strongly suggest that colonization rate in animals is likely higher than in humans.

Blastocystis is extremely heterogeneous genetically (Gentekaki et al., 2017). Based on the SSU rRNA gene, *Blastocystis* from avian and mammalian hosts is divided into 17 subtypes, which are considered separate species (Stensvold and Clark, 2016b). Nonetheless, there are many sequences originating from ectothermic hosts that do not belong to any of the designated subtypes (Yoshikawa et al., 2016). The various subtypes of *Blastocystis* do not seem to be host-specific. For example, ST1 to ST9 have been identified in humans, but also in other hosts (Stensvold and Clark, 2016b). The exception seems to be ST9, which has yet to be identified in a non-human host (Stensvold and Clark, 2016a). ST10 to ST17 have been found only in animals so far, with the exception of ST12, which has also been identified in humans (Ramirez et al., 2016).

Though *Blastocystis* has been found in individuals with gastrointestinal symptoms, asymptomatic carriage is also common (Scanlan et al., 2014; AbuOdeh et al., 2016; Nieves-Ramirez et al., 2018; Yowang et al., 2018; Mardani Kataki et al., 2019). *In vitro* experiments using cell lines have shown the invasion potential of some strains/subtypes of *Blastocystis* (Puthia et al., 2008; Wawrzyniak et al., 2012), with no evidence to date that this also occurs *in vivo* (Clark et al., 2013). Experimental infections in mouse models have been achieved only after an inoculum of considerable size (up to 4×10^7) is administered (Moe et al., 1997; Elwakil and Hewedi, 2010). Recent studies on animals have shown that *Blastocystis* exists asymptomatically in a broad array of hosts (Betts et al., 2018; Wang et al., 2018b). Collectively, these findings highlight the uncertainty surrounding pathogenicity status of *Blastocystis* in both humans and other animals.

Presence of multiple *Blastocystis* subtypes in humans is not often reported (Whipps et al., 2010; Scanlan and Stensvold, 2013). To our knowledge, only a few reports have demonstrated mixed colonization in animals (AbuOdeh et al., 2016; Cian et al., 2017; Betts et al., 2018). In our previous work, Betts et al. (2018) examined *Blastocystis* distribution in a wildlife park in the United Kingdom, and identified various genetic isolates in a number of different animals across the park. Importantly, we also demonstrated presence of up to four subtypes in healthy captive animals (Betts et al., 2018). At that time, while microscopically screening the fecal samples, we noted presence of other protists as well. Most previous studies have been focused on identifying single target protist species, but only a few have focused on co-occurrence of multiple microbial eukaryotes in the gut. Herein, we have expanded the study area to include an additional wildlife park. We aimed to further characterize presence of *Blastocystis* isolates along with additional microbial eukaryotes across a broad range of taxa in the two parks.

MATERIALS AND METHODS

Study Sites

Two zoos situated in the Southeast, United Kingdom were sampled in this study: 1) Wildwood Conservation Park, Herne Bay, Kent, United Kingdom (51°19′54.1″N 1°07′10.1″E). This is a small conservation park housing native vertebrate and invertebrate species from the United Kingdom and mainland Europe with the exception of the red-necked wallaby (*Macropus rufogriseus*). The park is actively involved in breeding and re-introduction programs for native animals including the European water vole (*Arvicola amphibious*) and Scottish wildcat (*Felis silvestris silvestris*), and 2) Howletts Wild Animal park, Canterbury, Kent, United Kingdom (51°16′11.8″N 1°09′25.0″E). This is a large zoo with over 400 animals from 50 vertebrate and invertebrate species from across the globe. The zoo has a large primate collection, including one of the largest family groups of western lowland gorilla (*Gorilla gorilla gorilla*) in the world. The zoo is involved in a number of re-introductory schemes, mainly into national parks. Both zoos closely monitor animal health, through licensed veterinarians once a month. To our knowledge none of the animals in this study presented symptomatic gastrointestinal diseases or diarrhea.

Sample Collection

A total of 231 fresh fecal samples have been collected from 38 vertebrate species between July 2016 and March 2019 (**Supplementary Table S1**). One hundred and eighteen samples were from a previous collection (Accession numbers of *Blastocystis* positive samples: MF186640-MF186709; Betts et al., 2018) and the rest were newly collected. Sixty-seven of these samples were from nine vertebrate species collected from Howletts Zoo between November 2017 and February 2019 and the remaining samples were collected form 31 species at Wildwood. Samples from gray wolf (*Canis lupus*) and European bison (*Bison bonasus*) were collected from both zoos. Sampling covered a total of 33 mammalian species, four bird species and one reptile (**Supplementary Table S1**). In both zoos, a minimum of one fecal sample was collected from each enclosure. In enclosures where more than one animal resided, between two and five samples were collected, each of which was considered as individual sample. For some water voles (*Arvicola amphibious*), a number of repeat collections were carried out over the course of 12 months (**Supplementary Table S1**). Fresh fecal samples were collected in the morning either before or shortly after enclosures were cleaned. For some animals, including avian species and the reptile; where age of fecal sample is difficult to determine, multiple samples were collected. Zookeepers supervised all collections.

Once collected, fecal samples were stored at 4°C in sterile falcon tubes within 1 h of collection until DNA extraction. In some instances, heat fixed slides were prepared. Within an hour of sampling, a small amount of fecal sample from the water voles and other randomly selected animals were separately inoculated in four sterile falcon tubes containing the following media: two tubes containing modified LYSGM [16 · 07 mM potassium

phosphate dibasic, 2 · 94 mM potassium phosphate monobasic, 128 · 34 mM sodium chloride, 2 · 5 g L^{-1} yeast extract, 0 · 5 g L^{-1} liver extract, 5% adult bovine (Sigma)/horse serum (Gibco); modified TYSGM-9, without mucin (Diamond, 1982)[1]], two tubes of TYM (22 · 2 g L^{-1} trypticase peptone, 11 · 1 g L^{-1} yeast extract, 16 · 23 mM maltose, 9 · 17 mML-cysteine, 1 · 26 mM L-ascorbic acid, 5 · 1 mM potassium phosphate dibasic, 6 · 53 mM potassium phosphate monobasic) (Diamond, 1957, 1983) enriched with 5% fetal bovine serum (FBS; Sigma) and 2 tubes with 0 · 5% Liver Digest (LD) medium (0 · 5 g L^{-1} Oxoid liver extract). The tubes were incubated at 35°C. samples were examined for *Blastocystis* under the microscope every 3–5 days. After initially leaving the cultures for 2 weeks, they were subcultured every 10 days.

DNA Extraction, Amplification of Target Gene and Molecular Characterization

Genomic DNA was extracted directly from a minimum of 250 mg of fresh fecal sample or culture pellet using the Microbiome DNA Purification Kit Purelink (Fisher, United Kingdom) to the manufacturer's instructions. DNA was eluted in 100 µl elution buffer and aliquotted. The working stock was stored at −20°C, while the rest was placed at −80°C for long-term storage. Extracted DNA was used for the polymerase chain reaction (PCR) with specific primers targeting regions of interest (**Supplementary Table S2**). PCR was carried out using the 2X PCRBIO Taq DNA Polymerase (PCRBIOSYSTEMS). Reagents per 25 µl reaction were as follows: PCRBIO Taq mix, 0.4 µM forward primer, 0.4 µM reverse primer, 19 µl nuclease free water and 2 µl DNA (ranging in concentration 10–50 ng/µl). Details of amplification conditions for all species in this study are provided in **Table 1**.

Fragments amplified to the correct size were excised and extracted using the Thermo Scientific GeneJET Gel Extraction Kit (following manufacturer's instructions) purified gel extracts were eluted in 30–50 µl of elution buffer. If PCR reactions were left for 7 days before ligation, a polyadenylation reaction was carried out with the following protocol: per reaction 0.25 µl GoTaq DNA Polymerase (Promega), 7 µl Gel extraction, 2 µl 5X GoTaq Buffer (Promega), 0.5 mM MgCl2, 2.5 mM dATP (Promega) and 0.3 µl nuclease water at 72°C for 30 min. 1.5 µl of polyadenylation product or gel extract was cloned using the pGEM-T easy vector system I (Promega) following manufacturer's protocol. Between 3 and 10 colonies per transformation were grown in 5 ml overnight cultures. Plasmid DNA was extracted using the GeneJET Plasmid Miniprep Kit (following manufacturer's instructions). Before sequencing, a restriction digest using *Eco*RI (Promega) was carried out to confirm fragment insertion, per 10 µl reaction, 0.25 µl *Eco*RI, 5 µl miniprep elution, 1 µl 10X buffer H and 3.75 µl dH20 was incubated at 37°C for 2 h and visualized on a 1.5% agarose gel. Positive samples were sequenced using both the T7 or SP6 universal primers by Eurofins, United Kingdom.

Phylogenetic Analysis

Raw reads were trimmed to remove remaining vector fragments and unambiguous bases at the ends of the reads. BLAST search using the newly obtained sequences against the non-redundant (nr) database was used to identify sequence positive clones. A dataset was assembled including all new sequences in addition to reference sequences encompassing the breadth of diversity of *Blastocystis* and an alignment was carried out using MAFFT v.7 (Katoh and Toh, 2010). Alignment contained four outgroup taxa for a total of 171 taxa. After aligning with MAFFT, ambiguous positions were masked with trimAl (Capella-Gutierrez et al., 2009). Following trimming, the alignment contained 1326 positions. A maximum likelihood tree was constructed using the RAxML software version 8 (Stamatakis, 2014, 2015) on the online platform CIPRES (Miller et al., 2010).[2] For each dataset bootstrap support was calculated from 1000 replicates.

[1]http://entamoeba.lshtm.ac.uk/xenic.htm

[2]http://www.phylo.org/

TABLE 1 | Summary of amplification conditions from this study.

Target Organism	Primer Pair	Primer Type	Initial Denaturation Conditions		Denaturation Conditions		Annealing Conditions		Extension Conditions		Cycle Number	Final Extension Conditions	
			Temp °C	Time min/s	Temp °C	Time min/s	Temp °C	Time min/s	Temp °C	Time min/s		Temp °C	Time min/s
Blastocystis	RD3/RD5	External	95	5 min	95	30 s	55	30 s	72	1 min 40 s	35	72	5 min
Blastocystis	RD5F/BhRDr	Internal	95	5 min	95	30 s	55	30 s	72	1 min 40 s	35	72	5 min
Cryptosporidium	CRY F1/CRY R1	External	94	2 min	94	50 s	53	50 s	72	1 min	24	72	10 min
Cryptosporidium	CRY F2/CRY R2	Internal	94	2 min	94	50	56	30 s	72	1 min	30	72	10 min
Giardia	RH11/RH4	-	96	2 min	96	45 s	58	30 s	72	45 s	30	72	4 min
Eimeria	EIF1/EIR3	External	94	5 min	94	30 s	57	30 s	72	2 mins	30	72	10 min
Eimeria	EIF3/EIR3	Internal	94	3 min	94	30 s	60	30 s	72	1 min 30 s	40	72	7 min
Entamoeba	542/543	-	94	5 min	94	30 s	55	30 s	72	30 s	35	72	2 min

RESULTS

Culturing

Blastocystis was cultured in tubes containing both types of media. Isolates from fox, lynx, wallaby, elk and otter grew at 35°C, while the ones from water voles grew at room temperature (**Supplementary Figure S1**). We were unable to establish cultures from other hosts.

Screening of Fecal Samples

Building upon sampling from a previous study, a total of 231 fecal samples from 38 vertebrate species were examined. It should be noted that the percent positive percentages herein are the minimum since PCR amplification rather than qPCR was used. *Blastocystis* was detected in 18/38 species (47%). A total of 255 clones were sequence positive for *Blastocystis*; 184 of these clones were from the current study. Of the 12-carnivorous species only three (pine marten, lynx and Scottish wild cat) were sequence positive for *Blastocystis* (25%, **Table 2**). There were no sequence positives for badger, European brown bear, otter, polecat, red and arctic foxes, stoat, gray and Iberian wolves, despite having multiple samples from different time points from these species. For non-carnivorous species, 15/26 (58%) were sequence positive, while barnacle and pink footed geese, four lined snake, hedgehog, water shrew, raven, red billed chough, black and brown rats, pied tamarind and black rhinoceros were negative (**Table 2**). *Blastocystis* was found in all artiodactyl species examined, but not all fecal samples were sequence positive. Sequence positive results for samples were as follows: Carnivora 3/50 (6%); Artiodactyla 20/36 (56%); Anseriformes 0/2 (0%); Squamata 0/1 (0%); Eulopotyphia 0/0 (0%); Passeriformes 0/4 (0%); Rodentia 29/81 (36%); Diprotodontia 2/5 (40%); Primates 27/43 (63%); Perissodactyla 0/0 (0%).

Regarding subtypes from cultures, we only looked at water voles as their cultures were numerous. We found only ST1 and ST4, while the rest of the STs found in the faces were not recovered.

Diversity and Distribution of Subtypes

In total, 10 known subtypes were detected: ST1, ST2, ST3, ST4, ST5, ST8, ST10, ST13, ST14, and ST15 (**Table 3**). Of those, ST2, ST3, ST8 and ST15 were not found in our previous collection. Subtype 4 was the most commonly isolated, found in 83/255 (33%) clones across 11 species. This was followed by ST2, isolated from 80/255 samples (31%); ST10 27/255 (11%); ST1 26/255 (10%); ST14 17/255 (7%); ST5 13/255 (5%); ST3 and ST15 4/255 (2%); ST13 1/255 (0.4%). Three sequences grouped with the *B. lapemi* clade.

All artiodactyls, except for the European Bison (*Bison bonasus*) housed at Howletts, had at least one positive ST identification. The subtypes found in this group coincided with published data with most isolates belonging to ST5, ST10 and ST14. ST5 was present in 6/36 (17%) samples; ST10 in 10/36 (28%) samples; ST14 in 7/36 (19%); ST4 in 2/36 (6%) samples; ST1 and ST13 both 1/36 (3%). 5/36 samples exhibited co-occurrence with two or more STs. The bongo calf (*Tragelaphus eurycerus*) –shared the same STs (10 and 14) with its mother as opposed to the father, who is housed separately and in whom we only detected ST14.

Eighty-one samples from four species belonging to the order Rodentia are presented in this study. Brown rat (*Rattus norvegicus*) and black rat (*Rattus rattus*) yielded no *Blastocystis* positive isolates. ST2 and ST4 were detected in three samples were from Red squirrel (*Sciurus vulgaris*). Water vole (*Arvicola amphibious*) samples accounted for a total of 26/81 (32%) positive *Blastocystis* samples and 88 positive clones. a total of 74 water vole samples have been taken to date, 26/74 (35%) are sequence positive for one or more STs. The large sample number is due to the sizable cohort in the study, which included repeat sampling over an extended period of time. Three groups of water vole were sampled: captive voles from Wildwood (22 samples) and wild caught voles from two areas in Essex, United Kingdom; Tilbury (17 samples) and Bulphan (35 samples). The wild caught voles were routinely screened over the course of 10–12 months. Amongst sequence positive samples the captive voles had a total of 30 positive clones obtained from 9/22 (41%) positive samples; Tilbury voles had 28 positive clones from 5/17 (29%) samples, while Bulphan voles yielded 29 clones from 11/35 (31%) positive samples. ST4 was the most commonly identified across both captive and wild voles, representing 76/88 (86%) of the clones and 23/26 (88%) samples. ST1, ST15 and a subtype placing with *B. lapemi* were all identified in two samples, ST1 and *B. lapemi* clade ST were isolated in captive voles, whereas ST15 was found in one wild vole across repeat sample time points. ST10 and ST14 were identified in one sample each from captive voles. Co-occurrence of two or more STs was identified in four voles, all of which were captive. ST4 was present in all of these co-occurrence instances along with ST1, ST10, ST14, and *B. lapemi* clade ST.

A total of 43 non-human primate (NHP) samples were collected from Howletts zoo as follows: 25 gorillas (*Gorilla gorilla gorilla*) samples from four family groups ranging in size (G1, G3 G4 and G5) and one individual were collected across two collection times, 13 Javan gibbon (*Hylobates moloch*) samples from individuals across seven groups ranging in size (A-G) and five pied tamarin (*Saguinus bicolor*) samples from group enclosures. Of these samples, 16/25 gorillas (64%); 11/13 (85%) Javan gibbons were sequence positive for at least one ST, while no *Blastocystis* was detected in any of the pied tamarins (**Table 4**). In terms of clones, for the gorillas, 64 positive clones were sequenced, of which 45/64 (70%) were ST2; 9/64 (14%) ST1; 8/64 (13%) ST3; and 2/64 (3%) were ST5. There were no notable differences observed among family groups. Specifically, all family groups had a relatively high incidence of ST2, while ST5 was only reported from family group 5. Co-colonization with two STs was seen in four of the gorilla samples (**Table 4**). The Javan gibbons represent one of the highest proportions of sequence positive clones for *Blastocystis* STs, from the 11 positive samples, 45 clones were sequenced. ST1 represented 18/45 (40%) of these clones; ST2 17/45 (38%); ST3 and ST5 both 4/45 (9%); ST8 1/45 (2%); ST15 1/45 (2%). Of the gibbon groups, Group F was the only one to not have any sequence positive data across two sample collections. Of all the groups, Group G was only sampled from once as its members were released to the wild between collections. Differences were observed among groups between the sample

TABLE 2 | Prevalence of *Blastocystis*, *Giardia*, *Cryptosporidium*, *Entamoeba,* and *Eimeria* in study animals.

Host	Scientific Name	Location	No. faecal samples collected	*Blastocystis* No. positive (% Positive)	*Giardia* No. Positive (% Positive)	*Cryptosporidium* No. Positive (% Positive)	*Entamoeba* No. Positive (% Positive)	*Eimeria* No. Positive (% Positive)
Carnivora (*T* = 50)								
Badger	*Meles meles*	Wildwood	2	0 (0)	0 (0)	0 (0)	0 (0)	1 (50)
European Brown Bear	*Ursus arctos arctos*	Wildwood	4	0 (0)	0 (0)	0 (0)	0 (0)	0 (0)
Lynx	*Lynx lynx*	Wildwood	5	2 (40)	0 (0)	0 (0)	0 (0)	0 (0)
Otter	*Lutra lutra*	Wildwood	7	0 (0)	0 (0)	0 (0)	0 (0)	0 (0)
Pine Marten	*Martes martes*	Wildwood	2	1 (50)	0 (0)	0 (0)	0 (0)	0 (0)
Polecat	*Mustela putarius*	Wildwood	1	0 (0)	0 (0)	0 (0)	0 (0)	0 (0)
Red Fox	*Vulpes vulpes*	Wildwood	3	0 (0)	0 (0)	0 (0)	0 (0)	0 (0)
Arctic Fox	*Vulpes lagopus*	Wildwood	2	0 (0)	0 (0)	0 (0)	0 (0)	0 (0)
Scottish Wild Cat	*Felis silvestris*	Wildwood	13	1 (8)	0 (0)	0 (0)	0 (0)	0 (0)
Stoat	*Mustela ermine*	Wildwood	3	0 (0)	0 (0)	0 (0)	0 (0)	0 (0)
Gray Wolf	*Canis lupus*	Howletts	3	0 (0)	0 (0)	0 (0)	0 (0)	1 (33)
Gray Wolf	*Canis lupus*	Wildwood	2	0 (0)	0 (0)	1 (50)	0 (0)	0 (0)
Iberian Wolf	*Canis lupus signatus*	Howletts	3	0 (0)	0 (0)	0 (0)	0 (0)	1 (33)
Anseriformes (*T* = 2)								
Barnacle Goose	*Branta leucopsis*	Wildwood	1	0 (0)	0 (0)	0 (0)	0 (0)	0 (0)
Pink Footed Goose	*Anser brachyrhynchus*	Wildwood	1	0 (0)	0 (0)	0 (0)	0 (0)	1 (100)
Artiodactyla (*T* = 36)								
Muntjac	*Muntiacus reevesi*	Wildwood	1	1 (100)	0 (0)	0 (0)	0 (0)	0 (0)
European Bison	*Bison bonasus*	Wildwood	5	3 (60)	0 (0)	0 (0)	2 (40)	1 (20)
European Bison	*Bison bonasus*	Howletts	4	0 (0)	0 (0)	0 (0)	2 (50)	2 (50)
Eurasian Elk	*Alces alces*	Wildwood	3	1 (33)	0 (0)	0 (0)	0 (0)	0 (0)
Pygmy Goat	*Capra aegagrus hircus*	Wildwood	2	2 (100)	0 (0)	0 (0)	2 (100)	0 (0)
Red Deer	*Cervus elaphus*	Wildwood	3	1 (33)	0 (0)	0 (0)	1 (33)	0 (0)
Reindeer	*Rangifer tarandus*	Wildwood	1	1 (100)	0 (0)	0 (0)	1 (100)	1 (100)
Soay Sheep	*Ovis aries*	Wildwood	1	1 (100)	0 (0)	0 (0)	1 (100)	0 (0)
Wild Boar	*Sus scrofa*	Wildwood	4	2 (50)	0 (0)	0 (0)	1 (25)	0 (0)
Red River Hog	*Potamochoerus porcus*	Howletts	6	3 (50)	0 (0)	1 (17)	1 (17)	0 (0)
Bongo	*Tragelaphus eurycerus*	Howletts	6	1 (17)	0 (0)	0 (0)	2 (33)	1 (17)
Squamata (*T* = 1)								
Four-lined Snake	*Elaphe quatuorlineata*	Wildwood	1	0 (0)	0 (0)	0 (0)	0 (0)	0 (0)
Eulopotyphla (*T* = 7)								
Hedgehog	*Erinaceus quatuorlineata*	Wildwood	1	0 (0)	0 (0)	0 (0)	0 (0)	0 (0)
Water Shrew	*Neomys fodiens*	Wildwood	6	0 (0)	0 (0)	0 (0)	1 (17)	0 (0)
Passeriformes (*T* = 4)								
Raven	*Corvus corax*	Wildwood	3	0 (0)	0 (0)	0 (0)	0 (0)	0 (0)
Red Billed Chough	*Pyrrhocorax pyrrhocorax*	Wildwood	1	0 (0)	0 (0)	0 (0)	0 (0)	0 (0)

(Continued)

TABLE 2 | Continued

Host	Scientific Name	Location	No. faecal samples collected	*Blastocystis* No. positive (% Positive)	*Giardia* No. Positive (% Positive)	*Cryptosporidium* No. Positive (% Positive)	*Entamoeba* No. Positive (% Positive)	*Eimeria* No. Positive (% Positive)
Rodentia (*T* = 81)								
Black Rat	*Rattus rattus*	Wildwood	1	0 (0)	0 (0)	0 (0)	0 (0)	0 (0)
Brown Rat	*Rattus norvegicus*	Wildwood	1	0 (0)	0 (0)	0 (0)	0 (0)	0 (0)
Red Squirrel	*Sciurus vulgaris*	Wildwood	5	3 (60)	0 (0)	0 (0)	0 (0)	0 (0)
Water Vole	*Arvicola amphibious*	Wildwood	22	10 (45)	4 (18)	15 (68)	0 (0)	0 (0)
Water Vole	*Arvicola amphibious*	Tilbury	17	5 (29)	7 (41)	2 (12)	1 (6)	1 (6)
Water Vole	*Arvicola amphibious*	Bulphan	35	12 (34)	17 (49)	4 (11)	2 (6)	4 (11)
Diprotodontia (*T* = 5)								
Wallaby	*Macropus rufogriseus*	Wildwood	5	2 (40)	0 (0)	0 (0)	0 (0)	0 (0)
Primates (*T* = 43)								
Western Lowland Gorilla	*Gorilla gorilla gorilla*	Howletts	25	16 (64)	0 (0)	1 (4)	2 (8)	2 (8)
Javan Gibbon	*Hylobates moloch*	Howletts	13	11 (85)	1 (8)	6 (46)	1 (8)	0 (0)
Pied Tamarin	*Saguinus bicolor*	Howletts	5	0 (0)	0 (0)	0 (0)	0 (0)	0 (0)
Perissodactyla (*T* = 2)								
Black Rhinoceros	*Diceros bicornis*	Howletts	2	0 (0)	0 (0)	0 (0)	0 (0)	0 (0)

collections. For example, ST5 and ST15 were detected in Group B upon first collection, yet in the second ST1 and ST2 were found.

In general, differences in ST distribution and prevalence are seen between the two zoos, the most obvious attribute to this is the differences in sampled taxa. Samples from Wildwood were comprised largely of members from the orders Rodentia, Artiodactyla and Carnivora, with Water voles and Scottish wild cats being sampled several times. Samples from Howletts were mainly from NHPs and other members of the Artiodactyla. The European bison and gray wolf were the only species sampled across both parks. Notably, *Blastocystis* was not isolated from any wolf or bison samples from Howletts, even though the bison housed at Wildwood and Howletts are related. The differences in ST distribution among the parks reflect the taxa housed within. Wildwood comprises largely of ST4 and ST10, STs commonly associated with rodents and hooved animals, whereas ST2, ST1 and ST5 are isolated on Howletts and are commonly associated with NHPs.

In total, 25 of the *Blastocystis* positive samples harbored more than one subtype; specifically, two subtypes were detected in 22 samples, three subtypes in two samples, while one sample contained four subtypes.

Newly generated sequences have been submitted to GenBank (MN526748- MN526930).

Co-occurrence of *Blastocystis* and Other Protists

Fecal samples were screened for *Cryptosporidium*, *Eimeria*, *Entamoeba*, *Giardia* and *Isospora*. Of the 81 *Blastocystis* positive samples, 43 (53%) harbored at least one of the above-mentioned protists in addition to *Blastocystis* (**Table 5**). Of those, 35 samples had one additional protist as follows: 14 cases from samples of Rodentia (all water voles), 13 from Artiodactyla (three from European bisons, three from bongos, two from Red river hogs, two from pygmy goats, one from wild boar, one from soay sheep, and one from red deer) and eight from NHPs (four from gorillas and three from Javan gibbons). Seven samples carried *Blastocystis* and two other protists: four Rodentia (all from water voles), two NHPs (both from Javan gibbons), and one from Artiodactyla (reindeer). A single sample from water vole was found with three other protists. The widest range of host species where co-occurrence was noted in the Artiodactyla. *Cryptosporidium* was detected in 31 (13%) samples and co-occurred with *Blastocystis* in 19 cases (61%); 22 (9%) samples were positive *Entamoeba*, 14 of which (64%) were found with *Blastocystis*; 29 (12%) samples harbored *Giardia* which co-occurred with *Blastocystis* in 10 cases (35%); 17 (7%) samples were positive for *Eimeria*, while nine were found with *Blastocystis*. Of the three (1%) *Isospora* positive samples, none co-occurred with *Blastocystis*.

Phylogenetic Analysis

All *Blastocystis* sequences grouped together with maximum support (100BS) (**Figure 1**). Newly acquired sequences belong to ST1, ST2, ST3, ST4, ST5, ST8, ST10, ST14, ST15, and the *B. lapemi* clade. In agreement with previous studies, ST15, ST16 and ST17 along with sequences originating from ectotherms placed in the

TABLE 3 | *Blastocystis* subtypes and co-occurrence with other microbial eukaryotes.

Host	Location	No. sequence positive clones	*Blastocystis* ST										Co-occurrence with other protists
			ST1	ST2	ST3	ST4	ST5	ST8	ST10	ST13	ST14	ST15	ST?	
Carnivora														
Pine Marten	Wildwood	1	–	–	–	1/1	–	–	–	–	–	–		–
Lynx	Wildwood	2	–	1/2	–	–	–	–	–	–	1/2	–		–
Scottish Wild Cat	Wildwood	2	–	–	–	1/2	–	–	–	–	1/2			–
Artiodactyla														
Muntjac	Wildwood	1	–	–	–	–	–	–	–	1/1	–	–		–
European Bison	Wildwood	11	–	–	–	–	–	–	11/11		–	–		*Entamoeba, Eimeria*
Eurasian Elk	Wildwood	6	–	–	–	1/6	–	–	1/6	–	4/6	–		–
Pygmy Goat	Wildwood	3	1/3	–	–	–	–	–	1/3	–	1/3	–		*Entamoeba*
Red Deer	Wildwood	8	–	–	–	3/8	–	–	5/8	–	–	–		*Entamoeba*
Reindeer	Wildwood	1	–	–	–	–	–	–	1/1	–	–	–		*Entamoeba, Eimeria*
Soay Sheep	Wildwood	1	–	–	–	–	–	–	–	–	1/1	–		*Entamoeba*
Wild Boar	Wildwood	2	–	–	–	–	2/2	–	–	–	–	–		*Entamoeba*
Red River Hog	Howletts	5	–	–	–	–	5/5	–	–	–	–	–		*Cryptosporidium, Entamoeba*
Bongo	Howletts	10	–	–	–	–	–	–	5/10	–	5/10	–		*Entamoeba, Eimeria*
Rodentia														
Red Squirrel	Wildwood	4	–	3/4	–	1/4	–	–	–	–	–	–		–
Water Vole	Wildwood	30	3/30	–	–	24/30	–		1/30		–	–	2/30	*Cryptosporidium, Giardia*
Water Vole	Tilbury	28	–	–	–	25/28	–	–	–	–	–	3/28		*Cryptosporidium, Entamoeba, Giardia, Eimeria*
Water Vole	Bulphan	29	–	–	–	29/29	–	–	–	–	–	–		*Cryptosporidium, Entamoeba, Giardia, Eimeria*
Diprotodontia														
Wallaby	Wildwood	2	–	–	–	–	–	–	2/2	–	–	–		–
Primates														
Western Lowland Gorilla	Howletts	64	9/64	45/64	8/64	–	2/64	–	–	–	–	–		*Cryptosporidium, Entamoeba, Eimeria*
Javan Gibbon	Howletts	45	18/45	17/45	4/45	–	4/45	1/45	–	–	–	1/45		*Cryptosporidium, Giardia, Entamoeba*

most basal positions (Alfellani et al., 2013; Yowang et al., 2018). Subtypes 3, 4, 8, and 10 grouped together, while subtypes 7, 9 and 6 formed a clade. Two of the water vole sequences grouped within the clade formed by *B. lapemi* and *B. pythoni*. Subtypes 1, 2 and 11 grouped together and sister to the clade formed by subtypes 5, 12, 13, and 14.

DISCUSSION

Animals from 38 species from two animal parks in the United Kingdom were sampled over a period of 3 years. Eighty-two samples from 47% of all animal species were sequence positive for *Blastocystis*. Of those 82, (21/82) 26% were found to harbor more than one ST, while 53% also harbored other protists. *Blastocystis* was present in animals from both parks. As expected, ST4 was dominant in rodents, whereas ST10 and ST14 dominated in artiodactyls. In primates, ST1 and ST2 were dominant. We reported *Blastocystis* presence in the Lynx and the Scottish wild cat for the first time. Both of these animals are carnivorous. Our study confirms previous findings on reduced presence and often absence of *Blastocystis* in carnivores and high prevalence in artiodactyls (Alfellani et al., 2013; Cian et al., 2017, Zhao et al., 2017). It is well known that dietary, behavioral and environmental factors shape bacterial communities, though this has yet to be shown for microbial eukaryotes. In that vein, a possible explanation for the above observation could be that captive carnivores consume a diet consisting of almost exclusively refrigerated meat, which is devoid of other eukaryotes. This considerably reduces contamination. Nonetheless, a recent study on free-living carnivorous animals confirmed presence of *Blastocystis* in only 1.6% of hosts (Calero-Bernal et al., 2019), suggesting that additional factors might account for the low prevalence. Artiodactyls are herbivorous animals that consume exclusively fiber, while carnivores consume only animal protein. Thus the two also differ considerably in the overall

TABLE 4 | *Blastocystis* subtyping in captive Javan gibbons (*Hylobates moloch*) and West Lowland gorillas (*Gorilla gorilla gorilla*) from two sample collections with co-occurrence of other protists within sampled groups.

Host	Collection Number	Family Group	No. Positive Sequences	*Blastocystis* ST						Co-occurrence with other protists
				ST1	ST2	ST3	ST5	ST8	ST15	
Javan Gibbon A	1	A	6	3			2	1		*Cryptosporidium*
Javan Gibbon B	1	B	3				2		1	–
Javan Gibbon C	1	C	3	2	1					–
Javan Gibbon D	1	D	3		3					*Giardia*
Javan Gibbon E	1	E	3		3					–
Javan Gibbon F	1	F	0							–
Javan Gibbon G	1	G	3		3					*Cryptosporidium*
Javan Gibbon A	2	A	4	1		3				–
Javan Gibbon B	2	B	2	1	1					*Cryptosporidium, Entamoeba*
Javan Gibbon C	2	C	12	11	1					–
Javan Gibbon D	2	D	2			2				–
Javan Gibbon E	2	E	4		4					–
Javan Gibbon F	2	F	0							–
Javan Gibbon G	2	G	0							N/A

Host	Collection Number	Family Group	No. Positive Sequences	*Blastocystis* ST				Co-occurrence with other protists
				ST1	ST2	ST3	ST5	
West Lowland Gorilla 1	1	5	4		4			*Entamoeba*
West Lowland Gorilla 2	1	5	5		5			*Eimeria*
West Lowland Gorilla 3	1	4	6		6			–
West Lowland Gorilla 4	1	4	5		5			–
West Lowland Gorilla 5	1	3	4			4		–
West Lowland Gorilla 6	1	3	6		6			–
West Lowland Gorilla 7	1	3	6		5	1		–
West Lowland Gorilla 8	1	3	4		4			–
West Lowland Gorilla 9	1	3	1	1				–
West Lowland Gorilla 10	1	3	3	3				–
West Lowland Gorilla 1	2	1	2	2				–
West Lowland Gorilla 8	2	3	5		4	1		*Cryptosporidium*
West Lowland Gorilla 4	2	3	4		2	2		*Eimeria*
West Lowland Gorilla 10	2	4	3		3			–
West Lowland Gorilla 11	2	5	3	3				–
West Lowland Gorilla 12	2	5	3		1		2	–

structure and physiology of their respective gastrointestinal tracts. Both diet and physiology likely contribute to microbiota composition, and as a result, the microbial communities of artiodactyls and carnivores differ considerably (Sanders et al., 2015; Nishida and Ochman, 2018). In general, herbivores, to which artiodactyls belong, harbor high microbial diversity, while carnivores encompass the least diverse microbial communities amongst mammals (Nishida and Ochman, 2018). High microbial diversity and specific microbial profiles are linked to presence of *Blastocystis* in human studies though a causative link has yet to be established (Andersen et al., 2015; Audebert et al., 2016; Iebba et al., 2016; O'Brien Andersen et al., 2016; Beghini et al., 2017; Forsell et al., 2017; Nieves-Ramirez et al., 2018; Tito et al., 2019). A similar result has also been obtained from a study focusing on wild chimpanzees (Renelies-Hamilton et al., 2019). Given the high prevalence of *Blastocystis* in artiodactyls it would be interesting to explore whether such specific profiles exist in these animals as well.

As in our previous study (Betts et al., 2018), we identified multiple subtypes of *Blastocystis* in the same host. In addition to the elk, pygmy goat, red deer and water vole hosts bearing multiple subtypes, we add the Scottish wildcat (ST4 and ST14), bongo (ST10, ST14), and lynx (ST2, ST14). Previous reports also noticed presence of multiple STs in animals (Fayer et al., 2012; Badparva et al., 2015; AbuOdeh et al., 2016). Cian et al., documented several instances of mixed colonization of subtypes (11%), especially in primates and artiodactyls (Cian et al., 2017), while Wang et al., reported mixed colonization in 58% of a pig population (Wang et al., 2014). Collectively these data strengthen previously raised hypotheses that occurrence of multiple subtypes in animals is not unusual, but rather common (Fayer et al., 2012; Betts et al., 2018). Thus, a logical extension of this study would

TABLE 5 | Co-occurrence of *Blastocystis* with other microbial eukaryotes.

Sample	Order	Location	*Blastocystis* ST	*Cryptosporidium*	*Giardia*	*Eimeria*	*Entamoeba*	*Isospora*
Water Vole TB30.1	Rodentia	Tilbury	4	yes	yes	yes		
Javan Gibbon Group D	Primate	Howletts	2	yes	yes			
Water Vole R22	Rodentia	Wildwood	4	yes	yes			
Water Vole TB32.1	Rodentia	Tilbury	4	yes	yes			
Reindeer	Artiodactyla	Wildwood	10			yes	yes	
Water Vole TB29.1	Rodentia	Tilbury	15			yes	yes	
Javan Gibbon Group B	Primate	Howletts	1, 2	yes			yes	
Water Vole Q52	Rodentia	Wildwood	unknown	yes	yes			
Javan Gibbon Group G	Primate	Howletts	2	yes				
Western Lowland Gorilla 1 G5	Primate	Howletts	2				yes	
Western Lowland Gorilla 2 G5	Primate	Howletts	2			yes		
Water Vole C3	Rodentia	Wildwood	4	yes				
Water Vole C3	Rodentia	Wildwood	4	yes				
Water Vole C4	Rodentia	Wildwood	4	yes				
Water Vole C4	Rodentia	Wildwood	4	yes				
Water Vole PP01.2	Rodentia	Bulphan	4	yes				
Water Vole PP03.1	Rodentia	Bulphan	4		yes			
Water Vole PP03.2	Rodentia	Bulphan	4		yes			
Water Vole PP03.3	Rodentia	Bulphan	4		yes			
Water Vole PP03.4	Rodentia	Bulphan	4		yes			
Water Vole PP04.1	Rodentia	Bulphan	4		yes			
Water Vole PP05.2	Rodentia	Bulphan	4			yes		
Water Vole PP05.3	Rodentia	Bulphan	4			yes		
Red River Hog 2	Artiodactyla	Howletts	5	yes				
Red River Hog 3	Artiodactyla	Howletts	5				yes	
Wild Boar 1	Artiodactyla	Wildwood	5				yes	
European Bison 1	Artiodactyla	Wildwood	10				yes	
European Bison 1	Artiodactyla	Wildwood	10			yes		
European Bison 2	Artiodactyla	Wildwood	10				yes	
Bongo M	Artiodactyla	Howletts	14				yes	
Pygmy Goat 1	Artiodactyla	Wildwood	14				yes	
Soay Sheep	Artiodactyla	Wildwood	14				yes	
Water Vole TB29.2	Rodentia	Tilbury	15		yes			
Pygmy Goat 2	Artiodactyla	Wildwood	1, 10				yes	
Javan Gibbon Group C	Primate	Howletts	1, 2	yes				
Water Vole R12	Rodentia	Wildwood	1, 4	yes				
Javan Gibbon Group A	Primate	Howletts	1, 5, 8	yes				
Bongo Calf	Artiodactyla	Howletts	10 14				yes	
Bongo F	Artiodactyla	Howletts	10, 14			yes		
Western Lowland Gorilla 8 G3	Primate	Howletts	2, 3	yes				
Western Lowland Gorilla 4 G3	Primate	Howletts	2,3			yes		
Red Deer 1	Artiodactyla	Wildwood	4, 10				yes	
Water Vole Q99	Rodentia	Wildwood	4, unknown	yes				
Javan Gibbon Group B	Primate	Howletts	5, 15	yes				

be to disentangle whether co-occurring subtypes occupy distinct functional niches in the complex gut ecosystem, a direction that has also been suggested by Beghini et al. (2017).

Co-occurrence of *Blastocystis* with *Entamoeba*, *Giardia*, *Cryptosporidium* and *Eimeria* in multiple animal species across the two parks was also examined. Most previous studies have either looked for multiple parasites from single animal species or have targeted one microbial eukaryote in various hosts (Fayer et al., 2012; Parsons et al., 2015; Enriquez et al., 2016, 2019; Jacob et al., 2016). Herein, *Blastocystis* did not co-occur with other protists in any of the carnivores, even though we did observe co-occurrence of *Cryptosporidium* and *Eimeria* in gray and Iberian wolves. The case of artiodactyls is particularly notable. Eight out of ten artiodactyls that were *Blastocystis* positives co-occurred with an *Entamoeba* species. Out of these, three co-occurred with *Blastocystis*, *Entamoeba* and

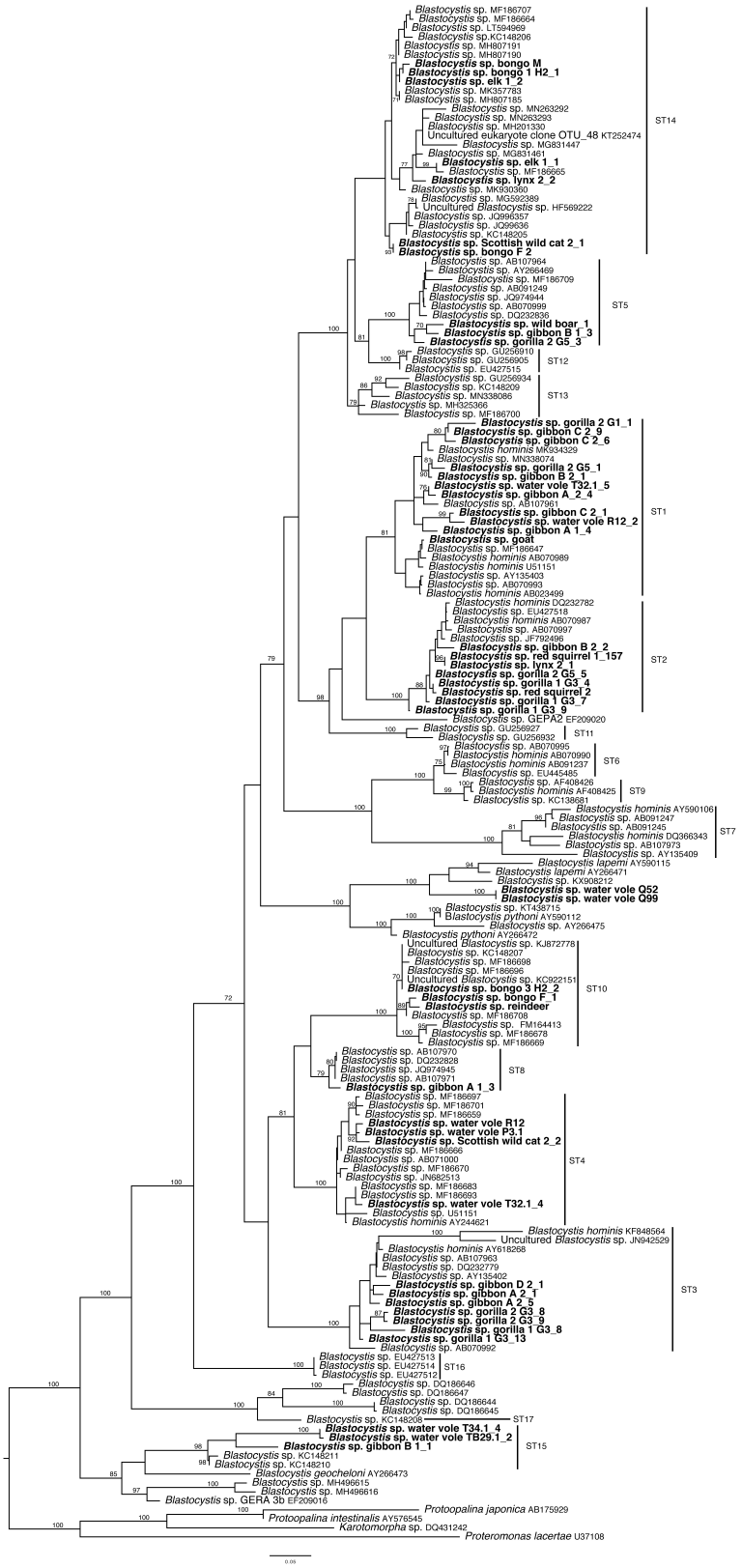

FIGURE 1 | Maximum likelihood phylogenetic tree inferred from 171 sequences and 1326 sites using RAxML v. 8. New sequences are in bold lettering. Numerical values indicate bootstrap support values and only those of over 70 are shown.

Eimeria (European bison, reindeer, bongo), while one animal had *Blastocystis*, *Entamoeba* and *Cryptosporidium* (red river hog). Significantly, none of the animals exhibited diarrheal episodes or other obvious gastrointestinal symptoms as confirmed by zookeepers and licensed veterinarians. Typically, microbial eukaryotes in animals are identified and reported upon onset of gastrointestinal symptoms. Herein, we sampled and detected gut protists before presentation of symptoms, though the possibility that some of the animals might have had symptoms before they were brought into the parks cannot be excluded. Asymptomatic carriage of a single or multiple protists in animals is not uncommon and the concern of zoonotic transmission has often been articulated (Fayer et al., 2012; Cian et al., 2017; Desoubeaux et al., 2018; Udonsom et al., 2018; Wang et al., 2018a; Enriquez et al., 2019). In case of zoonosis, detecting the reservoir is difficult as there is no reason to check the original host for presence of pathogens. The level and type of interaction among *Blastocystis*, other microbial eukaryotes (including fungi) and the rest of the host microbiome is unclear. Future animal studies should focus on exploring the eukaryotic component of the gut microbiome rather than targeting individual microbial species, in order to shed light on the role of eukaryome as a whole in the gut ecosystem. Combination of *in vitro* and *in vivo* targeted metagenomics and metabolomics approaches along with network analysis will greatly increase our understanding of these issues.

The case of *Blastocystis* is of interest. In the past, co-occurrence of *Blastocystis* with pathogens in stool samples of humans with gastrointestinal symptoms was likely one of the reasons for its controversial pathogenicity. Since adaptation of the subtyping system, the argument has been framed around specific subtypes or strains being pathogenic. Nonetheless, in a rather anthropocentric approach, assessment of the pathogenic potential of *Blastocystis* has focused primarily on humans and the "human" subtypes ST1 to ST9, while non-human metazoans and the rest of the subtypes have been largely overlooked. Moreover, the health status of animal subjects in many studies is not reported. When animals happen to have diarrhea the subtype present in these animals is often not mentioned, rather percent overall occurrence of individual subtypes is emphasized. Consequently, *Blastocystis* pathogenicity in animals is not well understood. It would be interesting to see whether any of the animals sampled herein will present any symptoms in the future. To that end, we have communicated with the zoo stuff to inform us in case symptoms develop in any of these animals.

To determine to which subtype the new sequences belonged, phylogenetic analysis was performed. Two of the newly generated sequences, both of which come from water voles, did not group with any of the known subtypes, but as sister to *Blastocystis lapemi*. There are two sequences designated as *B. lapemi* in the database, both of which originated from sea snakes (Yoshikawa et al., 2004; Noel et al., 2005). A third sequence that also groups within the clade and is genetically distinct comes from a monitor lizard. Therefore, either *B. lapemi* is not limited to sea snakes or all these sequences represent different species. In the absence of a culture and a full SSU rRNA sequence we designate those three sequences as *Blastocystis* sp. Four sequences – one coming from gibbon and three from water voles – group with ST15. Water vole is a newly reported host for ST15. Previously, Betts et al. (2018) had reported a potentially novel subtype, but had refrained from establishing it as such since the whole sequence was not available. Since then, several studies focusing on animals have contributed significantly toward populating previously isolate-sparse subtypes. As a result, the phylogenetic landscape of *Blastocystis* is changing. Expanded taxon sampling including several additional ST14 isolates from the database and from the current study has shown that ST14 is now divided into three distinct subclades, with new isolates populating all three. The previously suspected novel sequence (Betts et al., 2018) groups in one of the three. Thus, either ST14 has high intra-subtype divergence or it must be separated to at least two maybe even three subtypes. Nonetheless several subtypes harbor a high degree of genetic diversity except for ST4, which is the least genetically diverse (Stensvold and Clark, 2016b; Beghini et al., 2017). Given the variable degree of intra-subtype diversity, caution should be taken when establishing new subtypes. Genetic diversity within subtypes should be properly assessed. Commonly, closely related sequences from specific subtypes are included in the analysis, while more divergent representatives are not, leading to establishment of erroneous STs. Finally, the whole SSU rRNA region should be sequenced and phylogenies should include the breadth of *Blastocystis* diversity. Consistent approaches to subtyping *Blastocystis* will further elucidate the variety of subtypes that exist and their associations with specific hosts (El Safadi et al., 2016; Betts et al., 2018; Robertson et al., 2019).

In the current study, we employed cloning and demonstrated the presence of multiple subtypes within a single host and also presence of multiple eukaryotes within a host. We would like to emphasize that DNA was mainly extracted directly from fresh fecal samples without culturing in Jones media. Even though we still cannot guarantee that all subtypes present in the stool samples were amplified, selective pressures and constraints that culturing imposes were circumvented. In working with fecal samples other issues came to light. One of them is primer specificity. Eukaryotic microbe primers amplify the microbe of interest provided it is there. Our screening showed that all pairs of specific primers and most especially those of *Blastocystis* and *Entamoeba* also amplified several other eukaryotes. For example, approximately ∼40% of the sequenced clones did not correspond to *Blastocystis* specific sequences. Development of new *Blastocystis*-specific primers that will amplify a large fragment of the SSU rRNA gene are urgently needed, since this will reduce the costs of cloning and sequencing.

CONCLUSION

Herein we have identified asymptomatic carriage of multiple microbial eukaryotes in a number of animal species. This is defined as presence of multiple *Blastocystis* subtypes in single hosts and in many cases these co-occur with up to three other microbial eukaryotes. Given the higher prevalence of overlap of microbial eukaryotes in animals and especially in artiodactyls, the latter might provide a model not only for studying the spectrum

of parasitism (Rueckert et al., 2019), but also the associated microbial communities and how those relate with the different parts of this spectrum.

DATA AVAILABILITY STATEMENT

The raw data supporting the conclusions of this article will be made available by the authors, without undue reservation, to any qualified researcher.

AUTHOR CONTRIBUTIONS

EB carried out the collections, culturing, collected and analyzed all the data, and wrote a first draft of the manuscript. AT and EG directed research, planned experiments, analyzed data, and wrote the manuscript.

FUNDING

This research was supported by BBSRC research grant (BB/M009971/1) to Dr. AT. Dr. EG is supported by The Thailand Research Fund (RSA6080048). We would like to thank the University of Kent for sponsoring ADT's trip to Thailand under a GCRF grant. EB was supported by a Ph.D. studentship from the School of Biosciences at the University of Kent.

ACKNOWLEDGMENTS

We thank members of the Dr. Tsaousis laboratory, Adele Thomasz, Vicki Breakell, Angus I. Carpenter and Hazel Ryan from the Wildwood Trust and Adrian Harland from the Howllets Zoo and the zookeepers from both zoos for assisting with sample collection and accommodating us during our visitations.

SUPPLEMENTARY MATERIAL

The Supplementary Material for this article can be found online at: https://www.frontiersin.org/articles/10.3389/fmicb.2020.00288/full#supplementary-material

REFERENCES

AbuOdeh, R., Ezzedine, S., Samie, A., Stensvold, C. R., and ElBakri, A. (2016). Prevalence and subtype distribution of *Blastocystis* in healthy individuals in Sharjah, United Arab Emirates. *Infect. Genet. Evol.* 37, 158–162. doi: 10.1016/j.meegid.2015.11.021

Alfellani, M. A., Taner-Mulla, D., Jacob, A. S., Imeede, C. A., Yoshikawa, H., Stensvold, C. R., et al. (2013). Genetic diversity of *Blastocystis* in livestock and zoo animals. *Protist* 164, 497–509. doi: 10.1016/j.protis.2013.05.003

Andersen, L. O., Bonde, I., Nielsen, H. B., and Stensvold, C. R. (2015). A retrospective metagenomics approach to studying *Blastocystis*. *FEMS Microbiol. Ecol.* 91:fiv072. doi: 10.1093/femsec/fiv072

Audebert, C., Even, G., Cian, A., Blastocystis Investigation Group, Loywick, A., Merlin, S., et al. (2016). Colonization with the enteric protozoa *Blastocystis* is associated with increased diversity of human gut bacterial microbiota. *Sci. Rep.* 6:25255. doi: 10.1038/srep25255

Badparva, E., Sadraee, J., and Kheirandish, F. (2015). Genetic diversity of *Blastocystis* isolated from cattle in khorramabad, iran. *Jundishapur J. Microbiol.* 8:e14810. doi: 10.5812/jjm.14810

Beghini, F., Pasolli, E., Truong, T. D., Putignani, L., Caccio, S. M., and Segata, N. (2017). Large-scale comparative metagenomics of *Blastocystis*, a common member of the human gut microbiome. *ISME J.* 11, 2848–2863. doi: 10.1038/ismej.2017.139

Betts, E. L., Gentekaki, E., Thomasz, A., Breakell, V., Carpenter, A. I., and Tsaousis, A. D. (2018). Genetic diversity of *Blastocystis* in non-primate animals. *Parasitology* 145, 1228–1234. doi: 10.1017/S0031182017002347

Blaser, M. J. (2014). The microbiome revolution. *J. Clin. Invest.* 124, 4162–4165. doi: 10.1172/JCI78366

Calero-Bernal, R., Santín, M., Maloney, J. G., Martín-Pérez, M., Habela, M. A., Fernández-García, J. L., et al. (2019). Blastocystis sp. subtype diversity in wild carnivore species from Spain. *J. Eukaryot. Microbiol.* doi: 10.1111/jeu.12772 [Epub ahead of print].

Capella-Gutierrez, S., Silla-Martinez, J. M., and Gabaldon, T. (2009). trimAl: a tool for automated alignment trimming in large-scale phylogenetic analyses. *Bioinformatics* 25, 1972–1973. doi: 10.1093/bioinformatics/btp348

Chudnovskiy, A., Mortha, A., Kana, V., Kennard, A., Ramirez, J. D., Rahman, A., et al. (2016). Host-protozoan interactions protect from mucosal infections through activation of the Inflammasome. *Cell* 167, 444–456.e14. doi: 10.1016/j.cell.2016.08.076

Cian, A., El Safadi, D., Osman, M., Moriniere, R., Gantois, N., Benamrouz-Vanneste, S., et al. (2017). Molecular epidemiology of *Blastocystis* sp. in various animal groups from two french zoos and evaluation of potential zoonotic risk. *PLoS One* 12:e0169659. doi: 10.1371/journal.pone.0169659

Clark, C. G., van der Giezen, M., Alfellani, M. A., and Stensvold, C. R. (2013). Recent developments in *Blastocystis* research. *Adv. Parasitol.* 82, 1–32. doi: 10.1016/B978-0-12-407706-5.00001-0

Desoubeaux, G., Peschke, R., Le-Bert, C., Fravel, V., Soto, J., Jensen, E. D., et al. (2018). Seroprevalence survey for Microsporidia in common bottlenose Dolphin (*Tursiops truncatus*): example of a quantitative approach based on immunoblotting. *J. Wildl. Dis.* 54, 870–873. doi: 10.7589/2017-11-287

Diamond, L. S. (1957). The establishment of various trichomonads of animals and man in axenic cultures. *J. Parasitol.* 43, 488–490.

Diamond, L. S. (1982). A new liquid medium for xenic cultivation of *Entamoeba histolytica* and other lumen-dwelling protozoa. *J. Parasitol.* 68, 958–959.

Diamond, L. S. (1983). "Lumen dwelling protozoa: *Entamoeba*, trichomonads, and *Giardia*," in *In Vitro Cultivation of Protozoan Parasites*, ed. J. B. Jensen (Boca Raton, FL: CRC Press), 67–109.

El Safadi, D., Cian, A., Nourrisson, C., Pereira, B., Morelle, C., Bastien, P., et al. (2016). Prevalence, risk factors for infection and subtype distribution of the intestinal parasite *Blastocystis* sp. from a large-scale multi-center study in France. *BMC Infect. Dis.* 16:451. doi: 10.1186/s12879-016-1776-8

Elwakil, H. S., and Hewedi, I. H. (2010). Pathogenic potential of *Blastocystis hominis* in laboratory mice. *Parasitol. Res.* 107, 685–689. doi: 10.1007/s00436-010-1922-y

Enriquez, G. F., Garbossa, G., Macchiaverna, N. P., Argibay, H. D., Bua, J., Gürtler, R. E., et al. (2016). Is the infectiousness of dogs naturally infected with *Trypanosoma cruzi* associated with poly-parasitism? *Vet. Parasitol.* 223, 186–194. doi: 10.1016/j.vetpar.2016.04.042

Enriquez, G. F., Macchiaverna, N. P., Argibay, H. D., López Arias, L., Farber, M., Gürtler, R. E., et al. (2019). Polyparasitism and zoonotic parasites in dogs from a rural area of the Argentine Chaco. *Vet. Parasitol. Reg. Stud. Rep.* 16:100287. doi: 10.1016/j.vprsr.2019.100287

Fayer, R., Santin, M., and Macarisin, D. (2012). Detection of concurrent infection of dairy cattle with *Blastocystis, Cryptosporidium, Giardia*,

and *Enterocytozoon* by molecular and microscopic methods. *Parasitol. Res.* 111, 1349–1355. doi: 10.1007/s00436-012-2971-1

Forsell, J., Bengtsson-Palme, J., Angelin, M., Johansson, A., Evengard, B., and Granlund, M. (2017). The relation between *Blastocystis* and the intestinal microbiota in Swedish travellers. *BMC Microbiol.* 17:231. doi: 10.1186/s12866-017-1139-7

Gentekaki, E., Curtis, B. A., Stairs, C. W., Klimes, V., Elias, M., Salas-Leiva, D. E., et al. (2017). Extreme genome diversity in the hyper-prevalent parasitic eukaryote *Blastocystis*. *PLoS Biol.* 15:e2003769. doi: 10.1371/journal.pbio.2003769

Iebba, V., Santangelo, F., Totino, V., Pantanella, F., Monsia, A., Di Cristanziano, V., et al. (2016). Gut microbiota related to *Giardia duodenalis, Entamoeba* spp. and *Blastocystis hominis* infections in humans from Cote d'Ivoire. *J. Infect. Dev. Ctries.* 10, 1035–1041. doi: 10.3855/jidc.8179

Jacob, A. S., Busby, E. J., Levy, A. D., Komm, N., and Clark, C. G. (2016). Expanding the *Entamoeba* universe: new hosts yield novel ribosomal lineages. *J. Eukaryot. Microbiol.* 63, 69–78. doi: 10.1111/jeu.12249

Katoh, K., and Toh, H. (2010). Parallelization of the MAFFT multiple sequence alignment program. *Bioinformatics* 26, 1899–1900. doi: 10.1093/bioinformatics/btq224

Lukes, J., Stensvold, C. R., Jirka Pomajbaková, K., and Wegener Parfrey, L. (2015). Are human intestinal eukaryotes beneficial or commensals? *PLoS Pathog.* 11:e1005039. doi: 10.1371/journal.ppat.1005039

Mardani Kataki, M., Tavalla, M., and Beiromvand, M. (2019). Higher prevalence of *Blastocystis hominis* in healthy individuals than patients with gastrointestinal symptoms from Ahvaz, southwestern Iran. *Comp. Immunol. Microbiol. Infect. Dis.* 65, 160–164. doi: 10.1016/j.cimid.2019.05.018

Miller, M. A., Pfeiffer, W., and Schwartz, T. (2010). "Creating the CIPRES science gateway for inference of large phylogenetic trees," in *Proceedings of the Gateway Computing Environments Workshop (GCE)*, New Orleans, LA, 1–8.

Moe, K. T., Singh, M., Howe, J., Ho, L. C., Tan, S. W., Chen, X. Q., et al. (1997). Experimental *Blastocystis hominis* infection in laboratory mice. *Parasitol. Res.* 83, 319–325. doi: 10.1007/s004360050256

Nieves-Ramirez, M. E., Partida-Rodriguez, O., Laforest-Lapointe, I., Reynolds, L. A., Brown, E. M., Valdez-Salazar, A., et al. (2018). Asymptomatic intestinal colonization with Protist *Blastocystis* is strongly associated with distinct microbiome ecological patterns. *mSystems* 3:e00007-18. doi: 10.1128/mSystems.00007-18

Nishida, A. H., and Ochman, H. (2018). Rates of gut microbiome divergence in mammals. *Mol. Ecol.* 27, 1884–1897. doi: 10.1111/mec.14473

Noel, C., Dufernez, F., Gerbod, D., Edgcomb, V. P., Delgado-Viscogliosi, P., Ho, L. C., et al. (2005). Molecular phylogenies of *Blastocystis* isolates from different hosts: implications for genetic diversity, identification of species, and zoonosis. *J. Clin. Microbiol.* 43, 348–355. doi: 10.1128/jcm.43.1.348-355.2005

O'Brien Andersen, L., Karim, A. B., Roager, H. M., Vigsnæs, L. K., Krogfelt, K. A., Licht, T. R., et al. (2016). Associations between common intestinal parasites and bacteria in humans as revealed by qPCR. *Eur. J. Clin. Microbiol. Infect. Dis.* 35, 1427–1431. doi: 10.1007/s10096-016-2680-2

Parfrey, L. W., Walters, W. A., and Knight, R. (2011). Microbial eukaryotes in the human microbiome: ecology, evolution, and future directions. *Front. Microbiol.* 2:153. doi: 10.3389/fmicb.2011.00153

Parsons, M. B., Travis, D., Lonsdorf, E. V., Lipende, I., Roellig, D. M. A., Kamenya, S., et al. (2015). Epidemiology and molecular characterization of *Cryptosporidium* spp. in humans, wild primates, and domesticated animals in the greater gombe ecosystem, tanzania. *PLoS Negl. Trop. Dis.* 9:e0003529. doi: 10.1371/journal.pntd.0003529

Puthia, M. K., Lu, J., and Tan, K. S. (2008). *Blastocystis ratti* contains cysteine proteases that mediate interleukin-8 response from human intestinal epithelial cells in an NF-kappaB-dependent manner. *Eukaryot. Cell* 7, 435–443. doi: 10.1128/ec.00371-07

Ramirez, J. D., Sanchez, A., Hernandez, C., Florez, C., Bernal, M. C., Giraldo, J. C., et al. (2016). Geographic distribution of human *Blastocystis* subtypes in South America. *Infect. Genet. Evol.* 41, 32–35. doi: 10.1016/j.meegid.2016.03.017

Renelies-Hamilton, J., Noguera-Julian, M., Parera, M., Paredes, R., Pacheco, L., Dacal, E., et al. (2019). Exploring interactions between *Blastocystis* sp., *Strongyloides* spp. and the gut microbiomes of wild chimpanzees in Senegal. *Infect. Genet. Evol.* 74:104010. doi: 10.1016/j.meegid.2019.104010

Robertson, L. J., Clark, C. G., Debenham, J. J., Dubey, J. P., Kváč, M., Li, J., et al. (2019). Are molecular tools clarifying or confusing our understanding of the public health threat from zoonotic enteric protozoa in wildlife? *Int. J. Parasitol. Parasites Wildl.* 9, 323–341. doi: 10.1016/j.ijppaw.2019.01.010

Rueckert, S., Betts, E. L., and Tsaousis, A. D. (2019). The symbiotic spectrum: Where do the gregarines fit? *Trends Parasitol.* 35, 687–694. doi: 10.1016/j.pt.2019.06.013

Sanders, J. G., Beichman, A. C., Roman, J., Scott, J. J., Emerson, D., McCarthy, J. J., et al. (2015). Baleen whales host a unique gut microbiome with similarities to both carnivores and herbivores. *Nat. Commun.* 6:8285. doi: 10.1038/ncomms9285

Scanlan, P. D., and Stensvold, C. R. (2013). *Blastocystis*: getting to grips with our guileful guest. *Trends Parasitol.* 29, 523–529. doi: 10.1016/j.pt.2013.08.006

Scanlan, P. D., Stensvold, C. R., Rajilic-Stojanovic, M., Heilig, H. G., De Vos, W. M., O'Toole, P. W., et al. (2014). The microbial eukaryote *Blastocystis* is a prevalent and diverse member of the healthy human gut microbiota. *FEMS Microbiol. Ecol.* 90, 326–330. doi: 10.1111/1574-6941.12396

Stamatakis, A. (2014). RAxML version 8: a tool for phylogenetic analysis and post-analysis of large phylogenies. *Bioinformatics* 30, 1312–1313. doi: 10.1093/bioinformatics/btu033

Stamatakis, A. (2015). Using RAxML to infer phylogenies. *Curr. Protoc. Bioinformatics* 51, 6.14.1–14.14. doi: 10.1002/0471250953.bi0614s51

Stensvold, C. R. (2012). Thinking *Blastocystis* out of the box. *Trends Parasitol.* 28:305. doi: 10.1016/j.pt.2012.05.004

Stensvold, C. R., and Clark, C. G. (2016a). Current status of *Blastocystis*: a personal view. *Parasitol. Int.* 65, 763–771. doi: 10.1016/j.parint.2016.05.015

Stensvold, C. R., and Clark, C. G. (2016b). Molecular identification and subtype analysis of *Blastocystis*. *Curr. Protoc. Microbiol.* 43, 20A.2.1–20A.2.10. doi: 10.1002/cpmc.17

Tito, R. Y., Chaffron, S., Caenepeel, C., Lima-Mendez, G., Wang, J., Vieira-Silva, S., et al. (2019). Population-level analysis of *Blastocystis* subtype prevalence and variation in the human gut microbiota. *Gut* 68, 1180–1189. doi: 10.1136/gutjnl-2018-316106

Udonsom, R., Prasertbun, R., Mahittikorn, A., Mori, H., Changbunjong, T., Komalamisra, C., et al. (2018). *Blastocystis* infection and subtype distribution in humans, cattle, goats, and pigs in central and western Thailand. *Infect. Genet. Evol.* 65, 107–111. doi: 10.1016/j.meegid.2018.07.007

Wang, J., Gong, B., Liu, X., Zhao, W., Bu, T., Zhang, W., et al. (2018a). Distribution and genetic diversity of *Blastocystis* subtypes in various mammal and bird species in northeastern China. *Parasit. Vectors* 11:522. doi: 10.1186/s13071-018-3106-z

Wang, J., Gong, B., Yang, F., Zhang, W., Zheng, Y., and Liu, A. (2018b). Subtype distribution and genetic characterizations of *Blastocystis* in pigs, cattle, sheep and goats in northeastern China's Heilongjiang Province. *Infect. Genet. Evol.* 57, 171–176. doi: 10.1016/j.meegid.2017.11.026

Wang, W., Bielefeldt-Ohmann, H., Traub, R. J., Cuttell, L., and Owen, H. (2014). Location and pathogenic potential of *Blastocystis* in the porcine intestine. *PLoS One* 9:e103962. doi: 10.1371/journal.pone.0103962

Wawrzyniak, I., Texier, C., Poirier, P., Viscogliosi, E., Tan, K. S., Delbac, F., et al. (2012). Characterization of two cysteine proteases secreted by *Blastocystis* ST7, a human intestinal parasite. *Parasitol. Int.* 61, 437–442. doi: 10.1016/j.parint.2012.02.007

Whipps, C. M., Boorom, K., Bermudez, L. E., and Kent, M. L. (2010). Molecular characterization of *Blastocystis* species in Oregon identifies multiple subtypes. *Parasitol. Res.* 106, 827–832. doi: 10.1007/s00436-010-1739-8

Yoshikawa, H., Abe, N., and Wu, Z. (2004). PCR-based identification of zoonotic isolates of *Blastocystis* from mammals and birds. *Microbiology* 150, 1147–1151. doi: 10.1099/mic.0.26899-0

Yoshikawa, H., Koyama, Y., Tsuchiya, E., and Takami, K. (2016). *Blastocystis* phylogeny among various isolates from humans to insects. *Parasitol. Int.* 65, 750–759. doi: 10.1016/j.parint.2016.04.004

Yowang, A., Tsaousis, A. D., Chumphonsuk, T., Thongsin, N., Kullawong, N., Popluechai, S., et al. (2018). High diversity of *Blastocystis* subtypes isolated from asymptomatic adults living in Chiang Rai, Thailand. *Infect. Genet. Evol.* 65, 270–275. doi: 10.1016/j.meegid.2018.08.010

Zhao, G. H., Hu, X. F., Liu, T. L., Hu, R. S., Yu, Z. Q., Yang, W. B., et al. (2017). Molecular characterization of *Blastocystis* sp. in captive wild animals in Qinling Mountains. *Parasitol. Res.* 116, 2327–2333. doi: 10.1007/s00436-017-5506-y

Conflict of Interest: The authors declare that the research was conducted in the absence of any commercial or financial relationships that could be construed as a potential conflict of interest.

frontiers in Microbiology

REVIEW
published: 26 June 2020
doi: 10.3389/fmicb.2020.01468

Innate and Adaptive Immune Responses Against Microsporidia Infection in Mammals

Yinze Han[1,2], Hailong Gao[1,2], Jinzhi Xu[1,2], Jian Luo[1,2], Bing Han[3], Jialing Bao[1,2], Guoqing Pan[1,2], Tian Li[1,2] and Zeyang Zhou[1,2,4]**

[1] State Key Laboratory of Silkworm Genome Biology, Southwest University, Chongqing, China, [2] Chongqing Key Laboratory of Microsporidia Infection and Control, Southwest University, Chongqing, China, [3] Department of Pathology, Albert Einstein College of Medicine, The Bronx, NY, United States, [4] College of Life Sciences, Chongqing Normal University, Chongqing, China

OPEN ACCESS

Edited by:
Lihua Xiao, South China Agricultural University, China

Reviewed by:
Louis Weiss, Albert Einstein College of Medicine, United States
Hicham El Alaoui, Université Clermont Auvergne, France
Tian Luo, The University of Texas Medical Branch at Galveston, United States
Majid Pirestani, Tarbiat Modares University, Iran

***Correspondence:**
Tian Li
lit@swu.edu.cn
Zeyang Zhou
zyzhou@swu.edu.cn

Specialty section:
This article was submitted to Infectious Diseases, a section of the journal Frontiers in Microbiology

Received: *13 September 2019*
Accepted: *04 June 2020*
Published: *26 June 2020*

Citation:
Han Y, Gao H, Xu J, Luo J, Han B, Bao J, Pan G, Li T and Zhou Z (2020) Innate and Adaptive Immune Responses Against Microsporidia Infection in Mammals. Front. Microbiol. 11:1468. doi: 10.3389/fmicb.2020.01468

Microsporidia are obligate intracellular and eukaryotic pathogens that can infect immunocompromised and immunocompetent mammals, including humans. Both innate and adaptive immune systems play important roles against microsporidian infection. The innate immune system can partially eliminate the infection by immune cells, such as gamma delta T cell, natural killer cells (NKs), macrophages and dendritic cells (DCs), and present the pathogens to lymphocytes. The innate immune cells can also prime and enhance the adaptive immune response via surface molecules and secreted cytokines. The adaptive immune system is critical to eliminate microsporidian infection by activating cytotoxic T lymphocyte (CTL) and humoral immune responses, and feedback regulation of the innate immune mechanism. In this review, we will discuss the cellular and molecular responses and functions of innate and adaptive immune systems against microsporidian infection.

Keywords: microsporidia, mammal host, immune response, innate immunity, adaptive immunity

INTRODUCTION

Microsporidia are obligate intracellular parasites that infect nearly all vertebrates and invertebrates, including immunocompetent and immunocompromised humans. The Microsporidia phylum is composed of at least 200 genera and 1400 species (Cali et al., 2017). At least 17 species within nine genera (*Anncaliia, Encephalitozoon, Enterocytozoon, Microsporidium, Nosema, Pleistophora, Trachipleistophora, Tubulonosema, Vittaforma*) of microsporidia have been reported to be able to infect humans (Fayer and Santin-Duran, 2014; Han and Weiss, 2017). The human-infecting microsporidia are recognized as opportunistic pathogens, and frequently reported in immunocompetent and immunocompromised individuals, such as AIDS patients, cancer patients, transplant recipients, children and the elderly (Lores et al., 2002; Tumwine et al., 2002; Mor et al., 2009; Abu-Akkada et al., 2015; Wang et al., 2018; Ghoyounchi et al., 2019). Moreover, some microsporidia have a broad host range and can be transmitted among animals and humans, leading to zoonotic or interspecies transmission of microsporidiosis (Li et al., 2019; Udonsom et al., 2019).

When infecting, microsporidian spores extrude a polar tube, through which sporoplasms inside the spores are transported into host cells for development and proliferation (Franzen, 2005; Franzen et al., 2005b; Han et al., 2020). Inside host cell, the pathogen has to fight against host immune

systems, including innate immunity and adaptive immunity. A few years ago, several reviews summarized studies in the early time on the immune responses of mammals against microsporidian infections (Khan et al., 2001; Ghosh and Weiss, 2012; Valencakova and Halanova, 2012). These very early analyses had partially indicated that both immunities are crucial to the resistance against microsporidian infections, and had found that immune cells including macrophages, dendritic cells (DCs) and CD8+ T cell, and cytokines like IL-12 and IFN- γ are activated and contribute to the immune defense (Mathews et al., 2009). In recent years, some new and further studies have revealed more cellular and molecular interactions between host immune system and microsporidia. In this review, we will systematically discuss the cellular and molecular responses to microsporidian infections from aspects of innate and adaptive immunities, respectively.

INNATE IMMUNE RESPONSE TO MICROSPORIDIAN INFECTION

The innate immune system serves as the first line of defense and plays important roles in non-specific responses against infections. The innate immune system is composed of tissue barrier, innate immune cells, innate immune molecules, and cytokines (Beutler, 2004; Turvey and Broide, 2010; Sokol and Luster, 2015). The innate immune cells including macrophages, DCs, Natural Killer Cells (NKs) and innate-like lymphocytes have been proved to be essential for responses against microsporidian infections (Didier et al., 2010; Lawlor et al., 2010; Moretto et al., 2012). The innate immunity cannot completely clear microsporidian infection, but is necessary to activate the responses of adaptive immunities for a clearance.

Macrophage Response to Microsporidian Infection

Macrophages originate from blood monocytes, differentiate in tissues, and are involved in the detection, phagocytosis and destruction of harmful organisms. Macrophages can also present antigens to T cells and initiate inflammation by releasing cytokines to activate other immune cells. During microsporidian infection, macrophages can recognize the pathogens via pattern recognition receptors (PRRs) on the surface (Fischer et al., 2008a), and subsequently active defense mediators, such as chemokines, cytokines, reactive nitrogen, and radical oxygen, to control pathogen dissemination (Mathews et al., 2009). Macrophages are highly plasticity, can be activated and generate classically activated (M1) and alternatively activated (M2) types according to the activation state and functions, respectively (Martinez and Gordon, 2014). IFN-γ and lipopolysaccharide (LPS) are important activators for polarization of M1, which has intense phagocytic activity and higher microbicidal activity with NO and can secrete IL-12 and IFN-γ (Martinez and Gordon, 2014). It has been found that M1 can significantly reduce *Encephalitozoon* infection (Didier and Shadduck, 1994; Didier, 1995; Fischer et al., 2008b) depending on reactive nitrogen species (RNS) and reactive oxygen species (ROS) (Didier, 1995; Didier et al., 2010; Gonzalez-Machorro et al., 2019; **Figure 1**). The RNS- and ROS-deficient mice were shown to bear significantly higher peritoneal pathogen load and need longer time to eliminate the infection compared to the wild type of mice (Didier et al., 2010). Nonetheless, the deficient mice finally survived against *Encephalitozoon cuniculi* infection (Didier et al., 2010). Moreover, the phagocytosis of microsporidia significantly increased in LPS-activated murine macrophages, and the growth of pathogens inside the macrophages was inhibited, while the inhibitory effect lost after 72 h (Gonzalez-Machorro et al., 2019). These findings suggest that macrophages can control microsporidian infection to a certain extent, but the complete elimination likely requires other immunities. In addition, it was found that macrophage activities were associated with B-1 cells in microsporidian infection. In mice with B-1 cells, peritoneal macrophages had an M1 profile. In B-1 cell deficient mice, however, *E. cuniculi* modulated macrophages to M2, which is less phagocytic capacity and index and microbicidal activity, and inside which spore germination was observed, suggesting that B-1 cells are important in the modulation of macrophage in *E. cuniculi* infection (Pereira et al., 2019).

In fact, studies have tried to understand that how microsporidia escape the macrophage immunity. Early studies proved that microsporidian spores in vacuoles were able to block phagosome acidification and fusion with secondary lysosomes (Weidner and Sibley, 1985; **Figure 1**). Spore-containing phagocytic vacuoles fused with lysosomes can kill partial pathogens, while some sporoplasms can still escape from maturing lysosomes so that enter into host cytoplasm for successful infection (Franzen, 2005; Franzen et al., 2005b). When failing to inhibit the proliferation of microsporidia, macrophages can release chemokines (CCL3, CCL4) with TLR2-NF-κB signaling pathway to recruit phagocytes (Fischer et al., 2008a; **Figure 1**). However, this recruitment mechanism can be hijacked by the pathogens for infecting more monocytes and expanding the monocyte-derived-macrophage infections (Fischer et al., 2007). Meanwhile, the macrophage itself may also be hijacked as a "Trojan horse" to carry the parasites to other parts of the host body and spread the infection (Mathews et al., 2009). Furthermore, the macrophage immunity can be modulated by microsporidia via cytokines. In human macrophages infected with *Encephalitozoon*, the expression of IL-10 increased (Franzen et al., 2005a). This is consistent with the later study by Pereira et al. (2019) that macrophages were polarized to M2 type, in which the IL-10 expression is upregulated and the pathogens can escape from killing. Besides, the IL-10 belongs to an anti-inflammatory cytokine and can inhibit the production of nitric oxide and activity of macrophages and Th1 cells during infection (Popi et al., 2004; Couper et al., 2008). It was documented that early expression of IL-10 delayed the production of IFN-γ (Braunfuchsova et al., 1999), which was found to play an important role in macrophage-activating and resisting the microsporidian infection (Achbarou et al., 1996; El Fakhry et al., 1998, 2001; Khan and Moretto, 1999; Rodriguez-Tovar et al., 2016).

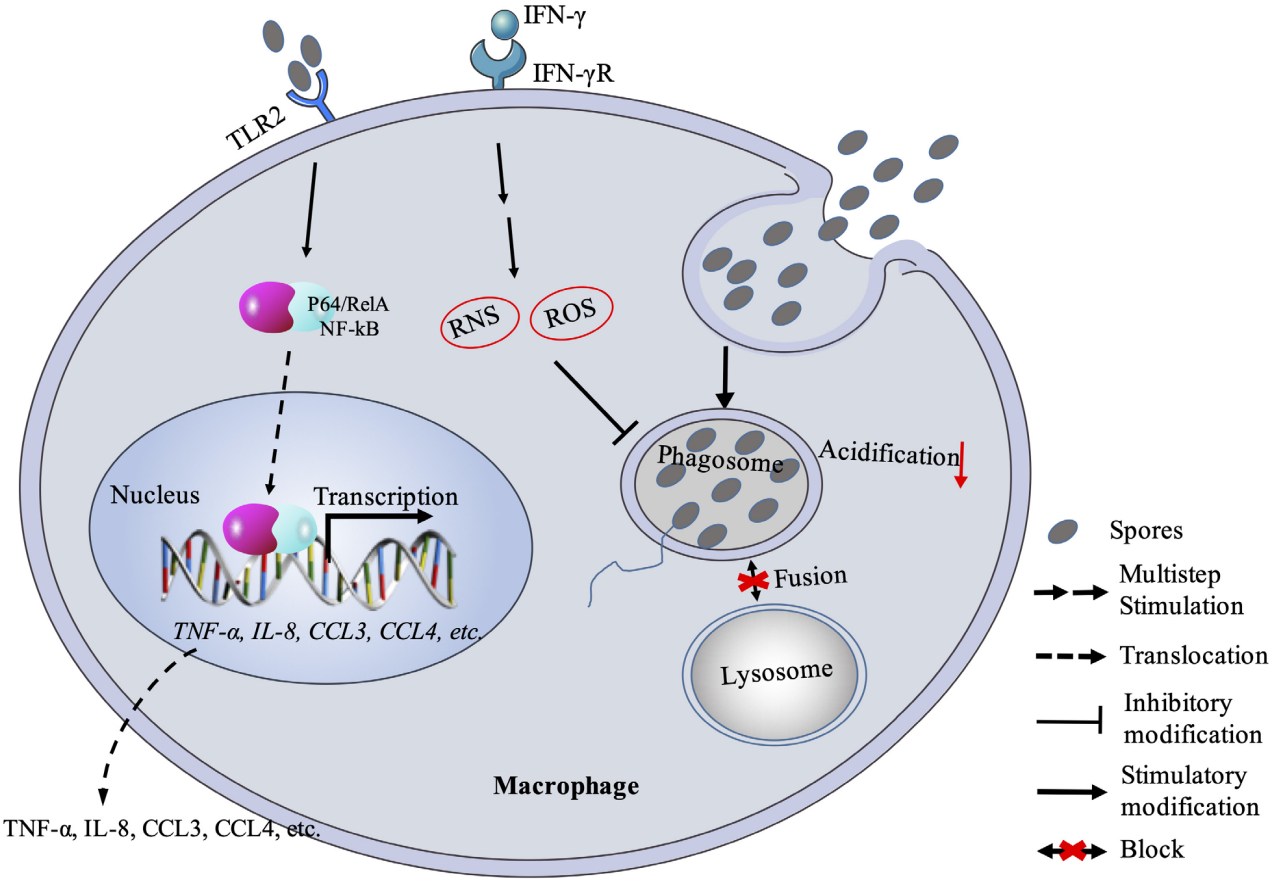

FIGURE 1 | Macrophage response against microsporidian infection. Macrophage recognizes microsporidia via MyD88-dependent TLR2 and stimulates downstream expression of cytokines and chemokines. Macrophage can also kill the pathogen with RNS and ROS mechanism. Besides, microsporidia can block the fusion between phagosome and lysosome. RNS, reactive nitrogen species; ROS: reactive oxygen species.

DCs Response to Microsporidian Infection

Dendritic cells are essential antigen presentation cells and thus function as a bridge between innate and adaptive immune systems (Mellman and Steinman, 2001). Antigens presented by DCs to T cells promote the adaptive immunity via activating naïve lymphocytes into effector T cells, which will significantly boost immunity against the infection (Steinman and Hemmi, 2006; Bieber and Autenrieth, 2020). Besides, DCs can secrete many cytokines, such as IL-12 and IFNs, which will trigger adaptive immune responses against the foreigner invasions (Mellman and Steinman, 2001; Trinchieri, 2003; von Stebut and Tenzer, 2018).

It was reported that IFN-γ and IL-12 play vital roles in DCs response against microsporidian infection. The IFN-γ secreted by DCs is important for priming the gut intraepithelial lymphocytes response (IEL) against *E. cuniculi* infection. Murine DCs lacking IFN-γ failed to induce IEL response and led to ineffective suppression of the infection (Moretto et al., 2007, 2012). The IL-12 is also an important cytokine responding to microsporidian infection. The mutant mice lacking IL-12 was found to be susceptible to the infection (Khan and Moretto, 1999), and CD8+ T cells showed poor immune response (Moretto et al., 2010). In infected DCs, IL-12 production was strongly induced, while the $p40^{-/-}$ DCs lacking IL-12 failed to develop robust CD8+ T cell-mediated immune response to *E. cuniculi* infection (Moretto et al., 2010). Studies also showed that the IL-12 can be induced during early infection of DC by *E. cuniculi*, suggesting that IL-12 is important to the initiation of innate immunity (Lawlor et al., 2010; **Figure 2**). Moreover, the PRRs of DCs, like Toll-like receptors (TLRs), are crucial for pathogen-recognition. It was shown that TLR4 is a key factor for DCs response (**Figure 2**), and is also essential for the expression of costimulatory molecules (CD80, CD86, and MHC class II), which induce optimal antigen-specific CD8+ T cells response to *E. cuniculi* infection (Lawlor et al., 2010). In *Enterocytozoon bieneusi* infection, however, TLR4 is not required for DCs response, but the myeloid differentiation factor 88 (MyD88) involved in Toll-like signaling pathway is needed (Zhang et al., 2011). Therefore, DCs probably recognize different microsporidia via different TLRs.

On the other hand, the differentiation of DCs was found to be inhibited by microsporidia via an IL-6-dependent mechanism so that the parasites can escape from stronger immune defense (Bernal et al., 2016; **Figure 3**). In addition, the ability of priming

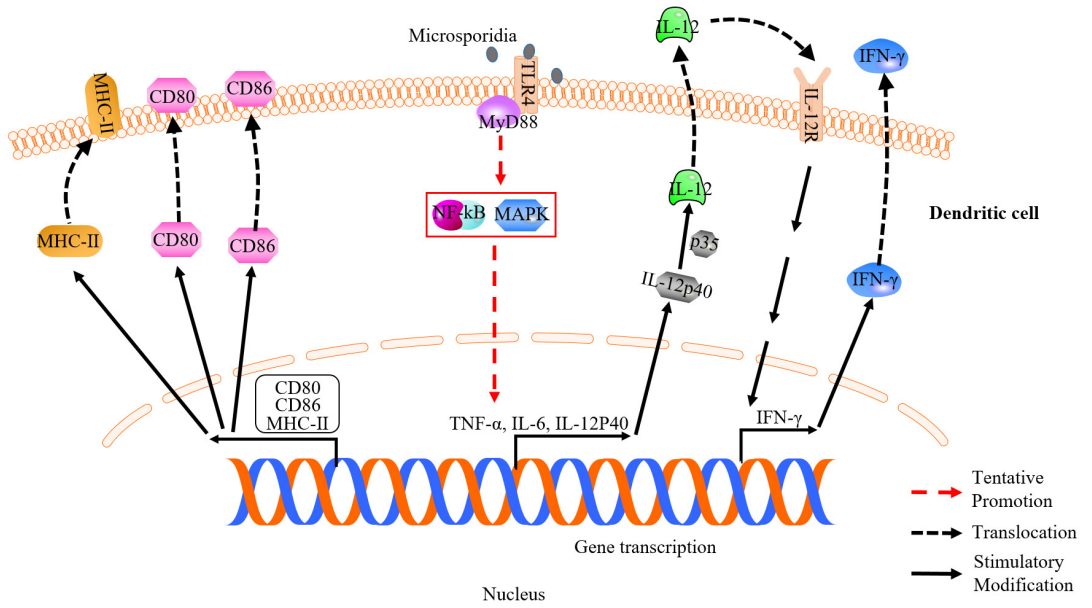

FIGURE 2 | Dendritic cell (DC) response against microsporidian infection. Surface molecules of CD80, CD86, MHC-II and toll-like receptor 4 are up-regulated in infected DC. Upregulation of CD80, CD86, and MHC-II is essential for induction of optimal T-cell response. DC can recognize microsporidia via TLR4. IL-12 and IFN-γ secreted by DC help to optimize and prime effector T cell immune response, respectively.

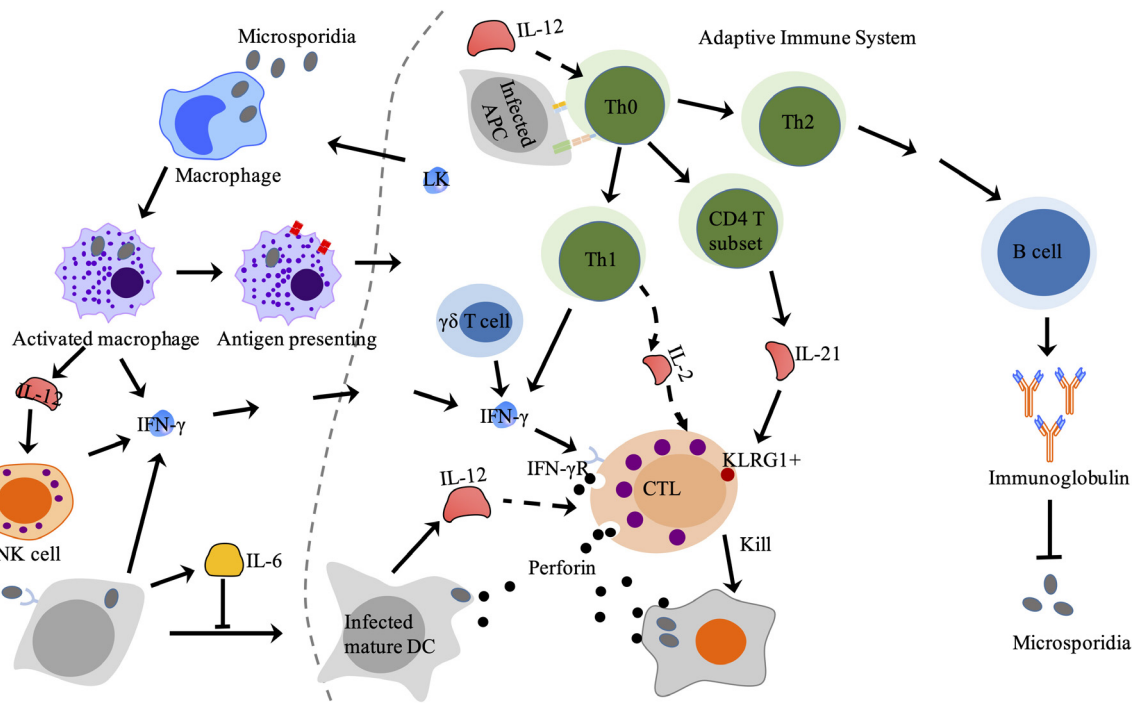

FIGURE 3 | Adaptive immune response against microsporidia in mammals. CTL is activated by APC and cytokines from innate immune cells and Th cell and then lyses target cell via perforin-dependent cytotoxicity. Antibodies produced by effector B lymphocytes can partially block microsporidian infection. LK produced by lymphocytes stimulates macrophage to secret IFN-γ. LK, lymphokines; CTL, cytotoxic T lymphocytes; Th cell, helper T cell; APC, antigen presenting cell.

antigen-specific T cell response in aged host decreases at the microsporidia-infected gut mucosal site (Moretto et al., 2008; Gigley and Khan, 2011). The maturation of DCs can be inhibited by the programmed death-ligand 1 (PD-L1), which expression is increased in aged mice leading to decrease of mature DCs and T cells immunity (Gigley and Khan, 2011). This probably is a

reason why the aged is susceptible to microsporidian infection (Lores et al., 2002).

NKs Response to Microsporidian Infection

The NKs are a type of cytotoxic lymphocytes and critical to the innate immune system. NKs can not only lyse infected cells, but also secret cytokines like IFN-γ to induce immunity of antigen specific T cells (Yokoyama, 2005). It was found that the activity of NKs was enhanced in mice infected with *E. cuniculi* (Niederkorn et al., 1983), and the number of NKs increased upon early infection of *E. cuniculi* but decreased to a normal level in late infection stage (Khan et al., 1999). Further studies indicated that NKs can also produce IFN-γ after stimulated by IL-12 secreted by macrophages (Braunfuchsova et al., 1999; Salat et al., 2004; **Figure 3**).

Intraepithelial Lymphocytes Response to Microsporidian Infection

The intestinal mucosa is an important defense line against microsporidia by inducing strong intraepithelial lymphocytes (IELs) response (Moretto et al., 2004, 2007, 2012). The population of IELs accompanied with the secretion of cytokines, such as IFN-γ and IL-10, rapidly increases in early infection by *E. cuniculi*. And the activated IELs are cytotoxic to infected syngeneic macrophages, which can kill more than 60% antigen-specific target cells (Moretto et al., 2004). These findings indicated that the early expansion of IELs not only serves as the first defense line, but also offers immunoregulators. Besides, the IFN-γ produced by DCs from mucosal sites is crucial for evoking antigen-specific IEL responses against microsporidia in the small intestine (Moretto et al., 2007).

Apoptosis Response to Microsporidian Infection

Apoptosis is a form of programmed cell death that also responses to pathogen infection and plays significant roles in the control of the immune response (Knodler and Finlay, 2001; Luder et al., 2001; Higes et al., 2013).

Intracellular parasites like microsporidia and *Toxoplasma gondii* can suppress host apoptosis in order to have more time for proliferation (Nash et al., 1998; Heussler et al., 2001; Higes et al., 2013; He et al., 2015; Kurze et al., 2015; Sinpoo et al., 2017; Sokolova et al., 2019). Microsporidia can inhibit host apoptosis via modulating apoptosis-related proteins. Buffy and BIRC5 are two host factors that suppress apoptosis. The buffy is a Bcl-2 like protein and can inhibit caspase-dependent cell death by activating downstream gene expressions in *Drosophila* (Quinn et al., 2003). And the BIRC5 is a member of the inhibitors of apoptosis family (IAP), which can inhibit caspase activation to reduce apoptosis (Heussler et al., 2001; Martin-Hernandez et al., 2017). Microsporidian *Nosema ceranae* and *Nosema apis* were reported to suppress host apoptosis via up-regulating expression of the *buffy* and *BIRC5* (Higes et al., 2013; Martin-Hernandez et al., 2017; **Figure 4A**). In mitochondria-mediated apoptosis pathway, the tumor suppressor protein p53 is activated for recruiting Bax (pro-apoptosis protein member of Bcl-2 family) to mitochondrial membrane. Then the Bax promotes the release of cytochrome c (CYT-C) from mitochondria to cytoplasm, where the CYT-C binds to apoptosis protease activated factor1 (APAF1). Finally, the APAF1, cytochrome c and caspase-9 assemble and form a protein complex to facilitate cell death (Heussler et al., 2001; **Figure 4A**). Microsporidian *Nosema bombycis* can also inhibit host apoptosis by down-regulating the expression of *apaf1* and *cyt-c* and up-regulating the expression of *buffy*, so that reduce caspase-3 activity and inhibit host apoptosis (He et al., 2015). Besides, *Encephalitozoon* infection can suppress apoptosis of Vero cells by inhibiting the cleavage of caspase-3, phosphorylation and translocation of p53 (del Aguila et al., 2006; **Figure 4B**). In the apoptosis process, the p53 activated the expressions of *p21* and *Bax* to induce apoptosis (Miyashita et al., 1994). However, expressional changes of the *Bcl-2* and *Bax* are not observed in *Encephalitozoon* infected Vero cells for unknown reasons (del Aguila et al., 2006). A previous study showed that *T. gondii* prevented the activation and cytosol-mitochondrial targeting of Bax but not the protein levels to inhibit host apoptosis (Hippe et al., 2009). It is possible that *Encephalitozoon* also utilize mechanisms similar to that of the *T. gondii* to modulate host Bax.

In a recent study, the expressions of 84 apoptosis-related genes were investigated in *E. cuniculi* and *Vittaforma corneae* infected THP1 cell line. As a result, both pathogens can manipulate intrinsic apoptosis pathway (Sokolova et al., 2019). The assayed pro-apoptosis genes including *LTA, CARD8, TRADD, BAX, CASP3, CASP1, CASP4, CASP9, BP2, DARK1*, and *BCLAF1* are all down-regulated, while some anti-apoptosis genes, such as *ABL1, BAG1, BAG3, BCL2, TNFRSF1A*, and *CD40LG*, are all up-regulated upon infection. This study suggests that host apoptosis pathway is deeply modulated by the pathogen. Similar to *Encephalitozoon,* other intracellular parasites, such as *T. gondii, Trypanosoma cruzi*, and *Cryptosporidium parvum*, were also found to inhibit host apoptosis via similar mechanisms (Heussler et al., 2001; Luder et al., 2001; Mammari et al., 2019), indicating that intracellular pathogens can modulate host apoptosis pathway with similar or conserved strategies.

Antimicrobial Peptides Response to Microsporidian Infection

Antimicrobial peptides are important components of the host innate immune system. It was reported that lactoferrin (Lf), lysozyme (Lz), human beta defensin 2 (HBD2), human alpha defensin 5 (HD5), and human alpha defensin 1 (HNP1) are capable of inhibiting microsporidian spore germination and reducing enterocytes infection (Leitch and Ceballos, 2008). For example, the germination of *Encephalitozoon hellem* spore can be inhibited by HNP1. And the germination of *Anncaliia algerae* spore can also be blocked by Lf, HBD2, HD5, and HNP1 (Leitch and Ceballos, 2008). However, this inhibitory ability of antimicrobial peptides is not applicable to all microsporidian species. The germination of *Encephalitozoon intestinalis* spores cannot be inhibited by any of the peptides listed above (Leitch and Ceballos, 2008). It is likely that microsporidia have different germination mechanisms.

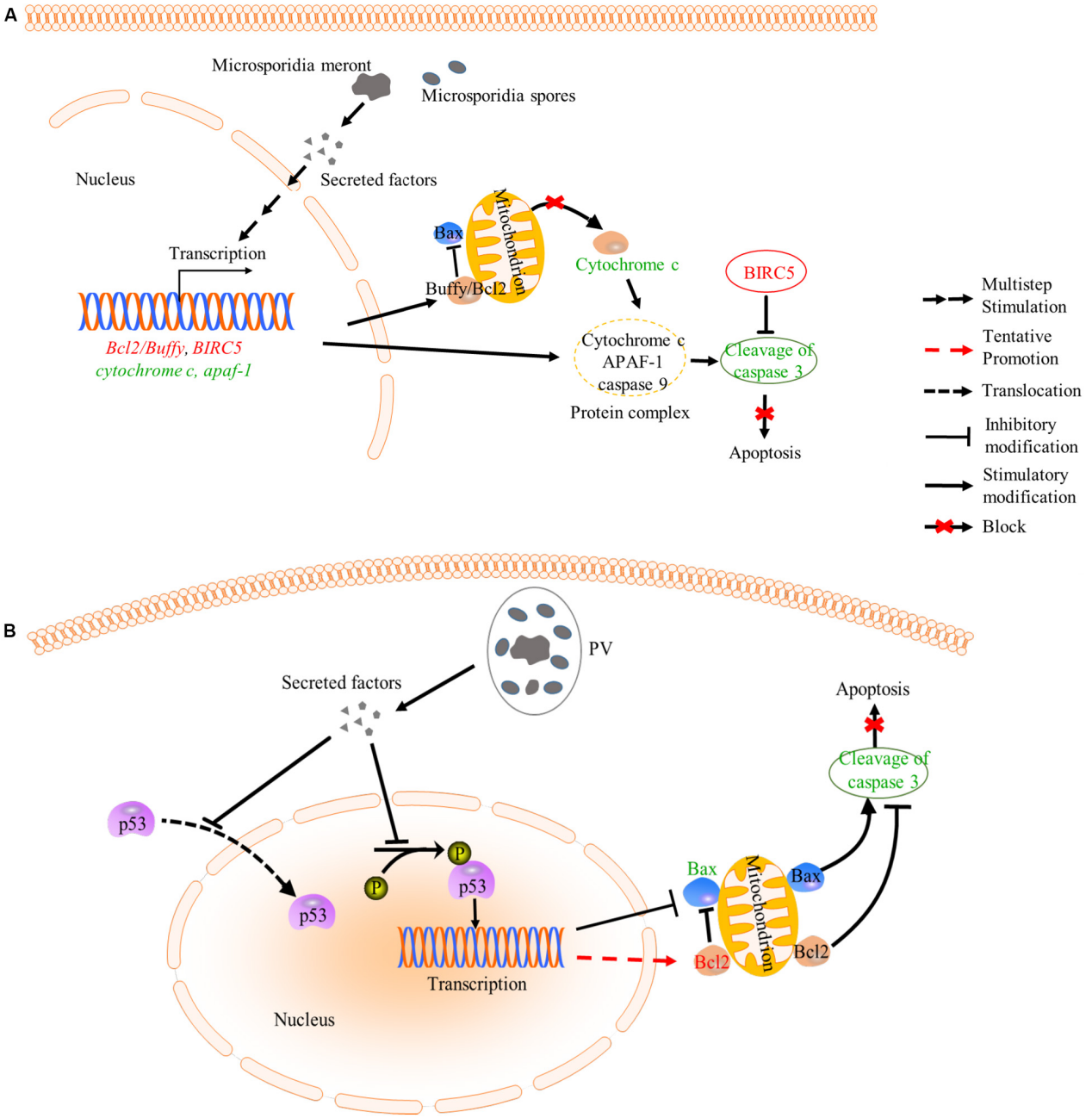

FIGURE 4 | Inhibition of apoptosis by microsporidia. **(A)** Microsporidian species which directly expose to host cytoplasm can inhibit the release of cytochrome c (CYT-C) by up-regulating the expression of *Bcl2/Buffy*. Besides, down-regulated expression of *cyt-c* and *apaf-1* may cause reduction of cytochrome-APAF1-Caspase 9 complexes, which decrease cleavage activity of caspase 3. And BIRC5 belongs to a member of IAP which can inhibit the capase3 activation. These changes caused the inhibition of host apoptosis. **(B)** Microsporidia species which live inside PV can inhibit host apoptosis by decreasing the phosphorylation and nuclear translocation of p53, which also leads to suppression of cleavage activity of caspase 3. words in red: up-regulated gene; Words in green: down-regulated gene; PV, parasitophorous vacuole.

ADAPTIVE IMMUNE RESPONSE AGAINST MICROSPORIDIAN INFECTION

Adaptive immunity is broader and more efficient protection against non-self antigens than innate immune system. Adaptive immunity involves T lymphocytes-mediated cellular immunity and B lymphocytes-mediated humoral immunity, which have a tightly regulated interplay with antigen-presenting cells and facilitate the pathogen-specific elimination (Bonilla and Oettgen, 2010). When the innate immunity fails to block pathogen invasion, the adaptive immunity with production of antibodies and cytotoxic T lymphocytes (CTLs) will be triggered to

resolve the infection. And T cell-mediated immunity plays a principal role in protection against microsporidia lethal infection (Valencakova and Halanova, 2012).

Humoral Immune Response to Microsporidian Infection

Humoral immunity is a very effective way to scavenge pathogens from the host (Casadevall, 2018). Treatment of Vero E6 cells with anti-exospore monoclonal antibody P5/H1 could reduce *E. cuniculi* infection *in vitro*. One explanation for the inhibition is that P5/H1 neutralizes sensitive epitopes on *E. cuniculi* spores so that the growth of the pathogens was suppressed (Schmidt and Shadduck, 1984). Antibodies binding to spores led to macrophages making more efficient phagocytosis and increase oxidative burst (Sak et al., 2004). In addition, the P5/H1 could prolong the survival of microsporidia-infected SCID mice, which were reconstituted with CD4+ T lymphocytes (Sak et al., 2006). Further studies showed that the protective effect of the antibodies on SCID mice depends on IFN-γ (Salat et al., 2008).

Microsporidia like *E. cuniculi* are able to induce a strong antibody response. Increase of IgA, IgM, and IgG were detected in infected mice (Cox, 1977; Sak and Ditrich, 2005; Omalu et al., 2007; **Figure 3**). However, these antibodies cannot protect IFN-γ knockout mice and athymic BALB/c (nu/nu) from death upon *E. cuniculi* infection (Schmidt and Shadduck, 1983; Salat et al., 2004; Valencakova and Halanova, 2012), suggesting that the antibody alone is not powerful enough to completely clear the infection.

T Cell-Mediated Immune Response to Microsporidian Infection

T cell-mediated immune response in host is crucial for prevention of infection. CD4+ and CD8+ T cells were found induced in infected mice and rabbits (El Naas et al., 1999; Soto-Dominguez et al., 2020), and were important in resisting against microsporidia (de Moura et al., 2019). And among T cell population, the CD8+ T cell subtype plays a major role during infection (Moretto et al., 2004). However, the activation of CD8+ T cell is associated with other immune cells and cytokines (Moretto et al., 2010; Langanke Dos Santos et al., 2017). The CD4+ T cells can be activated by infection and will develop to effective T cells. The number of CD4+ T cells increased upon microsporidian infection in mice (El Naas et al., 1999). In addition, spleen cells from wild mice inoculated with *E. intestinalis* were shown to have elevated levels of IFN-γ and IL-2 (El Fakhry et al., 2001), which are cytokines secreted by Th1 and involved in activation of CD8+ T cells. Adoptive transfer of pure CD4+ T cells can prolong the survival of SCID mice (Salat et al., 2006). However, adoptive transfer of CD4+ T cells from IFN-γ deficient mice cannot prolong the survival of SCID mice (Salat et al., 2008). These results indicate that CD8+ T lymphocytes-independent protection against the infection can be mediated by CD4+ T lymphocytes and the protective immunity is mediated by IFN-γ, which is a potential activator of macrophages. In other studies, the co-inhibitory receptor killer-cell lectin like receptor G1 (KLRG1) was found to be expressed in NKs and antigen-experienced T cells (Henson and Akbar, 2009). During the response against *E. cuniculi,* the KLRG1+ T cell subset was the majority of polyfunctional effector CD8+ T cells (Bhadra et al., 2014). A more recent study demonstrated that IL-21 secreted by the CD4+ T cells was important for inducing KLRG1^{+} effector CD8+ T cells against microsporidian infection (Moretto and Khan, 2016; **Figure 3**). These studies indicate that the CD4+ T cells play roles against microsporidian infection. However, mice lacking CD4+ T cell still can survive from microsporidian infection (Moretto et al., 2000), suggesting that CD4+ T cell is not a key immune defense against the infection.

Strong CD8+ T cell responses were also observed during microsporidian infection (Khan et al., 1999). The CD8$^{-/-}$ mice became more susceptible to *E. cuniculi* infection (Moretto et al., 2000). And SCID mice, deficient in T and B cells, reconstituted with CD8+ T cell-contained splenocytes resolved the infection (Braunfuchsova et al., 2001; Salat et al., 2002). These results suggest that the CD8+ T lymphocytes play a crucial role in resisting against *E. cuniculi*. And this protection depends on the activity of CD8+ CTLs, which lead to lysis of infected cells by perforin pathway (Khan et al., 1999; **Figure 3**). Moreover, trigger of CD8+ T cells into CTLs had been documented. The activation of the CD8+ T cells can be evoked by CD4+ T cells. For example, mice lacking CD4+ T cells show a lower CTLs response to virus infection (Matloubian et al., 1994). However, CD4+ T cell deficiency does not affect the effector CD8+ T cell responding against *E. cuniculi* infection (Moretto et al., 2000), suggesting CD4+ T cell is not the sole activator of CD8+ T cell response and another reason is associated with the route of infection (Moretto et al., 2004; de Moura et al., 2019). It was found that other immune cell types like DC, γδ T cell, and B-1 cell are also key roles in modulating the antigen-specific CD8+ T cell immunity (Moretto et al., 2001; Langanke Dos Santos et al., 2017). The γδ T cells were reported to be important for establishing primary immune response against pathogen infection by producing cytokines (Berguer and Ferrick, 1995; Ferrick et al., 1995; **Figure 3**). It was found that the γδ T cell significantly increases in early infection of mice by *E. cuniculi,* while lacking of γδ T cell causes down-regulation of CD8+ cell immune response (Moretto et al., 2001). In addition to γδ T cell, the B-1 cell was found to be able to decrease host susceptibility to *E. cuniculi* (da Costa et al., 2016). In microsporidia-infected BABL/c XID mice, which are B-1 cell deficient, the population of CD8+ T cell decreases compared with that of infected BABL/c mice (Langanke Dos Santos et al., 2017). This suggests that the B-1 cell can increase the immunity of the CD8+ T lymphocytes, in addition to increasing pro-inflammatory cytokines and modulating M1 prolife (Pereira et al., 2019). Probably, B-1 cell behaves as an APC to increase population of CD8+ T cell and promotes the activation of CD4+ T cell (Hardy, 2006; Margry et al., 2013). Besides, the CD8+ T cell response can also be activated by DCs-secreted IL-12 during infection by *E. cuniculi* (Moretto et al., 2010; **Figure 3**). These findings demonstrate that CD8+ T cell is vital in responses against microsporidia and also explain why CD8+ T cell can be induced in the absence of the CD4+ T cell.

In general, T cell-mediated immune protection is essential for elimination of microsporidian infection. However, microsporidian spores still can remain in some organs of immunocompetent mice and may become a source of infection onset (Kotkova et al., 2013; Sak et al., 2017). This raises an important question that how microsporidia escape the strong immunities.

CONCLUSION

The innate and adaptive immune systems play vital roles against microsporidian infection. Further understanding of host immune responses against the infection will greatly help with the diagnosis and treatment of microsporidiosis. The innate immune system not only directly resists the infection but also triggers the adaptive immunity. Innate immune cells, such as macrophages, DCs, γδ T cell, and NKs, can control microsporidia to some extent, and also secret cytokines and chemokines to assist both the innate and adaptive immunities against the infection. The cytokine IL-12 and IFN-γ can help to clear the parasite by activating related immune responses. However, early expression of IL-10 is benefit for the pathogen growth by negatively regulating the IFN-gamma expression. Yet the relation between IL-10 and microsporidia remains to be clarified. Besides, it is worth noting that lymphokines can also activate macrophages to kill microsporidia (Schmidt and Shadduck, 1984; **Figure 3**). With the innate immunities, however, the host cell cannot completely clear microsporidia probably due to the evasive mechanism of the pathogens (Weidner, 1975; Bernal et al., 2016).

To completely clear the infection, the host needs to initiate the adaptive immunity. First of all, the CTL can be activated to restrict the proliferation of microsporidia by lysing infected cells via perforin pathway (**Figure 3**). In addition, increase of IgA, IgM, and IgG was observed in microsporidia-infected mice (Cox, 1977; Sak and Ditrich, 2005; Omalu et al., 2007). Furthermore, specific antibodies have been found to have strong inhibitory effects against microsporidia (Sak et al., 2004, 2006). In the adaptive immunity, antibodies play important roles in resisting against microsporidia. However, humoral responses to microsporidian infection have not been clearly illuminated and further studies with microsporidia-infected mice models are needed.

In summary, the interactions between microsporidia and host immune systems have been further studied, but are far to be fully elucidated. For example, what are the key host cells and factors that confer the defense effects. And what are the mechanisms that microsporidia modulate host immune responses. Hopefully, genomics and proteomics studies on microsporidia have provided some important clues and candidates to dissect the questions (Katinka et al., 2001; Mittleider et al., 2002; Akiyoshi et al., 2009; Corradi et al., 2010; Reinke et al., 2017).

AUTHOR CONTRIBUTIONS

TL and ZZ contributed to conception and design of the study. TL and YH wrote the first draft of the manuscript. HG, JX, JL, BH, JB, and GP wrote sections of the manuscript. All authors contributed to manuscript revision, read and approved the submitted version.

FUNDING

This work was supported by grants from the National Natural Science Foundation of China (31772678, 31472151, and 31770159), Natural Science Foundation of Chongqing, China (cstc2019yszx-jcyjX0010), and Fundamental Research Funds for the Central Universities (XDJK2019TY002).

REFERENCES

Abu-Akkada, S. S., El Kerdany, E. D. H., Mady, R. F., Diab, R. G., Khedr, G. A. E., Ashmawy, K. I., et al. (2015). *Encephalitozoon cuniculi* infection among immunocompromised and immunocompetent humans in Egypt. *Iranian J. Parasitol.* 10, 561–570.

Achbarou, A., Ombrouck, C., Gneragbe, T., Charlotte, F., Renia, L., Desportes-Livage, I., et al. (1996). Experimental model for human intestinal microsporidiosis in interferon gamma receptor knockout mice infected by *Encephalitozoon intestinalis*. *Parasite Immunol.* 18, 387–392. doi: 10.1046/j.1365-3024.1996.d01-128.x

Akiyoshi, D. E., Morrison, H. G., Lei, S., Feng, X., Zhang, Q., Corradi, N., et al. (2009). Genomic survey of the non-cultivatable opportunistic human pathogen, *Enterocytozoon bieneusi*. *PLoS Pathog.* 5:e1000261. doi: 10.1371/journal.ppat.1000261

Berguer, R., and Ferrick, D. A. (1995). Differential production of intracellular gamma interferon in alpha beta and gamma delta T-cell subpopulations in response to peritonitis. *Infect. Immun.* 63, 4957–4958. doi: 10.1128/iai.63.12.4957-4958.1995

Bernal, C. E., Zorro, M. M., Sierra, J., Gilchrist, K., Botero, J. H., Baena, A., et al. (2016). *Encephalitozoon intestinalis* inhibits dendritic cell differentiation through an IL-6-dependent mechanism. *Front. Cell. Infect. Microbiol.* 6:4. doi: 10.3389/fcimb.2016.00004

Beutler, B. (2004). Innate immunity: an overview. *Mol. Immunol.* 40, 845–859. doi: 10.1016/j.molimm.2003.10.005

Bhadra, R., Moretto, M. M., Castillo, J. C., Petrovas, C., Ferrando-Martinez, S., Shokal, U., et al. (2014). Intrinsic TGF-beta signaling promotes age-dependent CD8+ T cell polyfunctionality attrition. *J. Clin. Invest.* 124, 2441–2455. doi: 10.1172/JCI70522

Bieber, K., and Autenrieth, S. E. (2020). Dendritic cell development in infection. *Mol. Immunol.* 121, 111–117. doi: 10.1016/j.molimm.2020.02.015

Bonilla, F. A., and Oettgen, H. C. (2010). Adaptive immunity. *J. Allergy Clin. Immunol.* 125, S33–S40. doi: 10.1016/j.jaci.2009.09.017

Braunfuchsova, P., Kopecky, J., Ditrich, O., and Koudela, B. (1999). Cytokine response to infection with the microsporidian, *Encephalitozoon cuniculi*. *Folia Parasitol. (Praha)* 46, 91–95.

Braunfuchsova, P., Salat, J., and Kopecky, J. (2001). CD8+ T lymphocytes protect SCID mice against *Encephalitozoon cuniculi* infection. *Int. J. Parasitol.* 31, 681–686. doi: 10.1016/s0020-7519(01)00134-5

Cali, A., Becnel, J. J., and Takvorian, P. M. (2017). "Microsporidia," in *Handbook of the Protists*, eds J. M. Archibald, A. G. B. Simpson, and C. H. Slamovits (Cham: Springer International Publishing), 1559–1618.

Casadevall, A. (2018). Antibody-based vaccine strategies against intracellular pathogens. *Curr. Opin. Immunol.* 53, 74–80. doi: 10.1016/j.coi.2018.04.011

Corradi, N., Pombert, J. F., Farinelli, L., Didier, E. S., and Keeling, P. J. (2010). The complete sequence of the smallest known nuclear genome from the

microsporidian *Encephalitozoon intestinalis*. *Nat. Commun.* 1:77. doi: 10.1038/ncomms1082

Couper, K. N., Blount, D. G., and Riley, E. M. (2008). IL-10: the master regulator of immunity to infection. *J. Immunol.* 180, 5771–5777. doi: 10.4049/jimmunol.180.9.5771

Cox, J. C. (1977). Altered immune responsiveness associated with *Encephalitozoon cuniculi* infection in rabbits. *Infect. Immun.* 15, 392–395. doi: 10.1128/iai.15.2.392-395.1977

da Costa, L. F. V., Alvares-Saraiva, A. M., Dell'Armelina Rocha, P. R., Spadacci-Morena, D. D., Perez, E. C., Mariano, M., et al. (2016). B-1 cell decreases susceptibility to encephalitozoonosis in mice. *Immunobiology* 222, 218–227. doi: 10.1016/j.imbio.2016.09.018

de Moura, M. L. C., Alvares-Saraiva, A. M., Pérez, E. C., Xavier, J. G., Spadacci-Morena, D. D., Moysés, C. R. S., et al. (2019). Cyclophosphamide treatment mimics sub-lethal infections with *Encephalitozoon intestinalis* in immunocompromised individuals. *Front. Microbiol.* 10:2205. doi: 10.3389/fmicb.2019.02205

del Aguila, C., Izquierdo, F., Granja, A. G., Hurtado, C., Fenoy, S., Fresno, M., et al. (2006). *Encephalitozoon* microsporidia modulates p53-mediated apoptosis in infected cells. *Int. J. Parasitol.* 36, 869–876. doi: 10.1016/j.ijpara.2006.04.002

Didier, E. S. (1995). Reactive nitrogen intermediates implicated in the inhibition of *Encephalitozoon cuniculi* (phylum microspora) replication in murine peritoneal macrophages. *Parasite Immunol.* 17, 405–412. doi: 10.1111/j.1365-3024.1995.tb00908.x

Didier, E. S., Bowers, L. C., Martin, A. D., Kuroda, M. J., Khan, I. A., and Didier, P. J. (2010). Reactive nitrogen and oxygen species, and iron sequestration contribute to macrophage-mediated control of *Encephalitozoon cuniculi* (Phylum Microsporidia) infection in vitro and in vivo. *Microbes Infect.* 12, 1244–1251. doi: 10.1016/j.micinf.2010.09.010

Didier, E. S., and Shadduck, J. A. (1994). IFN-gamma and LPS induce murine macrophages to kill *Encephalitozoon cuniculi* in vitro. *J. Eukaryot. Microbiol.* 41:34S.

El Fakhry, Y., Achbarou, A., Desportes, I., and Mazier, D. (2001). Resistance to *Encephalitozoon intestinalis* is associated with interferon-gamma and interleukin-2 cytokines in infected mice. *Parasite Immunol.* 23, 297–303. doi: 10.1046/j.1365-3024.2001.00386.x

El Fakhry, Y., Achbarou, A., Desportes-Livage, I., and Mazier, D. (1998). *Encephalitozoon intestinalis*: humoral responses in interferon-gamma receptor knockout mice infected with a microsporidium pathogenic in AIDS patients. *Exp. Parasitol.* 89, 113–121. doi: 10.1006/expr.1998.4267

El Naas, A., Levkut, M., Revajova, V., Levkutova, M., Hipikova, V., and Letkova, V. (1999). Immune response to *Encephalitozoon cuniculi* infection in laboratory mice. *Vet. Parasitol.* 82, 137–143. doi: 10.1016/s0304-4017(98)00261-1

Fayer, R., and Santin-Duran, M. (2014). "Epidemiology of microsporidia in human infections," in *Microsporidia: Pathogens of Opportunity*, 1st Edn, eds L. M. Weiss and J. J. Becnel (Oxford: Wiley Blackwell), 135–164. doi: 10.1002/9781118395264.ch3

Ferrick, D. A., Schrenzel, M. D., Mulvania, T., Hsieh, B., Ferlin, W. G., and Lepper, H. (1995). Differential production of interferon-gamma and interleukin-4 in response to Th1- and Th2-stimulating pathogens by gamma delta T cells in vivo. *Nature* 373, 255–257. doi: 10.1038/373255a0

Fischer, J., Suire, C., and Hale-Donze, H. (2008a). Toll-like receptor 2 recognition of the microsporidia *Encephalitozoon* spp. induces nuclear translocation of NF-kappaB and subsequent inflammatory responses. *Infect. Immun.* 76, 4737–4744. doi: 10.1128/IAI.00733-08

Fischer, J., Tran, D., Juneau, R., and Hale-Donze, H. (2008b). Kinetics of *Encephalitozoon* spp. infection of human macrophages. *J. Parasitol.* 94, 169–175. doi: 10.1645/GE-1303.1

Fischer, J., West, J., Agochukwu, N., Suire, C., and Hale-Donze, H. (2007). Induction of host chemotactic response by *Encephalitozoon* spp. *Infect. Immun.* 75, 1619–1625. doi: 10.1128/IAI.01535-06

Franzen, C. (2005). How do microsporidia invade cells? *Folia Parasitol. (Praha)* 52, 36–40. doi: 10.14411/fp.2005.005

Franzen, C., Hartmann, P., and Salzberger, B. (2005a). Cytokine and nitric oxide responses of monocyte-derived human macrophages to microsporidian spores. *Exp. Parasitol.* 109, 1–6. doi: 10.1016/j.exppara.2004.10.001

Franzen, C., Müller, A., Hartmann, P., and Salzberger, B. (2005b). Cell invasion and intracellular fate of *Encephalitozoon cuniculi* (Microsporidia). *Parasitology* 130(Pt 3), 285–292. doi: 10.1017/s0031182004006633x

Ghosh, K., and Weiss, L. M. (2012). T cell response and persistence of the microsporidia. *FEMS Microbiol. Rev.* 36, 748–760. doi: 10.1111/j.1574-6976.2011.00318.x

Ghoyounchi, R., Mahami-Oskouei, M., Rezamand, A., Spotin, A., Aminisani, N., Nami, S., et al. (2019). Molecular phylodiagnosis of *Enterocytozoon bieneusi* and *Encephalitozoon intestinalis* in children with cancer: microsporidia in malignancies as an emerging opportunistic infection. *Acta Parasitol.* 64, 103–111. doi: 10.2478/s11686-018-00012-w

Gigley, J. P., and Khan, I. A. (2011). Plasmacytoid DC from aged mice down-regulate CD8 T cell responses by inhibiting cDC maturation after *Encephalitozoon cuniculi* infection. *PLoS One* 6:e20838. doi: 10.1371/journal.pone.0020838

Gonzalez-Machorro, J. R., Rodriguez-Tovar, L. E., Gomez-Flores, R., Soto-Dominguez, A., Rodriguez-Rocha, H., Garcia-Garcia, A., et al. (2019). Increased phagocytosis and growth inhibition of *Encephalitozoon cuniculi* by LPS-activated J774A.1 murine macrophages. *Parasitol. Res.* 118, 1841–1848. doi: 10.1007/s00436-019-06310-0

Han, B., Takvorian, P. M., and Weiss, L. M. (2020). Invasion of host cells by microsporidia. *Front. Microbiol.* 11:172. doi: 10.3389/fmicb.2020.00172

Han, B., and Weiss, L. M. (2017). Microsporidia: obligate intracellular pathogens within the fungal kingdom. *Microbiol. Spectr.* 5:10.1128/microbiolspec.FUNK-0018-2016. doi: 10.1128/microbiolspec.FUNK-0018-2016

Hardy, R. R. (2006). B-1 B cells: development, selection, natural autoantibody and leukemia. *Curr. Opin. Immunol.* 18, 547–555. doi: 10.1016/j.coi.2006.07.010

He, X., Fu, Z., Li, M., Liu, H., Cai, S., Man, N., et al. (2015). *Nosema bombycis* (Microsporidia) suppresses apoptosis in BmN cells (*Bombyx mori*). *Acta Biochim. Biophys. Sin. (Shanghai)* 47, 696–702. doi: 10.1093/abbs/gmv062

Henson, S. M., and Akbar, A. N. (2009). KLRG1–more than a marker for T cell senescence. *Age (Dordr)* 31, 285–291. doi: 10.1007/s11357-009-9100-9

Heussler, V. T., Kuenzi, P., and Rottenberg, S. (2001). Inhibition of apoptosis by intracellular protozoan parasites. *Int. J. Parasitol.* 31, 1166–1176. doi: 10.1016/s0020-7519(01)00271-5

Higes, M., Juarranz, A., Dias-Almeida, J., Lucena, S., Botias, C., Meana, A., et al. (2013). Apoptosis in the pathogenesis of *Nosema ceranae* (Microsporidia: *Nosematidae*) in honey bees (*Apis mellifera*). *Environ. Microbiol. Rep.* 5, 530–536. doi: 10.1111/1758-2229.12059

Hippe, D., Weber, A., Zhou, L., Chang, D. C., Hacker, G., and Luder, C. G. (2009). *Toxoplasma gondii* infection confers resistance against BimS-induced apoptosis by preventing the activation and mitochondrial targeting of pro-apoptotic Bax. *J. Cell. Sci.* 122(Pt 19), 3511–3521. doi: 10.1242/jcs.050963

Katinka, M. D., Duprat, S., Cornillot, E., Metenier, G., Thomarat, F., Prensier, G., et al. (2001). Genome sequence and gene compaction of the eukaryote parasite *Encephalitozoon cuniculi*. *Nature* 414, 450–453. doi: 10.1038/35106579

Khan, I. A., and Moretto, M. (1999). Role of gamma interferon in cellular immune response against murine *Encephalitozoon cuniculi* infection. *Infect. Immun.* 67, 1887–1893. doi: 10.1128/.67.4.1887-1893.1999

Khan, I. A., Moretto, M., and Weiss, L. M. (2001). Immune response to *Encephalitozoon cuniculi* infection. *Microbes Infect.* 3, 401–405. doi: 10.1016/s1286-4579(01)01397-1

Khan, I. A., Schwartzman, J. D., Kasper, L. H., and Moretto, M. (1999). CD8+ CTLs are essential for protective immunity against *Encephalitozoon cuniculi* infection. *J. Immunol.* 162, 6086–6091.

Knodler, L. A., and Finlay, B. B. (2001). *Salmonella* and apoptosis: to live or let die? *Microbes Infect.* 3, 1321–1326. doi: 10.1016/s1286-4579(01)01493-9

Kotkova, M., Sak, B., Kvetonova, D., and Kvac, M. (2013). Latent microsporidiosis caused by *Encephalitozoon cuniculi* in immunocompetent hosts: a murine model demonstrating the ineffectiveness of the immune system and treatment with albendazole. *PLoS One* 8:e60941. doi: 10.1371/journal.pone.0060941

Kurze, C., Le Conte, Y., Dussaubat, C., Erler, S., Kryger, P., Lewkowski, O., et al. (2015). Nosema tolerant honeybees (*Apis mellifera*) escape parasitic manipulation of apoptosis. *PLoS One* 10:e0140174. doi: 10.1371/journal.pone.0140174

Langanke Dos Santos, D., Alvares-Saraiva, A. M., Xavier, J. G., Spadacci-Morena, D. D., Peres, G. B., Dell'Armelina Rocha, P. R., et al. (2017). B-1 cells upregulate CD8 T lymphocytes and increase proinflammatory cytokines serum levels in

oral encephalitozoonosis. *Microbes Infect.* 20, 196–204. doi: 10.1016/j.micinf.2017.11.004

Lawlor, E. M., Moretto, M. M., and Khan, I. A. (2010). Optimal CD8 T-cell response against *Encephalitozoon cuniculi* is mediated by Toll-like receptor 4 upregulation by dendritic cells. *Infect. Immun.* 78, 3097–3102. doi: 10.1128/IAI.00181-10

Leitch, G. J., and Ceballos, C. (2008). A role for antimicrobial peptides in intestinal microsporidiosis. *Parasitology* 136, 175–181. doi: 10.1017/s0031182008005313

Li, W., Feng, Y., Zhang, L., and Xiao, L. (2019). Potential impacts of host specificity on zoonotic or interspecies transmission of *Enterocytozoon bieneusi*. *Infect. Genet. Evol.* 75:104033. doi: 10.1016/j.meegid.2019.104033

Lores, B., Lopez-Miragaya, I., Arias, C., Fenoy, S., Torres, J., and del Aguila, C. (2002). Intestinal microsporidiosis due to *Enterocytozoon bieneusi* in elderly human immunodeficiency virus–negative patients from Vigo, Spain. *Clin. Infect. Dis.* 34, 918–921. doi: 10.1086/339205

Luder, C. G., Gross, U., and Lopes, M. F. (2001). Intracellular protozoan parasites and apoptosis: diverse strategies to modulate parasite-host interactions. *Trends Parasitol.* 17, 480–486. doi: 10.1016/s1471-4922(01)02016-5

Mammari, N., Halabi, M. A., Yaacoub, S., Chlala, H., Darde, M. L., and Courtioux, B. (2019). *Toxoplasma gondii* modulates the host cell responses: an overview of apoptosis pathways. *Biomed. Res. Int.* 2019:6152489. doi: 10.1155/2019/6152489

Margry, B., Wieland, W. H., van Kooten, P. J., van Eden, W., and Broere, F. (2013). Peritoneal cavity B-1a cells promote peripheral CD4+ T-cell activation. *Eur. J. Immunol.* 43, 2317–2326. doi: 10.1002/eji.201343418

Martinez, F. O., and Gordon, S. (2014). The M1 and M2 paradigm of macrophage activation: time for reassessment. *F1000Prime Rep.* 6:13. doi: 10.12703/P6-13

Martin-Hernandez, R., Higes, M., Sagastume, S., Juarranz, A., Dias-Almeida, J., Budge, G. E., et al. (2017). Microsporidia infection impacts the host cell's cycle and reduces host cell apoptosis. *PLoS One* 12:e0170183. doi: 10.1371/journal.pone.0170183

Mathews, A., Hotard, A., and Hale-Donze, H. (2009). Innate immune responses to *Encephalitozoon* species infections. *Microbes Infect.* 11, 905–911. doi: 10.1016/j.micinf.2009.06.004

Matloubian, M., Concepcion, R. J., and Ahmed, R. (1994). CD4+ T cells are required to sustain CD8+ cytotoxic T-cell responses during chronic viral infection. *J. Virol.* 68, 8056–8063. doi: 10.1128/jvi.68.12.8056-8063.1994

Mellman, I., and Steinman, R. M. (2001). Dendritic cells: specialized and regulated antigen processing machines. *Cell* 106, 255–258. doi: 10.1016/s0092-8674(01)00449-4

Mittleider, D., Green, L. C., Mann, V. H., Michael, S. F., Didier, E. S., and Brindley, P. J. (2002). Sequence survey of the genome of the opportunistic microsporidian pathogen, *Vittaforma corneae*. *J. Eukaryot. Microbiol.* 49, 393–401. doi: 10.1111/j.1550-7408.2002.tb00218.x

Miyashita, T., Krajewski, S., Krajewska, M., Wang, H. G., Lin, H. K., Liebermann, D. A., et al. (1994). Tumor suppressor p53 is a regulator of bcl-2 and bax gene expression in vitro and in vivo. *Oncogene* 9, 1799–1805.

Mor, S. M., Tumwine, J. K., Naumova, E. N., Ndeezi, G., and Tzipori, S. (2009). Microsporidiosis and malnutrition in children with persistent diarrhea, Uganda. *Emerg. Infect. Dis.* 15, 49–52. doi: 10.3201/eid1501.071536

Moretto, M., Casciotti, L., Durell, B., and Khan, I. A. (2000). Lack of CD4(+) T cells does not affect induction of CD8(+) T-cell immunity against *Encephalitozoon cuniculi* infection. *Infect. Immun.* 68, 6223–6232. doi: 10.1128/iai.68.11.6223-6232.2000

Moretto, M., Durell, B., Schwartzman, J. D., and Khan, I. A. (2001). Gamma delta T cell-deficient mice have a down-regulated CD8+ T cell immune response against *Encephalitozoon cuniculi* infection. *J. Immunol.* 166, 7389–7397. doi: 10.4049/jimmunol.166.12.7389

Moretto, M., Weiss, L. M., and Khan, I. A. (2004). Induction of a rapid and strong antigen-specific intraepithelial lymphocyte response during oral *Encephalitozoon cuniculi* infection. *J. Immunol.* 172, 4402–4409. doi: 10.4049/jimmunol.172.7.4402

Moretto, M. M., and Khan, I. A. (2016). IL-21 is important for induction of KLRG1+ effector CD8 T cells during acute intracellular infection. *J. Immunol.* 196, 375–384. doi: 10.4049/jimmunol.1501258

Moretto, M. M., Khan, I. A., and Weiss, L. M. (2012). Gastrointestinal cell mediated immunity and the microsporidia. *PLoS Pathog.* 8:e1002775. doi: 10.1371/journal.ppat.1002775

Moretto, M. M., Lawlor, E. M., and Khan, I. A. (2008). Aging mice exhibit a functional defect in mucosal dendritic cell response against an intracellular pathogen. *J. Immunol.* 181, 7977–7984. doi: 10.4049/jimmunol.181.11.7977

Moretto, M. M., Lawlor, E. M., and Khan, I. A. (2010). Lack of interleukin-12 in p40-deficient mice leads to poor CD8+ T-cell immunity against *Encephalitozoon cuniculi* infection. *Infect. Immun.* 78, 2505–2511. doi: 10.1128/IAI.00753-09

Moretto, M. M., Weiss, L. M., Combe, C. L., and Khan, I. A. (2007). IFN-gamma-producing dendritic cells are important for priming of gut intraepithelial lymphocyte response against intracellular parasitic infection. *J. Immunol.* 179, 2485–2492. doi: 10.4049/jimmunol.179.4.2485

Nash, P. B., Purner, M. B., Leon, R. P., Clarke, P., Duke, R. C., and Curiel, T. J. (1998). *Toxoplasma gondii*-infected cells are resistant to multiple inducers of apoptosis. *J. Immunol.* 160, 1824–1830.

Niederkorn, J. Y., Brieland, J. K., and Mayhew, E. (1983). Enhanced natural killer cell activity in experimental murine encephalitozoonosis. *Infect. Immun.* 41, 302–307. doi: 10.1128/iai.41.1.302-307.1983

Omalu, I. C., Duhlinska, D. D., Anyanwu, G. I., Pam, V. A., and Inyama, P. U. (2007). Immune responsiveness associated with experimental *Encephalitozoon intestinalis* infection in immunocompetent rats. *Indian J. Med. Microbiol.* 25, 209–213.

Pereira, A., Alvares-Saraiva, A. M., Konno, F. T. C., Spadacci-Morena, D. D., Perez, E. C., Mariano, M., et al. (2019). B-1 cell-mediated modulation of M1 macrophage profile ameliorates microbicidal functions and disrupt the evasion mechanisms of *Encephalitozoon cuniculi*. *PLoS Negl. Trop. Dis.* 13:e0007674. doi: 10.1371/journal.pntd.0007674

Popi, A. F., Lopes, J. D., and Mariano, M. (2004). Interleukin-10 secreted by B-1 cells modulates the phagocytic activity of murine macrophages in vitro. *Immunology* 113, 348–354. doi: 10.1111/j.1365-2567.2004.01969.x

Quinn, L., Coombe, M., Mills, K., Daish, T., Colussi, P., Kumar, S., et al. (2003). Buffy, a *Drosophila* Bcl-2 protein, has anti-apoptotic and cell cycle inhibitory functions. *EMBO J.* 22, 3568–3579. doi: 10.1093/emboj/cdg355

Reinke, A. W., Balla, K. M., Bennett, E. J., and Troemel, E. R. (2017). Identification of microsporidia host-exposed proteins reveals a repertoire of rapidly evolving proteins. *Nat. Commun.* 8:14023. doi: 10.1038/ncomms14023

Rodriguez-Tovar, L. E., Castillo-Velazquez, U., Arce-Mendoza, A. Y., Nevarez-Garza, A. M., Zarate-Ramos, J. J., Hernandez-Vidal, G., et al. (2016). Interferon gamma and interleukin 10 responses in immunocompetent and immunosuppressed New Zealand white rabbits naturally infected with *Encephalitozoon cuniculi*. *Dev. Comp. Immunol.* 62, 82–88. doi: 10.1016/j.dci.2016.05.003

Sak, B., and Ditrich, O. (2005). Humoral intestinal immunity against *Encephalitozoon cuniculi* (Microsporidia) infection in mice. *Folia Parasitol. (Praha)* 52, 158–162. doi: 10.14411/fp.2005.020

Sak, B., Kotkova, M., Hlaskova, L., and Kvac, M. (2017). Limited effect of adaptive immune response to control encephalitozoonosis. *Parasite Immunol.* 39:e12496. doi: 10.1111/pim.12496

Sak, B., Sakova, K., and Ditrich, O. (2004). Effects of a novel anti-exospore monoclonal antibody on microsporidial development in vitro. *Parasitol. Res.* 92, 74–80. doi: 10.1007/s00436-003-0988-1

Sak, B., Salat, J., Horka, H., Sakova, K., and Ditrich, O. (2006). Antibodies enhance the protective effect of CD4+ T lymphocytes in SCID mice perorally infected with *Encephalitozoon cuniculi*. *Parasite Immunol.* 28, 95–99. doi: 10.1111/j.1365-3024.2005.00813.x

Salat, J., Braunfuchsova, P., Kopecky, J., and Ditrich, O. (2002). Role of CD4+ and CD8+ T lymphocytes in the protection of mice against *Encephalitozoon intestinalis* infection. *Parasitol. Res.* 88, 603–608. doi: 10.1007/s00436-002-0620-9

Salat, J., Horka, H., Sak, B., and Kopecky, J. (2006). Pure CD4+ T lymphocytes fail to protect perorally infected SCID mice from lethal microsporidiosis caused by *Encephalitozoon cuniculi*. *Parasitol. Res.* 99, 682–686. doi: 10.1007/s00436-006-0208-x

Salat, J., Jelinek, J., Chmelar, J., and Kopecky, J. (2008). Efficacy of gamma interferon and specific antibody for treatment of microsporidiosis caused by *Encephalitozoon cuniculi* in SCID mice. *Antimicrob. Agents Chemother.* 52, 2169–2174. doi: 10.1128/AAC.01506-07

Salat, J., Sak, B., Le, T., and Kopecky, J. (2004). Susceptibility of IFN-gamma or IL-12 knock-out and SCID mice to infection with two microsporidian

species, *Encephalitozoon cuniculi* and *E. intestinalis*. *Folia Parasitol. (Praha)* 51, 275–282. doi: 10.14411/fp.2004.033

Schmidt, E. C., and Shadduck, J. A. (1983). Murine encephalitozoonosis model for studying the host-parasite relationship of a chronic infection. *Infect. Immun.* 40, 936–942. doi: 10.1128/iai.40.3.936-942.1983

Schmidt, E. C., and Shadduck, J. A. (1984). Mechanisms of resistance to the intracellular protozoan *Encephalitozoon cuniculi* in mice. *J. Immunol.* 133, 2712–2719.

Sinpoo, C., Paxton, R. J., Disayathanoowat, T., Krongdang, S., and Chantawannakul, P. (2017). Impact of *Nosema ceranae* and *Nosema apis* on individual worker bees of the two host species (*Apis cerana* and *Apis mellifera*) and regulation of host immune response. *J. Insect. Physiol.* 105, 1–8. doi: 10.1016/j.jinsphys.2017.12.010

Sokol, C. L., and Luster, A. D. (2015). The chemokine system in innate immunity. *Cold Spring Harb. Perspect. Biol.* 7:a016303. doi: 10.1101/cshperspect.a016303

Sokolova, Y. Y., Bowers, L. C., Alvarez, X., and Didier, E. S. (2019). *Encephalitozoon cuniculi* and *Vittaforma corneae* (Phylum Microsporidia) inhibit staurosporine-induced apoptosis in human THP-1 macrophages in vitro. *Parasitology* 146, 569–579. doi: 10.1017/S0031182018001968

Soto-Dominguez, A., Davila-Martinez, C., Castillo-Velazquez, U., Nevarez-Garza, A. M., Rodriguez-Rocha, H., Saucedo-Cardenas, O., et al. (2020). Variation of the CD4, CD8, and MHC II cell population in granulomas of immunocompetent and immunosuppressed rabbits in *Encephalitozoon cuniculi* infection. *Comp. Immunol. Microbiol. Infect. Dis.* 68:101387. doi: 10.1016/j.cimid.2019.101387

Steinman, R. M., and Hemmi, H. (2006). Dendritic cells: translating innate to adaptive immunity. *Curr. Top. Microbiol. Immunol.* 311, 17–58. doi: 10.1007/3-540-32636-7_2

Trinchieri, G. (2003). Interleukin-12 and the regulation of innate resistance and adaptive immunity. *Nat. Rev. Immunol.* 3, 133–146. doi: 10.1038/nri1001

Tumwine, J. K., Kekitiinwa, A., Nabukeera, N., Akiyoshi, D. E., Buckholt, M. A., and Tzipori, S. (2002). *Enterocytozoon bieneusi* among children with diarrhea attending mulago hospital in Uganda. *Am. J. Trop. Med. Hyg.* 67, 299–303. doi: 10.4269/ajtmh.2002.67.299

Turvey, S. E., and Broide, D. H. (2010). Innate immunity. *J. Allergy Clin. Immunol.* 125(2 Suppl. 2), S24–S32. doi: 10.1016/j.jaci.2009.07.016

Udonsom, R., Prasertbun, R., Mahittikorn, A., Chiabchalard, R., Sutthikornchai, C., Palasuwan, A., et al. (2019). Identification of *Enterocytozoon bieneusi* in goats and cattle in Thailand. *BMC Vet. Res.* 15:308. doi: 10.1186/s12917-019-2054-y

Valencakova, A., and Halanova, M. (2012). Immune response to *Encephalitozoon* infection review. *Comp. Immunol. Microbiol. Infect. Dis.* 35, 1–7. doi: 10.1016/j.cimid.2011.11.004

von Stebut, E., and Tenzer, S. (2018). *Cutaneous leishmaniasis*: distinct functions of dendritic cells and macrophages in the interaction of the host immune system with Leishmania major. *Int. J. Med. Microbiol.* 308, 206–214. doi: 10.1016/j.ijmm.2017.11.002

Wang, Z.-D., Liu, Q., Liu, H.-H., Li, S., Zhang, L., Zhao, Y.-K., et al. (2018). Prevalence of Cryptosporidium, microsporidia and Isospora infection in HIV-infected people: a global systematic review and meta-analysis. *Parasites Vectors* 11, 28–28. doi: 10.1186/s13071-017-2558-x

Weidner, E. (1975). Interactions between *Encephalitozoon cuniculi* and macrophages. Parasitophorous vacuole growth and the absence of lysosomal fusion. *Z Parasitenkd*, 47, 1–9. doi: 10.1007/BF00418060

Weidner, E., and Sibley, L. D. (1985). Phagocytized intracellular microsporidian blocks phagosome acidification and phagosome-lysosome fusion. *J. Protozool.* 32, 311–317. doi: 10.1111/j.1550-7408.1985.tb03056.x

Yokoyama, W. M. (2005). Natural killer cell immune responses. *Immunol. Res.* 32, 317–325. doi: 10.1385/IR:32:1-3:317

Zhang, Q., Feng, X., Nie, W., Golenbock, D. T., Mayanja-Kizza, H., Tzipori, S., et al. (2011). MyD88-dependent pathway is essential for the innate immunity to *Enterocytozoon bieneusi*. *Parasite Immunol.* 33, 217–225. doi: 10.1111/j.1365-3024.2010.01269.x

Conflict of Interest: The authors declare that the research was conducted in the absence of any commercial or financial relationships that could be construed as a potential conflict of interest.

The reviewer LW declared a shared affiliation with the author BH at the time of review.

Advantages of publishing in Frontiers

OPEN ACCESS
Articles are free to read for greatest visibility and readership

FAST PUBLICATION
Around 90 days from submission to decision

HIGH QUALITY PEER-REVIEW
Rigorous, collaborative, and constructive peer-review

TRANSPARENT PEER-REVIEW
Editors and reviewers acknowledged by name on published articles

Frontiers
Avenue du Tribunal-Fédéral 34
1005 Lausanne | Switzerland

Visit us: www.frontiersin.org
Contact us: frontiersin.org/about/contact

REPRODUCIBILITY OF RESEARCH
Support open data and methods to enhance research reproducibility

DIGITAL PUBLISHING
Articles designed for optimal readership across devices

FOLLOW US
@frontiersin

IMPACT METRICS
Advanced article metrics track visibility across digital media

EXTENSIVE PROMOTION
Marketing and promotion of impactful research

LOOP RESEARCH NETWORK
Our network increases your article's readership